Winners and losers in a changing ocean: Impact on the physiology and life history of pteropods in the Scotia Sea; Southern Ocean

University of East Anglia

A thesis submitted to the School of Environmental Sciences of the University of East Anglia in partial fulfilment of the requirements for the degree of Doctor of Philosophy

By Jessie Gardner

June 2019

Abstract

The Scotia Sea (Southern Ocean) is a hotspot of biodiversity, however, it is one of the fastest warming regions in the world alongside one of the first to experience ocean acidification (OA). Thecosome (shelled) pteropods are planktonic gastropods which can dominate the Scotia Sea zooplankton community, form a key component of the polar pelagic food web and are important contributors to carbon and carbonate fluxes. Pteropods have been identified as sentinel species for OA, since their aragonitic shells are vulnerable to dissolution in waters undersaturated with respect to aragonite.

In this thesis I investigate the impact of a changing ocean on the physiology and life history of pteropods in the Scotia Sea. Firstly, I culture early stage pteropods within OA and warming conditions predicted to occur in 2100 (Chapter 2). I demonstrate that larval shell morphology and survival rates are detrimentally affected in these conditions. Secondly, I constrain the life cycle and population dynamics of pteropods collected over a year from a sediment trap deployed on a moored platform (Chapter 3). I show that *Limacina helicina* and *Limacina retroversa* both have distinct life history strategies, although, spawning of both species corresponds to phytoplankton blooms. Thirdly, I establish a baseline vertical and biogeographical distribution of pteropods using historical samples (Chapter 4). I elucidate the geographical range edges of *L. retroversa* and *L. helicina*, as well as vertical migration patterns in relation to predation threat. Finally, I examine *in-situ* pteropod shell condition in relation to carbonate chemistry using net and oceanographic samples collected during two recent cruises (Chapter 5). I demonstrate that larval shells are susceptible to dissolution on exposure to aragonite undersaturation, however, later life stages display some resilience, since shell dissolution is confined to breaches in the periostracum. Overall, I recommend that continued monitoring, combined with bioassays and mesocosm work, will be essential in identifying the continued threat to pteropods from rapid environmental changes.

Contents

List of Figures

List of Tables

Acknowledgements

First and foremost, I would like to express a sincere thank you to my four supervisors, Clara Manno (British Antarctic Survey; BAS), Dorothee Bakker (University of East Anglia; UEA), Geraint Tarling (BAS) and Victoria Peck (BAS) for their guidance, encouragement and critical appraisal of this work. I am grateful for the freedom and support they gave me, making my PhD experience genuinely enjoyable and exciting.

Thank you to the brilliant captains and crew members of JR304 and JR15002 for all the support and enthusiasm, whatever the time or weather. Thanks also to the PSO's Jon Watkins and Gabi Stowasser for keeping everything running smoothly on the cruises and for tolerating the countless times I asked for another BONGO. I am extremely grateful for the help and support by Cecilia Liszka; covering the night/day shifts, being an awesome lab buddy and generally a great friend.

I also owe my deepest gratitude to those which helped me analyse my samples. Katrin Linse and Eric Tapley spent much time training and helping me to use the environmental scanning electron microscopes, to which I am extremely grateful. I would also like to thank Guy Hillyard, Elaine Fitzcharles and Paul Geissler for all the friendly support during my lab work at BAS. Many thanks go to Pete Ward, for teaching me invaluable skills with plankton and sharing your fantastic identification knowledge. I am extremely indebted to Stephen Humphrey and Marcos Cobas-Garcia for the very early and long mornings with the VINDTA (Laural) at UEA. I would also like to thank Gareth Lee for his technical expertise in seawater analysis and the training and support he gave while Laural was running. Ollie Legge wrote a Matlab script to process the VINDTA output; without it (and the training to use it) I would not have been able to process any of the carbonate chemistry output, so thank you.

I would also like to acknowledge the EnvEast cohort of 2014, being united as the first cohort and sticking together throughout our PhD's. There are also many awesome people at UEA who have helped me tremendously over the past few years. Particularly I would like to mention; Natasha, Jen, Dave C, Cecilia, Laurie, Claire, Phil, Dave L, Bio floor 01 crew, Env/Bio drinkers and the UEA fencers. My enthusiasm for my PhD would have faded without the comfort of Vlad, Alucard, Crumpet and Witcher. Finally, thanks to my amazing partner, Kris Sales, for tolerating me, keeping me sane and feeding me.

This PhD research was funded by the EnvEast doctoral training partnership, to which I am extremely grateful. All photographs included in this thesis were taken by the author.

1 Introduction

Ocean acidification and warming are currently a threat to most marine ecosystems and are likely to have large societal ramifications (Gattuso *et al.,* 2015). Forecasting the ecological impacts of anthropogenic change has become a top priority for research, policy and management (Rudd, 2014; IPCC, 2013; Kroeker *et al.,* 2013). While research on oceanic change is rapidly expanding, international advisory groups (OSPAR/ICES, 2013) have recommended to focus on species that may act as indicators for anthropogenic change. Thecosome pteropods have been identified as a possible sentinel species for anthropogenic ocean acidification, since their shells have been demonstrated to be particularly vulnerable to dissolution (Bednaršek *et al.,* 2017). Alongside being a potential biological indicator, pteropods in high-latitude ecosystems are important members of polar ecosystems as well as biogeochemical cycles. Therefore, changes to their life history and population dynamics could have wider ramifications.

1.1 Pteropod biology and role in the marine ecosystem

Pteropods are free-floating, holoplanktonic gastropods that are ubiquitous and abundant within the world's oceans (Figure 1-1) (Hunt *et al*., 2008; Lalli and Gilmer, 1989). Their foot is modified into elaborate paired wings to facilitate swimming, from which their name is derived (ptero- wings, poda- foot). The superorder pteropoda consists of two evolutionarily distinct clades, the Thecosomata (shelled) and Gymnosomata ('naked', but with larval shells) (Lalli and Conover, 1976).
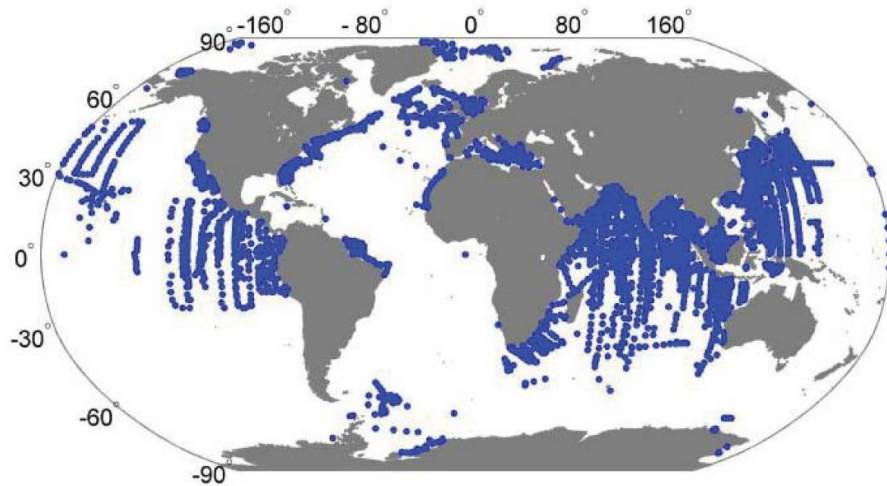
Figure 1-1 The global distribution of pteropods (Taken from Bednaršek *et al.,* 2012c)

The superorder pteropoda (Class Gastropoda, infraclass: Opisthobranchia) is split into two orders: Thecosomata (shelled pteropods) and Gymnosomata ('naked' pteropods with larval shells only) (Lalli and Conover, 1976). These orders have distinct trophic positions since Gymnosomes are active predators that specialise on capturing Thecosomes, which instead produce mucous webs to feed on plankton (Gilmer and Harbison, 1986). Thecosome shells comprise of a diverse range of forms, including coiled, triangular, coned and globose, all formed from thin, transparent aragonite structures (Lalli and Gilmer, 1989). Thecosome pteropods are further divided into the suborders Euthecosomata and Pseudothecosomata. Classification is mainly based on shell morphology with forma assigned to particular geographical regions, making species identification relatively simple. The euthecosomes possess an external aragonite shell throughout their life cycle, while in the pseudothecosomes each family is distinct, namely Cymbuliidae (larval shell is shed, and adults have internal gelatinous pseudoconcha), Peralididae (adults are shell bearing) and Desmopteridae (no adult shell or pseudoconcha) (Lalli and Gilmer, 1989). Within Euthecosomate are the superfamilies Limacinoidea and Cavolinioidea which are characterised by their sinistrally coiled and uncoiled adult shells, respectively. The full classification of pteropoda from WoRMS (2017) and Janssen (2003) is presented in Table 1.1.

Table 1.1 Subdivision of the superfamily Pteropoda (based on WoRMS, 2017; Janssen, 2003)

Class: Gastropoda
    Subclass: Opisthobranchia
      <u>Order: Thecosomata</u>
        - Suborder: Euthecosomata
          • Superfamily: Limacinoidea
            · Family: Limacinidae (e.g. *Limacina helicina, Limacina retroversa*)
          • Superfamily: Cavolinioidea
            · Family: Creseidae (*e.g. Creseis acicula*)
            · Family: Cliidae (e.g. *Clio pyramidata, Clio piatkowskii*)
            · Family: Cuvierinidae (e.g. *Cuvierina atlantica*
            · Family: Cavoliniidae (e.g. *Cavolinia inflexa*)
            · Family: Sphaerocinidae (e.g. *Sphaerocina formai*)
        - Suborder: Pseudothecosomata
          • Superfamily: Peraclidoidea
            · Family: Peraclididae (e.g. *Peraclis reticulate*)
            · Family: Cymbuliidae (*Cymbulia peroni*)
            · Family: Desmopteridae (e.g. *Desmopterus papilio*)
      <u>Order: Gymnosomata</u>
        - Suborder: Gymnosomata
            · Family: Pneumodermatidae (e.g. *Spongiobranchaea australis*)
            · Family: Notobranchadeidae (e.g. *Notobranchaea macdonaldi)*
            · Family: Cliopsidae (e.g. *Cliopsis krohni*)
            · Family: Clionidae (e.g. *Clione limacina antarctica*)
        - Suborder: Gymnoptera
            · Family: Hydromylidae (e.g. *Hydromyles globulosa*)
            · Family: Laginiopsidae (e.g. *Laginiopsis trilobata*)

Euthecosomata (a suborder of Thecosomata) pteropods have received the most research interest, since members of this suborder secrete an aragonite shell. Aragonite is a polymorph of calcium carbonate which is 50% more soluble than calcite, which could cause Euthecosomata shells to be susceptible to ocean acidification (Mucci, 1983; Fabry *et al.,* 2009). There are two families within Euthecosomata; Limacinidae, which have sinistrally coiled shells, and Cavoliniidae, which have uncoiled shells.

Most species of thecosome pteropods are thought to share similar reproductive biology, being protandric hermaphrodites that first function as males and subsequently mature into females (Lalli and Wells, 1978; Lalli and Gilmer, 1989).

Females are capable of producing high numbers of eggs, with up to 10,000 being reported for *L. helicina* inhabiting polar waters (Lalli and Gilmer, 1989). Pteropods in high-latitude ecosystems can be particularly abundant and a significant part of zooplankton biomass (Crelier *et al.,* 2010; Pakhomov and Froneman, 2004; Ward *et al.,* 2003). Pteropods are also major components within polar food webs, being a food source for carnivorous zooplankton, seabirds, commercially important fish and even bowhead whales (Pomerleau *et al.* 2012; Hunt *et al.,* 2008; Węsławski *et al.,* 1999). Furthermore, pteropods themselves are extensive omnivorous scavengers, with polar *Limacina* species accounting for up to 40% of community grazing impact (Pakhomov *et al.,* 2002). Since pteropods play such an important role within the polar food web, changes to their populations due to anthropogenic change could have wider ramifications within the polar ecosystem.

Pteropods significantly contribute to carbon and carbonate export to the deep ocean via the rapid sinking of dead individuals and large faecal pellets (Manno *et al.,* 2007; 2009). For example, Berner and Honjo (1981), estimated that pteropods may constitute at least 12% of the global total carbonate flux. Furthermore, individuals facilitate the aggregation of particles, since shells and discarded mucous feeding webs act as nuclei for sinking organic matter. Pteropods are estimated to account for up to 42% of the carbonate produced in the ocean (Bednaršek *et al.,* 2012c), however, ocean acidification could impact carbonate production as well as encourage carbonate dissolution at shallower depths, altering the efficiency of the carbonate pump.

Pteropods are major parts of polar food webs with *Limacina* accounting for 40% of community grazing impact in the Southern Ocean (Hunt *et al.,* 2008; Bernard and Froneman, 2005). Thecosome pteropods are omnivorous suspension feeders, producing mucous webs to entrap a diverse range of food. The size, shape and production of mucous webs is highly dependent on species and life stage however, they can reach ≥2 m in diameter and are secreted in as little as 5 seconds (Gilmer and Harbison, 1986; Gilmer, 1974). Once deployed the pteropod hangs motionlessly while particles and prey are trapped (Gilmer and Harbison,

1986). Prey include phytoplankton, zooplankton, sinking aggregates and even other pteropods (Bernard and Froneman, 2009; Gilmer and Harbison, 1991; Noji *et al.,* 1997). The webs are drawn into the gut by small radula, while exoskeletons (e.g. diatom frustules) are crushed via the gizzard (Morton, 1954a). Mucous webs are not essential for feeding, with ciliary action also being employed to waft particles into the food groove (Howes *et al.,* 2013; Morton, 1954). Incubations have shown *L. helicina helicina* can survive starvation for <4 weeks (Lischka and Riebesell, 2012) and *L. helicina antarctica* for >2 weeks (Maas *et al.,* 2011; Bednarsek *et al.,* 2012b). During the polar night pteropods cope with little to no food through reducing metabolism and/or relying on internal lipids reserves during the winter (Lischka and Riebesell, 2012).

1.2 Pteropod life history and physiology

Currently there are large variations in the estimations of pteropod longevity, life cycle, life stage phenology and growth patterns. For example, the longevity of *L. helicina antarctica* is proposed to be either 1 or 3 years, with disagreement as to whether early life stages overwinter (Bednaršek *et al*., 2012a; Hunt *et al*., 2008). Knowledge of a pteropod's life history is critical in determining their responses to anthropogenic oceanic change, since different life stages may have different tolerances of environmental drivers. For example, in most species, early life history stages are especially vulnerable in comparison to later life stages to anthropogenic change in comparison to adult stages (Hodgson *et al.,* 2016; Byrne, 2013; Kroeker *et al.,* 2013; Pechenik, 1987). Within the Southern Ocean, pH and temperature exhibits large spatiotemporal variation with water mass, upwelling, freshwater input, season and biological activity (Matson *et al.,* 2011; Kapsenberg *et al.,* 2015). Therefore, it is relevant to understand which life stage might coincide with more acidified and warm conditions since this may impact recruitment and long-term population stability (Dupont and Thorndyke, 2009; Manno *et al.,* 2017). Furthermore, defining the population dynamics, particularly the generation time and longevity, will enable us to elucidate the ability of pteropods to adapt to oceanic change (Manno *et al.,* 2017) since species with

faster generation turnover tend to have higher rates of molecular evolution (Thomas *et al.,* 2010).

Baseline data are vital starting points for monitoring population level changes associated with environmental climate change. The need to establish baselines is particularly pressing in rapidly changing regions such as high-latitude ecosystems (Manno *et al.,* 2017; Doney *et al.,* 2009; Fabry *et al.,* 2009). Long-term time series of abundance and size distribution have indicated a variety of trends suggesting multiple life history possibilities (Howes *et al.,* 2015; Loeb and Santora, 2013; Ohman *et al.,* 2009). However, variability may be due to the use of large regional averages and generalisation across multiple species and life stages, illustrating the need for regional, species-specific studies. As well as alterations in abundance, pteropods can also respond on a population level to environmental change by modifying vertical distribution and phenology of life history events, however, currently our knowledge of these aspects is lacking.

1.3 Pteropods in a changing world: an overview of current experimental research

1.3.1 Ocean acidification

Ocean acidification is the reduction in the pH of the ocean, caused primarily by uptake of carbon dioxide (CO_2) from the atmosphere. When CO_2 absorbed into the ocean it reacts with seawater to form H_2CO_3. Most of the H_2CO_3 quickly dissociates into a hydrogen ion (H^+) and HCO_3^-. Hydrogen ions can react with a carbonate ion (CO_3^{2-}) to form a bicarbonate ion (HCO_3^-). Therefore, the overall effect of dissolving CO_2 into seawater is an increase in the concentrations of H_2CO_3, HCO_3^-, and H^+, and decrease the concentration of CO_3^{2-} and a lower pH (Figure 1-2). Furthermore, increasing CO_2 concentrations will continue to decrease the [CO_3^{2-}] and thereby lower the saturation states of biologically important calcium carbonate ($CaCO_3$) minerals, including calcite (Ω_{ca}) and aragonite (Ω_{ar})$CaCO_3$ saturation levels (Orr *et al.*, 2005).

a.

$$CO_{2\ (atm)} \Leftrightarrow CO_{2\ (aq)} + H_2O \Leftrightarrow H_2CO_3^- \Leftrightarrow H^+ + HCO_3^- \Leftrightarrow 2H^+ + CO_3^{2-}$$

b. Present day conditions

c. Future conditions
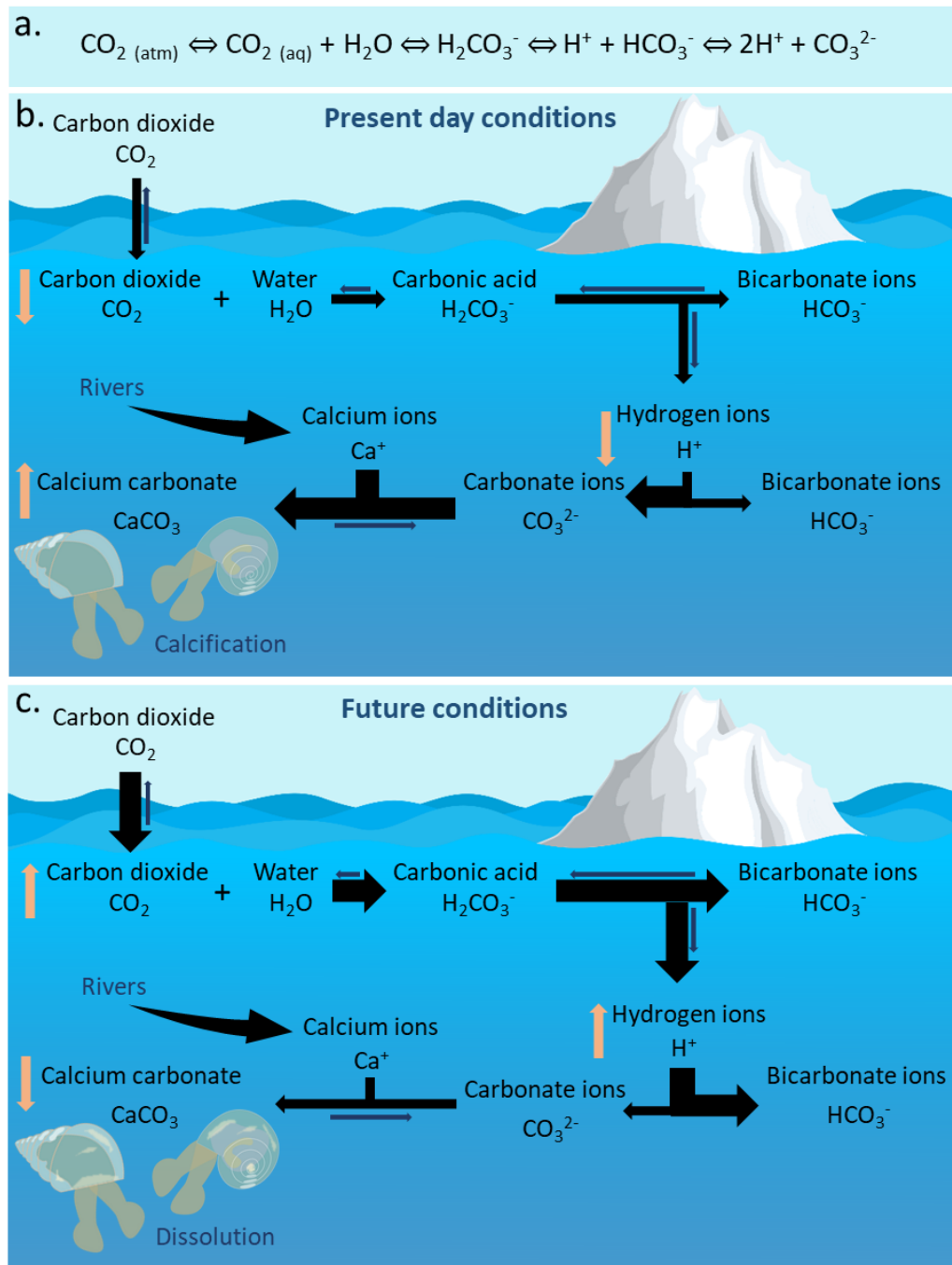
Figure 1-2 (**a.**) Atmospheric carbon dioxide ($CO_{2(atm)}$) absorbed by the oceans reacts with water and alters the speciation of total inorganic carbon. Total inorganic carbon exists in a thermodynamic equilibrium of aqueous carbon dioxide ($CO_{2(aqu)}$), carbonic acid ($H_2CO_3^-$), bicarbonate ions (HCO_3^-) and carbonate ions (CO_3^{2-}). (**b.**) Under present day concentrations of $CO_{2(atm)}$, CO_3^{2-} are readily available for marine calcifiers to form calcium carbonate ($CaCO_3$) structures, on combination with calcium ions (Ca^{2+}). (**c.**) Under future conditions, when the concentration of $CO_{2(atm)}$ has increased, the equilibrium (**a.**) is shifted towards the right, causing an increase in HCO_3^- and H^+ ions and a decrease in CO_3^{2-} ions, leading to the dissolution of $CaCO_3$ structures. The orange arrows indicate increases and decreases in specific species.

High-latitude ecosystems are experiencing ocean acidification at the fastest rate due to decreased buffering capacity from freshening and low temperatures enhancing CO_2 solubility (McNeil and Sasse, 2016; Sabine *et al.,* 2004; Doney *et al.,* 2009). Climate models estimate that the pH in the South Atlantic fell below the natural range of inter-annual variability between 1900- 1930 (Henson *et al.,* 2017). Regions in Southern Ocean are projected to become undersaturated with respect to aragonite within wintertime surface waters by 2030, while seasonal long-term aragonite undersaturation is predicted to become commonplace from 2050 (Hauri *et al.,* 2016; Friedrich *et al.,* 2012; McNeil and Matear, 2008) (Figure 1-3). Areas of aragonite undersaturation in polar regions are already being observed in association with upwelling (Bednaršek *et al.,* 2012) and glacial meltwater (Yamamoto-Kawai *et al*., 2009; 2011). If the saturation state of $CaCO_3$ is greater than 1, precipitation will occur, however, if it is less than 1, dissolution will ensue. This poses a significant challenge to organisms that form calcium carbonate shells, skeletons or internal structures such as pteropods (Gazeau *et al*., 2013; Kroeker *et al*., 2010; Parker *et al*., 2013).
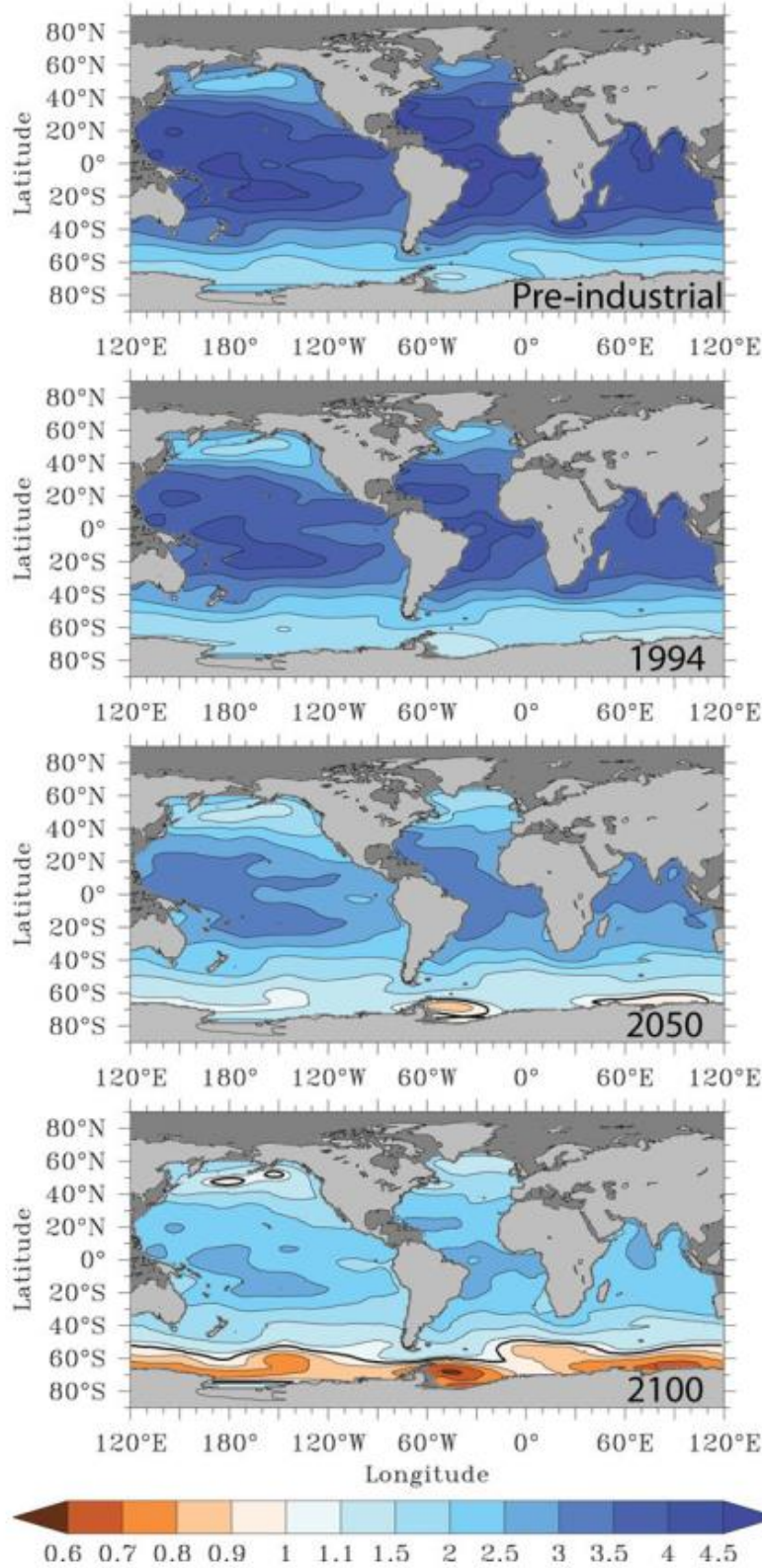
Figure 1-3. Surface water aragonite saturation state (Ωarag) for the pre-industrial ocean (nominal year 1765), 1994, 2050, and 2100. Original figure and details of computation can be found in Fabry *et al.* (2008).

Previous studies investigating historical pteropod assemblages within sediment cores have observed that pteropod shells are more abundant during colder periods in history and either absent or at low abundance during interglacial periods (Chen, 1968). This trend appears to be caused by variations in the ocean carbonate saturation levels. For example, during cold periods, reduced atmospheric CO_2 levels created lower dissolved CO_2 and higher carbonate saturation in the water column. Higher saturation levels of carbonate allowed pteropods to produce and maintain stronger shells, as well as reach the ocean floor and become buried in sediments without being dissolved. In contrast, the higher CO_2 levels and thus lower carbonate saturation levels during interglacial periods lead to in-life shell dissolution and increased dissolution of shells on the sea floor (Almogi-Labin et al., 2000; Wang et al., 1997).

Within conditions undersaturated with $CaCO_3$, pteropods are prone to shell dissolution and reduced calcification rates (Table 1.2). Pteropod shells are vital for swimming, protection, escape and feeding, therefore, alteration of shell weight and integrity could have severe implications for survival (Adhikari et al., 2016; Lalli and Gilmer, 1989). Furthermore, breaches within the pteropod shells or mechanical weakening could increase potential risk of predation, parasitism and bacterial infection, further increasing vulnerability (Green et al., 2009). For calcification to occur, pteropods take up bicarbonate ions from the surrounding seawater and concentrate them within the extrapallial space, which is isolated by an organic membrane called the periostracum (Harper, 1997). With ocean acidification, the concentration of surrounding carbonate ions declines, and more energy is needed to build a sufficient gradient between the internal and external spaces for calcification. A disruption of homeostasis heightens the energetic requirement needed to balance acid-base concentrations, which may influence numerous physiological processes.

The melting of ice in Arctic regions has led to freshening of the surface waters, contributing to carbonate undersaturation. Manno et al., (2012) demonstrated that lower salinity negatively impacts swimming ability of Arctic *Limacina retroversa,* while concurrent reduced pH reduces shell mass and survival. The

northern Scotia Sea has little variation in salinity due to the influence of ice being

relatively small, therefore, freshening was not considered in the current study.

However, reduced salinity is likely to act as an additional stressor on pteropods

residing in more ice-influenced regions further south in the Southern Ocean.

Table 1.2. A review of perturbation experiments investigating the impact of Ocean acidification (OA) and/or warming (Temperature [Temp'], °C) on thecosome pteropods across various areas and species (Spp). For OA, numbers <5 are the saturation state of aragonite (Ω_{ar}) and numbers >100 are atmospheric pCO2 concentrations (µatm). The effect of OA is given by blue arrows, warming by orange arrows and interactions between OA and warming by purple arrows. The direction of metabolic rates, calcification rates and mortality responses have been summarised. Metabolism also includes respiration measurements. Shell dissolution is considered as a failure to repair the shell and thus included as a reduction in calcification. Stage is whether the pteropods incubated were adult, juvenile, veligers or eggs, a ? indicates that the stage was unknown. Area abbreviations are NWA: Northwest Atlantic, CC: California current, EP: Eastern Pacific, NEP: Northeast Pacific, MED: Mediterranean, SO: Southern Ocean, AO: Arctic Ocean, PO: Pacific Ocean. Species abbreviations are LHH: *Limacina helicina helicina,* LR: *Limacina retroversa,* LHA: *Limacina helicina antarctica,* CP: *Clio pyramidata,* CI: *Cavolinia inflexa,* CA: *Creseis acicula.* Where blank, information was not available.

Spp	Area	Stage	OA	Temp'	Metabolism	Calcification	Mortality	Study
LHH	CC	Juvenile	Ω_{ar} 0.5-2.5	16-8		↘ (blue)		1
LHH	NEP	Adult	~760, ~1600, ~2800	12		↘ (blue)	→ (blue)	2
LHH	AO	Juvenile	362, 530, 704	-1.6		↘ (blue)	→ (blue)	3
LHH	AO	Adult	350, 765	5		↘ (blue)		4
LHH	AO	Juvenile	180, 350, 650, 880	2.3, 5.6, 6.8	↗ (blue/orange), → (purple), ↘ (orange)			5
LHH	AO	Adult	280, 380, 550, 760, 1120	0, 4	↗ (blue/orange), → (purple)	↗ (blue), → (purple/orange)		6
LHH	AO	Juvenile	130, 380, 750, 1150	3, 5.5, 8		↘ (blue/orange)	→ (purple), ↗ (blue/orange)	7
LHH	AO	Juvenile	350, 650	2, 7		↘ (purple/blue), → (orange)	→ (purple/blue)	8
LHH	PO	?	Ω_{ar} 0.5-1.79	14.4		↘ (blue)		9
LR	AO	Juvenile	350, 650, 880	2, 7		↘ (blue), → (orange)	↗ (orange), → (purple/blue)	10
LR	AO	Juvenile	350, 650, 880	2.3, 5.6, 6.8	→ (purple/blue/orange)			10
LR	AO	Adult	280, 350, 750, 1000	7		↘ (blue)	→ (blue)	11

Winners and losers in a changing ocean: Impact on the physiology and life history of pteropods in the Scotia Sea; Southern Ocean.

LR	NWA	Veliger	380, 753, 993	8	↗	12
LHA	SO	Juvenile	375, 500, 750, 1200	4	↘	13
LHA	SO	Juvenile /Adult	318, 387, 455, 704, 940, 894	4	↘	14
LHA	SO	Eggs	387, 750, 1200	2	↘	15
LHA	SO	Adult	180, 380, 560, 790, 1000, 1500,1800	-1.8	↘	16
LHA	SO	Juvenile	315, 427, 901	-0.8, 4	↗	17
CP	EP	?	380, 1000	20	→	18
CP	NWA	?	380, 800	15	→	19
CP	NEP	?	Ω_{ar} = 2.6 to Ω_{ar}>1		↘	20
CP	NWA	?	Ω_{ar}= 0.66		↘	21
CI	Med	Veligers	380, 857, 1713	13	↘	22
CA	Med	Adult	134, 240, 654, 2427, 1671, 835, 475	~19	↘ ↘	23

1. Bednaršek and Ohman, 2015; 2. Busch *et al.,* 2014; 3. Comeau *et al.,* 2012a; 4. Comeau *et al.,* 2009; 5. Lischka and Riebesell, 2016; 6. Comeau *et al.,* 2010a, 7. Lischka *et al.,* 2011; 8. Lischka and Riebesell, 2012; 9. Bausch *et al.,* 2018; 10. Lischka and Riebesell, 2016; 11. Manno *et al.*, 2012; 12. Thabet *et al.,* 2015; 13. Bednaršek *et al.,* 2012; 14. Bednaršek *et al.*, 2014; 15. Manno *et al.,* 2016; 16. Seibel *et al.,* 2012; 17. Hoshijima *et al.,* 2017; 18. Maas *et al.,* 2012a; 19; Maas *et al.,* 2015; 20. Fabry *et al.,* 2008; 21. Orr *et al.,* 2005; 22. Comeau *et al.,* 2010b; 23. Comeau *et al.,* 2012b.

All incubation experiments on pteropods which investigate the impact of future ocean acidification have demonstrated pteropod shell dissolution and/or reduced calcification (Table 1.2). Whether pteropods are physiologically able to tolerate ocean acidification remains ambiguous, with perturbation experiments revealing a variety of responses (Table 1.2). For example, oxygen consumption of *L. helicina antarctica* was supressed by 20% under future ocean acidification conditions (Seibel *et al.,* 2012), while *L. helicina helicina* and *L. retroversa retroversa* showed no response (Lischka and Riebesell, 2016; Comeau *et al.,* 2010a). Similarly, there is disagreement between studies as to whether mortality rate is unaffected or increases with ocean acidification (Table 1.2). Local acclimatization and local adaptation are likely to result in wide variation in the tolerance of pteropod populations (Bednaršek *et al*., 2017), therefore, it may be difficult to extrapolate findings to other species and regions.

Incubations of pteropods under ocean acidification conditions suggest there is no difference in the response of juveniles and adults with respect to mortality, metabolism or shell calcification (Table 1.2). Furthermore, Bednaršek *et al.,* (2014) found no difference in shell dissolution between juvenile and adult *Limacina helicina antarctica* that were treated identically. Only two studies have focused on the impact of ocean acidification on larval pteropod stages. Thabet *et al.* (2015) found increased mortality of embryo and larvae and possible developmental delay of *Limacina retroversa* when exposed to undersaturated conditions. Comeau *et al.* (2010) demonstrated when the larvae of *Cavolinia inflexa* are exposed to low pH, they develop malformations and reduce growth rates and at a very low pH veligers were viable but shell-less. Both of these studies suggest that early life stages of pteropods are vulnerable to ocean acidification, however, there are currently no investigations into the impact of anthropogenic change on larval *L. helicina antarctica* within the Southern Ocean.

The literature is currently divided over the effectiveness of the periostracum for pteropods in protecting the underlying aragonite shell from aragonite undersaturation (Peck *et al.,* 2016a; 2016b; Bednaršek *et al.,* 2014; 2016a). Peck *et al.,* (2016a; 2016b) stipulate that shell dissolution only occurs when there has

been a breach or perforation in the periostracum which, for example, may occur from bacterial damage (Bausch *et al.,* 2018). Alternatively, Bednaršek *et al.,* (2014a; 2012b) state that the periostracum is ineffective, providing insufficient protection against undersaturation since it is extremely thin. Further investigation into the effectiveness of the periostracum in protecting pteropod shells is needed to resolve this debate.

1.3.2 Oceanic warming

Temperature has been shown to have a significant effect on biomineralisation processes and growth across many calcifying species (Gazeau *et al.,* 2013). Within an organism's tolerance window, warming can increase metabolic rates and boost shell growth, however, when this optimum is exceeded shell microstructure can become degraded, reducing mechanical strength (Somero, 2010; Mackenzie *et al.,* 2014).

Associations between pteropods and temperature could manifest via effects on metabolism, growth, reproduction and survival. Metabolic studies have revealed that *L. helicina antarctica* and *L. helicina helicina* increase their respiration and metabolic rates with elevated temperatures of 4-5 °C (Table 1.2). Temperate pteropod species that undertake diurnal migration encounter a greater temperature range than polar species of ±3°C and so have a greater tolerance to warming (Maas *et al.,* 2016; 2012). This contrasts to high-latitude pteropod species which have a narrower thermal tolerance (Van der Spoel and Hayman, 1983) and experience a narrower thermal range so may be more vulnerable to warming, as demonstrated in cod (Pörtner, 2002) (*see* Section 3.4.1. for details on thermal tolerances and ranges of *Limacina*). For example, the true polar *L. helicina helicina* showed an increase in metabolic rate with warming, while the sub-polar *L. retroversa retroversa* had no response (Lischka and Riebesell, 2016) suggesting the subpolar species may be better acclimated to temperature variations. Despite this, across numerous high latitude ecoregions, increased sea surface temperature has been identified as the most likely cause of reduced *L. helicina* abundances (Mackas and Galbraith 2011; Beaugrand *et al.* 2013; Howes

et al., 2015), as well as driving a poleward range shift (Mackas and Galbraith 2011; Beaugrand *et al.,* 2013). Elevated temperature was shown to have a significant effect on the mortality of juvenile *L. retroversa retroversa* and *L. helicina helicina* (Lischka and Riebesell 2012; Lischka *et al.,* 2011), but not on adults (Lischka and Riebesell, 2012; Comeau *et al.,* 2010a), suggesting earlier life stages could be more vulnerable to warming than later ones (Byrne *et al.,* 2013). However, there are currently no investigations into the impact of warming on early life stages of polar pteropods, despite high-latitude regions experiencing some of the fastest rates of warming.

1.3.3 Multiple drivers

Rising CO_2 levels may cause numerous concurrent changes including changes to nutrient cycling, stratification, storminess, water column mixing, water chemistry, oxygenation, freshwater input and temperature. Understanding the impact of these environmental perturbations on marine biota remains a major challenge since a range of intra- and inter-specific responses to multiple environmental drivers have been observed (Kroeker *et al.,* 2013; Wernberg *et al.,* 2012). While temperature alone can increase growth and metabolism in invertebrates (Pörtner, 2001), ocean acidification can increase the metabolic demands of acid-base regulation and reduce the amount of energy available for vital homeostatic processes (Francis-Pan *et al.,* 2015; Stumpp *et al.,* 2012; Dupont *et al*., 2009; Watanabe *et al.,* 2006). Therefore single-parameter manipulation experiments may under or over estimate an organism's response to any one variable (Byrne and Przeslawski, 2013).

The potential of warming to offset the negative impacts of ocean acidification has been demonstrated for a range of organisms (Brennand *et al.,* 2010; Waldbusser, 2011; McCulloch *et al*., 2012), although, other studies have revealed additive (Anthony *et al.,* 2008; Boyd *et al.,* 2015) and even synergistic responses (Baragi and Anil, 2015; Lischka and Riebesell., 2012). A synergistic response is one that produces an effect greater than the sum of the individual responses (Begon *et al.,* 2006). The impact of these environmental drivers on an organism

depends on numerous factors including the rate of change (Suckling *et al.,* 2014a), frequency of change (Pansch *et al.,* 2013), plasticity (Poloczanska *et al*., 2013; Lavergne *et al.,* 2010; Parmesan and Yohe, 2003), tolerance threshold (Pörtner, 2008), life stage (Small *et al.,* 2016; Cripps *et al.,* 2015) and food availability (Ramajo *et al.,* 2016). Therefore, predicting the impact of concurrent ocean acidification and warming on pteropods remains a major scientific challenge (Manno *et al.,* 2017).

Comeau *et al.* (2010a) investigated the combined impact of elevated temperature and pCO_2 on *Cavolinia inflexa* and revealed respiration rates increased as a function of pCO_2 at higher temperature. However, calcification rate was independent of temperature, being reduced as a function of elevated pCO_2 instead. Juvenile *L. helicina helicina* also show increased dissolution as a function of increased pCO_2 (Comeau *et al.,* 2012). With both elevated temperature and ocean acidification there was a synergistic increase in *L. helicina helicina* shell degradation (Lischka and Riebesell, 2012), although, this synergism is not universal (Lischka *et al.,* 2011). Mortality did not increase in either juvenile or adult *L. retroversa* and *L. helicina helicina* when exposed to a combination of ocean acidification and warming suggesting at levels predicted in 2100 they are sub-lethal stressors (Lischka and Riebesell, 2012; Lischka *et al.,* 2011; Comeau *et al.,* 2010a).

Table 1.2 gives a summary of previous perturbation experiments and their main findings. Most of the perturbation experiments investigating the impact of concurrent warming and OA focus on the Arctic pteropod species *L. helicina helicina, L. retroversa balea* and *L. helicina retroversa*. All pteropods displayed shell dissolution or a reduction in calcification on exposure to conditions undersaturated with respect to aragonite. However, it is clear that metabolic and mortality responses vary by species, highlighting a need also to focus on Southern Ocean species. Furthermore, all of the multiple driver investigations have concentrated on adult and juvenile life stages therefore, we have limited knowledge on the impacts of oceanic change on early life stages which are potentially more vulnerable. Larval survivorship and fitness underpin recruitment

success and any negative impacts from anthropogenic change could ultimately reduce long-term population viability within a region (Przeslawski *et al.,* 2008).

1.4 An overview of *in-situ* pteropod conditions in a changing world

Localised ocean acidification hotspots can occur naturally as a result of extensive ice melt (Robbins *et al.,* 2013) or deep water upwelling (Bednaršek *et al.,* 2012a; Feely *et al.,* 2009). Regions with horizontal gradients of surface aragonite saturation states provide excellent natural laboratories for considering the *in-situ* response of pteropods to anthropogenic ocean acidification. Studies investigating *in-situ* pteropod shell condition in upwelling regions along the U.S. west coast (Pacific Ocean) and the Scotia Sea (Southern Ocean) have found shell dissolution of *L. helicina* where Ω_{ar} ≤1, with increased severity with further undersaturation (Bednaršek and Ohman 2015; Bednaršek *et al.,* 2016; 2014a; 2014b; 2012a). Similarly, *in-situ* shell dissolution has been found along ice margins in the Greenland Sea (Peck *et al.,* 2016a). Currently there is little overlap between *in-situ* sampling of pteropod condition with water column carbonate chemistry in the Southern Ocean (a single study exists in the literature: Bednaršek *et al.,* 2012a) therefore, we have limited understanding of the baseline conditions in which pteropods reside. A recent review of the present state of pteropod research (Manno *et al.,* 2017) recommended that further assessment of pteropod shell condition in relation to carbonate chemistry is needed, particularly in regions of rapid change such as high-latitude ecosystems.

1.5 Study region

Most of the open Southern Ocean is classed as High Nutrient Low Chlorophyll (HNLC) where lack of iron limits phytoplankton growth (Wadley *et al.,* 2014; Boyd *et al.,* 2000). However, parts of the Scotia Sea have significant productivity (Whitehouse *et al.,* 2012; Atkinson *et al.,* 2012; Hogg *et al.,* 2011), since the Polar Front transports iron into the region, fuelling one of the largest phytoplankton blooms in the Southern Ocean (Korb *et al.,* 2005; Korb and Whitehouse, 2004) (Figure 1-4). The Scotia Sea supports high mesozooplankton biomass and

biodiversity (Atkinson *et al.,* 2012), including extremely high abundances of pteropods (Hunt *et al.,* 2008; Ward *et al.,* 1995; Bednaršek *et al.,* 2012a). However, the Scotia Sea's unique hotspots of biodiversity are under threat, as the region is experiencing some of the fastest rates of environmental change in the Southern Ocean (Henson *et al.,* 2017). Around South Georgia surface temperatures have increased between 1925 and 2006 by ~2.3°C (~0.5 S.E.) in winter and by ~0.9°C (~0.3 S.E.) in summer (Whitehouse *et al.,* 2006; 2008). Furthermore, wintertime and summertime aragonite undersaturation is predicted to occur by 2030 south of the Polar Front (Bjork *et al.,* 2014; Friedrich *et al.,* 2012; McNeil and Matear, 2008). Thus, the Scotia Sea is an ideal natural laboratory setting to investigate the vulnerability of pteropods to ocean change.

a.

Sea-surface nitrate [mmol N m^{-3}]

b.
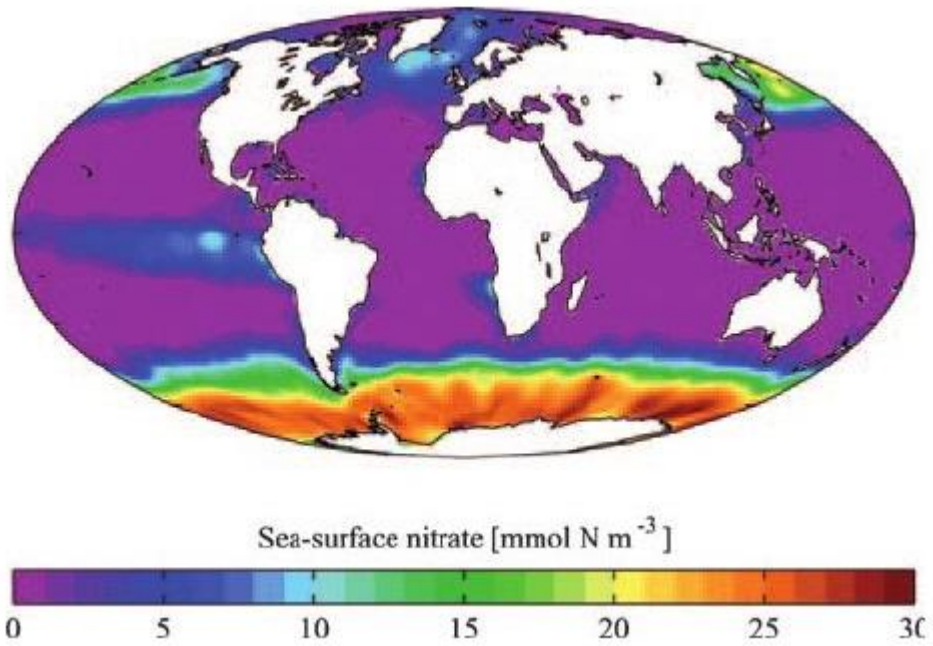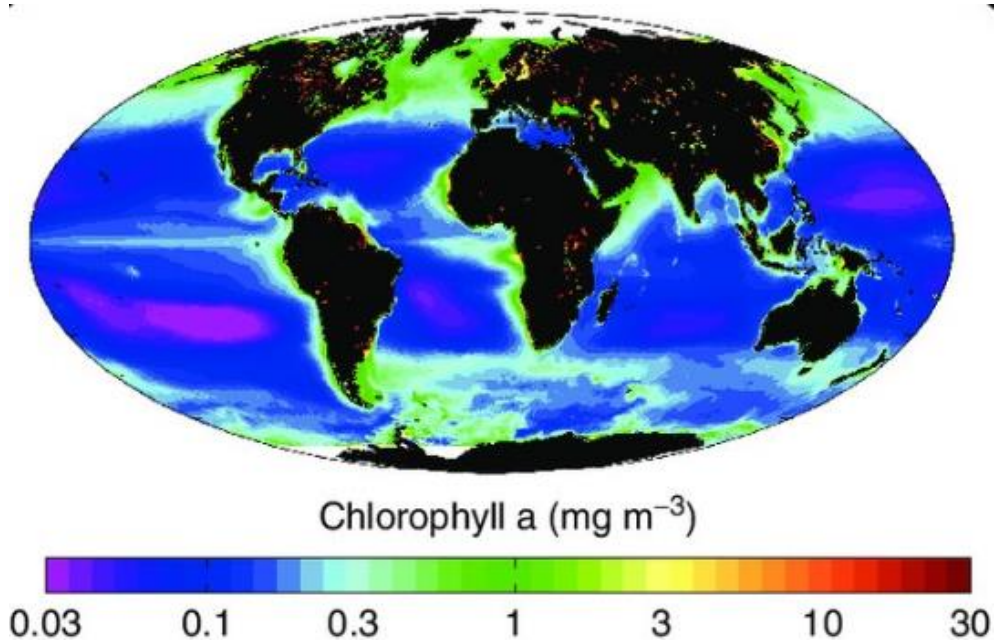
Chlorophyll a (mg m^{-3})

Figure 1-4. A comparision of the locations of (a.) High Nutrient–Low Chlorophyll (HNLC) regions around the world, represented by nitrate concentration with (b.) regions of high productivity, represented by chlorophyll concentration. Images were taken from a. Mock *et al.* (2008) and b. Hopes and Mock (2001).

1.6 Thesis aims and approach

In this thesis I investigate the impact of changing seawater properties on the physiology and life history of pteropods in the Scotia Sea; Southern Ocean. In order to assess pteropods in a changing world, a range of approaches were utilised including experimental (Chapter 2), long-term monitoring (Chapter 3), historical datasets (Chapter 4) and *in-situ* sampling (Chapter 5). These approaches assess the state of pteropod populations in the past (Chapter 4), present (Chapter 3 and 5) and future (Chapter 2) in order to advance ocean acidification and pteropod research. An outline of the main aims for each results Chapter is given below.

Chapter 2: The impact of ocean acidification and warming on early life stage *Limacina helicina antarctica*

In Chapter 2 I cultivate the polar pteropod *Limacina helicina antarctica* and observe the potential impact of exposure to increased temperature and aragonite undersaturation resulting from ocean acidification (OA) for the first time. Larval *Limacina helicina antarctica* were incubated within acidified and warm conditions using a fully-factorial experimental design for 5 days to assess whether there was an impact on post-hatch shell development, morphology and survival. These short-term incubations simulate the experience of larvae to variations in their environment because of present day and predicted heterogeneity in warm and acidified waters in the Southern Ocean. Larval survivorship and fitness underpin recruitment success and any negative impacts from a high CO_2 world can ultimately reduce long-term population viability in this region.

Chapter 3: Southern Ocean pteropod life history and population dynamics

In Chapter 3 I attempt to elucidate the population dynamics and life history of pteropods collected within a shallow (400 m) sediment trap at site P3 (Scotia Sea) between December 2014 and November 2015. The *in-situ*, long-term presence and abundance of pteropod species is assessed in relation to environmental conditions. For *L. helicina* and *L. retroversa* a cohort analysis was carried out to describe seasonal spawning phenology, growth patterns,

population dynamics and generation time. The improvement of current knowledge of pteropod population dynamics and life history is critical in determining their responses to oceanic change since different life stages and species may have different tolerances and vulnerabilities.

Chapter 4: A historic baseline for the vertical and biogeographical distribution of pteropods across the Polar Front.

In Chapter 4 I develop a baseline to define *in-situ,* species-specific population dynamics and abundances of pteropods across the Polar Front between South Georgia and the Falkland Islands. Pteropods examined in this Chapter were collected around 90 years ago during the *Discovery Investigations,* before most of the influence of anthropogenic ocean acidification and warming in the Southern Ocean. Furthermore, for *L. helicina* and *L. retroversa,* the vertical distribution and diurnal migration activities were also defined. This baseline will allow future studies to assess any subsequent changes to this population of pteropods within the rapidly changing Scotia Sea.

Chapter 5: *In-situ* pteropod shell condition in relation to carbonate chemistry during the summer within the Scotia Sea

In Chapter 5 I define the present day, *in-situ* condition of pteropod shells in relation to summer carbonate chemistry at key research stations within the Scotia Sea. Pteropods were collected during two research cruises during the summers of 2014 (JR304) and 2015 (JR15002). Water samples and vertical CTD profiles (conductivity, temperature, Chl-*a*) representing the full water column were collected alongside the pteropods to elucidate the current conditions in which pteropods reside. The shell condition of pteropods from areas of aragonite undersaturation ($\Omega_{ar} \leq 1$) and supersaturation ($\Omega_{ar} \geq 1$) was inspected for signs of dissolution using both light and scanning electron microscopy to give a current baseline state of pteropods within the Scotia Sea.

 Finally, in Chapter 6 I aim to assimilate the results of the previous Chapters in order to give an overall conclusion of this thesis in the light of recent research. Furthermore, areas for future investigation are highlighted.

2 Southern Ocean pteropods at risk from ocean acidification and warming

The majority of the work in this Chapter has been published as:

Gardner, J., Manno, C., Bakker, D.C., Peck, V.L. and Tarling, G.A., 2018. Southern Ocean pteropods at risk from ocean warming and acidification. *Marine Biology*, 165(1), pp.8-18.

The full paper has been included at the end of the thesis.

2.1 Introduction

2.1.1 A changing world

A multitude of concurrent drivers pose a pernicious, global threat to marine ecosystems and their services (Bijma *et al.,* 2013). With increases in seawater temperature of 0.6-2.0˚C, decreases in pH of 0.1-0.4 units and shoaling of the carbonate compensation depth forecast to occur by 2100 (RCP 2.6- 8.5), ocean acidification (OA) and warming pose an acute threat to marine organisms (IPCC 2013; Heinze *et al.,* 2015). Understanding the impact of these environmental perturbations on marine biota remains a major challenge (Kroeker *et al.,* 2013) since a range of intra- and inter-specific responses to multiple environmental drivers have been observed (Wernberg *et al.,* 2012).

2.1.2 Early life history stages and oceanic change

Early life history stages are suspected to be especially vulnerable to environmental change (Guo *et al.,* 2015; Byrne, 2011; Clark *et al.,* 2009; Gosselin and Qian, 1997) although large variations in tolerance have been observed as some species are highly sensitive and others resistant to change (Foo and Byrne, 2017). This is hypothesised to be related to organ and immune systems being undeveloped, the higher surface to volume ratio, differential rates of absorption/detoxification and an inability to avoid unfavourable conditions (Mohammed, 2013). In invertebrates, early stages are often ecologically and physiologically distinct from adult forms (Gosselin *et al.,* 1997), as observed in pteropods. Furthermore, life cycles often consist of several ontogenic phases that may exhibit different responses to environmental perturbations (Small *et al.,* 2016; Green *et al.,* 2004). Despite this, many studies focus on adults, generalising outcomes across entire life cycles and potentially over or under estimating vulnerability. For example, Cripps *et al.,* (2014) demonstrated adverse effects (such as increased mortality and reduced reproductive fitness) of ocean acidification on early life stages of copepods where prior investigations considered them insensitive due to focus on adult females. Stage specific survival rates may have serious consequences on demographics. Viability and survival of these stages are vital for successful recruitment and long-term population

stability. Furthermore, early exposure to environmental stressors could alter vulnerability of later developmental stages through latent effects (such as mortality, egg production, fecundity and shell size), adding to the overall impact (Kroeker *et al.,* 2013; Suckling *et al.,* 2014).

OA is expected to occur in high-latitude ecosystems at one of the fastest rates in the world due to seasonal amplification, freshening and colder temperatures enhancing CO_2 solubility (Doney *et al.,* 2009; Fabry *et al.,* 2009). Such processes alter the ratio of dissolved inorganic carbon (DIC) and total alkalinity (TA) to values where calcium carbonate becomes susceptible to dissolution. This poses a significant threat to polar marine organisms that form calcium carbonate shells, skeletons or internal structures (Mostofa *et al.,* 2016). In the Southern Ocean carbonate undersaturation events have already been observed (Bednaršek *et al.,* 2012a) and are predicted to occur more frequently over the coming decades (McNeil and Matear, 2008).

2.1.3 Southern Ocean pteropods

Thecosome pteropods (holoplanktonic gastropods) can dominate high-latitude zooplankton communities (Hunt *et al.,* 2008). In polar regions shelled pteropods are one of the major components within food webs, acting as a food source of carnivorous zooplankton, fishes and a number of higher predators such as whales and birds (Falk-Petersen and Sargent, 2001). Furthermore, polar pteropods contribute significantly to carbon and carbonate export to the deep ocean through the sinking of dead individuals and faecal pellets (Manno *et al.,* 2007; 2009). *Limacina helicina* are true polar pteropods, with its two species, *Limacina helicina antarctica* and *Limacina helicina helicina* occurring within the Antarctic and Arctic respectively (Hunt *et al.,* 2010). They are considered potential sentinels of OA since their shells consist of aragonite; a polymorph of calcium carbonate which is 50% more soluble than calcite (Mucci, 1983; Bednaršek *et al.,* 2014a). In the Southern Ocean, *Limacina helicina antarctica* reside within the surface ocean where aragonite undersaturation events and 'hotspots' of rapid warming have already been identified and are predicted to become more frequent (McNeil and Matear, 2008; Gutt et al., 2015; Vaughan *et*

al., 2003). This is of particular concern in the northern Scotia Sea region, since it has the largest measured seasonal cycle of surface ocean CO_2 in the Southern Ocean (Jones *et al.,* 2012; 2015) as well as upwelling events of CO_2 enriched deep water to the surface and hotspots of warming (Bednaršek *et al.,* 2012a; Whitehouse *et al.,* 2008; Gille, 2002).

2.1.4 Larval pteropods in a changing world

Shell dissolution of juvenile *L. helicina antarctica* has already been reported in natural populations within the Scotia Sea (Bednaršek *et al.,* 2012a), while numerous incubation experiments under predicted OA levels of polar pteropod juveniles and adults suggest a range of other negative physiological responses (Comeau *et al.,* 2009; Lischka *et al.,* 2011; Manno *et al.,* 2012; Peck *et al.,* 2016; Seibel *et al.,* 2012) (Table 1.2). Manno *et al.* (2016) demonstrated that maternal and embryonic exposure of *L. helicina antarctica* to acidified conditions reduced the percentage of eggs developing to later stages by 80%. However, responses to concurrent OA and warming remain unresolved (Bednaršek *et al.,* 2016) particularly with regard to the responses of larval *L. helicina antarctica* to multiple concurrent environmental drivers*.* To date, studies of larval pteropods have focussed on incubating North Atlantic and Mediterranean species with *Limacina retroversa* exhibiting increased mortality (Thabet *et al.,* 2015) and *Cavolinia inflexa* shell malformations (Comeau *et al.,* 2010b) as a result of ocean acidification. Due to the key ecological and biogeochemical role of *L. helicina antarctica* in polar regions (see Section 1.1.)*,* alteration of larval shell morphology alongside reduced recruitment to adulthood could have major implications on the Southern Ocean ecosystem.

2.1.5 Chapter aims

Here, early life stages of *Limacina helicina antarctica* were experimentally exposed to acidification and warming which are predicted to occur by 2100. Currently we have little knowledge of the impact of acidification and warming on early life stages of polar pteropods. Short-term incubation experiments were utilised to cultivate shelled pteropod (*Limacina helicina antarctica*) larvae within present day and predicted conditions in the Southern Ocean. Individuals were exposed to acidification and warming in a fully factorial experimental design to

examine responses to the singular and combined stressors on post-hatch shell development, morphology and survival.

In this Chapter, I aim to cultivate polar shelled pteropods (*Limacina helicina antarctica*) and use these to examine responses to the singular and combined impact of acidification and warming on post-hatch shell development, morphology and survival. These short-term incubations (5 days) aim to simulate the experience of larvae (veligers) to variations in their environment because of present day and predicted heterogeneity in warm and acidified waters in the Southern Ocean (McNeil and Matear, 2008; Gutt *et al.,* 2015; Vaughan *et al.,* 2003). Larval survivorship and fitness underpin recruitment success and any negative impacts from a high CO_2 world can ultimately reduce long-term population viability in this region (Przeslawski *et al.,* 2008).

2.2 **Methods**

2.2.1 **Pteropod collection and culturing**

Limacina helicina antarctica were collected onboard the *RRS James Clark Ross* (Cruise number JR304) within the Scotia Sea (57°36'20.5" S, 43°40'22.2" W) in November 2014 using a motion-compensated Bongo net (100 µm and 200 µm mesh sizes), vertically hauled from 200 m (Figure 2-1). The motion compensation corrects for the pitching and rolling of the ship using a spring mechanism that helps maintain a constant upward velocity of the net through the water. This reduces stress on pteropods during collection and avoids mechanical damage to shells. Ambient sea-surface conditions at 10 m were characterised by a sea surface temperature and salinity of 1.62°C and 34.3 respectively, with a total alkalinity (TA) of 2320 µmol/kg and a pH of 8.09. pH was measured in total scale using a pH meter (pH mobile 826, Metrohm) connected to a combined electrode (double juncture), calibrated using buffers Tris (pH = 8.089) y 2-Aminopiridine (pH = 6.786) at 4°C within a temperature controlled cold room.

Figure 2-1. Pteropod adults were collected within the Scotia Sea (Southern Ocean) from (**a.**) *R.R.S. James Clark Ross* in November 2014 (Cruise number JR304) using a (**b.**) motion-compensated Bongo net.

Live adult females were identified following the description of Lalli and Wells (Lalli and Wells, 1978) and examined under a light microscope (Olympus SZX16 fitted with a Cannon EOS 60D). Actively swimming individuals with no signs of damage (shell and body) and fully translucent shells were acclimated within filtered seawater (0.22 μm) for 8 hours at 1.66 ± 0.03°C (Spartel incubator with a C-400 circulator unit and an FC-500 in-line cooler, temperature measured every 2 hours). Filtered seawater was prepared from seawater collected via the ships underway system and passing it through a 0.22 μm filter (MasterFlex C/P 77600-62). Seawater was collected at the same location as the adult pteropods in an attempt to mimic the seawater chemistry of the pteropods locality. After acclimatisation, individuals that were actively swimming were placed individually within 500 ml incubation jars (nonpyrogenic polystyrene, Corning®) filled with filtered seawater and maintained at 1.22 ± 0.41°C. This temperature was in the range measured (-0.2- 1.8 °C) between 0 and 200 m at a station near where the adult was collected (55°15′10.0″ S, 41°18′08.5″ W). Jars were stored in darkness and sealed with no headspace to limit CO_2 exchange and inspected at least every 6 hours.

After 9 days within the 500 ml incubation jars, some adults spawned eggs within a 2-hour period. These were immediately removed using a wide mouthed Pasteur pipette to avoid egg cannibalism and damage. Mothers were in a good state of health during egg production (i.e. swimming and maintaining fully transparent shells) (Peck *et al.,* 2016) (Figure 2-2.). Egg ribbons were placed separately into ambient incubatory conditions within 65 ml jars of filtered seawater (1.02 ± 0.31°C). Following a further 7 days of incubation, veligers emerged simultaneously from 4 egg ribbons, each having been laid by a different female. These were mixed and randomly transferred into experimental conditions via stretched glass pipettes.
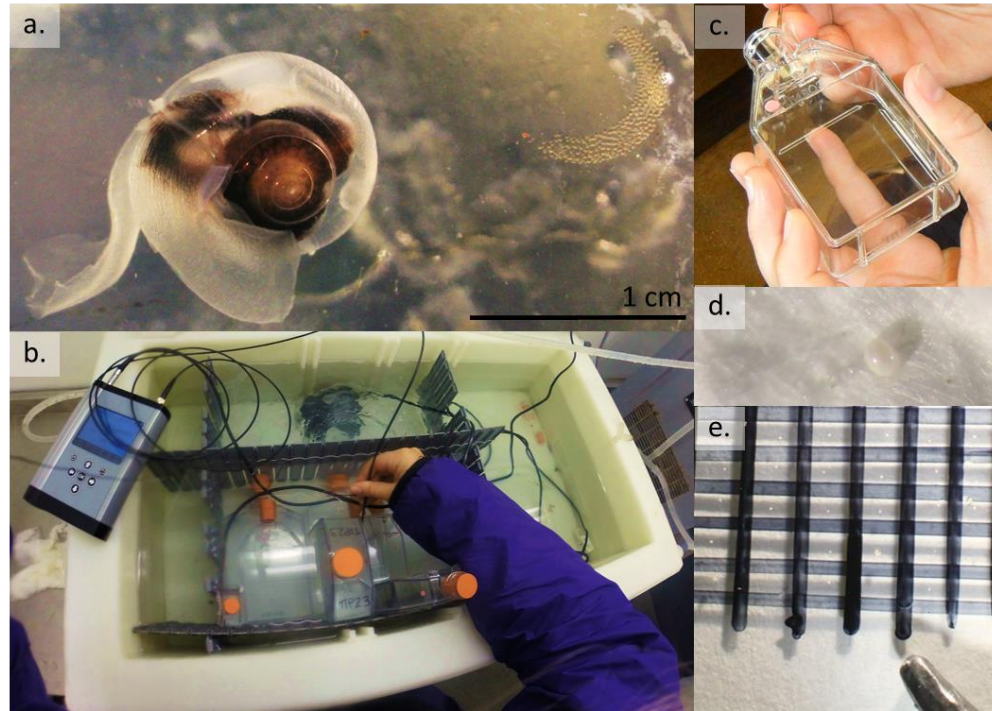
Figure 2-2. (**a.**) Adult *L. helicina antarctica* spawning eggs within experimental conditions. (**b.**) Egg ribbons were placed separately into ambient incubatory conditions (mimicking the collection environment) within (**c.**) 65 ml jars of filtered seawater. (**d.**) After incubation some veligers were air dried. (**e.**) Veligers were placed on a microscope slide for further microscope analysis (Pencil tip for scale).

2.2.2 Experimental design

All incubations took place within a controlled temperature room aboard the *RRS James Clark Ross*. Post hatch veligers were examined under a light microscope and five actively swimming individuals with fully translucent shells were placed together into each of the 60 incubation jars (65 ml, non-pyrogenic polystyrene, Corning®). 15 jars were placed into each of the four treatments exemplifying ambient (1.7˚C and pH 8.1), warm (3.5˚C and pH 8.1), acidified (1.7˚C and pH 7.6) or acidified-warm (3.5˚C and pH 7.6) conditions based upon predictions in 2100. All seawater was filtered (0.22 µm) since current evidence suggests *L. helicina antarctica* spawn in the autumn and overwinter as larvae when food availability is lower than in the summer (Hunt, 2008; Lischka and Riebesell, 2016). Although, the feeding habit and diet of pteropods over the winter in the Southern Scotia Sea remains poorly understood. Furthermore, filtration reduces most biological activity from altering the carbonate chemistry within the treatment bottles from the target values. Bacterial activity may still occur after filtration however, it was

assumed that chemistry was not altered by bacteria due to the short incubation period. To examine the impact of exposure time, three bottles were removed from each treatment every day for five days (Figure 2-3.). Each bottle was gently decanted into deep welled glass petri dishes and veligers were inspected under a light microscope for five minutes each. Those that were actively swimming and/or showed ciliate velum activity were classed as alive. Veligers that showed no ciliate velum activity, were not swimming and had no signs of internal movement after 5 minutes of observation were classed as dead. Maximum shell length was measured using a graticule and condition of the larvae noted before preservation, ensuring no secondary preservation effects (i.e. artificial shell features resulting from preservation) occurred (Oakes *et al.,* 2018). All veligers were subsequently rinsed with de-ionised water three times. For preservation, two specimens from each bottle were air dried upon a filter while the remainder were placed into Eppendorf tubes filled with 70% buffered ethanol.

Ethanol preserved veligers were dehydrated through a series of ethanol solutions (50, 70, 80, 90, 95 and 100 %, 5 min each) to stop shell collapse while dried veligers needed no further preparation. All veligers were subsequently mounted on carbon tape and imaged at x1200 magnification using a variable pressure scanning electron microscope (SEM) (TM3000, Hitachi) at the British Antarctic Survey. Only specimens that were living at the end of the incubation were considered for shell analysis (n= 233). Using the SEM, the apical shell surface was inspected for presence or absence of pitting (deep holes in the shell surface), etching (the partial dissolution of the upper shell surface observed by exposure of the granular or prismatic layer beneath) and malformation (deviation of growth from the expected smooth spiral) (Figure 2-4). Since statistically there was complete separation in the presence/absence of etching and pitting (for example in etching, presence was either on 100% or 0% of veligers) this resolution of shell analysis was considered appropriate. The maximum shell diameter (see Section 3.2.7) was also measured using the SEM and light microscope graticule to approximate shell size over the exposure period.
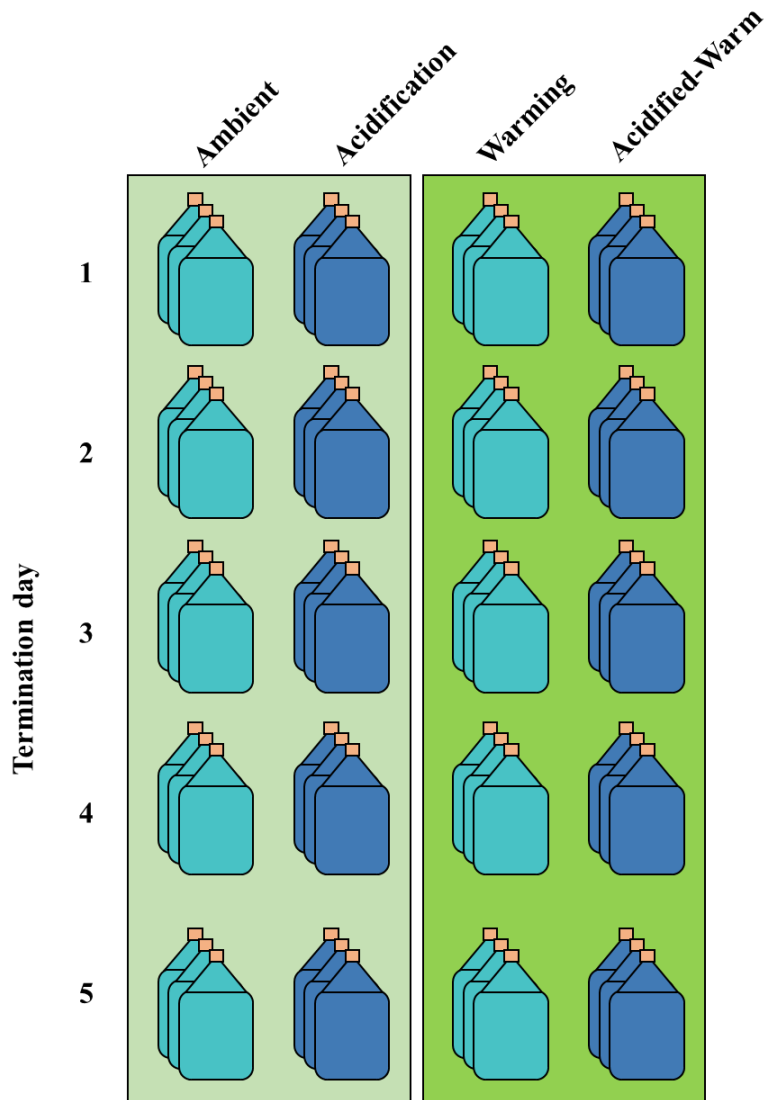
Figure 2-3. Schematic representation of the experimental design used to investigate the impact of acidification and warming on early life stage *L. helicina antarctica*. A fully factorial design was adopted with 4 treatments representing ambient (1.7°C, pH 8.1), warming (3.5°C, pH 8.1), acidified (1.7°C, pH 7.6) and acidified-warm (3.5°C, pH 7.6) conditions. Five pteropods were placed in each bottle with three bottles being removed from each treatment every day for five days.
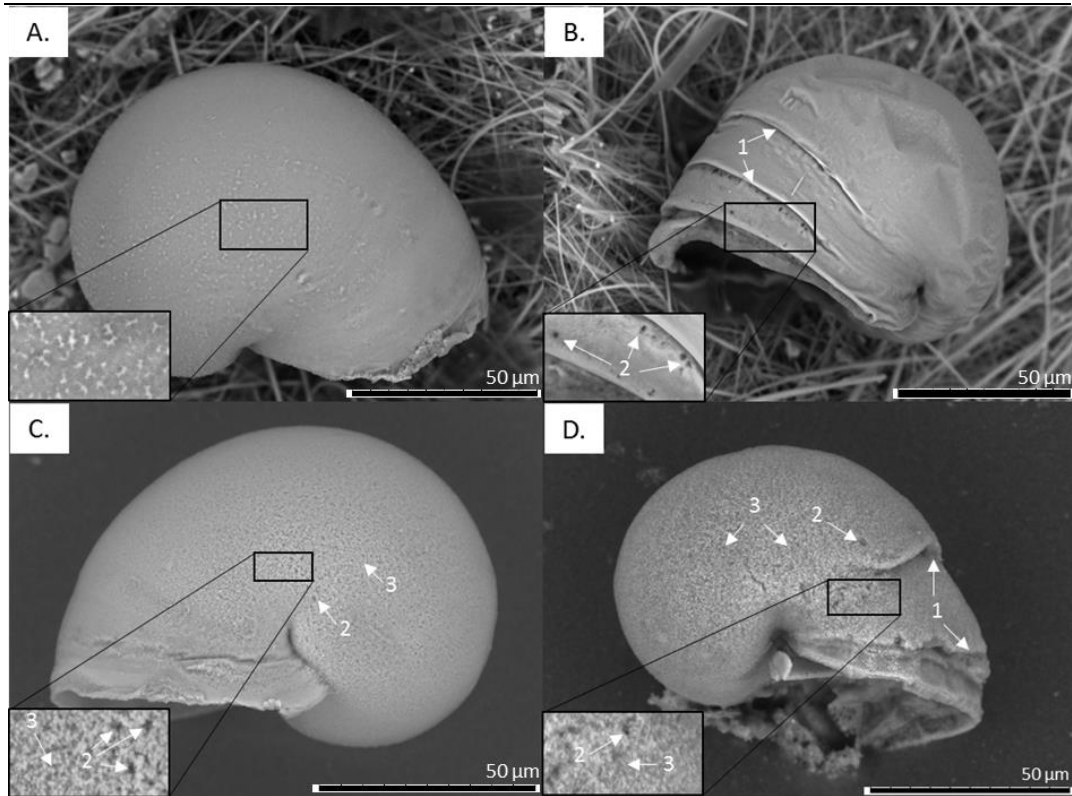
Figure 2-4. *Limacina helicina antarctica* larval shell morphology as a result of 5 days of exposure to ambient (**A.**), warm (**B**.), acidified (**C.**) and acidified-warm (**D**.) conditions. Examples of malformation (**1.**), pitting (**2.**) and etching (**3.**) are highlighted with arrows. Larvae were alive upon harvesting.

2.2.3 Seawater manipulation

A Spartel incubator with a C-400 circulator unit and an FC-500 in-line cooler housed within the ship's cold room was used to control incubation temperature. Temperature was measured every 4 hours throughout the entire incubatory period (PreSens fibox 4).

Seawater pH was manipulated through additions of HCl (hydrochloric acid) and NaHCO$_3$ (sodium bicarbonate) calculated by the *seacarb* software and maintained in a closed system (Lavigne and Gattuso, 2010). Gas bubbling is considered the best method to mimic ocean acidification (Gattuso *et al.,* 2011) however, acid/base addition was used in this instance due to logistical restraints. This method has been shown to be effective for the short incubation periods and small bottle volumes (Howes *et al.,* 2014; Gattuso and Lavigne, 2009). Using the acid/base addition technique does not alter the dissolved inorganic carbon within

the sample but modifies total alkalinity. Furthermore, pH may be lower than expected from this technique, the values are within the range suggested to occur by 2100 (RCP 8.5) in the Southern Ocean (Table 2.1) (IPCC 2013; Gattuso *et al.,* 2011; Gattuso and Lavigne, 2009; SCAR, 2009; Schulz *et al.,* 2009; McNeil and Matear, 2008). The calculation utilised measurements of pH (total scale) made with a pH electrode (Metrohm 826) and TA through applying a sea surface salinity (S) and temperature (T) algorithm based on Lee *et al.* (2006) and refined through a recent spatially-intensive carbonate chemistry survey in this region (M.P. Humphreys*, pers. comm*.) (Equation 1).

Equation 1: $TA = 683.41S - 9.139S^2 - 1.37T - 0.896T^2 - 10364.16$

To determine the impact of the manipulations on the incubation water, we extracted a 250 mL sub-sample of initial incubatory conditions, fixed with mercuric chloride and stored in a borosilicate bottle for subsequent analysis of TA and DIC. TA was measured by potentiometric titration and DIC by coulometry using a VINDTA (Versatile Instrument for the Determination of Titration Alkalinity, version 3C). Accuracy (TA= 2.5 µmol/kg; DIC= 1.1 µmol/kg) was determined using certified reference materials (Scripps Institution of Oceanography). pH was determined at the start and end of the incubation experiment. Aragonite saturation state was indirectly estimated from TA and DIC values using CO_2SYS software with the constants of Mehrbach *et al.* (1973) refitted by Dickson and Millero (1987) and sulphate dissolution constants by Dickson (1990). Carbonate system parameters of the incubations are in Table 2.1.

Table 2.1. Mean (± SD) values of carbonate system parameters determined from water samples from each treatment. Treatment refers to the target incubation conditions. Temperature (°C) was measured every 4 hours while pH (total scale) at the start and end of each incubatory period. Salinity, TA (µmol/kg) and DIC (µmol/kg) were determined from samples taken at the start of the experiment (accuracy TA= 2.5 µmol/kg; DIC= 1.1 µmol/kg) and subsequently used to calculate pCO_2 (partial pressure of CO_2, µatm) and Ω_a (aragonite saturation state) using CO_2SYS. Salinity was 34.5.

Treatment	Temperature	TA	DIC	Start pH End pH	Ω_a	pCO_2
Adults	1.22 ± 0.41	2293	2140	8.12 ± 0.01 8.10 ± 0.02	1.12	364
Ambient	1.71 ± 0.05	2322	2162	8.11 ± 0.01 8.10 ± 0.01	1.38	342
Warm	3.50 ± 0.09	2319	2154	8.09 ± 0.01 8.09 ± 0.01	1.49	343
Acidified	1.71 ± 0.05	2329	2332	7.60 ± 0.01 7.60 ± 0.01	0.62	1180
Acidified-warm	3.50 ± 0.09	2325	2320	7.60 ± 0.01 7.60 ± 0.01	0.61	1194

2.2.4 Statistical analysis

Data were analysed using R (2015). All larvae were considered when estimating mortality between treatment and days (n= 300) exposed however, only larvae that were living at the end of the incubatory period and were not damaged during processing were included within the analysis of shell morphology and size (n= 233 where ambient n= 66, acidified n= 44, warm= 59, acidified-warm= 54). A binomial (logit) generalised linear model (GLM) was used to estimate whether there were any differences in etching, pitting and malformation presence between treatments and days exposed. A gamma (identity) GLM and a binomial (logit) GLM estimated differences in shell size and mortality between treatments and days of exposure respectively. Complete separation between treatments for the presence of shell etching and pitting was found, therefore a Bayesian analysis with non-informative prior assumptions (Gelman *et al.*, 2008) was utilised from

the *arm* package (Gelman and Su, 2016). Model selection was informed using the information theoretic approach using the *MuMIn* package (Barton, 2016) to identify the models with delta Akaike information criterion <4 and the highest Akaike weights (Table A2.1) alongside comparisons of R^2 and likelihood ratio tests using the *lmtest* package (Zeileis and Hothorn, 2002). Model validation included checking the normalised residuals for normal distribution through plotting histograms, ploting the residuals versus fitted values to check for homoscedasticity (equal variances), checking that the independant varaibles are independant of each other (i.e. no collinearity) using 'base{corVIF}', calculating overdispersion using 'base{overdisp_fun}' and whether there was serial autocorrelation using 'car{ durbin.watson}'. For post-hoc analysis, tukey pairwise comparisons were performed using the *lsmeans* (Lenth, 2002). A two-way factorial analysis was also used within the same model frameworks as above to highlight the presence of any interactions between warming, acidification and exposure time on larval shell morphology, size and mortality.

Confidence intervals (CIs) for mean mortality x were calculated by:

Equation 2: $CI = x \pm \frac{Z\alpha}{2}\sigma/\sqrt{n}$

Where n is the number of living larvae per incubation bottle at the start of the incubation, σ the standard deviation and $Z\alpha/2$ the Z-table value for a given α value. Confidence intervals for the mean occurrence of shell malformation, pitting and etching as well as larval mortality were calculated by the modified Wald method (Agresti and Coull, 1998).

2.3 Results

2.3.1 Change in larval pteropod mortality

Significantly more larval fatalities occurred within acidified and acidified-warm conditions overall in comparison to ambient treatments ($p<0.01$) (Figure 2-5a). However, the number of fatalities did not change with the amount of time exposed to these conditions ($p>0.05$) (Table A2.2). A post-hoc analysis showed

that throughout, mortality was significantly higher in acidified conditions (38.7%, n=29) and acidified-warm conditions (25.3%, n=19) compared to that in warm (12%, n=9) and ambient conditions (2.7% n=2) ($p<0.001$). Furthermore, a factorial analysis indicated that acidification ($p<0.001$), rather than warming ($p>0.05$), increases larval mortality. However, larval mortality significantly increases when warming and acidification are combined ($p<0.01$) (Table A2.3). For a summary of mortalities see Table A2.4.

2.3.2 Change in larval pteropod shell size

Larvae in all treatments significantly increased their shell size during the incubation ($p<0.001$). Over the entire exposure time, larvae experiencing acidified ($p<0.05$) and acidified-warm ($p<0.01$) conditions were smaller than in ambient and warm conditions, which were similar (p>0.05) (Figure 2-5b) (Table A2.5). Post-hoc analysis indicated that shells incubated in acidified-warm conditions were significantly smaller than those in ambient conditions ($p>0.001$) but were not different from those in acidified conditions ($p>0.05$). Furthermore, during the first 3 days of exposure, shell size was similar between ambient, warm and acidified conditions but subsequently, shell size was smaller in warm and acidified conditions relative to ambient conditions ($p<0.01$). The rate of change in shell size was significantly lower in acidified-warm conditions on day 2 ($p<0.05$), warm conditions on day 4 and 5 ($p<0.001$) and acidified conditions on day 5 ($p<0.05$) (Table A2.6). This resulted in shell size on day 5 being smaller on exposure to warming (104.5 ± 1.11 µm, n=13, $p<0.001$), acidified (106.0 ± 2.0 µm, n=10, $p<0.001$) and acidified-warm conditions (105.2 ± 1.2 µm, n=12, $p<0.001$) compared to ambient conditions (113.0 ± 0.9 µm, n=14). The factorial analysis indicated that shell growth was primarily reduced by exposure to acidified conditions ($p<0.001$) rather than warm ($p>0.05$) with no interaction between them ($p>0.05$) (Table A2.9).
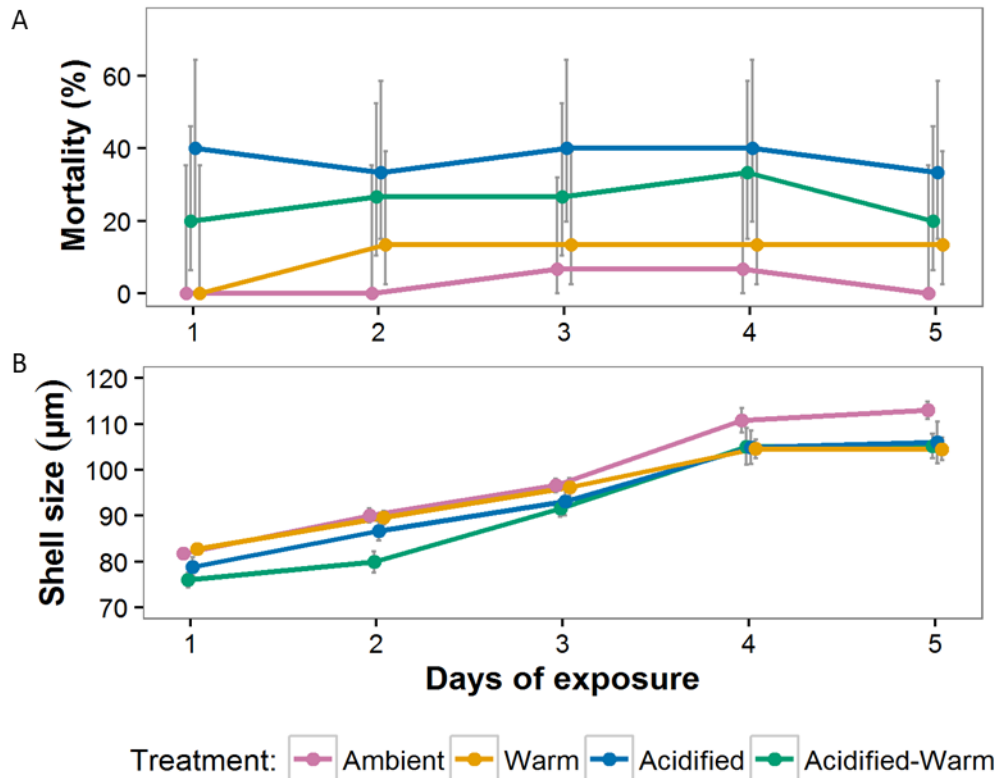
Figure 2-5. *Limacina helicina antarctica* larval mortality (A) and shell size (B) over time during incubation under ambient (pink), warm (orange), acidified (blue) and acidified-warm (green) conditions. Only larvae that were alive upon harvesting are included in the analysis of shell size. Bars denote 95% confidence intervals between treatment bottles.

2.3.3 Change in larval pteropod shell morphology

2.3.3.1 *Malformation*

Significantly more larval shell malformations were present in response to warm and acidified-warm conditions compared to ambient and acidified conditions ($p<0.0001$) (Figure 2-6a) (Table A2.7). Post-hoc analysis indicated a similar number of larvae developed malformations on exposure to acidified-warm (62.5%, n=35) and warm conditions (49.2%, n=29) ($p>0.05$). Likewise, there was no difference in the number of malformations between acidified (9.1%, n=4) and ambient conditions (3%, n=2) ($p>0.05$). Malformations occurred as a result of exposure to warm conditions ($p>0.001$) rather than acidification ($p>0.05$) with no interaction between them ($p>0.05$) (Table A2.8). The number of shell malformations was highly dependent on the amount of time that the individuals were exposed to each condition ($p<0.0001$, n=223), with larval malformation instances significantly

increasing after 3 days of exposure ($p<0.001$). There was an 82% increase in malformation occurrence within acidified-warm conditions after the first 3 days of exposure. Furthermore, the number of malformations gradually increased in warming conditions with none being present on day 1 to 92% being malformed after 5 days.

2.3.3.2 Pitting

Larvae that experienced warm, acidified and acidified-warm conditions all displayed significantly higher amounts of shell pitting than those incubated in ambient conditions (Figure 2-6b) ($p<0.001$, n=223) (Table A2.7). Larval shells with the most pitting (47%, n=28) were found in warm conditions although this was not statistically different from the pitting instances on larval shells exposed to acidified-warm (40%, n=20) or acidified (23%, n=10) conditions ($p>0.05$). Warming and acidification both increased the instances of pitting however, the combination of acidified-warm conditions does not increase pitting instances as much as would be expected from an additive or a synergistic response ($p<0.01$, n=223) (Table A2.8). The amount of time larvae were exposed to each condition did not alter the number of pitting instances ($p>0.05$, n=223).

2.3.3.3 Etching

There were significantly more cases of shell etching in acidified and acidified-warm conditions compared to ambient and warm conditions ($p<0.001$, n=223) (Figure 2-6c) (Table A2.7). The presence of etching was attributable to acidification only ($p<0.001$, n=223) with no effect of exposure to warm conditions or an interaction ($p>0.05$, n=223) (Table A2.8). Larvae incubated in ambient and warm conditions exhibited either no or few cases (2.97%, n=3) of etching respectively, with no significant difference between the conditions ($p>0.05$). Conversely, after 1 day (24 hours) of exposure to acidified and acidified-warm conditions, all larvae had shell etching present, and there was no change in the instances of etching over time ($p>0.05$, n=223).
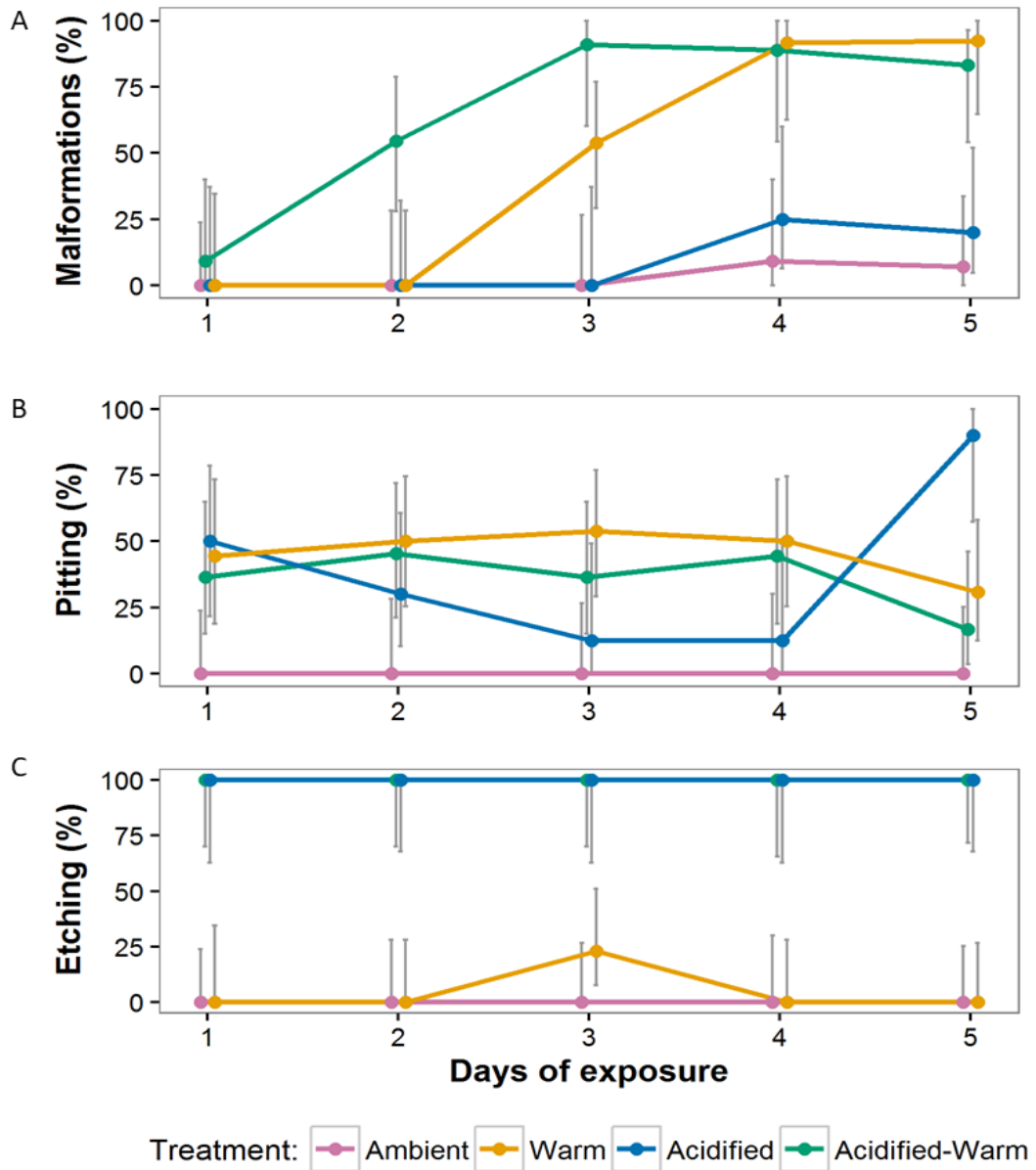
Figure 2-6. *Limacina helicina antarctica* larval shell condition showing percentage occurrence of A. Malformation, B. Pitting and C. Etching over time during incubation under ambient (pink), warm (orange), acidified (blue) and acidified-warm (green) conditions. Bars denote 95% confidence intervals between treatment bottles. Only larvae that were alive upon harvesting are included (n= 223).

2.3.4 Overall shell morphology

Those individuals that exhibited etching and malformations together without pitting most frequently occurred within acidified-warm conditions (87%, n=34), with 10% (n=4) in acidified and 3% (n=1) in warm conditions. A similar number of larvae developed malformation and pitting without etching within warm and acidified-warm conditions at 45% (n=12) and 55% (n=10) respectively. Larvae developed both shell etching and pitting without malformations within acidified-warm (66%, n=19) and acidified (35%, n=10) conditions only. All the larvae that displayed shell pitting, malformation and etching together occurred within acidified-warm conditions (Figure 2-7). The SEM images in Figure 2-4. and Figure A2.1. highlight these general combinations of shell morphology.
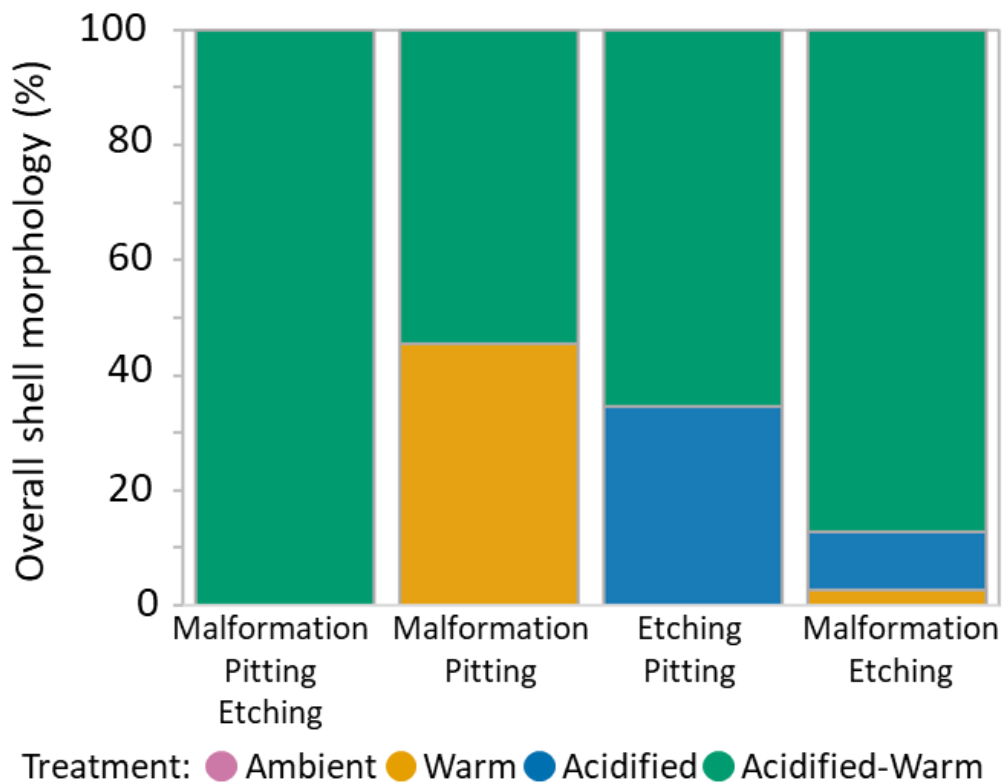
Figure 2-7. Larval *Limacina helicina antarctica* shell morphology over 5 days of exposure to ambient, warm, acidified and acidified-warm conditions. Each bar shows the treatments where a combination of different shell morphologies (pitting, malformation and etching) developed on the same single larval shell. Only larvae that were alive upon harvesting are included (n=223).

2.4 Discussion

2.4.1 Ocean acidification increases larval mortality

I demonstrated that veligers the shells of *L. helicina antarctica* are sensitive to warm, acidified and acidified-warm oceanic conditions predicted for 2100 in the Scotia Sea (IPCC 2013; McNeil and Matear, 2008), given that there was higher larval mortality on exposure to these conditions in comparison to ambient conditions. Previous studies on Arctic juvenile and adult pteropods incubated in acidified conditions (over 5 and 8 days to 1 month) found survivorship of 80-100% (Comeau *et al.,* 2009; Manno *et al.,* 2012; Lischka and Riebesell, 2012). Here I showed lower survival (down to 61%) of larval *L. helicina antarctica*. A similar survivorship was also found on incubation of larval *L. retroversa* in acidified conditions indicating increased sensitivity of early life stages (Thabet *et al.,* 2015). This fits the general trend that early stage molluscs are more vulnerable to acidification than adults (Kroeker *et al.,* 2013; Waldbusser *et al.,* 2015a). Acidification, rather than warming, appears to be the main driver of increased mortality. Furthermore, there was no synergistic or additive increase in mortality through the addition of warming to acidification. Acidification therefore poses the greatest threat to survivorship of larval *L. helicina antarctica.* However, warming has other sub-lethal influences on shell production and maintenance that may increase vulnerability in the natural environment. Interestingly, mortality did not change with exposure time suggesting either fatalities were sensitive phenotypes that would have died regardless of the exposure timeframe or because larvae were more sensitive in the first day of exposure and the more vulnerable died sooner. The short time-scale over which these effects were observed has particular relevance to the environmental experience of pteropods, which are most likely to be exposed to such conditions through contact with mesoscale bodies of water where such altered conditions prevail (Bednaršek *et al.,* 2012a). In the Southern Ocean, pH exhibits spatiotemporal variation with water masses, meltwater, season and phytoplankton productivity (Kapsenberg *et al.,* 2015; Schram *et al.,* 2015). Furthermore, the continued uptake of anthropogenic CO_2 by the surface ocean is predicted to make undersaturation events occur more frequently over the

coming decades where water bodies may become corrosive to aragonite during wintertime by 2038 and will be widespread across the Southern Ocean by 2100 (McNeil and Matear, 2008).

2.4.2 Ocean acidification and warming decreased shell size

For shell growth to occur, larvae take up bicarbonate ions from the surrounding seawater and concentrate them within the isolated extrapallial space (Harper *et al.,* 1997) (see Section 5.1.2). With acidification, the concentration of surrounding carbonate ions declines and therefore more energy is needed for calcification (See section 5.1.2.). Larval shell size increased in all treatments, even when exposed to acidified and warm conditions. Continuing shell calcification, despite exposure to acidified conditions and Ω_{ar}<1, has also be observed in Arctic *L. retroversa* (Manno *et al.,* 2012) and *L helicina helicina* (Lischka *et al.,* 2011; Comeau *et al.,* 2010a). Previously, Comeau *et al.,* (2009; 2010a) demonstrated that calcification stopped when the saturation state of aragonite was below 0.7 in Arctic *L. helicina helicina.* Larvae in the present study were incubated at Ω_{ar}= 0.62 and 0.61 in acidified and acidified-warm conditions respectively and shell growth continued. This suggests some resilience of these early life stages to short term exposure to OA (Lischka *et al.,* 2011; Comeau *et al.,* 2010b) however, shell morphology was still altered. Larval shell sizes were smaller upon exposure to acidified and acidified-warm conditions than in ambient conditions. Smaller shell size with exposure to acidification has also been observed in *L. helicina* juveniles and adults (Comeau *et al.,* 2009; Lischka *et al.,* 2011; Comeau *et al.,* 2012). I found that warming and acidification did not interact and further impact larval shell growth, indicating that warming did not mitigate the impact of OA.

Decreased shell size and delayed growth can be attributed to impeded shell deposition, dissolution exceeding calcification and reduced energetic capacity (Watson *et al.,* 2009). Since larval shell growth increased on exposure to acidified conditions initially and shell etching was observed throughout the 5-day period, it is unlikely that the mechanistic capacity of shell formation was exceeded. However, increased acid-base regulation in acidified conditions is energetically

demanding and may explain smaller shell sizes (See section 5.1.2.). Altering external conditions increases the energetic demand of maintaining homeostasis and where these costs cannot be met, complete or partial metabolic suppression may be induced as an adaptive strategy to extend survival time (Pörtner, 2008).

Juvenile *Limacina helicina antarctica* exposed to acidic conditions supressed their metabolic rate (Seibel *et al.,* 2012) while Arctic *Limacina helicina helicina* exposed to acidified warm conditions increased their metabolic rate (Lischka and Riebesell, 2016). Altering metabolic rate enables energetic allocation to essential physiological processes at the expense of other processes, including shell formation (Pörtner, 2008). Food availability has been shown to mediate the impact of ocean acidification in calcifying organisms therefore, it is possible that with food acquisition, the impacts observed within this study could decline (Seibel *et al.,* 2012; Ramajo *et al.,* 2016). *L. helicina antarctica* veligers are able to feed directly after hatching and are therefore probably not dependent on egg stores (Paranjape *et al.,* 1968; Böer *et al.,* 2005). Current estimations vary in whether *L. helicina antarctica* overwinter as larvae, when food availability is naturally low or in the summer, when it is high (Hunt *et al.,* 2008; Bednaršek *et al.,* 2012b; Wang *et al.,* 2017). Since shell growth reduced by day 3 and ceased by day 4 in all treatments I hypothesise that here, larvae may have been initially utilising endogenous reserves and that these were depleted at differing rates between treatments depending on the energetic cost of maintaining homeostasis, finally inducing a stasis in shell size.

2.4.3 Shell morphology is altered in a high CO₂ world

I show that larvae incubated under acidified-warm conditions displayed a combination of both shell etching and shell malformation. Previous studies suggested that warming may offset the negative impacts of ocean acidification (sea urchin: Brennand *et al.,* 2010, coral: McCulloch *et al.,* 2012) although others have revealed cumulative (diatom: Boyd *et al.,* 2015) and even synergistic interactions (pteropod: Lischka and Riebesell, 2012). Here I demonstrated that the impacts of warming and acidification on larval shell morphology are

separate, with warming initiating shell malformations and acidification resulting in shell etching. This lack of interaction between warming and acidification has also been observed in Arctic *L. helicina helicina* and *L. retroversa* juveniles (Lischka *et al.,* 2011; Comeau *et al.,* 2010a; Lischka and Riebesell, 2012). It suggests that warming and acidification impact different metabolic processes, thus resulting in malformation and etching respectively in pteropod larvae.

Temperature has been shown to have a significant effect on biomineralisation processes and growth across a number of calcifying species (Gazeau *et al.,* 2013). Increased temperature can boost shell growth within an organism's thermal tolerance window and aid acclimatisation to warming (Somero, 2010), but shell microstructure can be altered when this optimum is exceeded (Mackenzie *et al.,* 2014), resulting in shell malformations and pitting, as observed in the current study (Figure 2-4). Regions of strain on a shell, such as areas of attachment, are particularly susceptible to disruption which could explain the banding of malformations occurring parallel to the aperture observed in Section 2.3.3.1. Since pitting and malformation occurred in warm and acidified-warm conditions this suggests that pitting is a result of malformation, perhaps as points of failure where shells surpass their physical limits and causing deformation. Acidification was also shown to cause shell pitting, which is consistent with prior studies (Auzoux-Bordenave *et al.,* 2010; Bednaršek *et al.,* 2012b). Shell pitting can therefore occur as a result of two different processes and could signify exposure to acidification, warming or both. Overall this demonstrates the structural fragility and loss of integrity of larval shells in high CO_2 conditions.

In contrast to warming, the ability of larvae to counteract acidification depends on a combination of the energetic capability to repair shell damage internally (Lischka *et al.,* 2011; Waldbusser *et al.,* 2015b: 2013), the effectiveness and intactness of the protective organic matrix (periostracum) surrounding the shell (Peck *et al.,* 2016) and the ability to regulate ion and acid-base balance to maintain pH at the site of calcification (Thorp and Covich, 2009). On exposure of *L. helicina antarctica* larvae to acidified conditions, shell etching occurred in 100% of individuals from day 1, suggesting a failure in one of these mechanisms.

This percentage is higher than previously observed in later life stages (Bednaršek *et al.,*2012b: 2014; Siebel *et al.,* 2012), indicating *L. helicina antarctica* larvae may be particularly sensitive to shell etching although, direct comparison is difficult due to variation in species, origin and methodology (Gazeau *et al.,* 2013). Many early life history stages of gastropods lack specialised ion-regulatory mechanisms required for acid-base maintenance (Ries, 2011). However, since shell size continued to increase, and etching occurred on the upper shell surface, it is unlikely that this was the main cause of shell dissolution. Numerous early larval stages of benthic gastropods secrete amorphous calcium carbonate, which is more prone to dissolution, before a transition to aragonite (Weiss *et al.*, 2002; Melzner *et al.*, 2011; Duquette *et al.,* 2017). If this were true for pteropods it would explain why the protoconches of Arctic *Limacina helicina helicina,* that represent larval shells, are particularly susceptible to shell dissolution compared to outer whorls formed in later life stages (Peck *et al.,* 2016). Regardless of the shell composition, the periostracum may have been breached, ineffective or absent for etching to have occurred (Peck *et al.,* 2016), although the exact role of a pteropod's periostracum as protection against ocean acidification requires further investigation (Ries, 2011; Bednaršek *et al.,* 2016). Since etching did not occur in patterns indicative of abrasion or cracking and there was no mechanism for this to occur, it is unlikely that the periostracum was breached. Furthermore, a mechanism allowing isolation of the extrapallial space from the surrounding undersaturated seawater is needed for calcification to proceed, suggesting a periostracum is present. I suggest that the periostracum is not as developed in the newly hatched larvae as in later life stages of pteropods and is therefore inadequate in protecting larval shells from acidification.

2.4.4 Concluding remarks and summary

The capacity of pteropods to maintain a viable population distribution and abundance in the Southern Ocean depends on their capability to recruit successfully. I show OA and warming do not act synergistically, with the nature of the impacts on viability being recognisably different between the two. Survivorship was mainly influenced by the level of acidification, while the effects

of warming were more likely to be sub-lethal and did not increase mortality levels when combined with acidification. I demonstrate that the short-term exposures that are likely to be experienced in the natural environment of larval *Limacina helicina antarctica* will have a major impact on survivorship and consequently, population stability in these regions.

3 Southern Ocean pteropod life history and population dynamics

3.1 Introduction

An essential part of predicting the impact of environmental change on pteropods (see Section 1.3.) is knowing their life history and population dynamics (Manno *et al.,* 2017). The life history of an individual includes their reproductive development and behaviour, life span, growth and post-reproductive behaviour. The population dynamics of a species describes the size, structure and age composition of a defined population (Begon *et al.,* 2006).

Currently, our knowledge of pteropod population dynamics and life history phenology remains uncertain; particularly within the Southern Ocean due to seasonal inaccessibility. In the Southern Ocean, acidification and warming are predicted to be seasonally and spatially heterogeneous (McNeil and Matear, 2008; Gutt *et al.,* 2015; Vaughan *et al.,* 2003). For example, the upper 1,000 m north of the Antarctic Circumpolar Current are warming rapidly (0.1°–0.2°C per decade) but further south of this region is not warming or is slightly cooling (Sallée *et al.,* 2018). The tolerance and impact of oceanic change on pteropods are thought to vary in severity and outcome, depending on the life stage affected. For example, early life history stages are suspected to be especially vulnerable to environmental change in comparison to adult stages (Byrne, 2011; Kroeker *et al.,* 2013; Pechenik, 1987) although, this is not ubiquitous across all taxa (Foo and Byrne, 2017). Therefore, it is relevant to understand which life stage of each pteropod species might coincide with acidification and warming since this may impact recruitment and long-term population stability (Manno *et al.,* 2017; Gaylord *et al.,* 2015).

3.1.1 Southern Ocean pteropod life cycle and population dynamics

Currently there is considerable variation in estimates of polar pteropod development period, growth rates, longevity, spawning season(s) and seasonal population size structures (Table 3.1). This reduces the certainty of predictions for the response of pteropods to future environmental change. Such wide-ranging estimations may arise from different sampling equipment (McGowan and Vernie, 1966), protocols (Cermeño *et al.,* 2014) and scales (Wiens, 1989)

between studies but also, they could be real biological signals. For example, different mesh sizes of sampling nets select for particular size cohorts, leading to exaggerated estimations of selected population size frequencies (Hunt *et al.,* 2008). Furthermore, each pteropod species spans several geographical ecoregions, therefore regional differentiation of life cycles in response to ambient environmental conditions is likely. For example, pteropods may time specific life stages which require higher energetic budgets, such as the high growth veliger phase, to local phytoplankton blooms to meet a greater energetic demand (Maas *et al.,* 2011). Seasonal acclimatization and regional adaptation could lead to differences in the environmental tolerances of a pteropod population based on past experiences (Bednaršek *et al*., 2017). Variation may also occur genetically between taxonomic sub-units since *Limacina helicina* comprises of numerous morphotypes (not classed as separate species) both in the Arctic Ocean (*acuta*, *helicina*, and *pacifica*) and Southern Ocean (*antarctica* and *rangi*). Several *L. retroversa* formea are found in the Arctic (*balea* and *retroversa*) and in the Southern Ocean (*australis*) (Hunt *et al.,* 2010; Jennings *et al.,* 2010).

Table 3.1. Summary of current literature on the life cycle of on thecosome pteropods (excluding tropical and Mediterranean studies). The species (Spp.) abbreviations are LR: *Limacina retroversa,* LHA: *Limacina helicina antarctica,* LHH: *Limacina helicina helicina,* CP: *Clio pyramidata.* Size is shell width except * where it is the largest whorl diameter. Spawning behaviour is the type of spawning (Discrete, Protracted or Continuous) and the peak seasons this occurs in (Sum: Summer, Aut: Autumn, Spr: Spring). The bloom timing is the timing of the phytoplankton bloom in that region. References (Ref) are given below the table. Ind is individuals. Kongsf'is Kongsfjorden ** were not investigated within the study. Adapted from Wang *et al.,* 2017.

Spp.	Spawning behaviour	Bloom timing	Longevity (years)	Generations per year	Size range (mm)	Region	Sample size (ind, sites)	Ref
LHH	Discrete: Sum- Aut	Spr	1	1-2	5	Kongsf'	(276, 6)	1
LHH	Protracted: Sum-Win	Sum	1.5-2	1	0.8-3.7	Canada Basin	(ND, 42)	2
LHH	**	Sum	~1 (330 days)	1	1.5-3.5	North Pacific	(ND, ND)	3
LHH	Continuous: Spr- Aut	Spr	2	2	5.5	North-East Pacific	(ND, 35)	4
LHA	Discrete: Sum	Spr	>3	1	~9	Scotia Sea	(ND, 56)	5
LHA	Protracted: Sum	Spr	1	1	<10	Antarctic Peninsula	(ND, ND)	6
LR	Continuous: Sum	Spr/Sum	1	**	0.96	English Channel	(ND, ND)	7
LR	Protracted: Sum	Spr	1	**	>1.8*	Gulf of Maine	(ND, ND)	8
LR	Discrete: Spr + Aut	Spr	1	2	0.99-3.25	Southern Argentine Sea	(134, 7)	9
LR	Discrete: Spr + Aut	Spr	0.5	2	0.58-2.5	Gulf of Maine	(ND, ND)	10
CP	**	Sum	~1 (310 days)	1	5.5-12.8	North Pacific	(ND, ND)	5
CP	Continuous: Spr- Aut	Spr	1	2	**	Southeast of Bermuda	(ND, ND)	11

References: 1. Gannefors *et al*. (2005). 2. Kobayashi (1974). 3. Fabry (1989). 4. Wang *et al*. (2017). 5. Bednaršek *et al*. (2012a). 6. Hunt *et al*. (2008). 7. Lebour (1932). 8. Hsiao (1939). 9. Dadon and Cidre (1992). 10. Thabet *et al.* (2015). 11. Van der Spoel (1973).

3.1.2 Life stage identification

Most species of Limacinidae are thought to share similar reproductive biology, being protandric hermaphrodites that first function as males and subsequently mature into females (Lalli and Wells, 1978; Lalli and Gilmer, 1989). All *Limacina* spp observed develop through a trochophore stage into planktonic veligers (Lebour, 1932; Paranjape, 1968; Bandel and Hemleben, 1995). Veliger locomotion is initially via ciliated velums (Figure 3-174a) which are eventually replaced with the characteristic wings when they mature into females (Figure 3-1b) (Thabet *et al.,* 2015; Lalli and Gilmer, 1989).
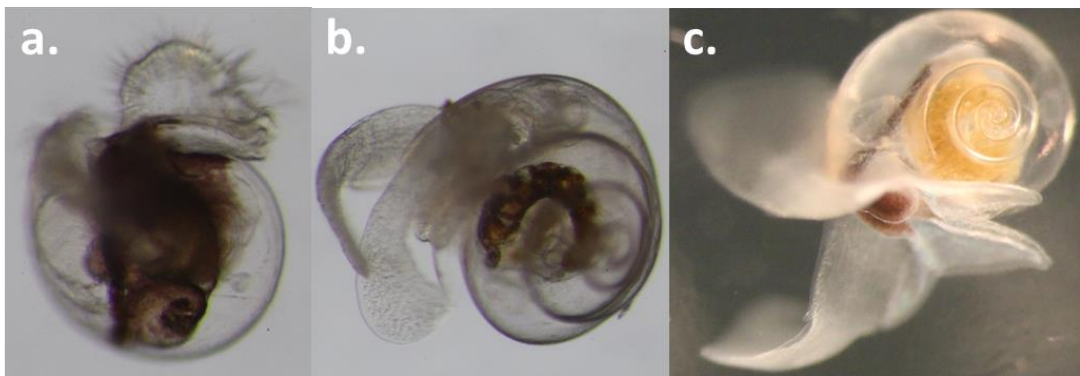
Figure 3-1. The three major life stages of Limacinidae species where individuals develop through a (**a.**) trochophore stage, (**b.**) a male stage and (**c.**) a female stage.

As the rate of shell extension is hypothesised to be linear throughout Limacinidae life cycles (Lalli and Gilmer, 1989; Lalli and Wells, 1978), maturity and gender are thought to relate to size (Lalli and Gilmer, 1989; Lalli and Wells, 1978; Kobayashi, 1974; Hsiao, 1939). Developmental stages can be identified based on shell size with the shell width of *L. helicina* veligers, juveniles and adults being <0.3 mm, 0.3-4 mm and >4 mm, respectively, and the shell spire height of *L. retroversa* veligers, juveniles and adults being <0.3 mm, 0.3-1 mm and 1 mm (Lalli and Gilmer, 1989; Lalli and Wells, 1978).

While these estimates of developmental stage from shell sizes are a good baseline, these assume that the growth of *Limacina* is constant and that maturity is size dependent (Lalli and Gilmer, 1989; Kobayashi, 1974). However, growth rate is likely to be influenced by environmental conditions and time of spawning,

with poor nutrition and late spawning resulting in smaller mature individuals (Hunt *et al.,* 2008; Dadon and de Cidre, 1992). For example, the summer generation of *L. retroversa australis* matured at a shell spire height of 1.2 mm after an abundance of food, while the spring generation matured at 0.66 mm, when food was scarcer, with all under 0.66 mm being immature (Dadon and de Cidre, 1992). Currently, there is one study that investigates the growth of *L. helicina antarctica* (Bednaršek *et al.,* 2012b) and no studies for *L. retroversa australis* in the Southern Ocean.

3.1.3 Sediment traps as tools for pteropod population studies

Sediment traps are commonly used to estimate year-round vertical fluxes of organic matter and are usually deployed below the euphotic zone for prolonged time-periods. Swimmers, which are organisms deemed to be alive upon entering the sediment trap, are often discarded during processing (Chiarini *et al.,* 2013). However, swimmers represent the local population present within the water column and so could offer an insight into localised, year-round and inter-annual population dynamics (Makabe *et al.,* 2016). This is particularly valuable in remote and difficult to access areas such as the Southern Ocean.

Currently, very few winter zooplankton samples exist in the Southern Ocean due to its remoteness, inaccessibility and hostility (Bednaršek *et al.,* 2012c), however, moored sediment traps continuously sample a fixed geographical location in user-defined intervals. Therefore, the swimmers collected in the winter by sediment traps could assist in filling these winter absences in the zooplankton records. Since there are few records of pteropods during the winter months, there is a gap in our understanding of pteropod life history and population dynamics.

Spring- autumn net samples of pteropods in the Southern Ocean show a high degree of spatiotemporal variability both in abundance and distribution (Hunt *et al.,* 2008; Ward *et al.,* 2004). This is likely due to the intense seasonality of phytoplankton blooms and the oceanographical zonation of environmental conditions (Deppeler and Davidson, 2017). Consequently, localised sampling over

prolonged time periods is necessary to parameterise regional pteropod population dynamics.

The entrapment of pteropod swimmers by sediment traps depends on their behaviour, swimming activity and abundance in the surrounding water column (Makabe *et al.,* 2016; Harbison and Gilmer, 1996; Peterson and Dam, 1990). These organisms are entrapped due to attraction to the organic matter inside or interference of swimming from turbulence around the trap (Buesseler *et al,* 2007). Sediment traps are not suitable for sampling all zooplankton swimmers since the capture of individuals relies on them actively swimming at that depth and not being able to escape once in the trap. Pteropods are widely distributed throughout the water column (see Section 4.4.4.) and their escape mechanism involves rapidly sinking (rather than swimming away), therefore, they are commonly captured as swimmers (Makabe *et al.,* 2016). Pteropod swimmer abundances have been shown to correlate well with samples from nets indicating that sediment trap samples are representative of the biological community (Makabe *et al.,* 2016; Almogi-labin *et al.,* 1988; Wells, 1976).

3.1.4 Sampling area

The Southern Ocean is the largest high nutrient, low chlorophyll area in the global ocean, where productivity is limited by the availability of iron which is an essential component of phytoplankton photosynthesis (Martin *et al.,* 1990; Boyd *et al.,* 2000). However, some regions are enriched in iron from nearby landmasses, shelf-sediment interactions, glacial melt and vertical mixing of deeper waters causing hotspots of intense productivity (Blain *et al.,* 2001; Robinson *et al.,* 2016). The site P3 (Figure 3.2a) is situated within the South Georgia Basin, bounded by the Polar Front to the north and the Southern Antarctic Circumpolar Current Front to the south and east (Orsi *et al.,* 1995; Meredith *et al.,* 2003) (See Figure 4.1 for an overview of frontal positions).
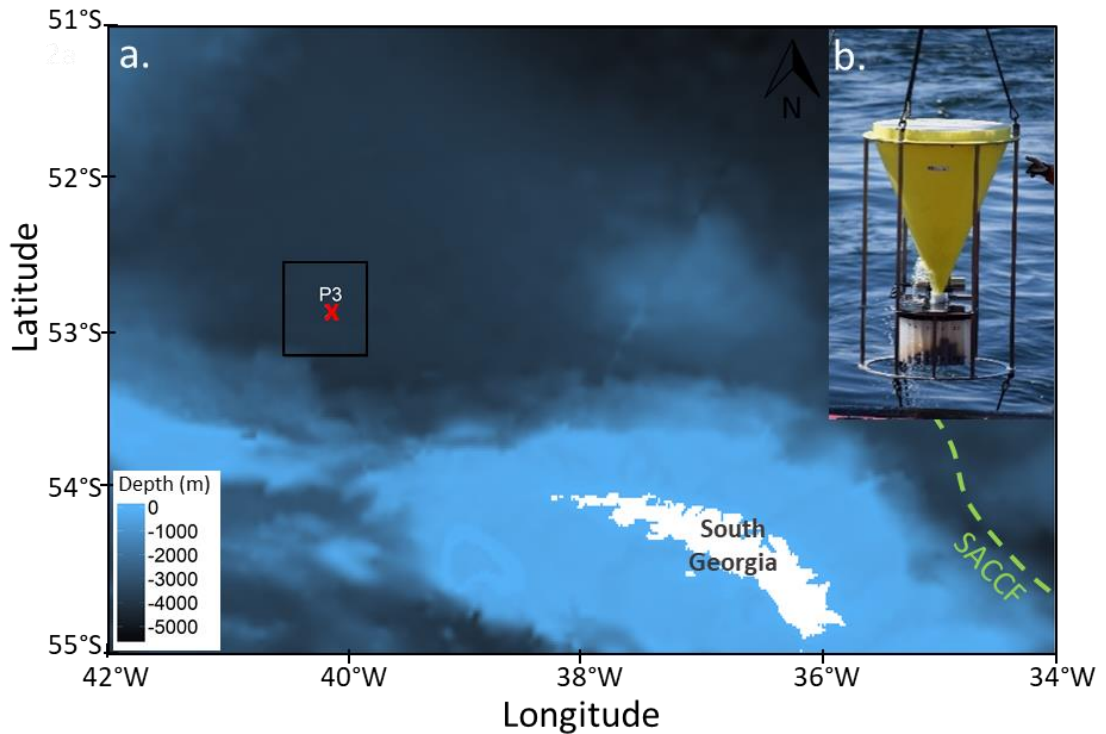
Figure 3-2. Bathymetric map indicating the location of P3 (52°48.7"S, 40°06.7"W) sampling site (a) and an image of the sediment trap as it was recovered in November 2015 (b). The blue shading indicates the seafloor depth, while the white represents land. The dashed line (━ ━) indicates the position of the Southern Antarctic Circumpolar Current Front (SACCF) (Orsi *et al.,* 1995). The rectangle around P3 shows the area over which MODIS 4 km resolution monthly temperature and chlorophyll satellite data was averaged.

Since P3 is oceanographically downstream of South Georgia, it is naturally iron fertilised. High iron availability fuels a hotspot of productivity, with extensive phytoplankton blooms until late summer (Borrione and Schlitzer, 2013). These phytoplankton blooms support high abundances of organisms with zooplankton biomass being ~6x greater than in the rest of the Southern Ocean (Ward *et al.,* 1995). The region to the north of South Georgia also has the largest seasonal cycle of surface ocean pCO$_2$ in the open Southern Ocean (Jones *et al.,* 2012; 2015) as well as enhanced carbon export to the deep ocean (Manno *et al.,* 2015; Blain *et al.,* 2007). However, the region to the north of South Georgia is experiencing one of the fastest rates of environmental change in the Southern Ocean (Henson *et al.,* 2017). Around South Georgia surface temperatures have increased between 1925 and 2006 by ~2.3°C in winter and by ~0.9°C in summer (Whitehouse *et al.,* 2006; 2008). Furthermore, wintertime (McNeil and Matear, 2008) and summertime

(Bjork *et al.,* 2014) aragonite undersaturation is predicted to occur by 2030 south of the Polar Front. Since pteropods are extremely abundant in these bloom areas around South Georgia (Hunt *et al.,* 2008; Ward *et al.,* 1995; Bednaršek *et al.,* 2012a), it makes a perfect natural laboratory for studying their response to this oceanic change. An understanding of pteropod population dynamics in areas where they are keystone components of ecosystem (Lalli & Gilmar 1989; Hunt *et al.,* 2008; Hunt *et al.,* 2010; Manno *et al.,* 2017), such as in the Scotia Sea, is vital in order to discern any responses or vulnerabilities to localised events such as warming or undersaturation. However, caution should also be taken in generalising the results from these small-scale studies over wider areas.

3.1.5 Chapter Aims

Chapter 3 aims to elucidate the population dynamics and life history of pteropods from samples collected using a sediment trap (400 m) moored at site P3 (Scotia Sea) between December 2014- November 2015. I aim to adopt a local scale sampling regime which uses the same sampling equipment and protocols to reduce possible bias. Four specific aspects will be addressed:

1. Species presence and abundance in relation to environmental conditions
2. Spawning and growth patterns of *L. helicina* and *L. retroversa*
3. Cohort and life stage dynamics of *L. helicina* and *L. retroversa*.
4. Longevity of *L. helicina* and *L. retroversa*

3.2 Materials and Methods

3.2.1 Sample collection

A McLane PARFLUX sediment trap (0.5 m^2 capture area, McLane Labs, Falmouth, MA, USA) was deployed at 400 m depth (sea floor depth of 3787 m) on a bottom-tethered mooring line for 350 days (12.12.2014- 28.11.2015) at site P3 in the Northern Scotia Sea (52°48.7"S, 40°06.7"W) (Figure 3.2b). An overview schematic of the entire mooring is given in Figure A3.1. P3 is a sustained observation site within the SCOOBIES deep ocean observatory project (https://www.bas.ac.uk/project/scoobies). The sediment trap was equipped with 21 x 500 ml collection cups filled with 4% formaldehyde buffered with excess sodium tetraborate (borax). This preservative reduces physical damage by swimmers, arrests biological degradation and stops pteropod shell dissolution. Cups rotated on a 14-17 (spring and summer) and 30-31 (autumn and winter) day schedule with 15 cups being utilised within the sampling period. Sampling dates and lengths are given in Figure 3.3.
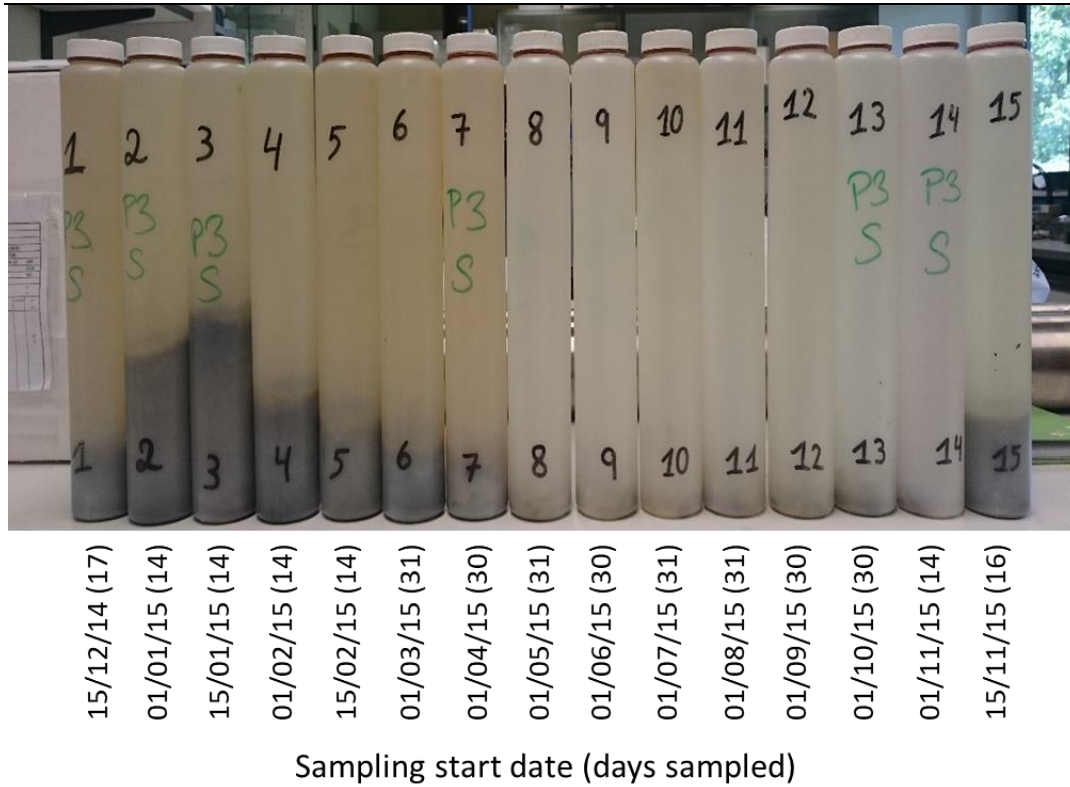
Figure 3-3. Sample bottles (500 ml) collected from a sediment trap deployed at 400 m depth for a year within the Scotia Sea (Southern Ocean), before processing. Dates below the bottles are the sampling start dates with the numbers in brackets being the number of days that each bottle was sampling.

3.2.2 Trapping efficiency

Sediment trap efficiency can be reduced due to hydrodynamic bias at high current speeds, errors from tilting and variations in depth (Gardner *et al.,* 1997; Gust *et al.,* 1994: 1992; Baker *et al.,* 1988). However, depth was 400 m ± 50 m indicating no serious impact of the variation in depth on zooplankton entrapment. A current meter 1 m underneath the sediment trap recorded mean current speeds of 0.05 (range: 0- 0.22) cm/s (SeaGuard TD262a). Current speed measurements were taken adjacent to the sediment trap every 15 minutes and averaged over a 1 minute interval. Current speeds over the sampling period were below the level where trapping efficiency is considered to decrease (Figure 3.4), and where considerable lateral advection might occur (10-12 cm/s) (Baker *et al.,* 1988; Whitehouse *et al.,* 2012). Therefore, hydrodynamic bias was negligible. On retrieval samples had a pH of 8.1 (total scale; Metrohm 826 pH electrode) and pteropod shells were primarily free of areas of frosting which are indicative of dissolution (Peck *et al.,* 2018).
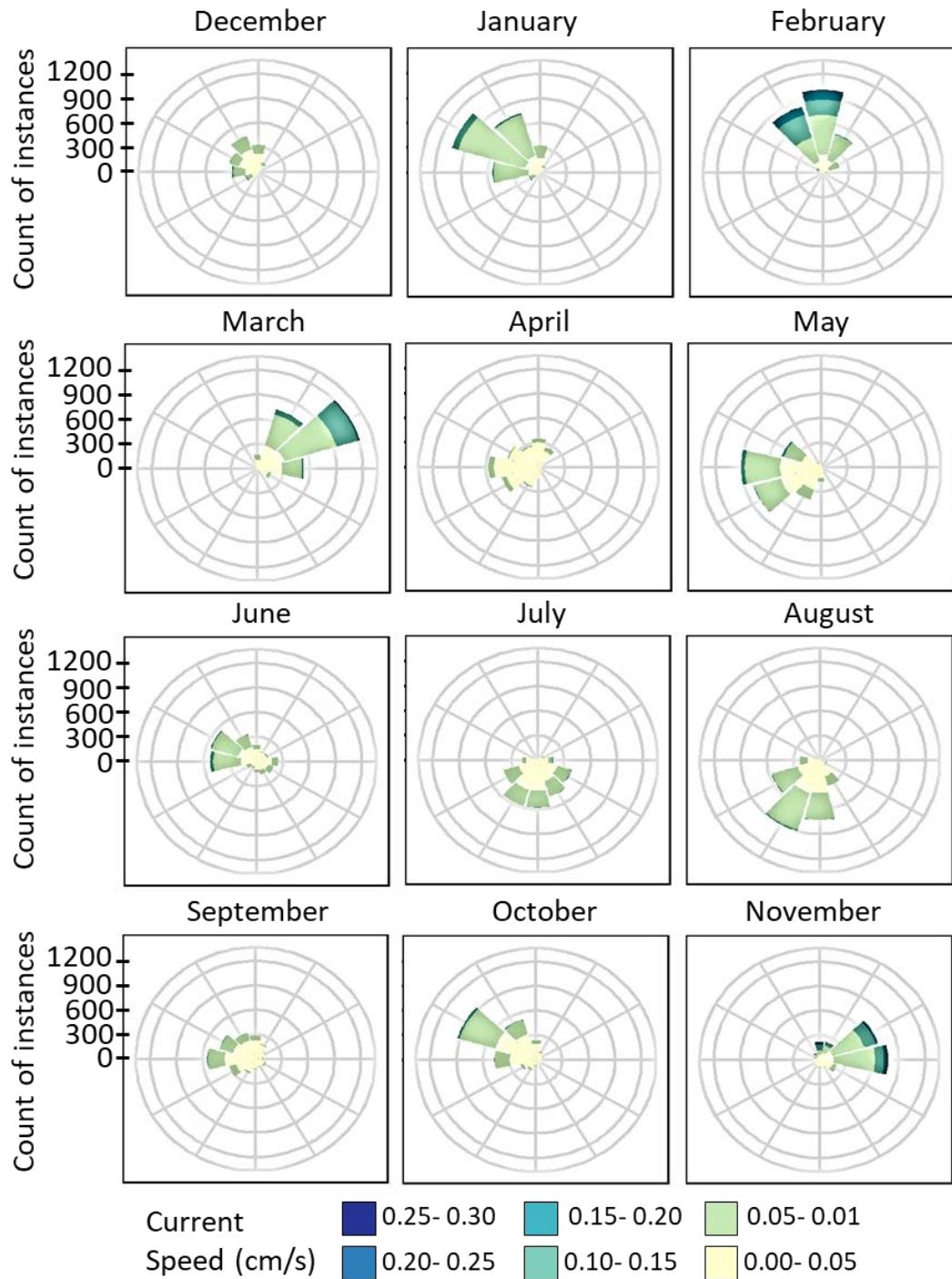
Figure 3-4. Monthly current speeds (cm/s) and direction recorded for a year (December 2014- November 2015) at 400 m depth at site P3 (Southern Ocean). Current speed measurements were taken each second for 1 minute every 15 minutes and averaged over 1 minute intervals.

3.2.3 Sample processing

Sediment trap samples are rarely analysed in full, being too time costly, however not splitting the samples considerably reduces bias and increases the accuracy of pteropod abundance estimates. A range of techniques exists to split sediment trap samples that often rely on the sample being mixed into a homogeneous suspension (Chiarini *et al.,* 2013). Since pteropods have a high sinking rate samples taken at the end of the splitting process are likely to include more individuals. Furthermore, Gerhardt *et al.* (2000) noted the fragility of pteropod shells and their susceptibility to damage during washing and sieving of samples. To avoid processing issues, no splitting of samples was undertaken. Larger organisms were removed first by handpicking from a white sorting tray. After this, samples were inspected under a dissection microscope (Olympus SZX16) using a Doncaster plankton sorting tray (Figure 3.5.). Each pteropod was removed via a stretched glass Pasteur pipette. Pteropods were then placed dorsoventrally and photographed under a light microscope (Olympus SZX16 fitted with a Canon EOS 60D).
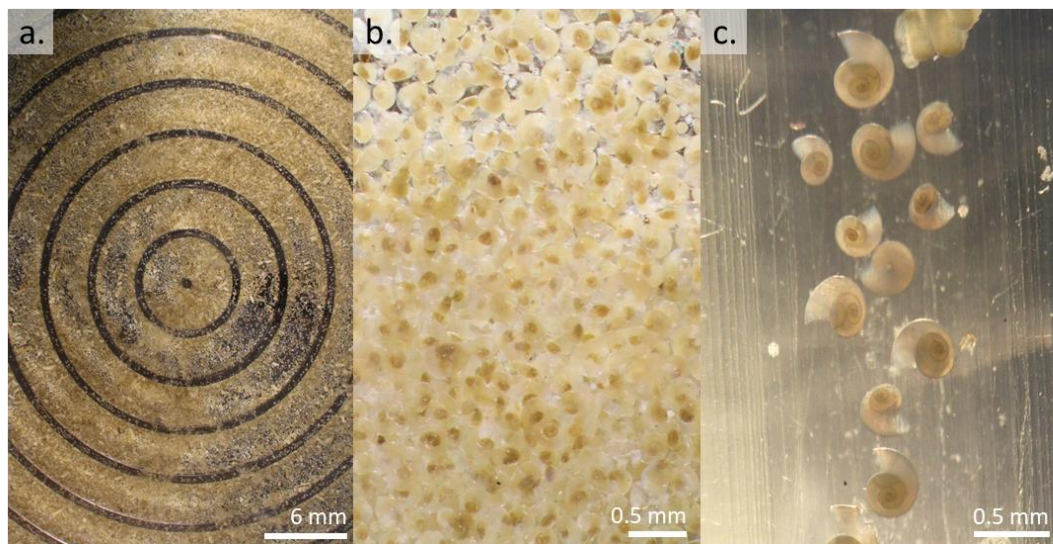
Figure 3-5. Overview of the processing of sediment trap samples collected within the Scotia Sea (Southern Ocean) in order to separate out pteropods for further analysis. Firstly, the sample was sorted through using a Doncaster plankton sorting tray (**a.**) to separate every pteropod from the main sample (**b.**). Pteropods were then arranged dorsoventrally before being imaged (**c.**).

3.2.4 Species identification and shell morphometrics

Extant Euthecosome pteropod species are well described, so identification of unbroken specimens from the sediment trap was to species and formae level using Lalli and Gilmer, (1989), Van der Spoel, (1973) and MSIP (2017). Within the Southern Ocean two formae of *L. helicina antarctica* (f. *antarctica* and f. rangi) exist where *L. helicina antarctica antarctica* attains twice the maximum shell width (6.5 mm) of *L. helicina antarctica rangi* (3.5 mm) (Van der Spoel and Dadon, 1999). Hunt *et al.* (2008) demonstrated that each forma has a distinct geographic range with f. rangi predominantly occurring to the north of the Polar Front and f. *antarctica* to the south. Furthermore, f. rangi have a taller spire within the adult stages than in f. antarctica. Since the Polar Front was north of P3 (indicated by the MODIS 4 km resolution, monthly satellite temperature data) and individuals around 3.5 mm wide all had depressed spires, it is unlikely that those recorded were *L. helicina antarctica rangi*. Therefore, *L. helicina antarctica anatarctica* will be the forma referred to by *L. helicina antarctica* hereafter in this chapter.

After species identification, shell diameter, shell width (otherwise called the line of aperture or aperture length), spire height and the number of whorls were measured using ImageJ (Schneider *et al.,* 2012) (Figure 3.6a- e). These shell morphometrics are the most common measurements used to characterise linear shell extension (Chiu *et al.,* 2002; Wilber and Owen, 1964). On *L. helicina* and *Limacina* spp veligers the shell width was determined by passing through both the growing edge and the protoconch (the embryonic shell), while the shell diameter was measured almost perpendicular to the shell width, going across the widest part of the shell (Figure 3.6a). On *L. retroversa* the spire height passed from the protoconch and down the axis of coiling to the shell edge, while the shell width was perpendicular to this, measuring from the growing edge over the widest shell portion (Figure 3.6b). On *C. pyramidata* the shell width started from the protoconch and ended in the centre of the aperture whereas the shell diameter was perpendicular to the shell width and orientated across the widest part of the growing edge (Figure 3.6c). The number of whorls was only recorded

for *Limacina* species, as a complete 360° revolution of shell growth, rounded to the nearest quarter (Figure 3.6d-e). The shell width, shell diameter (not measured on *L. retroversa*) and spire height (*L. retroversa* only) were all measured since the apertures of pteropods are commonly (and sometimes invisibly) damaged. Creating a ratio between the shell width and shell diameter for each pteropod group reflects the true shell size more accurately than one parameter alone (Van der Spoel, 1973). Whether a pteropod shell was damaged or not was also recorded. Pteropods were generally in good condition, however, some fragments were found. These were only counted as an individual if a protoconch was present, since there is only one protoconch per pteropod. Those that were damaged were excluded from shell size analyses.
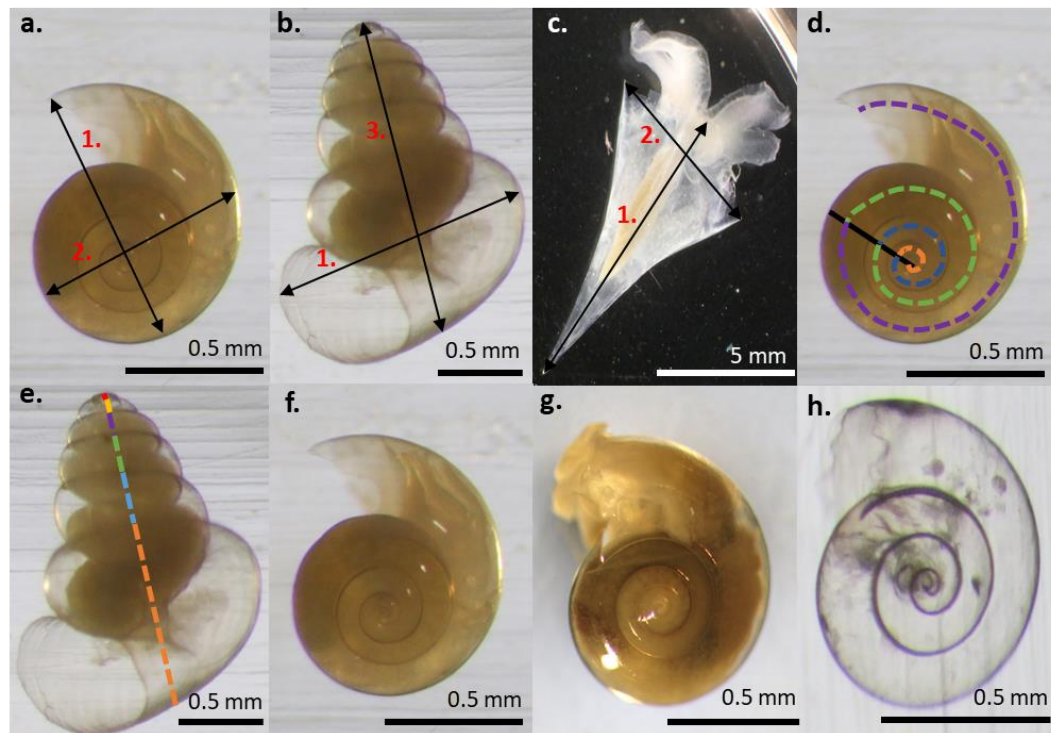
Figure 3-6. Shell morphometrics used to define pteropod cohorts of **a)** *L. helicina* **b)**, *L. retroversa* and **c)** *C. pyramidata* where **1.** is the shell width (otherwise known as the line of aperture), **2.** the shell diameter and **3.** the spire height (for *L. retroversa* only). Insets **d.** and **e.** indicate how the number of whorls were measured on *L. helicina* and *L. retroversa,* respectively, where each colour corresponds to one whorl. Pteropod shell condition was also classified as either alive **(f)**, dead **(g)** or predated **(h)** upon preservation.

From the values obtained for each linear measurement the following ratios were calculated: 1. (shell diameter or spire height)/shell width, 2. Number of whorls/(shell diameter or spire height) and 3. Number of whorls/ shell width. Furthermore, the area of each shell was estimated using the shell diameter/spire height and shell width, assuming *L. helicina* were roughly elliptical (*Equation. 1.1*) and *L. retroversa* and *C. pyramidata* were triangular (*Equation. 1.2*).

$$A = \frac{1}{4}\pi a d \qquad \qquad \text{Equation. 1.1}$$

$$A = \frac{1}{2} a d \qquad \qquad \text{Equation. 1.2}$$

Where *a* is the shell width and *d* is the shell diameter/spire height. A Principal Component Analysis (PCA) was run using 'prcomp{base}' to highlight which shell morphometric variables represented the most variation over the sampling period.

3.2.5 Classification of shell condition

Pteropod condition was classed into three categories (Figure 3.6f- h) being 1. Un-degraded soft body with a completely, transparent shell, 2. Signs of degradation of the soft body and/or the shell is uniformly frosted or 3. The soft body is missing but the shell is intact and completely transparent. All pteropods fitting category 1 were assumed to be alive upon entering the trap (swimmers) and so representative of the living cohort present within the area at that time. Those in category 2 were most likely dead when entering the trap (passive sinkers) with uniform shell frosting occurring due to internal dissolution (Peck *et al.,* 2016b). This frosting pattern is different from that caused by contact with external undersaturated conditions, since here the frosting would be localised to breaches within the periostracum (Peck *et al.,* 2016b) (see Section 2.4.1). Pteropod shells can become uniformly frosted and degraded with poor health of the animals since the individuals are unable to maintain acid-base homeostasis, therefore, some individuals may still have been alive in category 2 (Peck *et al.,* 2016b). Consequently, category 1 represented individuals that were significantly healthy enough to maintain their shell condition. Pteropods in category 3 are

most likely to have been predated since the shells bear no signs of frosting internally from contact with the degrading body. Furthermore, the aperture of these empty shells was often damaged perhaps due to gymnosomes attaching here while extracting the pteropod body from the inside of the shell. Gymnosomes are specialised predators on thecosome pteropods and have modified mouth parts adapted for the extraction of the soft body inside by grasping the aperture and thrusting their mouth parts within (Lalli and Gilmer, 1989).

3.2.6 Cohort and group identification

Following Lalli and Wells (1978), *L. helicina* with a shell width of <0.3 mm were classified as veligers, of 0.3-4 mm as juveniles and of >4 mm as adults. Similarly, *L. retroversa* individuals with a spire height of <0.3 mm, 0.3-1 mm and 1 mm were classified as veligers, juveniles and adults, respectively (Lalli and Gilmer, 1989). While shell morphometric measurements are a good indicator of shell growth rates it is difficult to link these to age since shell accretion may vary with season, diurnal rhythms or periods of inactivity (Linsley and Javidpour, 1980). Furthermore, size classes are based on Arctic *Limacina,* where ambient conditions are likely to be different to those in the Southern Ocean (Kobayashi, 1974). However, every pteropod cohort (individuals with the same period of birth) from the same region should experience similar biochemical conditions and so will grow at similar rates thus enabling identification of cohorts in the same life stage.

Shell width measurements (see Section 3.2.4.) were fed into size-frequency histograms constructed using the R package 'mixdist{plot}' (Macdonald and Du, 2012) to define pteropod monthly cohorts. Each pteropod cohort was considered to be of a similar age-class, being represented by discrete modal peaks on a size-frequency histogram. These size-frequency histograms were used to constrain Mixture models created using 'mixdist{mix}' (Macdonald and Du, 2012). 'mix{mixdist}' uses Newton-type and expectation-maximisation (EM) algorithms (iterative methods to find the maximum likelihood of parameters) to separate

the components (i.e. the cohorts) from a finite Mixture distribution (i.e. the overall shell morphometric measurements). Each component can be modelled with a variety of Mixture distributions and is constrained by user-defined parameters estimates (i.e. the number of components and the mean and standard deviation of each of these). By defining constraints, the risk of overparameterization is reduced. For each month, Mixture models were fitted using normal, lognormal, gamma and Weibull distributions to one, two and three components extracted based on peaks observed on the size-frequency histograms. The best-fitting models from the Mixture distributions and component number combinations were selected based on the chi-square goodness of fit and visual inspection of histograms by comparing the modelled modal peaks with the pteropod shell width measurements.

3.2.7 Shell growth, spawning behaviour and longevity

Cohorts identified using the Mixture analysis were tracked throughout the year, from recruitment to when they no longer appear within the population (due to die-off or migration out of the sample area). Tracking cohorts enables identification of pteropod shell width variation. To estimate the mean increase in shell width per day (the growth rate) of each cohort, the difference in mean shell width between two dates of observation was divided by the intervening time (*Equation 1.3*).

$$r = \frac{S_b - S_a}{\Delta t} \qquad \textit{Equation 1.3}$$

Where S is the mean shell width of each cohort (given by the modal size from the Mixture analysis), S_a is the shell width when a cohort was first recorded and S_b, when it was last recorded. t is the number of days between these observations. This equation assumes that sampling was representative of a single population with little influence of immigration and emigration and that growth was linear.

A discrete spawning event can be identified as the sudden increase in abundance of veligers (immature pteropod stages that have yet to grow wings). Prior studies have defined veligers of *L. helicina* and *L. retroversa* as having a shell width and spire height of <0.3 mm (Akiha *et al.,* 2017; Lalli and Gilmer, 1989; Lalli and

Wells, 1978). Veligers of *Limacina helicina* and *Limacina retroversa* are difficult to identify to species level since they only have a single shell whorl therefore, individuals with a shell width below 0.3 mm were classed as *Limacina* species. We therefore assumed modal peaks below <0.3 mm to signify a hatching event of *Limacina* individuals from egg masses. Previous studies on *Limacina* species have indicated that hatching occurs between 1- 10 days after spawning (Akiha *et al.*, 2017; Howes *et al.*, 2014; Lalli and Wells, 1978; Paranjape, 1968; Lebour, 1932) with rapid growth and development of parapodia within 30 days (Akiha *et al.*, 2017; Howes *et al.*, 2014; Paranjape, 1968). The factors which control the time of emergence of *Limacina* from egg sacs needs further investigation, however, it is likely that the variance in emergence times is predominantly controlled by temperature (Howes *et al.*, 2014). Rapid growth after emergence means spawning events can be identified to within 10 days of occurrence. Continuous spawning can be detected by the constant presence of this smaller size class.

Pteropods with signs of degradation (category 2) of the soft body and/or uniform frosting on the shell were considered dead upon entering the sediment trap, giving indication as to whether a large die-off event occurred (e.g. a pre-programmed event after spawning) (Gannefors *et al.*, 2005; Kobayashi, 1974). Longevity can be estimated from the date of a cohort's recruitment until its disappearance from size-frequency histograms, however, this assumes no migration out of the sampling region. Since in the current study some life stages were not sampled by the sediment trap (e.g. adult *L. helicina antarctica*) this cohort method of estimating longevity is unlikely to be fully accurate. Instead, we utilised growth rates calculated from tracking the change in each cohort's mean shell width and then used these to estimate the amount of time it would take to reach the maximum sizes recorded within the literature.

3.2.8 Environmental parameters

A number of sensors were fitted to the mooring alongside the sediment trap to monitor the environment alongside sediment trap sampling. xCO_2 (parts per million, Pro-Oceanus), temperature (°C, SAMI) and pH (total scale, SAMI) were

measured at 200 m depth. Oxygen (µM, optode within the Aquadopp current meter) was measured at 400 m depth, alongside pteropod sampling. The first and last days of temperature, xCO_2, oxygen and pH measurements were not included in the analysis. Since xCO_2 measurements were only made between December and March (with a large gap in January) and the instrument did not calibrate (i.e. the value of standard pH was not corresponding to the reading of the sensor) as well as there being a systematic offset in the data collected, xCO_2 measurements were not considered further for analysis (Figure A3.2). All environmental variables were averaged on a monthly and seasonal resolution, being the same resolution used for pteropod analysis. The categorisation of bottles, months and seasons is in Table 3.2.

Bloom events and phytoplankton activity were identified using monthly satellite chlorophyll-*a* data (mg m^{-3}) from Aqua MODIS with a 4 km resolution, (NASA Ocean Biology) from a 12 x 12 km box centred on P3 (Figure 3.2a). The co-ordinates of each corner of this box were; top-left: 52°42'19.4"S 39°56'35.3"W, bottom-left: 52°55'06.9"S 39°56'05.9"W, bottom-right: 52°54'45.7"S 40°17'33.5"W and top-right: 52°42'22.9"S 40°17'04.1"W. The chlorophyll-*a* data, alongside monthly temperature data from Aqua MODIS at 4 km resolution, can also be used to identify the proximity of any fronts, eddies or currents to P3 that could alter the pteropod population being sampled. For all satellite measurements, gaps in data are due to cloud cover, which is particularly prevalent during the winter.

Table 3.2. The start date, month and season of each sediment trap bottle used to determine the population dynamics of pteropods at site P3 (Scotia Sea; Southern Ocean).

Bottle	Sampling start date	Number of days sampled	Month	Season
1	15/12/14	17	December	Summer
2	01/01/15	14	January	Summer
3	15/01/15	14	January	Summer
4	01/02/15	14	February	Summer
5	15/02/15	14	February	Summer
6	01/03/15	31	March	Autumn
7	01/04/15	30	April	Autumn
8	01/05/15	31	May	Autumn
9	01/06/15	30	June	Winter
10	01/07/15	31	July	Winter
11	01/08/15	31	August	Winter
12	01/09/15	30	September	Spring
13	01/10/15	30	October	Spring
14	01/11/15	14	November	Spring
15	15/11/15	16	November	Spring

3.3 Results

3.3.1 Species presence

Five species out of the six previously recorded in the Southern Ocean were entrapped within the sediment trap. The thecosome pteropods identified within the sediment traps were: *Limacina helicina* f. *antarctica*, *Limacina retroversa* f. *australis*, *Clio pyramidata* f. *sulcata*, *Clio pyramidata* f. *excise*, *Clio piatkowski* and *Peraclis* f. *valdiviae* (Figure 3.7) (Van der Spoel, and Dadon, 1999). No *C. pyramidata* f. *antarctica*, *Clio pyramidata* f. *martensii* and *Clio andreae* were present, nor any 'aberrant' *C. pyramidata* individuals (which arise from schizogamy) (Van der Spoel, 1986). Individuals with a shell width below 0.3 mm were classed as *Limacina* spp veligers, since it was difficult to identify the difference between *L. retroversa* and *L. helicina*.
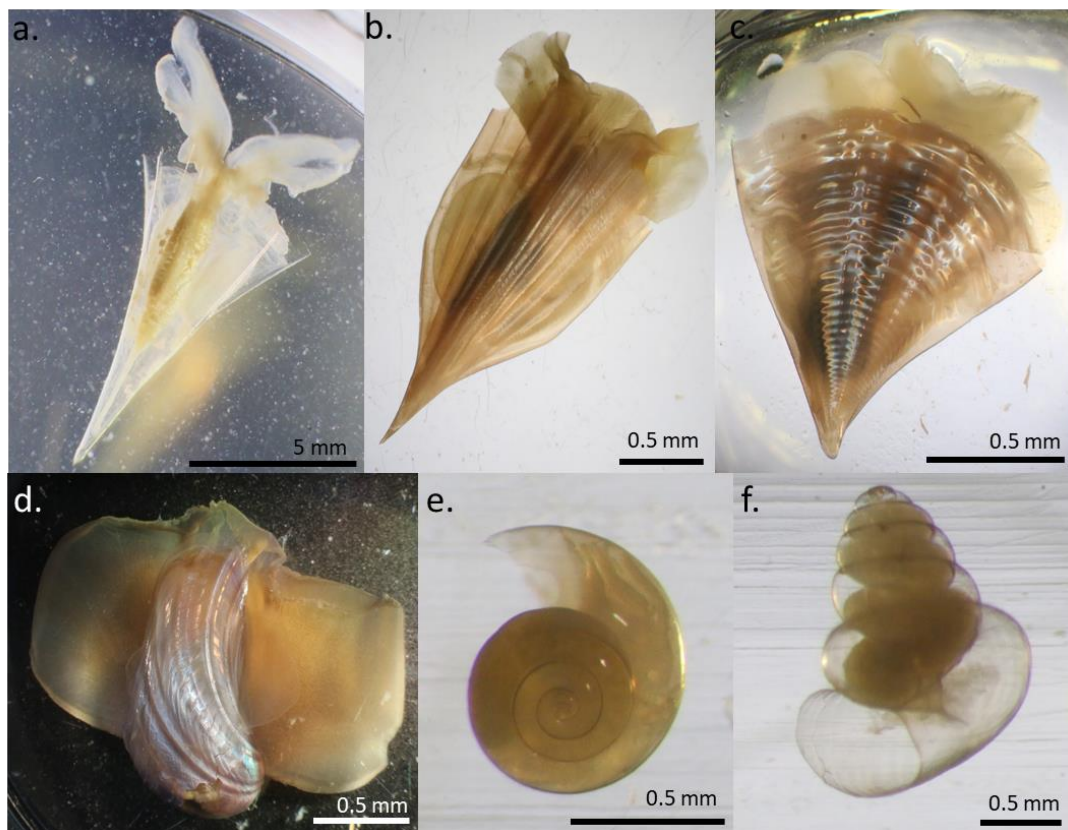
Figure 3-7. Thecosome pteropod species captured within a sediment trap deployed at 400 m depth within the Scotia Sea, Southern Ocean between December 2014 and November 2015. Species are: **a.** *C. pyramidata* f. *sulcata,* **b.** *C. pyramidata* f. *excise,* **c.** *Clio piatkowskii,* **d.** *Peraclis* cf. *valdiviae,* **e.** *L. helicina antarctica* and **f.** *L. retroversa australis*.

3.3.2 Species and life stage abundance

Limacina helicina were the most abundant pteropod species throughout the year, particularly in the summer (peaking in January at 6696 individuals) (Figure 3.8a). However, *L. helicina* abundance was very seasonal with the summer peak rapidly declining into autumn, and winter and spring abundances being much lower (Figure 3.9). There was a particularly rapid drop in abundance of living *L. helicina* between March (5466) and April (174) (Figure 3.8b and d). The abundance of dead individuals followed the same pattern as those that were alive, mainly being found in January, February and March (718, 325 and 419 individuals, respectively). There was little increase in abundance of dead individuals after the sudden decline of living individuals (Figure 3.8c) (Figure A3.4).

Based on the shell sizes within the literature (Lalli and Gilmer, 1989; Lalli and Wells, 1978), no adult *Limacina helicina* were found dead, alive or predated over the entire sampling period, with all identifiable individuals being juveniles. *Limacina helicina* juveniles were most abundant in January, February and March (5914, 4921 and 5029 individuals respectively) but were present in all other months at much lower abundances (30-164 individuals).

L. retroversa were less abundant than *L. helicina* in the summer, however, during the winter they became the dominant species (Figure 3.9). *L. retroversa* were most abundant during the winter and least in the spring with several monthly peaks being observed throughout the year (February: 196, May: 188, June: 166) (Figure 3.8e). Like *L. helicina,* there was a drop in abundance in April (32 individuals), however, this was immediately followed by a peak in abundance in May (188 individuals) (Figure 3.8f) with no increase in instances of dead individuals. The greatest die-off occurred in February (47 individuals) followed by January (26 individuals) with a fairly constant number of dead individuals being found over the rest of the year (mean 8.20 ± 1.89) (Figure 3.8g) (Appendix A.3.b).

Both adult and juvenile *Limacina retroversa* were present. Except for December, living adult *Limacina retroversa* were found in every month however, they were particularly abundant in the winter with a peak occurring in June (86 individuals)

93

which gradually declined through to spring and into summer (Figure 3.8f). Peaks of juvenile abundance occurred in both summer (February: 144 individuals) and autumn (May: 131 individuals). Juveniles were still found throughout winter (111 individuals) with the lowest abundance found in spring. Very few dead adult *Limacina retroversa* were found (May: 4, November: 1, all others: 0 individuals). Most dead juveniles were found in January (26 individuals) and February (47 individuals) with very few occurring over the rest of the year.

Limacina veligers (shell width ≤0.3 mm) were predominantly found during the summer and early autumn, with peak abundance in January (2260 individuals) (Figure 3.8i). Veligers were rare within the winter and spring (Figure 3.9). Almost all dead or predated veligers were found in the summer (Figure 3.8j).

Clio pyramidata were most abundant in the summer and autumn, but were overall much rarer than *Limacina* pteropods (Figure 3.9). There was a sudden increase in abundance from January (11 individuals) to February (55 individuals) when they were at their peak (Figure 3.8h). Abundance gradually declined in autumn and winter where they became much rarer (3 and 4 individuals, respectively). Dead *Clio pyramidata* were only found in the autumn (2 individuals). Predated individuals were not found. Over the entire sampling period, four *Clio piatkowski* and three *Peraclis* cf. *valdiviae* were entrapped. Due to the lower sample sizes of *Clio pyramidata, Clio piatkowski* and *Peraclis* cf. *valdiviae* no further analysis on cohorts, growth rates or shell morphometrics is performed.
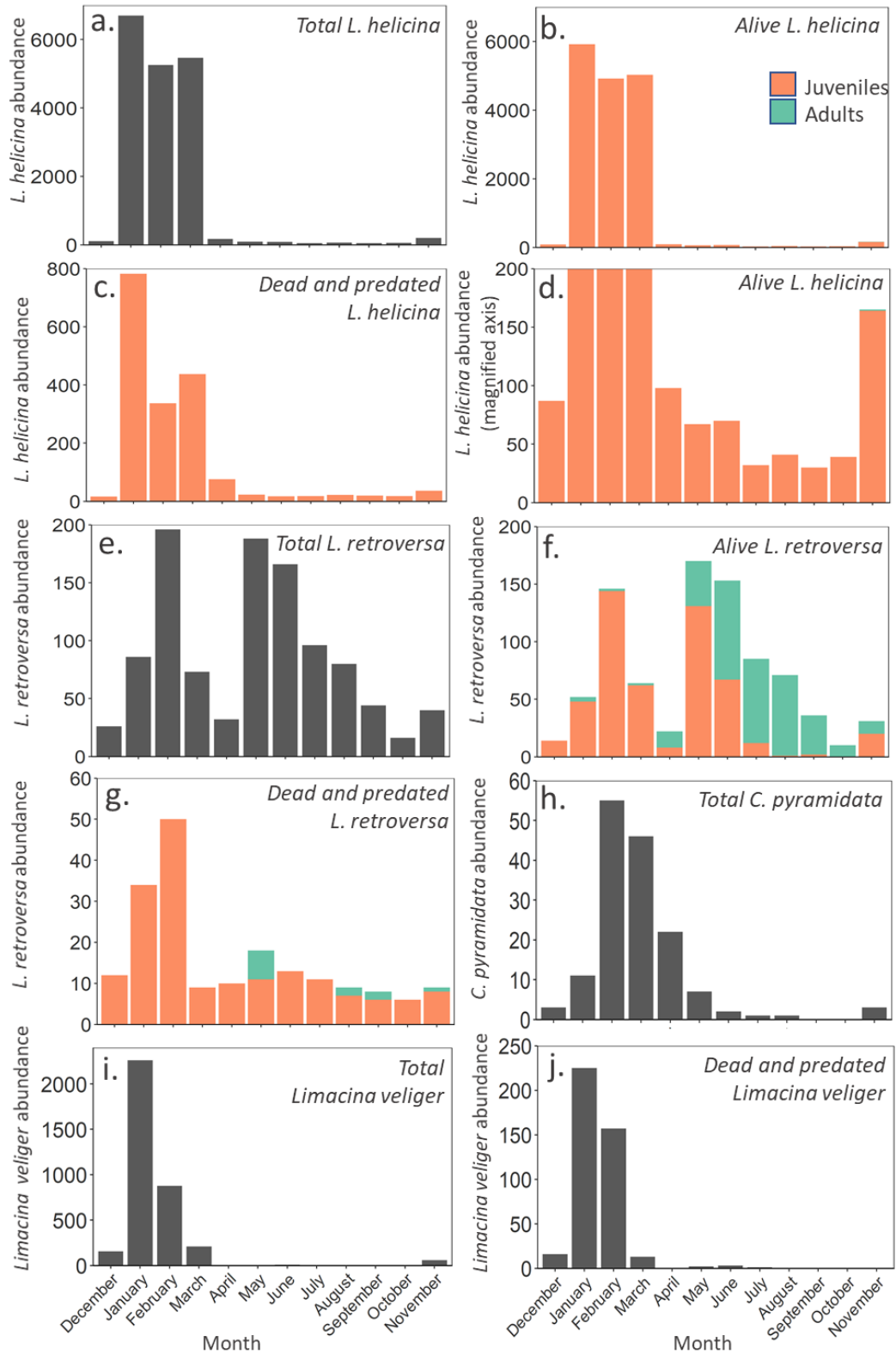
Figure 3-8. Monthly abundance of *L. helicina* (**a-d**), *L. retroversa* (**e-g**), *C. pyramidata* (**h**) and *Limacina* spp veligers (**i-j**) within the sediment trap deployed at P3 (Scotia Sea; Southern Ocean) at 400 m depth between December 2014 and November 2015. Orange bars are the number of juveniles and green bars are the number of adult pteropods based on size measurements given by Lalli and Gilmer (1989). Only 2 dead *Clio pyramidata* were found in the autumn and so not plotted.
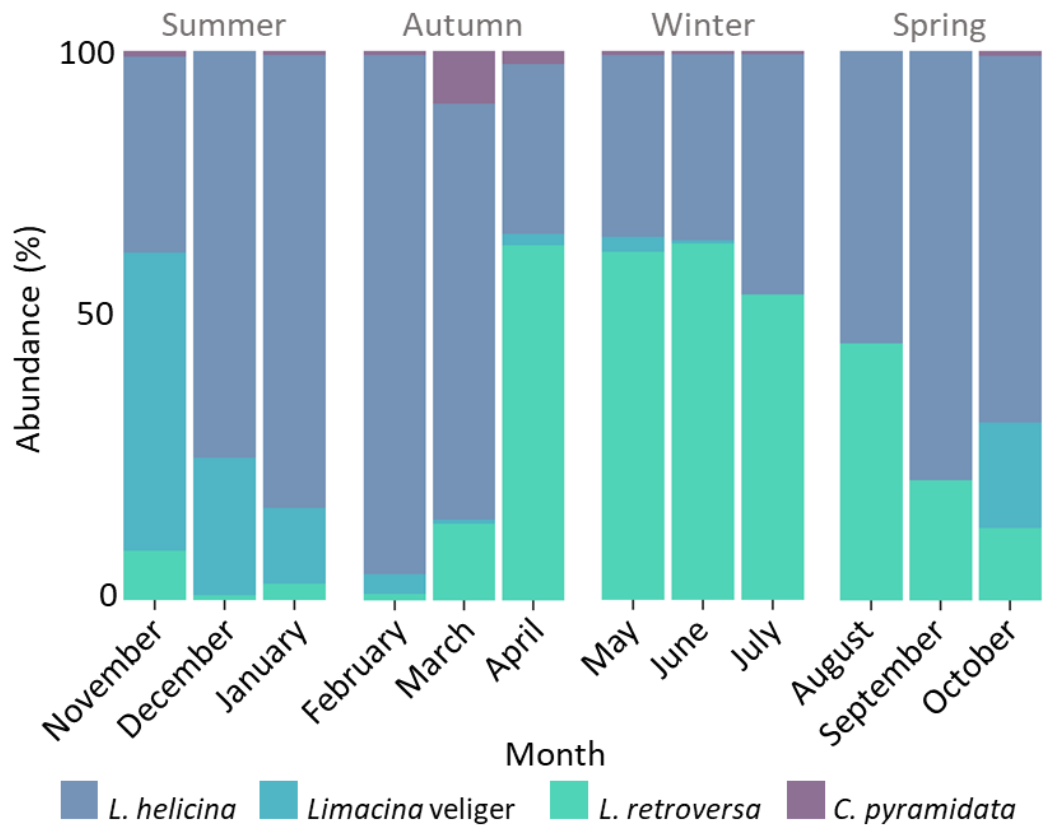
Figure 3-9. Proportional abundance (%) of the number of living pteropods recorded each month between December 2014 and November 2015 within a sediment trap deployed at 400 m depth at site P3 (Scotia Sea, Southern Ocean).

3.3.3 Shell morphometrics

Outliers were retained after being independently removed during PCA re-runs and not impacting the overall result. Correlations were investigated via a correlation matrix, revealing that all shell morphometric measurements were correlated (>0.3). The Kaiser-Meyar-Olkin (KMO{base}) sampling adequacy measure suggested that the ratios for shell width:number of whorls, diameter:number of whorls and shell width:diameter had poor factorability (i.e. the variables had an extreme degree of collinearity) (L.H.: 0.22, 0.51 and 0.15; L.R.: 0.21, 0.21 and 0.18, respectively) and so they were removed from further analysis. A Bartlett's test of sphericity indicated that the remaining morphological variables were suitable for factorability for both *Limacina* species (L.H.: $x^2{}_3$= 693060, *P*<0.001; L.R.: $x^2{}_3$= 108570, *P*<0.001). Catell's (1966) scree-plot indicated that Principal Component 1 (PC1) explained most of the variance for both *L. helicina* (89.2%) and *L. retroversa* (95.8%). For both species PC1

comprised of shell width/spire height, shell diameter, shell area and number of whorls with similar loadings that varied little between sampling months (Figure 3.10). Pearson's correlation analysis ('cor.test{base}') revealed that shell width/spire height and shell diameter had a strong positive association with the number of whorls of *L. helicina* (width: r_{16489} = 0.90, p<0.001; diameter: r_{16489} = 0.79, p<0.001) and *L. retroversa* (spire height: r_{852} = 0.96, p<0.001; diameter: r_{852} = 0.92, p<0.001) as well as being correlated together (L.H.: r_{16489} = 0.86, p<0.001; L.R.: r_{852} = 0.96, p<0.001. Therefore, any one of the shell morphometrics would be a good representation of pteropod shell size throughout the sampling period. Hereafter, shell width for *L. helicina* and *Limacina* veligers and spire height for *L. retroversa* will be utilised, since these are common measures in the literature (Dadon and Cidre, 1992; Gannefors *et al.,* 2005; Kobayashi, 1974; Wang *et al.,* 2017; Gilmer and Harbison, 1991).

Simple linear regressions were calculated to define the relationship between shell diameter/spire height, shell width and the number of whorls for *L. helicina* and *L. retroversa* (Table 3.3.).

Table 3.3. Simple linear relationships between shell diameter (mm) (**sd**), spire height (mm) (**sh**), shell width (mm) (**sw**) and number of whorls (**nw**) of *L. helicina* and *L. retroversa.*

Species	Association	Linear regression parameters
L. helicina	sd= 0.003 + 0.796*sw	$F_{1, 19580}$= 1.35, *p*<0.001, R^2= 0.87
	nw= 0.122 + 4.53*sw	$F_{1, 19580}$= 2.17, *p*<0.001; R^2= 0.92
	nw= 0.37 + 5.01*sd	$F_{1, 19580}$= 8.58, *p*<0.001; R^2= 0.81
L. retroversa	sd= 0.07 + 0.71*sh	$F_{1, 920}$= 1.38, *p*<0.001; R^2= 0.94
	nw= 0.88 + 2.86*sh	$F_{1, 920}$= 9672, *p*<0.001; R^2= 0.91
	nw= 0.73 + 3.82*sd	$F_{1, 920}$= 6698, *p*<0.001; R^2= 0.88
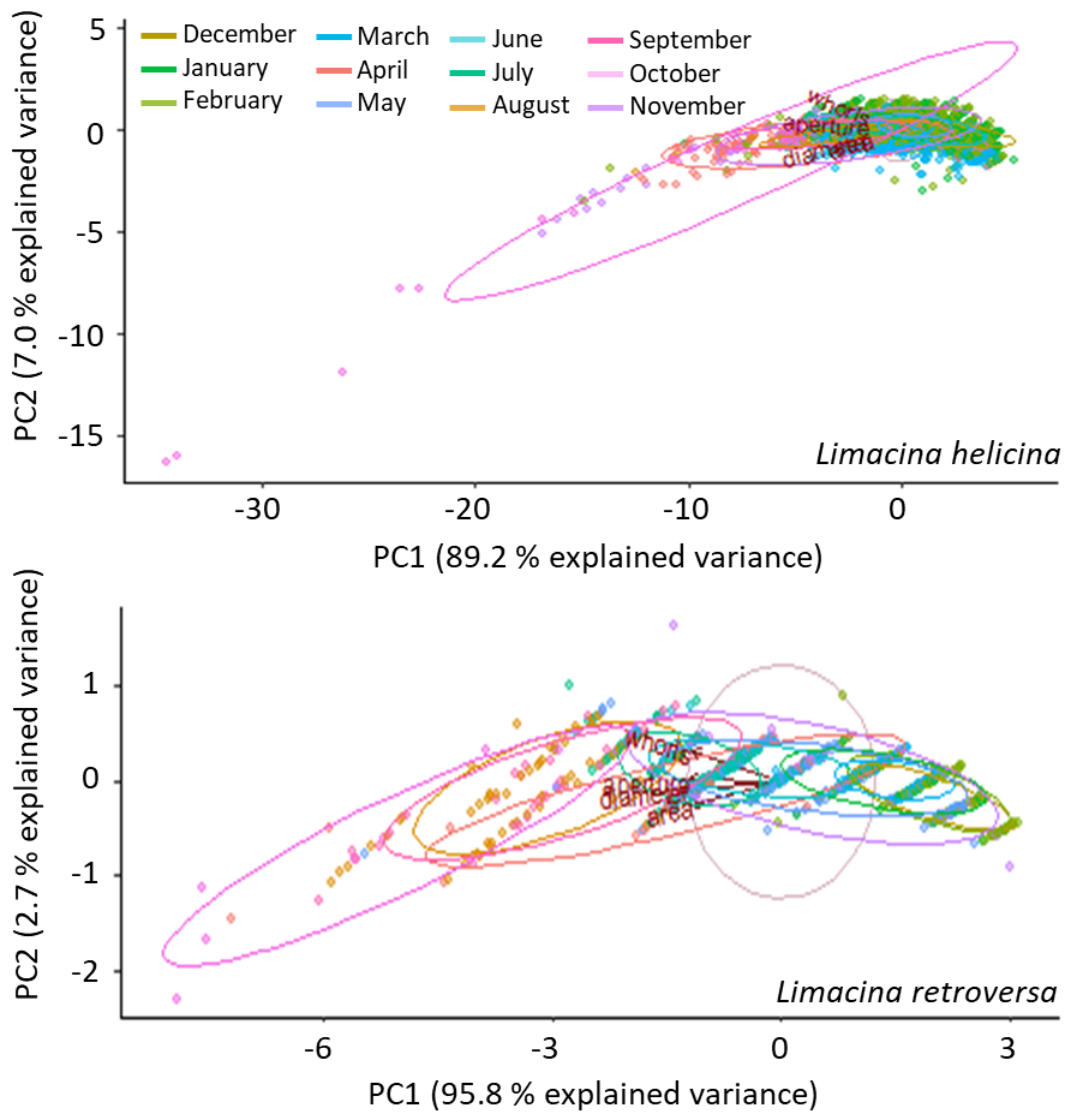
	PC1 (L.H.)	PC1 (L.R.)	PC2 (L.H.)	PC2 (L.R.)
Shell width/Spire height	-0.44	-0.51	-0.28	0.03
Shell diameter	-0.46	-0.50	0.06	-0.21
Area	-0.44	-0.49	-0.19	-0.58
Whorl	-0.42	-0.49	-0.02	-0.77
S.D.	2.11	1.96	1.16	0.33

Figure 3-10: Principal Component Analysis (PCA) biplots indicating the direction and relationship between pteropod shell morphometrics measured on *Limacina helicina* (L.H.) and *Limacina retroversa* (L.R.). Ellipses give the monthly normal data distributions in relation to the principal components. The table gives the shell morphometrics included and the associated loadings on each component and the standard deviation (S.D.).

3.3.4 Cohort identification

Cohorts of pteropods are groups of individuals that hatched at the same time (therefore, they are at the same life stage) which can be tracked throughout the year (see Section 3.2.6. for methodology). Cohorts were only calculated for *L. helicina* and *L. retroversa* since there was an insufficient sample size of the other species entrapped. Cohorts were based on the shell width of *L. helicina* and spire height of *L. retroversa* individuals (see Section 3.3.4. for shell morphometric analyses). From December to June, the population of *L. helicina* was represented by two cohorts of small juveniles with mean shell widths between 0.34-0.47 mm and 0.50-0.59 mm (Figure 3.11). May was an exception, with only a single size group being present (mean: 0.50 mm). Furthermore, a small number (n= 53) of larger individuals made up a second cohort in April with a mean shell width of 1.01 mm. From July, the shell width of these two size groups started to increase, from a mean size of 0.57 and 0.75 mm and reaching 0.76 and 1.79 mm in October. In contrast, *L. retroversa* had four cohorts over the year sampled. These were present December to January (0.31-1.17 mm), February to April (0.35-1.96 mm), May to October (0.54-2.29 mm) and November (0.39-1.10 mm) (Figure 3.12). For a full table of the Mixture analysis chi-squared, means and standard errors see Table A3.1.
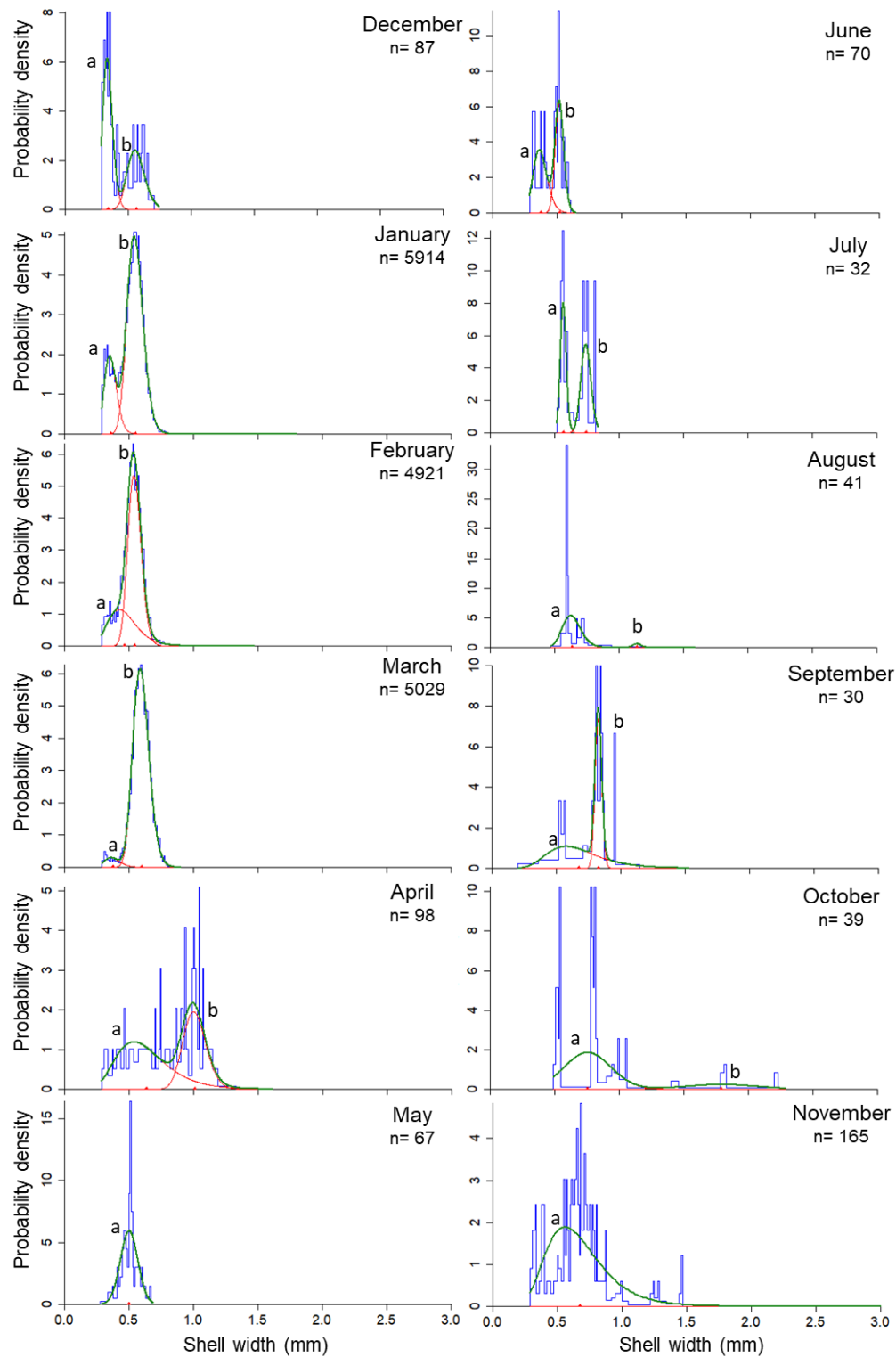
Figure 3-11. Mixture models fit to length-frequency data based on the shell width of living *L. helicina antarctica* for each month of a year-long sampling period. Mixture distributions were analysed using the *Mixdist* to identify cohorts within each month (identified by **a** and **b**). These cohorts can then be tracked throughout the year. **Blue** lines represent the original length-frequency distribution, **red** lines are the individual fitted distributions and **green** lines are the sum of fitted distributions.
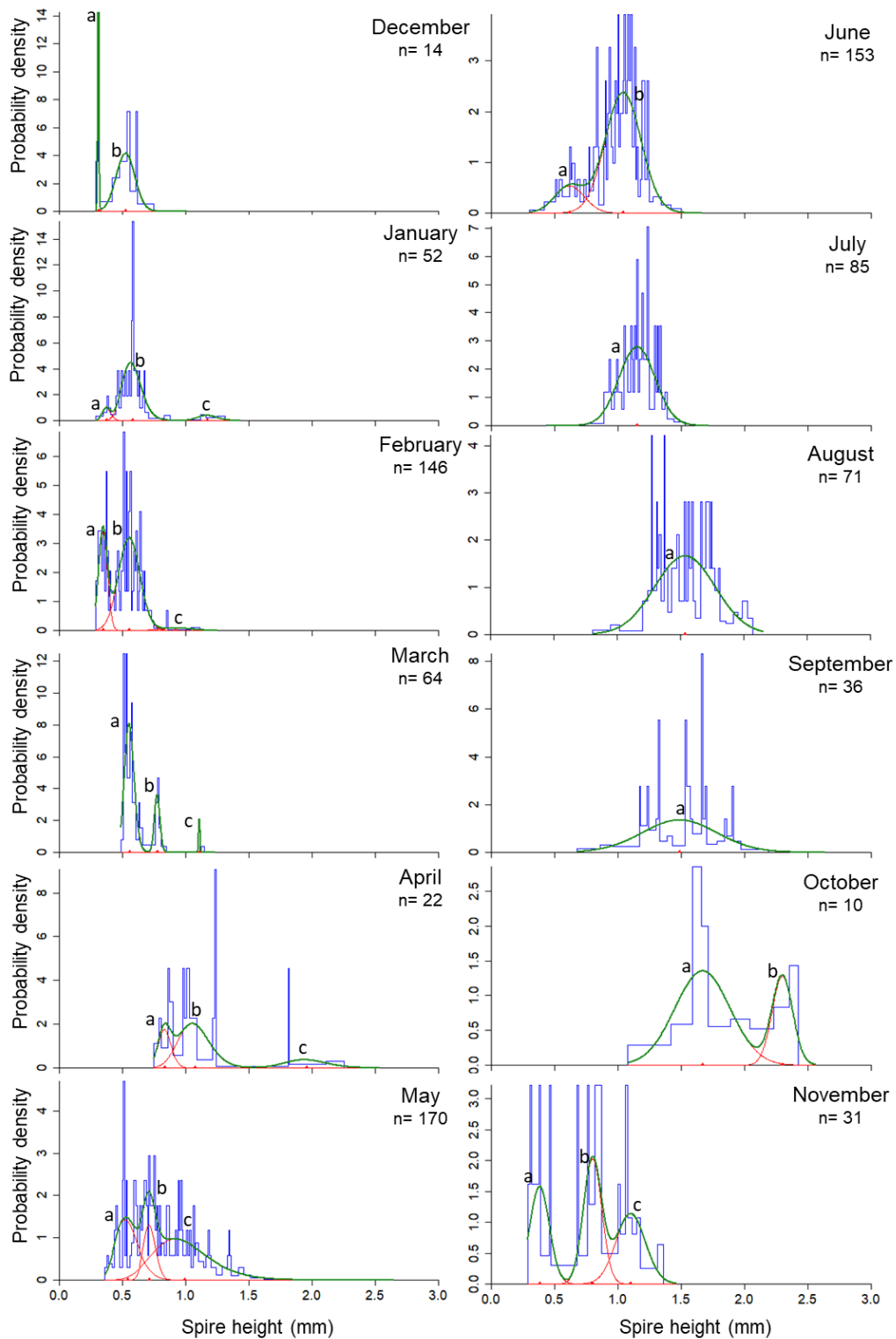
Figure 3-12. Mixture models fit to length-frequency data based on the spire height of living *L. retroversa* for each month of a year-long sampling period. Mixture distributions were analysed using the *Mixdist* to identify cohorts within each month (identified by **a-c**). These cohorts can then be tracked throughout the year. **Blue** lines represent the original length-frequency distribution, **red** lines are the individual fitted distributions and **green** lines are the sum of fitted distributions.

3.3.5 Shell growth

3.3.5.1 *Limacina helicina*

Unlike *L. retroversa* (LR)*,* the full population of *L. helicina* (LH) was not sampled since no adult individuals were captured. Since adults were absent, this makes it difficult to predict the number of cohorts present over the sampling period. However, I can describe the recruitment of *L. helicina* into juvenile stages and identify a number of distinct groups (LH1-5) using a mixture analysis (Figure 3.13). The first small juveniles of *L. helicina* in December probably emerged from their egg sacs in November since very few veligers were recorded in prior months. The persistence of this small size class (shell width 0.34- 0.37 mm) between December and June suggest protracted spawning throughout the entire summer (LH1). Larger juvenile individuals were also present over this period (shell width 0.47- 1.01 mm) (LH2) however, due to their presence each month, it is difficult to suggest when these individuals were recruited from LH1. These calculations assume that the population is static, with no advection of the *L. helicina* population in and out of the sampling area.

Groups LH3 (shell width 0.50 mm) and LH4 (shell width 0.38 mm) are small juveniles first recorded in May and June, respectively. The last spawning event, indicated by the presence of veligers, occurred in March, therefore, a range of growth rates can be estimated from this time lag. Depending on whether individuals were spawned in February or March, the growth rate of LR3 would be 0.005- 0.008 mm/day shell growth while the growth rate of LH4 would be 0.004- 0.003 mm/day (Table 3.4.). This assumes that individuals emerged from the egg-sac 9 days after spawning with a shell size of 0.07 mm, based on findings in Section 2.3.2.

Table 3.4. The growth rates of *Limacina helicina antarctica* to reach the shell sizes of the small juvenile groups found in May (LH3) and June (LH4). Two growth rates are given for each size group depending on whether they were spawned in February or March. Individuals were entrapped within a sediment trap deployed at P3 (Scotia Sea; Southern Ocean) at 400 m depth between December 2014 and November 2015.

Group	Month Spawned	Number of days growth	Shell width (mm)	Shell width minus embryonic shell growth (mm)	Growth rate (mm/day)
LH3	March	52	0.50	0.43	0.008
LH3	February	80	0.50	0.43	0.005
LH4	March	83	0.38	0.31	0.004
LH4	February	111	0.38	0.31	0.003
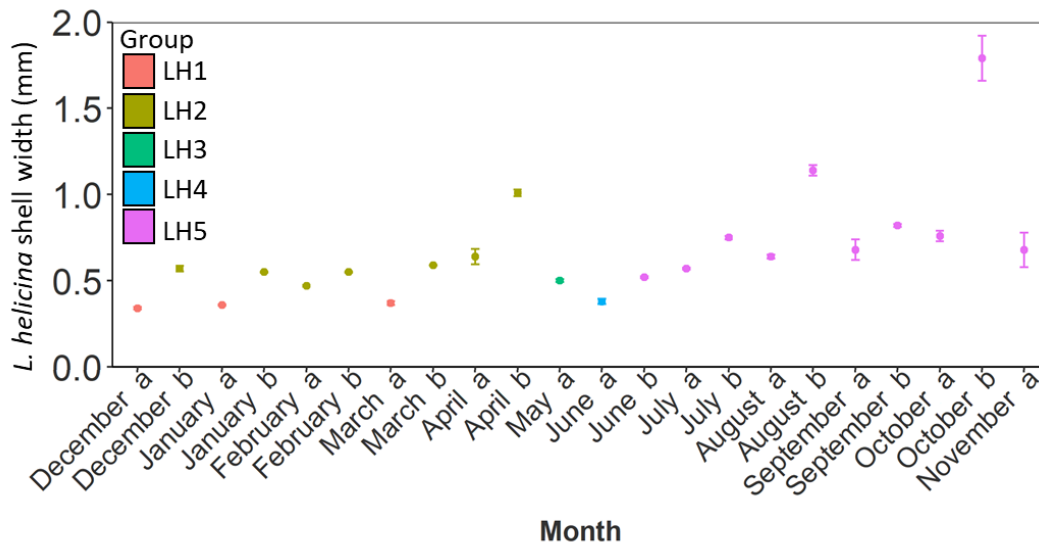
Figure 3-13. The mean shell width of *L. helicina* with standard error of each size group. Colours indicate assemblages of size groups (LH1-5) rather than a cohort, since cohorts could not be reliably identified. Groups were computed by a Mixture analysis for each month. *L. helicina* were collected within a sediment trap deployed at P3 (Scotia Sea; Southern Ocean) at 400 m depth between December 2014 and November 2015.

3.3.5.2   Limacina retroversa

There were four periods of *L. retroversa* shell growth identified via a Mixture analyses of monthly size frequencies (see Section 3.3.6.) making up four cohorts. These periods of growth occurred between December- January (cohort LR1), February- April (cohort LR2), May- October (cohort LR3) and November (cohort LR4) (Figure 3.14) with growth rates of 0.014, 0.018, 0.014 and 0.24 mm/day, respectively (Table 3.5.). There may have been some overlap between the LR1 and LR2 cohorts, since veligers and recruitment into the smaller size class occurred continuously between December and March. However, there is a small decrease in mean shell size in the smaller groups, making this unlikely (Table 3.6.). The absences of smaller individuals in March-April and June-October, and the disappearance of larger individuals, suggest there was no overlap between cohorts LR2-LR3 and LR3-LR4. Cohort LR4 may only be partially recorded since sampling ceased after November. The maximum spire height reached at the end of each growth period varied with the season, with adult individuals in summer reaching 1.17 mm (LR1), in autumn: 1.96 mm (LR2), in winter: 2.29 mm (LR3) and in spring: 1.10 mm (LR4).

The emergence of veligers from their eggs sacs which were recruited into cohort LR1 may have occurred in November although, if it is assumed that veligers have a similar growth rates to juveniles (0.014 mm/day) only ~12 days would have been needed to reach the mean shell size in December (0.31 mm) therefore, they could also have emerged in December. Hence, individuals that make up LR2, assuming similar growth rates to LR1, emerged in January/February. Since LR3 first appeared in May (mean shell size of 0.54 mm), and veligers were only found until March, the growth rate of these veligers was a maximum of 0.007 mm/day. LR4 juveniles first appeared in November (mean shell size 0.39 mm) therefore, must have arisen from the veligers that emerged in the same month, since few veligers were recorded between April and October (n= 16). This timing suggests that the growth rate of veligers was likely to match that of LR1.

Table 3.5. The growth rates of *Limacina retroversa australis* which were calculated based on the number of days between the recruitment of the smallest size group and the appearance of the largest size group within a single cohort. Individuals were entrapped within a sediment trap deployed at P3 (Scotia Sea; Southern Ocean) at 400 m depth between December 2014 and November 2015.

Cohort	Month recruited	Number of days growth	Minimum cohort spire height (mm)	Maximum cohort spire height (mm)	Overall spire growth (mm)	Growth rate (mm/day)
LR1	December	62	0.31	1.17	0.86	0.014
LR2	February	89	0.35	1.96	1.61	0.018
LR3	May	184	0.54	2.29	1.75	0.010
LR4	November	30	0.39	1.1	0.71	0.024
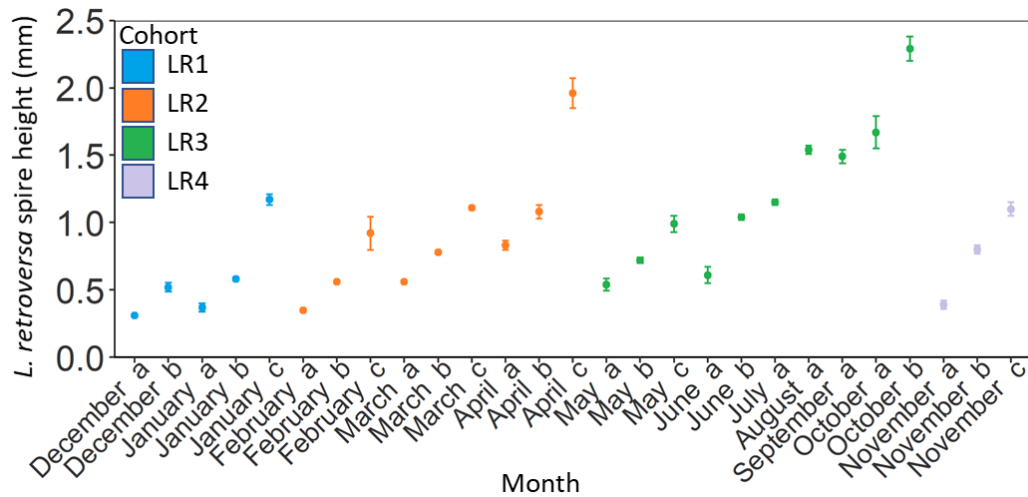
Figure 3-14. The mean spire height of *L. retroversa* with standard error of each size group computed by a Mixture analysis for each month. Colours indicate which cohort (LR1-4) each group belongs to. *L. retroversa* were collected within a sediment trap deployed at P3 (Scotia Sea; Southern Ocean) at 400 m depth between December 2014 and November 2015.

Table 3.6. Mean *L. retroversa* (L.R.) spire height (mm) and *L. helicina* (L.H.) shell width (mm) of each monthly cohort computed using a Mixture analysis within a sediment trap deployed at 400 m depth at site P3 (Scotia Sea; Southern Ocean) between December 2014 -November 2015. The growth rate (GR) was calculated as the increase in mean shell size of each cohort divided by the number of days (mm/day).

Month	L.R. shell width (S.E.)	L.R. cohort	L.R. GR	L.H. shell width (S.E.)	L.H. cohort
December	0.31 (0.01)	LR1		0.34 (0.01)	LH1
	0.52 (0.02)	LR1		0.57 (0.02)	LH2
January	0.37 (0.02)	LR1		0.36 (0.00)	LH1
	0.58 (0.01)	LR1		0.55 (0.00)	LH2
	1.17 (0.04)	LR1	0.014		
February	0.35 (0.01)	LR2		0.47 (0.01)	LH2
	0.56 (0.01)	LR2		0.55 (0.00)	LH2
	0.92 (0.12)	LR2			
March	0.56 (0.01)	LR2		0.37 (0.01)	LH1
	0.78 (0.01)	LR2		0.59 (0.00)	LH2
	1.11 (0.01)	LR2			
April	0.83 (0.04)	LR2		0.64 (0.05)	LH2
	1.08 (0.05)	LR2		1.01 (0.01)	LH2
	1.96 (0.11)	LR2	0.018		
May	0.54 (0.46)	LR3		0.50 (0.01)	LH3
	0.72 (0.02)	LR3			
	0.99 (0.06)	LR3			
June	0.61 (0.06)	LR3		0.38 (0.02)	LH4
	1.04 (0.02)	LR3		0.52 (0.01)	LH5
July	1.15 (0.02)	LR3		0.57 (0.01)	LH5
		LR3		0.75 (0.01)	LH5
August	1.54 (0.03)	LR3		0.64 (0.01)	LH5
		LR3		1.14 (0.03)	LH5
September	1.49 (0.05)	LR3		0.68 (0.06)	LH5
		LR3		0.82 (0.01)	LH5
October	1.67 (0.12)	LR3		0.76 (0.03)	LH5
	2.29 (0.09)	LR3	0.014	1.79 (0.13)	LH5
November	0.39 (0.03)	LR4		0.68 (0.10)	LH5
	0.80 (0.03)	LR4			
	1.10 (0.05)	LR4	0.24		

3.3.5.3 Limacina veligers

Previous studies have calculated that takes 3 days for *L. retroversa* to hatch from egg sacs (at 8 ± 1 °C) and another 3-4 days to develop shells (Thabet *et al.,* 2015; Lebour, 1932) while *L. helicina* veligers take 7-9 days to emerge, but already with a shell width of ~0.07 mm (Chapter 2; Pasternak *et al*, 2017; Paranjape, 1968). Therefore, these emergence times and initial shell sizes were assumed when calculating growth rates for *L. retroversa* and *L. helicina* veligers. However, since these values are based from data collected from populations in different regions and in different temperatures, it should be noted that there is some uncertaintly surrounding hatching time.

As *L. retroversa's* winter cohort (LR3) first appeared in May and small veligers were only found until March, the growth rate of these individuals would be 0.005 mm/day if spawning occurred in March or 0.006 mm/day if it occurred in April (Figure 3.15). This is assuming that the absence of small veligers is due to an absence of spawning rather than another factor (such as advection) removing the larvae from the sampling location. In contrast, if individuals spawned in the same month as the appearance of the summer (LR1) and Autumn (LR2) cohorts then their growth rates would be like those in the juvenile stages (LR1 veligers: 0.013 mm/day; juveniles: 0.014 mm/day and LR2 veligers: 0.017 mm/day; juveniles: 0.018 mm/day). Alternatively, if individuals were spawned the month before, growth rates of veligers would be much less than that of juveniles (LR1: 0.006 mm/day; LR2: 0.007 mm/day). Since veligers were first recorded in November and small juveniles of both species were present in the same month, it must have taken both species less than 31 days to reach 0.3 mm. Therefore, it is most feasible for *L. retroversa* veligers to have the same growth rate as juveniles.

It is more difficult to discern the growth rates of *L. helicina* veligers since no distinct cohort could be defined from *L. helicina* juveniles. Group LH3 are small juveniles (shell width 0.38 mm) first recorded in June, however, the last spawning event occurred in March. Therefore, to reach a shell width of 0.38 mm individuals in LH3 would have a growth rate of 0.006 mm/day. Similarly, group

LH4 individuals appeared in May therefore, if they emerged in March, they would have a growth rate of ~0.008 mm/day.
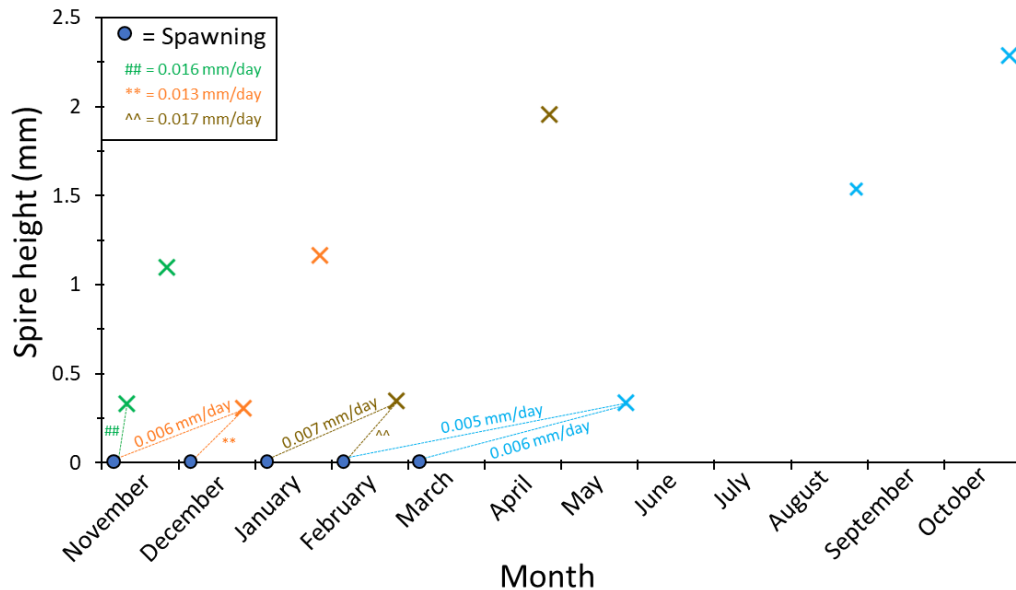
Figure 3-15. The average growth rate of *L. retroversa* veligers (dashed lines) and mean spire height (crosses) of each *L. retroversa* size group computed by a Mixture analysis. *L. retroversa* were collected within a sediment trap deployed at P3 (Scotia Sea; Southern Ocean) at 400 m depth between December 2014 and November 2015. Colours indicate interpretation of cohorts (LR1-4) based upon these size groups.

3.3.6 Environmental conditions

3.3.6.1 Temperature

There were differences in monthly (AOV: $F_{11,2093}$= 48.85, $p<0.001$) and seasonal (AOV: $F_{11,2101}$= 19.53, $p<0.001$) temperatures at 200 m, with the average being 0.92 ± 0.31°C S.D. (Figure 3.16a-b). Spring (0.84 ± 2.64°C S.D.) and summer (0.93 ± 1.99°C S.D.) exhibited a greater range in temperature compared to the autumn (0.93 ± 1.36°C S.D.) and winter (0.98 ± 0.96°C S.D.) (Figure 3.16b). August (1.1 ± 0.65°C S.D.) had the least variation in temperature, while November (1.03 ± 2.19°C S.D.) had the most. This indicates winter ventilation, with the upper ocean being mixed to 200 m during winter months and less mixing in the summer. Temperature did not change between the summer and autumn (TukeyHSD: *p*

>0.05) however, it was colder in the winter (TukeyHSD: p <0.001) and spring (TukeyHSD: p <0.001).

Sea surface temperatures (Aqua MODIS 4km resolution satellite data) were higher on average (3.18°C) than temperatures at 200 m depth, with a much wider standard deviation (1.14°C) (Figure 3.17a). There were monthly (AOV: $F_{11,3168}$= 1649, p<0.001) and seasonal differences (AOV: $F_{11,3175}$= 1009, p<0.001). Summer and autumn temperatures were similar (3.50 ± 3.59°C and 3.58 ± 5.63°C respectively) (TukeyHSD: p >0.05). In contrast, surface winter temperatures varied the least and were the coolest (-0.53 ± 1.62°C) (TukeyHSD: p <0.001) suggesting deeper winter mixing (Figure 3.17b). Little satellite data was available for June and July as there was too much cloud cover. The satellite data revealed warmer water to the north-west of P3 with eddies to the north and none of these warmer patches crossed P3 (Figure 3.18).

3.3.6.2   Chlorophyll-a

Surface chlorophyll-a concentration ranged from a minimum of 0.01 mg m^{-3} (August) to a maximum of 8.78 mg m^{-3} (February) (Figure 3.17c) with monthly (AOV: $F_{11,4481}$= 419.4, p<0.001) and seasonal differences (AOV: $F_{3,4486}$= 436.3, p<0.001). Phytoplankton bloom events were evident from spring into early summer with mean chlorophyll-a concentrations of 1.23 (± 3.65 mg m^{-3}) increasing to 2.05 (± 8.31 mg m^{-3}), respectively (Figure 3.17d). Chlorophyll-a concentration was highest in the summer (TukeyHSD: p <0.001) and lowest in the winter (TukeyHSD: p <0.001). The greatest mean chlorophyll-a concentrations were in December 2014 (2.07 ± 2.93 mg m^{-3}), November 2015 (2.03 ± 3.06 mg m^{-3}) and February 2015 (2.32 ± 6.91 mg m^{-3}). The spring bloom started in December 2014, covering a large area to the north of South Georgia and shrinking in size over the rest of summer into autumn (Figure 3.19). Cloud cover was too great from May to July to see large scale chlorophyll-a concentrations, but mean winter values dropped to 0.19 mg m^{-3} (± 0.06 mg m^{-3}). A smaller bloom started to form in October (1.32 ± 2.68 mg m^{-3}), which then rapidly expanded and intensified over a large area around P3 by November (2.03 ± 3.06 mg m^{-3}).

3.3.6.3 pH

pH at 200 m depth differed among months (AOV: $F_{11,2093}$= 196.6, p <0.001) and seasons (AOV: $F_{3,2101}$= 662.3, p<0.001). There was no difference in pH between the summer (7.9 ± 0.6) and autumn (7.9 ± 0.4) (TukeyHSD: p> 0.05), however, pH increased into the winter (8.0 ± 0.4) (TukeyHSD: p <0.001) and was highest in the spring (8.1 ± 0.4) (p <0.001) (Figure 3.16c). The greatest variation in pH occurred in late-spring to early summer (November: 8.1 ± 0.4 and December: 7.9 ± 0.7) with pH dropping to 7.6 in December and reaching a maximum of 8.4 in November (Figure 3.16d).

3.3.6.4 Oxygen

Oxygen concentration fluctuated from one month to the next ($F_{11,4157}$= 454.6, p<0.001) and seasonally ($F_{3,4165}$=859.7, p<0.001) at 400 m. There was no difference in the oxygen concentration in autumn and winter, with a mean 195.6 ± 10.4 µM) (TukeyHSD: p> 0.05) (Figure 3.16e). However, there was an increase in oxygen concentration during the spring (TukeyHSD: p <0.001), while the lowest concentration was in the summer (TukeyHSD: p <0.001). The high oxygen concentration between autumn and spring is likely due to deep mixing entraining surface water to 200 m depth. With a reduction in mixing during the summer, local remineralisation and respiration reduced the oxygen concentration, resulting in the lowest mean values occurring in December and January (191.3 ± 10.9 µM and 192.6 ± 7.9 µM, respectively) (Figure 3.16f).
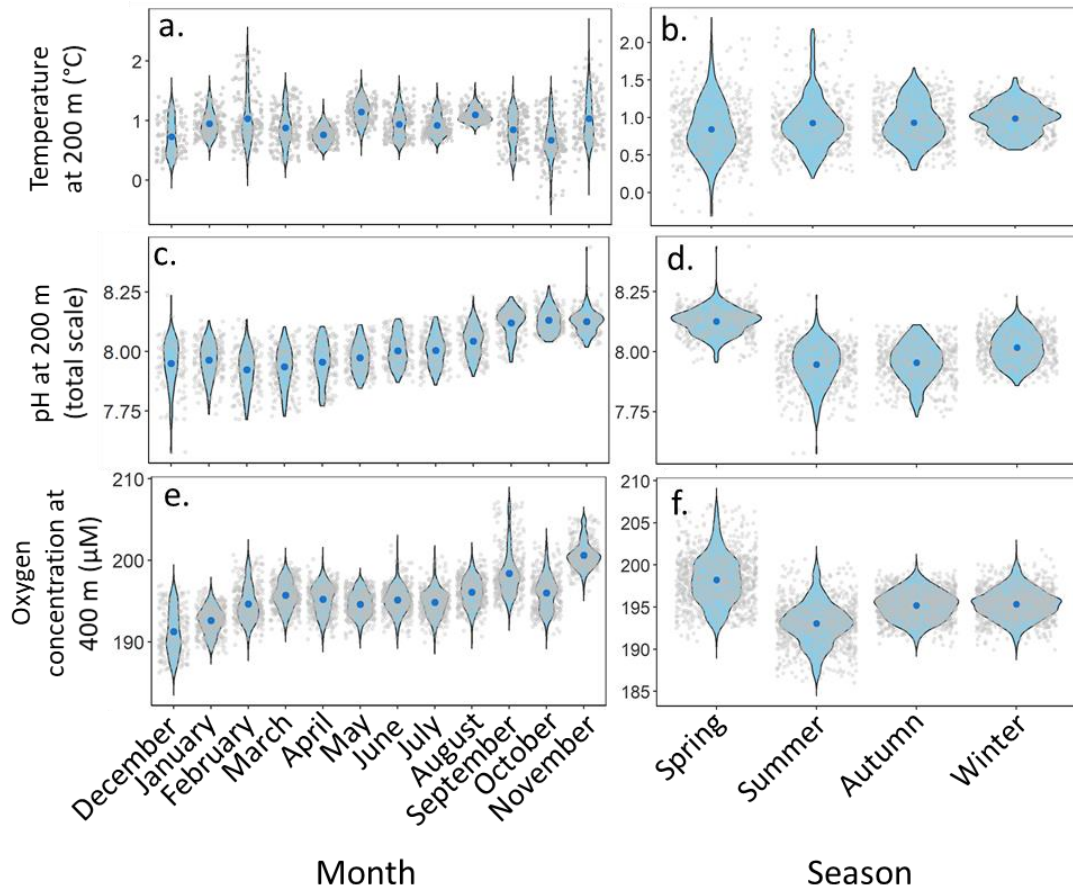
Figure 3-16. Monthly and seasonal environmental conditions associated with the sediment trap deployed at P3 (Scotia Sea; Southern Ocean) between December 2014- November 2015. Inset **a-b** are temperatures recorded *in-situ* at 200 m, **c-d** are *in-situ* pH measurements at 200 m and **e-f** *in-situ* oxygen concentrations at 400 m. Grey dots are individual data points, Blue dots are the means and the thickness of the violin plot represents data probability density.
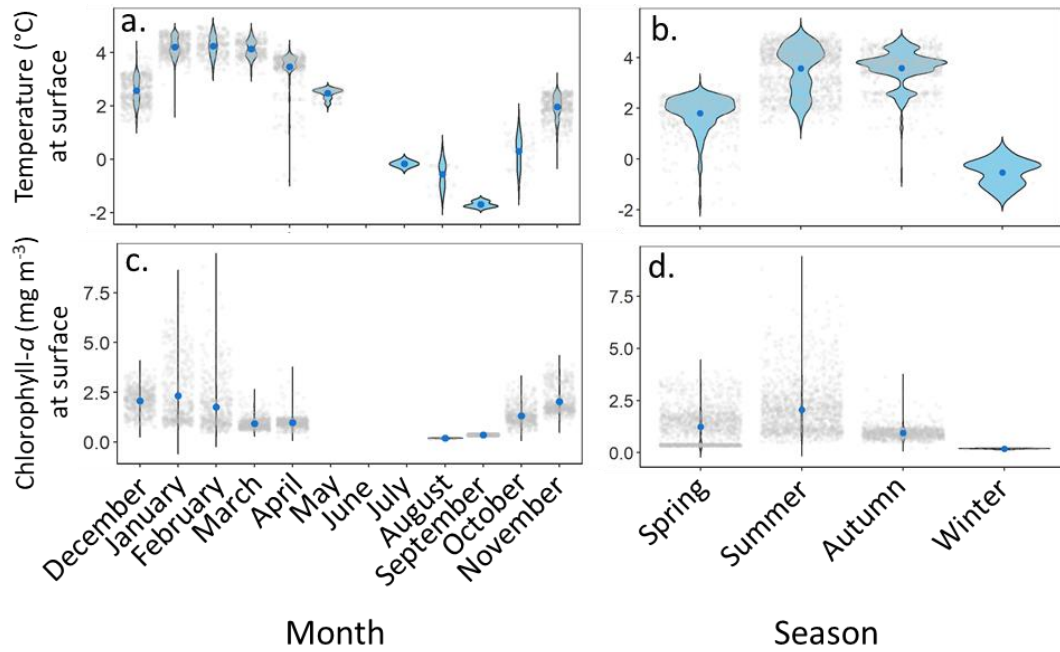
Figure 3-17. Monthly and seasonal environmental conditions at the surface associated with the sediment trap deployed at P3 (Scotia Sea; Southern Ocean) between December 2014- November 2015. **a-b** are surface temperatures, **b-c** are surface chlorophyll. Measurements were taken from Aqua MODIS at 4 km resolution satellite data (NASA; Ocean Biology). Grey dots are individual data points, Blue dots are the means and the thickness of the violin plot represents data probability density.
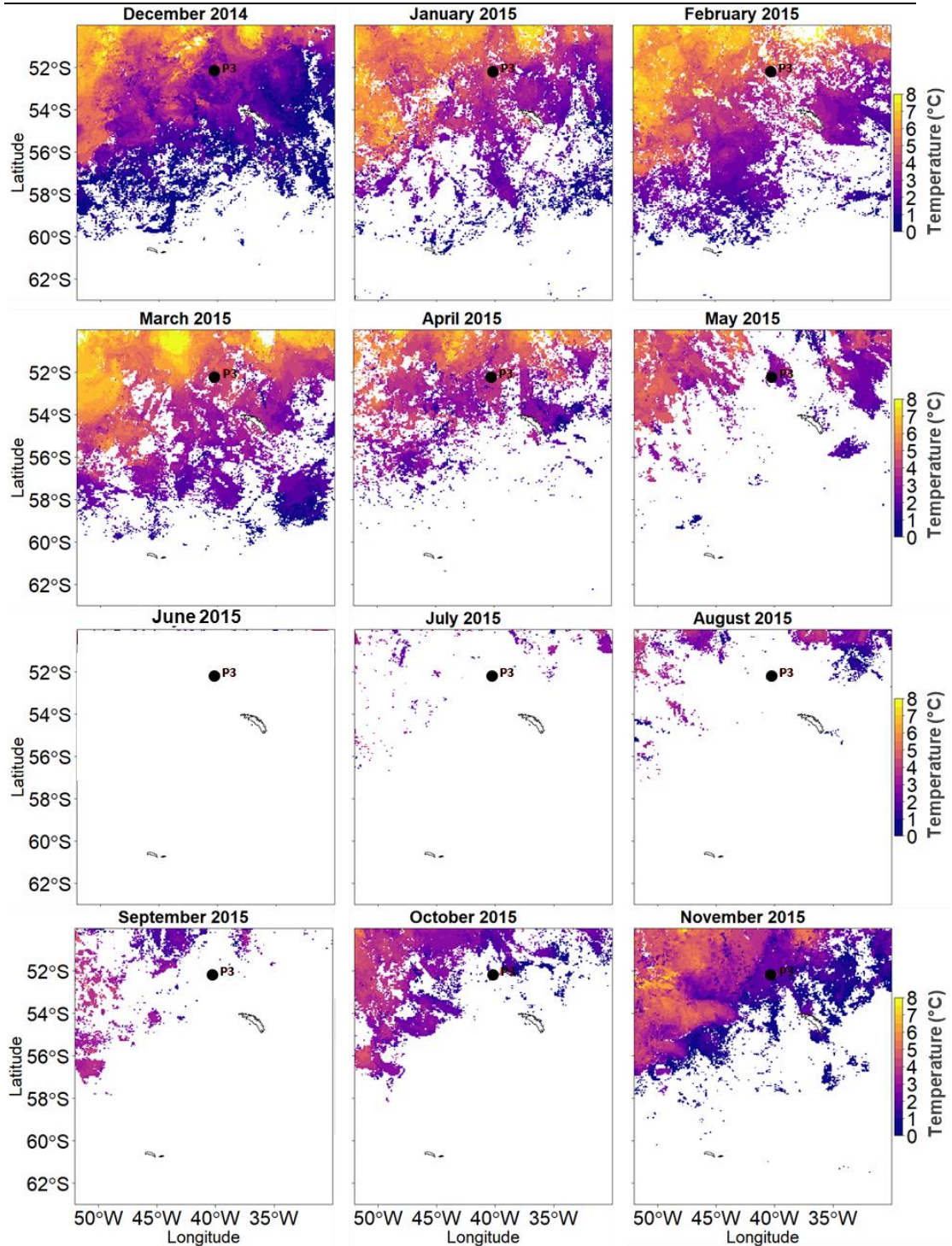
Figure 3-18. Monthly temperature conditions associated with the sediment trap deployed at P3 (Scotia Sea; Southern Ocean) over a year (December 2014- November 2015). P3 is labelled with a black circle. Measurements were taken from Aqua MODIS at 4 km resolution satellite data (NASA; Ocean Biology).
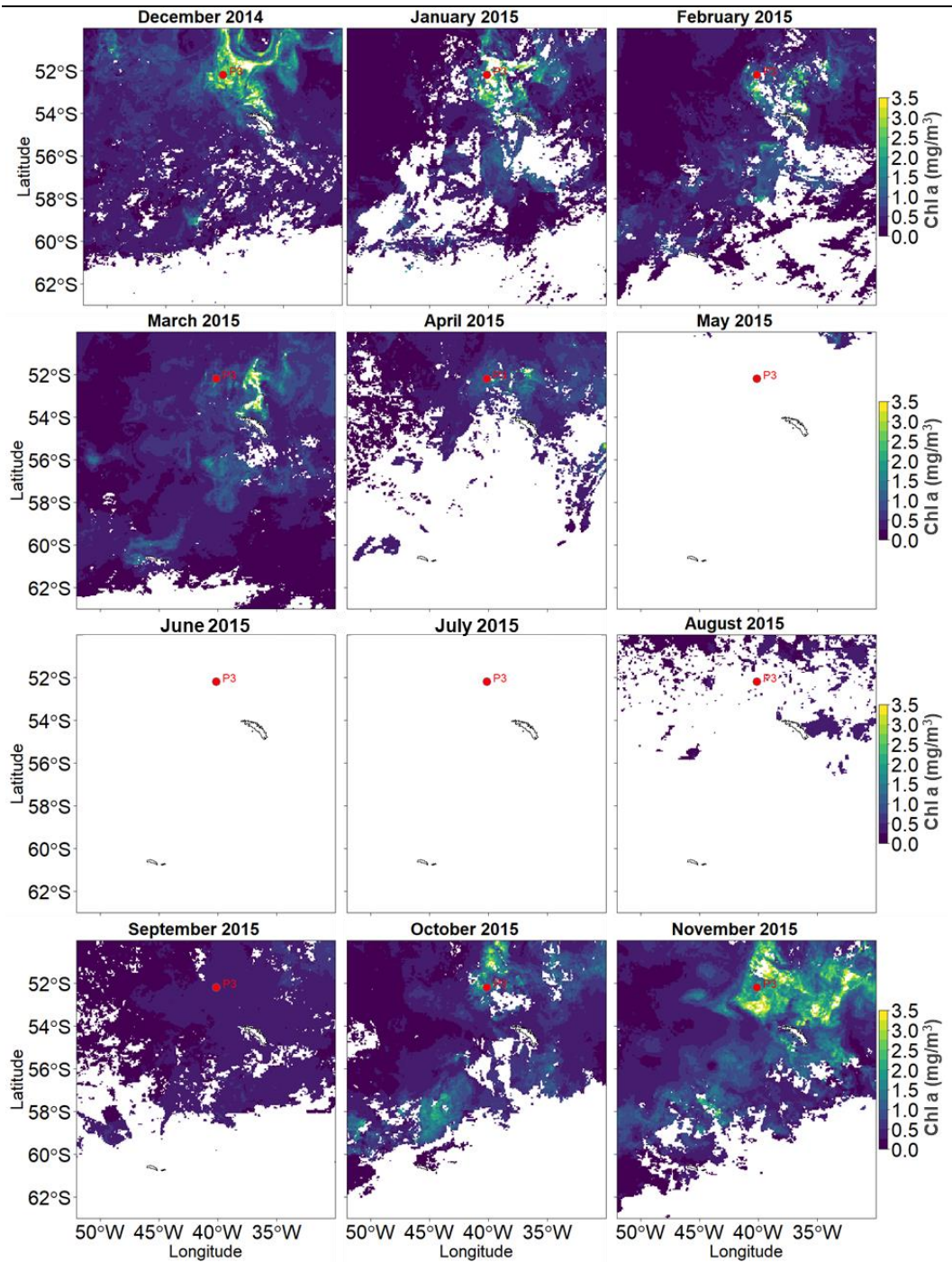
Figure 3-19. Monthly chlorophyll a (mg m^3) associated with the sediment trap deployed at P3 (Scotia Sea; Southern Ocean) over a year (December 2014-November 2015). P3 is labelled with a red circle. Measurements were taken from Aqua MODIS at 4 km resolution satellite data (NASA; Ocean Biology).

3.4 Discussion

3.4.1 Pteropod species

As in previous studies, the genus *Limacina* dominated the pteropod community with both *L. helicina* and *L. retroversa* being present (Hunt *et al.*, 2008; Bernard and Froneman, 2009; Van der Spoel and Dadon, 1999; Roberts *et al.,* 2011; Howard *et al.,* 2011). *C. pyramidata* forma *sulcata* were also present throughout the sampling period. This forma is commonly captured alongside *Limacina* species throughout the Southern Ocean, although, not in as high abundances as *Limacina* spp (Hunt *et al.*, 2008). No *Clio pyramidata* forma *antarctica* were recorded, however, they are mainly found north of the Polar Front (Hunt *et al.,* 2008), so this was not unexpected. Additionally, no *Clio pyramidata martensii* and *Clio andreae* were present, though these are extremely rare so it would be unlikely to capture them.

The thecosome pteropods *Clio piatkowskii*, *Peraclis* cf. *valdiviae* and *C. pyramidata* f. *excise* were recorded within the Scotia Sea for the first time. Therefore, sediment traps not only represent the known biodiversity within the Scotia Sea, but they also provide a good overview of local pteropod species presence which may otherwise be missed with discrete net sampling. Since several individuals of these pteropods were entrapped throughout the sampling period, it would suggest that they are resident at site P3 at 400 m, which increases the known range of all three pteropods. Previous records of *C. piatkowskii* are scarce, being found in the Weddell Sea (Van der Spoel *et al.,* 1992; 1999), Lazarev Sea (Flores *et al.,* 2011) and near Bouvetøya (Hunt *et al.,* 2008) at 300- 1000 m depth. *Peraclis* cf. *valdiviae* has previously been recorded south of Tasmania, within the Sub-Antarctic Zone down to 150 m (Roberts *et al.,* 2011; Howard *et al.,* 2011; Van der Spoel and Dadon, 1999). *C. pyramidata* f. *excise* has only previously been recorded in the Lazarev Sea. Interestingly, the maximum size of *C. pyramidata* f. *excise* forma in the literature is 20 mm long and 11 mm wide (MSIP, 2017), however, we show they can reach greater dimensions (24.17 mm long and 12.37 mm wide).

3.4.2 Temporal variation in abundance

The most abundant pteropod species throughout the entire year was *L. helicina* with 18,295 individuals being entrapped. Abundance was highly seasonal, with 66% of individuals being present in the summer, with 37% of individuals in early summer alone. *L. retroversa* was the next most abundant species of pteropod, although the total number of individuals was 6% of the total abundance of *L. helicina.* The abundance of *L. retroversa* was less seasonal, with 30% present in the summer, and similar numbers in the winter and autumn. *L. helicina* is a true polar pteropod compared to the sub-polar *L. retroversa,* and typically reaches high abundances south of the Polar Front (Akiha *et al.,* 2017; Bernard and Froneman, 2009; Hunt, 2008; Ward *et al.,* 2004; Dadon, 1990), while *L. retroversa* is more abundant in warmer waters north of the Polar Front (Van der Spoel, 1967, 1976; Chen and Be, 1964). *L. retroversa* tolerates a wider, but higher, temperature range than *L. helicina. L. retroversa* have been recorded to occupy temperatures between 5-9°C in the Southern Ocean (Dadon, 1990) and 2-18°C in the Northern hemisphere (Beckmann *et al.,* 1987; Bigelow, 1924; Chen and Be, 1964; Maas *et al.,* 2016) with an optimum of 2-7°C (Van der Spoel and Hayman, 1983). Mean temperatures in the winter at 200 m ranged between 0.93-1.10 °C which is lower than these ranges. Therefore, since the winter temperature range is at the lower end of the thermal tolerance of *L. retroversa,* it is possible that these individuals are not performing optimally, which may also explain why abundance is more generally lower than *L. helicina*.

There was a sudden drop in the abundance of *L. helicina* in early autumn, with the abundance in April being 97% lower than that in March. This sudden drop in abundance may well correspond to a sedimentation peak phenomenon, which has previously been observed within deeper (>1000 m) sediment traps the same time of year (Accornero *et al.*, 2003; Collier *et al.,* 2000; Gardner *et al.,* 2000). Peak sedimentation of pteropods within sediment traps has been observed in the autumn both within the Southern Ocean (Accornero *et al.,* 2003; Collier *et al.,* 2000; Gardner *et al.,* 2000) and the North-Eastern Atlantic (Bathmann *et al.,* 1991). This sedimentation peak has been postulated to occur due to: 1. a fatal

environmental perturbation; 2. or a 'pre-programmed' die-off (perhaps after spawning); 3. or an ontogenic vertical migration to deeper/much shallower waters; 4. or a starvation event or relocation in response to a concurrent decline in food supply (Maas *et al*., 2011; Hunt *et al.,* 2010; Seibel and Dierssen, 2003; Gilmer and Harbison, 1986). The feasibility of each of these scenarios will be discussed over the following paragraphs.

No significant difference in oxygen concentration, temperature at 200 m or pH between each month was found. However, there was a drop in mean sea surface temperature (3.5°C from 4.1°C) alongside increased temperature fluctuation (to 1°C) after May. Temperature has been shown to be an important influence on pteropod abundance and metabolic rate (Wang *et al.,* 2017; Maas *et al.,* 2011). However, *L. helicina antarctica* are true polar pteropods and are commonly found in temperatures down to -2°C in the Ross Sea (Maas *et al.,* 2011; Seibel *et al*., 2007, 2012) which means the temperatures experienced are within their thermal tolerance. Therefore, the sudden decline in abundance of *L. helicina* was not likely due to a fatal environmental perturbation.

It is possible that a mass die-off of adult individuals occurs at the end of autumn after a period of prolonged spawning, however, adult *L. helicina* were not observed in the current study, only immature juveniles. Furthermore, Collier *et al.,* (2000) found that large autumnal flux of pteropods within sediment traps in the Ross Sea mainly comprised of juveniles. Since individuals at P3 are juveniles, there is no reason for individuals to undertake a pre-programmed die-off before spawning as this is not an evolutionarily stable strategy. Therefore, the sudden decline in abundance of juvenile *L. helicina* was not due to a mass die-off after spawning or as a 'pre-programmed' life history event.

Individuals may have undertaken an ontogenic vertical migration to deeper or much shallower waters, reducing the number captured within the sediment trap at 400 m. Bednaršek *et al.* (2012a) collated a large database of global pteropod abundance data between 0 and 2000 m, which indicated no seasonal differences in pteropod depths however, this was averaged over numerous species and

regions which could have masked regional migration events. Ontogenic migration is the vertical movement of an organism with development, where adults often reside at deeper depths than the juvenile stage. Individuals were in early juvenile phase, with possibly a year before reaching adulthood (see Section 3.4.8.), which does not correspond to a specific developmental milestone therefore, it is unlikely that the decline in abundance was due to an ontogenic migration.

It is most likely that individuals migrated out of the sampling area as a response to altered food supply. The phytoplankton bloom occurs from spring to late autumn, with the deterioration in the bloom intensity corresponding to the decline in the abundance of *L. helicina* (see Section 3.3.6.2.)*.* It is also likely that the composition of the phytoplankton bloom altered in late autumn (Kopczyńska *et al.,* 1998) so that is was less nutritious for pteropods. Since there was no increase in the number of dead *L. helicina*, individuals most likely migrated out of the sampling region (discussed further in Section 3.4.3.). Migration out of the sampling region was not universal, since numerous individuals were caught throughout the winter at 400 m, indicating a variety of strategies are adopted within the population of *L. helicina.*

3.4.3 Pteropod population dynamics

Limacina spp veligers (shell width <0.3 mm) and *L. helicina* populations were highly seasonal in abundance, being most abundant in the summer and early autumn. During these months, temperatures (surface and 200 m) and chlorophyll-*a* concentration were highest, while oxygen concentration and pH were lowest. Oxygen concentration and pH were lower in the summer, perhaps due to the breakdown of organic matter from the surface phytoplankton bloom event, indicated by the higher chlorophyll-*a* concentration, although this is mainly speculative. Primary productivity has previously been shown as an important factor in determining the abundance of pteropods (Seibel and Dierssen, 2003; Maas *et al*., 2011; Atkinson *et al.,* 1996) and is most likely to

contribute towards the intense seasonality of pteropod populations within the Scotia Sea.

Limacina adults in the Scotia Sea synchronised spawning with the phytoplankton bloom. The highest chlorophyll-*a* concentration occurred between November and February, which corresponds to spawning between November and March and the highest abundance of small juvenile *L. helicina*. Both spawning and growth of early life stages is energetically expensive, therefore, this strategy of spawning during periods of high food sources ensures the rapid growth of pteropod veligers to maturity (Manno *et al.,* 2017; Bednaršek et al., 2016; Seibel *et al.,* 2012). Early life stages may be particularly prone to starvation under less favourable environmental conditions (Gannefors *et al.,* 2005; Lischka *et al.,* 2011), therefore, timing spawning where conditions are closest to optimal would ensure maximum recruitment. This synchrony between phytoplankton blooms and spawning is common across a multitude of species (Starr *et al.,* 1990; Highfield *et al.,* 2010) and has been observed in both Arctic *L. helicina helicina* (Gannefors *et al.,* 2005; Kobayashi, 1974; Wang *et al.,* 2017) and Antarctic *L. helicina antarctica* (Akiha *et al.,* 2017; Bednaršek *et al.,* 2012b; Bernard and Froneman *et al.,* 2009; Accornero *et al.,* 2003). The summer phytoplankton blooms to the north of South Georgia occur regularly and may last between 4-6 months (Korb *et al.,* 2008; 2004; Atkinson *et al.,* 2001). Such prolonged and extensive bloom events support the protracted spawning observed for both *L. helicina* and *L. retroversa*. This contrasts with *L. helicina helicina* in Kongsfjorden, Svalbard which are mainly limited to a discrete spring spawning event due to the limited phytoplankton blooming period (Gannefors *et al.,* 2005; Hop *et al.,* 2002).

Mean chlorophyll-*a* concentration dropped from 1.7 mg m^{-3} to 0.9 mg m^{-3} in March, consequently there was a reduction in food supply. As pteropods could continue growth throughout the winter (see Section 3.4.7), individuals are able to overcome this food shortage either through utilisation of lipid reserves, or the ability to survive on an alternative food supply. Healthy *L. helicina antarctica* at −2°C (Maas *et al.*, 2011) and 4°C (Bednaršek *et al.*, 2012a) could survive starvation for up to 1 month by living off energetic reserves. Furthermore, lipid

reserves were utilised by Arctic *L. helicina* during life stage transitions as well as during the polar winter (Gannefors *et al.,* 2005). Gut content analysis has revealed that pteropods can scavenge particulate matter as well as small organisms, selecting food based on size rather than its substance (Kobayashi, 1974; Gannefors *et al.,* 2005; Noji *et al.,* 1997). Therefore, it is likely that individuals in the Southern Ocean utilise both these strategies, switching to an alternative food source when phytoplankton becomes scarce, as well as utilising lipid reserves if needed.

The reduction in abundance observed in early autumn of *L. helicina* may either be due to individuals being advected out of the sampling area due to individuals not building up sufficient lipid reserves before the drop in food supply and being unable to undergo metamorphosis or survive a short starvation period. Since there was no concurrent change in current speed, I believe the latter is most likely. This would not be reflected in a sudden increase in dead individuals since the depletion of energetic reserves is a gradual process. Thecosome pteropods are negatively buoyant, so to maintain the same depth in the water column, active swimming must be maintained for 25% of the time (Seibel, 2007; Conover and Paranjape, 1977). With less energy or poor health, individuals are unable maintain this costly swimming and buoyancy regulation regime and so gradually sink from the upper water column and out of the sampling region. Individuals which enter the trap will still be alive and classed as swimmers, despite being in poor health while the number of dead individuals will not increase. Meanwhile, the number of dead individuals will increase in the deeper sediment traps, explaining the sedimentation peak phenomenon (Accornero *et al.,* 2003; Collier *et al.,* 2000; Gardner *et al.,* 2000). Unfortunately, the deeper sediment trap on the P3 mooring was not inspected for this phenomenon therefore, this relationship remains speculative.

3.4.4 Seasonal trends of cohorts and life stages

There were four distinct generations of *L. retroversa* over the year covering all life stages, with no overlapping of cohorts. These cohorts were identified between December- January (Summer; LR1), February- April (Autumn; LR2), May- October (Winter; LR3) and November (Spring; LR4) (see Section 3.3.5.2.). Between December and March, there was a continuous presence of veligers and recruitment into the smaller size classes, however, cohort LR1 and LR2 are distinct groups since all the size classes in February were smaller than those in January. Furthermore, the largest size class in January, which comprised of adults, was not present in February. Since veligers were only found until March, spawning must have ceased at this point as well. While it is possible that the relevant individuals were advected away from the sampling areas at this point, I believe this is unlikely since there is no corresponding change in the current speed or environmental conditions. Since a smaller size class was recruited in April, these individuals must have been spawned in March, which defines the LR3 cohort. LR2 adults that were present in April 'disappeared' after this spawning event. Finally, no smaller individuals were recruited during the winter indicating that LR4 is one cohort of *L. retroversa.* This cohort increased in size until the spring where adults, like for the other cohorts 'disappeared' and veligers were entrapped once again, signalling spawning. This defines the final cohort (LR4) although, since sampling did not continue, unclear whether this cohort is fully represented.

At the end of each growth period, adult individuals 'disappeared' from the sampling region. The disappearance of adult pteropods from the upper water column has previously been attributed to 1. a die-off after spawning (Gannefors *et al*. 2005; Kobayashi, 1974; Dadon and de Cidre, 1992) or 2. an ontogenic migration to deeper water. No dead or predated individuals larger than 1 mm were found in any month except May so it is unlikely that a die-off occurred after spawning. Therefore, it is most likely that adult *L. retroversa,* like many other *Limacina* species worldwide (Spoel and Heyman, 2013; Almogi-Labin *et al*., 1988), undergo an ontogenic migration to deeper water after spawning.

Adults of *L. retroversa* were relatively more abundant within the winter than in the other seasons, since there were few veligers and little recruitment into the juvenile stage. Juveniles then continued to grow and were then recruited into the adult size class. I speculate that overwintering adult pteropods delayed spawning until conditions were more favourable for the survival of more vulnerable early life stages in the subsequent spring/summer, which was also observed by Dadon and de Cidre, (1992) in the Argentine Sea.

The overwintering *L. retroversa* adults did not undergo migration to deeper waters until after spawning, instead, staying within the sampling region during the winter. During the winter, adults continued to increase their shell size (see Section 4.3.7.2.) which enables a greater number of eggs to be spawned once conditions are more favourable (Lalli and Gilmer, 1989; Lalli and Wells, 1978).

Five groups of *L. helicina* were identified from which part of the life history can inferred (LH1-5) (see Section 3.3.5.1.). However, no adult or large juvenile *L. helicina* were entrapped over the sampling period, therefore the full life history or specific cohorts could not be tracked. Group LH1 are small juveniles which are recruited from the veliger phase between December and March. The group LR2 comprises of larger *L. helicina* juveniles. These larger juveniles were present throughout the summer and autumn suggesting there was continuous recruitment into this size group. As both LH1 and LH2 coincide throughout the summer and early autumn, a specific cohort cannot be tracked. However, since adults must also be present during this period for spawning to occur, there is an overlap of veligers, juveniles and adults. This contrasts to *L. retroversa* where no overlap was found between each cohort.

No small juveniles were entrapped in April, but they were present once again in May (LH4) and June (LH3), with those in June being smaller than those in May. Therefore, these are likely to be distinct cohorts. Veligers were only found until March therefore, individuals in LH3 and LH4 must have emerged from their egg sacs during March at the latest, which allows calculation of growth rates (see

Section 3.4.7.1.). It is likely that individuals in LH3 and LH4 were recruited into the smaller juvenile size groups of LH5 in July, however, at this point they cannot be singled out. Since veliger presence, and so spawning, ceased in March, LR5 represents a distinct subpopulation of *L. helicina* juveniles throughout the winter and spring. Within LR5 there are two growth strategies, with some entering diapause (a state of suspended growth) throughout the winter and early spring, and others continuing to grow. This suggests that a variety of growth strategies are adopted by *L. helicina* however, it should be noted that no adult *L. helicina* were entrapped and so these samples do not represent the entire *L. helicina* population meaning there is large amount of uncertaintly surrounds these conclusions.

While adults of *L. retroversa* were present within the sediment traps, those of *L. helicina* were not. However, this must have been due to sampling, since adults need to be present for spawning to occur. Interestingly, Akiha *et al.* (2017) also did not find any adult *L. helicina* within sediment traps, despite capturing them in plankton nets in December in the South Atlantic, supporting that this bias originates from using a sediment trap. It is possible that *L. retroversa* adults were entrapped, and *L. helicina* were not because of the ability of adults to escape, although this is speculative. However, *L. helicina* adults are much faster and stronger swimmers than *L. retroversa,* having a swimming speed of 21 mm/s as opposed to 8 mm/s and so they are more likely to be able to escape the sediment trap (Adhikari *et al.,* 2016; Gilmer and Harbinson, 1987). Due to this bias in sampling swimmers, sediment traps may only be useful for assessing the life cycle of smaller organisms with weaker escape abilities.

3.4.5 Spawning behaviour

The continuous presence of *Limacina* spp veligers and small juveniles of both *L. helicina* and *L. retroversa* (see Section 3.4.2.) indicates protracted spawning throughout the spring and summer. Spawning was identified via the presence of veligers (individuals with a shell width <0.30 mm), since it takes 3 days for *L. retroversa* to hatch from egg sacs and another 3-4 days to develop shells (at ~4-

8 ° C) (Thabet *et al.,* 2015; Lebour, 1932) while *L. helicina* veligers take 7 days to emerge, but already with a shell of 0.08 mm (Pasternak *et al*, 2017; Paranjape, 1968) (see Section 3.4.7.3). Spawning concluded by autumn and winter since 99.55% of *Limacina* veligers were found between November and March. A clear peak in *Limacina* veliger abundance in January signalled that the majority of *Limacina* egg masses were released in December and January, in synchrony with the phytoplankton bloom (see Section 3.4.3.). Spring and summer spawning agrees with previous studies on *L. retroversa australis* within the Argentinian Sea (Dadon and Cidre, 1992). Bednaršek *et al.* (2012b) inferred from net samples in the Scotia Sea that the spawning of *L. helicina antarctica* was discrete, occurring predominantly during the summer. While this corresponds to the peak of spawning at P3, the continuous recruitment of small *L. helicina antarctica* juveniles indicates that spawning occurred over a much longer period (spring to early autumn). It is likely that the difference in spawning period between Bednaršek *et al.* (2012b) and this study arises from the differences in scale utilised. The sediment trap samples represent the region north of South Georgia where phytoplankton blooms are intense and prolonged, supporting spawning and early stage growth for a prolonged period (see Section 3.4.3.). Bednaršek *et al.* (2012b) generalised spawning time estimates over the entire Scotia Sea, which has large regions with shorter, less intense phytoplankton blooms, therefore, on average spawning is limited to the summer.

Hunt *et al.* (2008) and Van der Spoel (1967) postulated that *L. helicina antarctica* could spawn twice in a year, with the first occurring during the summer, and the second in the autumn. Thereafter, veligers that emerge during the autumn enter a diapause and overwinter without growth. The autumnal spawning theory was based on observations of Arctic *L. helicina helicina* (Kobayashi, 1974; Gannefors *et al*., 2005) and limited winter net samples in the Southern Ocean (Hunt *et al.,* 2008). While some spawning occurred in early autumn at P3, *L. helicina antarctica* veligers continued to grow and overwintered as juveniles rather than veligers. Early life stages may be particularly prone to starvation when food resources are scarce since they have smaller energetic reserves than later life

stages (see Section 3.4.3.), therefore, both *L. retroversa* and *L. helicina* might have overwintered at P3 as juveniles and adults to reduce this risk of starvation.

3.4.6 Variation in growth rates

The shell morphometric analyses (see Section 3.3.3.) revealed that both *L. helicina* and *L. retroversa* shell width/spire height, diameter, area and whorl number all increased linearly over each life stage. Furthermore, there was little change in these relationships over the year, indicating that growth is mostly uniform. In the literature a number of shell morphometric measurements are adopted being 1) the number of whorls (Chen and Be, 1964), 2) line of aperture/shell width (Lebour, 1932; Hsiao 1939; Conover and Lalli, 1974) and 3) shell diameter/spire height (Lalli and Wells 1978; Beckmann *et al.*, 1987). Here, it is demonstrated that these parameters are highly correlated to growth and a simple conversion can be used for comparison.

3.4.6.1 L. helicina

The only other study which investigated the growth of *L. helicina antarctica* in the Scotia Sea was performed by Bednaršek *et al.* (2012b). This study combined 50 plankton nets samples taken between October and March (1996-2005) (excluding November) from across the Scotia Sea to examine the population dynamics of *L. helicina.* Bednaršek *et al.* (2012b) measured shell diameter rather than shell width, therefore the conversions calculated in Section 2.3.4. were used to allow direct comparisons of shell size. Bednaršek *et al.* (2012b) identified three cohorts from all the plankton samples combined, being small juveniles (0.03-1 mm; "G2"), larger juveniles (1.5-4 mm; "G1") and adults (>4 mm; "G"). Based upon this, the sediment trap samples mainly included individuals from the G2 generation and a small number from G1. The absence of "G" individuals from the sediment trap samples is likely due to a sampling bias of the sediment trap (see Section 3.4.2.).

The rate of growth for veligers to reach the small juvenile size group (LH3 and LH4) was calculated as between 0.008 and 0.005 mm/day (LH3) or 0.004 and

0.003 mm/day (LH4) depending on whether spawning occurred in February or March (see Section 3.3.5.1.). These growth rates are based upon a time-lag between the last spawning event and the recruitment of LH3 and LH4 therefore there is greater certainty in the upper limit than the lower. Bednaršek *et al.* (2012b) calculated the growth rate of the equivalent size cohort ("G2") as 0.007 mm/day, based on a cohort analysis. During the autumn and winter, they estimated the same growth rate (0.007 mm/day) to occur, based on the minimum size that individuals reached in the spring (Figure 3.20). Averaging growth over autumn and winter assumes that it is constant, however, Section 3.2.5.2. suggests that *L. retroversa's* growth was highly variable with season, with a sudden increase in rates during the spring and a decrease in the autumn, corresponding to an increase and decrease in chlorophyll-*a* concentration, respectively (see Section 3.3.6.2). The growth rates estimated for LH3 occurred at the end of summer through to early autumn, and agree with the estimates by Bednaršek *et al.,* (2012b). However, the growth rates estimated for LH4 at P3 during the autumn were lower than those estimated by Bednaršek *et al.,* (2012b) due to the difference in the sampling season and period covered. Based upon the difference in growth rates between LH3 and LH4, it is possible that there is variation in growth rates with season, as observed for *L. retroversa* (see Section 3.2.7.1.).
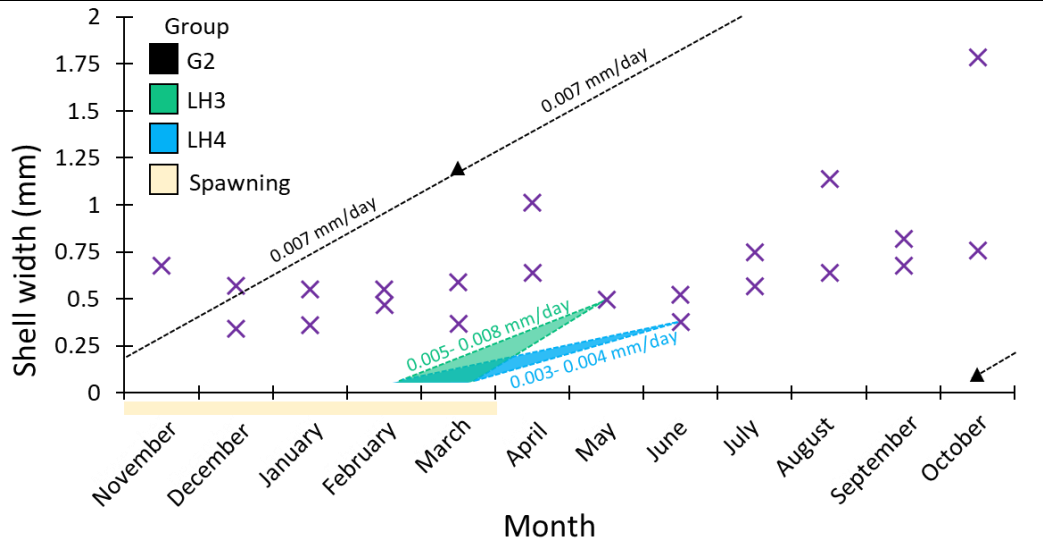
Figure 3-20. A comparison of average *Limacina helicina antarctica* shell growth rates (dashed lines) estimated within the current Chapter (groups **LR3** and **LH4**) and by Bednaršek *et al.* (2012b) (group **G2**). The purple crosses (**X**) are the average shell widths of *L. helicina* groups entrapped within a sediment trap at site P3 (Scotia Sea; Southern Ocean). The black triangles (▲) are the maximum and minimum shell width of the G2 size group estimated from individuals collected in plankton tows across the Scotia Sea.

3.4.6.2   *L. retroversa*

Four, non-overlapping cohorts of *L. retroversa* were identified (LR1-LR4) with maximal spire heights and growth rates varying with season. The maximal spire height of *L. retroversa* cohorts in the winter and autumn were larger than those in the summer and spring (2.29 mm, 1.96 mm, 1.17 mm and 1.10 mm, respectively). Arctic *L. retroversa* that have been observed spawning had spire heights of 1.3-2 mm (Pasternak *et al.*, 2017; Lalli and Wells, 1978) with the largest reported being >2.5 mm (Thabet *et al.,* 2015; Hsiao, 1939; Redfield, 1939). In contrast, Sub-Antarctic *L. retroversa* reach larger sizes of 1.25-3.2 mm (Dadon and de Cidre, 1992) and 1.10-2.29 mm (*Current study)*. Since individuals in the Sub-Antarctic do not experience the polar night, and the limited food resources that accompany this, they are able to continue growing during the winter rather than entering diapause (Lischka and Riebesell, 2012; 2017), thus attaining a larger shell size by spring. In many gastropods, fecundity is directly related to gonad volume, which increases with size (Ghiselin, 1969; Dillon, 2000), therefore investing in shell growth while conditions are less suitable for more

vulnerable early life stages, increases possible reproductive output during the spring as a larger shell size will be ascertained and thus greater gonad volume. Based on the maximum cohort size before "disappearance", individuals that spawned during the spring were larger in both the current study (2.19-2.42 mm) and in the Argentine Sea (1.99-3.20 mm) (Dadon and de Cidre, 1992) compared to those that spawned in the summer (1.15-1.19 and 1.25-1.80 mm, respectively). It appears that in the summer, *L. retroversa* adopt a different strategy which involves growing rapidly until maturity is reached and spawning as soon as possible. This allows veligers to hatch during the summer, where conditions are more favourable for growth and survival, so that these individuals can reach juvenile phase before the winter.

Dadon and de Cidre (1992) performed the only other study on the *L. retroversa* life cycle and seasonal growth rates in the Sub-Antarctic. They found that *L. retroversa* in the Argentine Sea had a two-generation per year life cycle, where individuals that emerged in the spring spawned by the summer (A1) and those that emerged in the summer overwintered and spawned in the spring (A2). This was based on 4 sampling times per year and so uncertainty surrounds these estimates. The minimum spawning spire heights were given, however, all other spire heights and spawning events were only presented for each season (Figure 8 in Dadon and de Cidre, 1992). From this figure, spire heights of spring spawning individuals (A1) ranged between 1.99-3.2 mm and spire heights of summer spawning individuals (A2) ranged between 1.25-1.8 mm. If it is assumed that spawning occurred at the beginning of spring (01/10/1978) and the end of summer (01/02/1979), with emergence after a week (see Section 3.4.7.3.), then the spring emerging cohort A1 would have a maximum growth rate of 0.008 mm/day to reach 1.25 mm and 0.012 mm/day to each 1.8 mm (Figure 3.21). Following the same assumptions, the cohort A2, which emerged in the summer and spawned in the spring would have a minimum growth rate of 0.009 mm/day to reach 1.99 mm and 0.015 mm/day to reach 3.2 mm.

In the Scotia Sea, protracted spawning of *L. retroversa* occurred between November and March, indicated by the constant recruitment of veligers into the

small juvenile size groups. In comparison, there were two discrete spawning events in the Argentine Sea, occurring in September and February. The spring discrete spawning event in the Argentine Sea corresponds with the rapid increase in temperature and primary production in September (Dadon, 1990), allowing this generation of *L. retroversa* to take advantage of the abundant food supply during the summer for rapid spawning by February. In the Scotia Sea the bloom event is intense and prolonged, allowing veliger growth to continue over a longer period.

Each of the cohorts at P3 had seasonal variation in shell growth rates (Figure 3.21). Cohort LR3 (late autumn- early spring) had the slowest rate of shell growth (0.010 mm/day) (Figure 3.21) however, if the growth rates of LR3 are re-calculated for each season, then the growth rate for the winter drops to 0.008 mm/day and increases during the spring at 0.013 mm/day. In the Argentine Sea, the difference between spire heights within cohort A2 was only 0.1 mm between autumn (0.3-2.4 mm) and winter (0.3-2.5 mm) with growth to 3.2 mm seemingly occurring in spring alone (Figure 3.21). In the Arctic, during the polar night, *L. retroversa* and *L. helicina* can cope with little to no food through reducing metabolism, shell growth and relying on internal lipids reserves during the winter (Lischka and Riebesell, 2012; 2017). However, the Sub-Antarctic does not experience the polar night so it is likely that there was a sufficient food supply sustain winter shell growth.

Based upon season, cohort A1 (spring-summer) within the Argentine Sea is the equivalent to LR1 and LR4 in the Scotia Sea while cohort A2 (autumn-winter) would be equivalent to LR2 and LR3. The greatest rate of shell growth occurred during the spring in both the Argentine Sea and the Scotia Sea. Despite this, the rate of growth was much higher in the Scotia Sea (0.019-0.024 mm/day) than the Argentine Sea (0.008-0.012 mm/day). Furthermore, the autumn-winter growth rates were similar between the Argentine Sea (0.009-0.015 mm/day) and Scotia Sea (0.010-0.018 mm/day), however the rates in the Scotia Sea were greater over all. These increased rates of growth are likely to arise from the phytoplankton bloom in the Scotia Sea being more prolonged and stable

between spring and autumn (see Section 3.3.6.2.) in comparison to the

Argentine Sea, which has more defined phytoplankton blooms (Dadon, 1990;

Dadon and de Cidre, 1992; Lutz *et al.,* 2009).
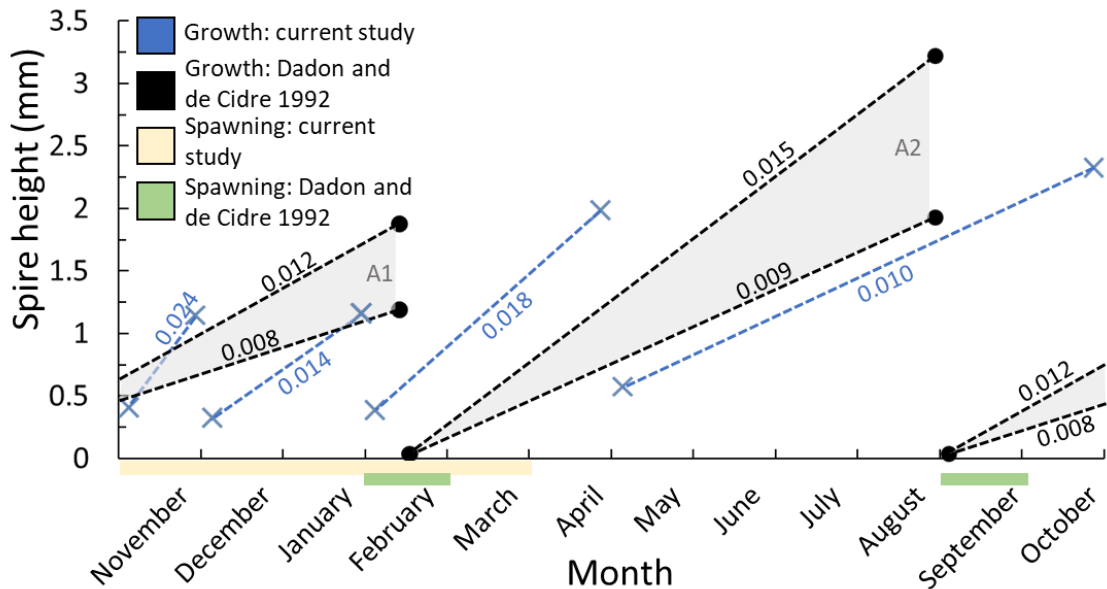
Figure 3-21. A comparison of average shell growth rates (dashed lines, mm/day) estimated within the Scotia Sea (**Blue**) (Current Study) and in the Argentine Sea (**Black**) (Dadon and de Cidre, 1992). The blue crosses (**x**) are the mean spire heights of *L. retroversa* cohorts entrapped within a sediment trap at site P3 (Scotia Sea). The black circles (●) are the maximum and minimum spire heights of the spring spawning (A1) and summer spawning (A2) cohorts estimated from individuals entrapped in plankton tows within the Argentine Sea (Dadon and de Cidre, 1992).

3.4.7 Longevity

Based on the cohort identification, it took between one (LR4) and seven (LR3)

months for *L. retroversa australis* to transition from the small juvenile stage to

adult stage however, since adults 'disappeared' from the samples, there was no

evidence of a die-off. Therefore, there is a large degree of uncertainty surrounding

this conclusion. This 'disappearance' was also evident in samples from the

Argentine Sea, which Dadon and de Cidre, (1992) concluded was due to a die-off

based upon observations of *L. retroversa retroversa* in the Arctic. Therefore, it is

most likely that *L. retroversa* in the Scotia Sea has a longevity of 1-7 months. Dadon

and de Cidre (1992) concluded that individuals lived for a year, with two

generations however, it is unclear how the authors came to this conclusion. In the Northern hemisphere, *L. retroversa retroversa* have longevities between 0.5 years (Thabet *et al.,* 2015) and 1 year (Lebour, 1932; Hsiao, 1939), which agrees with the longevity estimates in the Scotia Sea.

The longevity of *L. helicina antarctica* can be calculated using growth rates of LH3 and LH4 and extrapolating from these how long it would take to reach the maximum shell width. However, this method leads to a large degree of uncertaintly and so interpretation of longevity should be taken with caution. This method was also used by Bednaršek *et al.,* (2012b) for *L. helicina antarctica* in the Scotia Sea. Lalli and Wells (1978) reported of individuals with a shell width of >6 mm spawning eggs, therefore with a growth rate of 0.006 mm/day it would take 2.7 years to reach this size or with a growth rate of 0.008 mm/day, it would take 2.1 years to reach this size. This interpretation agrees with the longevity estimates of Bednaršek *et al.* (2012b) (2.5-3 years), however, Hunt *et al.* (2008) suggested that individuals did not live longer than 1 year (Table 3.1). The lower longevity predicted by Hunt *et al.,* (2008) could be a product of generalising over the entire Southern Ocean as opposed to just the Scotia Sea as performed by Bednaršek *et al.* (2012b), however, the methodologies of Hunt *et al.* (2008) for estimating longevity are unclear making any comparisons difficult.

3.4.8 Life cycle overview and conceptual schematic

Taking into consideration the life stage abundance, growth rate and spawning behaviour of *L. retroversa,* there is a seasonal life cycle strategy. Individuals that reach adulthood in late summer/autumn, stay in the upper 400 m and overwinter as adults until the spring, where they spawn. The veligers then hatch and undergo a rapid period of growth to reach adulthood in the summer and spawn. Veligers that hatch in late summer will then reach adulthood in the autumn and thus overwinter. This means *L. retroversa* in the northern Scotia Sea live for 1-7 months depending on the season (Figure 3.22).
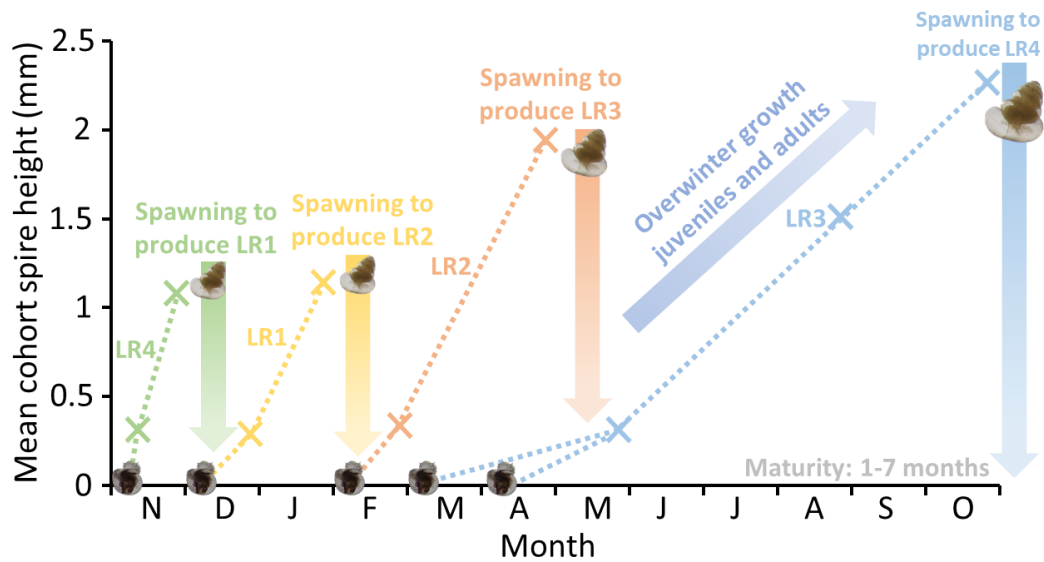
Figure 3-22. A conceptual schematic of the life cycle of *L. retroversa* captured within a sediment trap deployed at P3 (Scotia Sea; Southern Ocean) at 400 m depth between December 2014 and November 2015. **Crosses** represent the mean spire height of each growth stage computed by a Mixture analysis for each month with **dashed lines** indicating the average growth rate between these stages. Four separate cohorts of *L. retroversa* were identified between December- January (Summer; LR1; yellow), February- April (Autumn; LR2; orange), May- October (Winter; LR3; blue) and November (Spring; LR4; green).

Conversely, *L. helicina* populations are most likely made from several overlapping generations, although the lack of representation from all life stages in the samples adds uncertaintly to this. Spawning occurs in between November and May with several cohorts of small juveniles being recruited into the population. These individuals grow throughout the spring/summer period until the autumn where most individuals migrate to deeper or shallower water to overwinter. Those that reside in at 400 m continue to grow to large juveniles although, they are not large enough to spawn by the end of the winter. Based on the highly extrapolated growth rates it takes between 2.7 and 2.1 years to reach adulthood, although caution should be taken with these estimates due to a high degree of uncertainty (Figure 3.23).
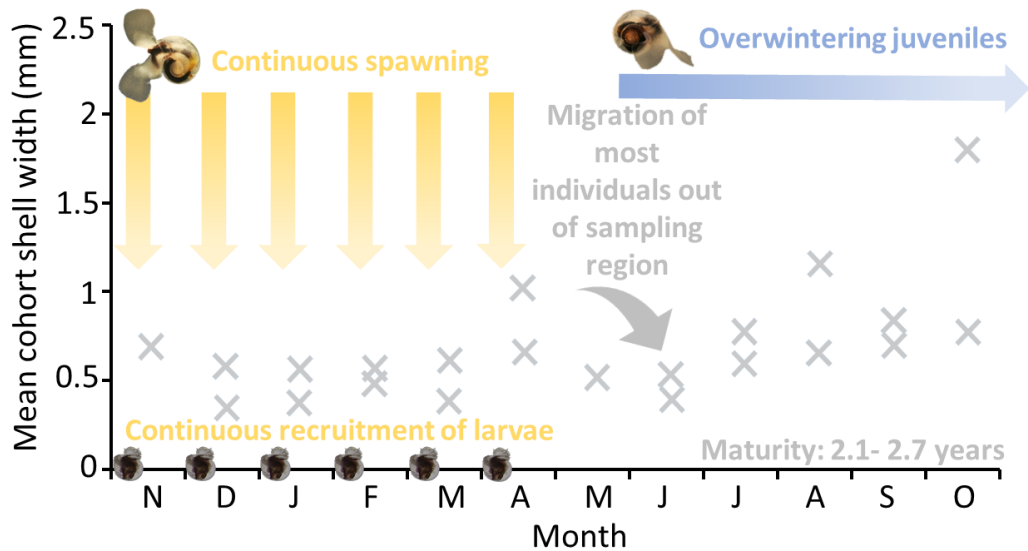
Figure 3-23. A conceptual schematic of the life cycle of *L. helicina* captured within a sediment trap deployed at P3 (Scotia Sea; Southern Ocean) at 400 m depth between December 2014 and November 2015. **Crosses** represent the mean shell width of each growth stage computed by a Mixture analysis for each month with **dashed lines** indicating the average growth rate between these stages.

A strategy with overlapping generations is more robust against unfavourable environmental conditions in comparison to one without overlap. For *L. helicina,* if a single cohort is removed there is potential for its replacement, since all life stages co-exist, therefore, the population will survive. Conversely, there is no overlap of life stages in the life cycle of *L. retroversa*, meaning if one cohort is removed, there are no replacements. If such an event occurred when *L. retroversa* are at early life stages, and thus particularly vulnerable to adverse conditions (Manno *et al.,* 2017; Thabet *et al.,* 2015), this could cause a population bottleneck or even a local extinction, which has been observed for *Limacina* by Maas *et al.* (2011) and Seibel and Dierssen (2003). Despite this, the repeated or prolonged exposure to unfavourable conditions is likely to impact all cohorts and if there is no recruitment over a prolonged period, the population of *L. helicina* will also be under threat.

Undersaturation events in surface waters are expected to occur first during the winter in the Southern Ocean, and then become more prolonged and intense with time (McNeil and Matear, 2008; Landschützer *et al.,* 2018). Therefore,

stages and cohorts which overwinter are most at risk. Current estimations vary as to whether *Limacina* spp. overwinter as larvae, when food availability is naturally low or only occur during the summer, when it is high (Hunt *et al.,* 2008; Bednaršek *et al.,* 2012b; Wang *et al.,* 2017; Kobayashi, 1974). However, I show that *L. retroversa* and *L. helicina* overwinter as juveniles and adults, making these stages most vulnerable to environmental change first. Numerous studies have found a decrease in calcification, metabolism and an increase in mortality under ocean acidification conditions (See Table 1.3). Stage specific survival rates may have serious consequences on demographics. For *L. retroversa,* the viability and survival of overwintering stages is vital for successful spawning the following spring, and thus long-term population stability. The capacity of pteropods to maintain a viable population distribution and abundance in the Southern Ocean depends on their capability to recruit successfully. Reduced calcification and metabolism could reduce the maximum shell size attained by spring, which is directly linked to the number of eggs produced, thus reducing productivity (Ghiselin, 1969; Dillon, 2000). Furthermore, exposure of adults and juveniles to environmental drivers during the winter could alter vulnerability of later developmental stages through latent effects (such as survivorship and shell size), adding to the overall impact (Kroeker *et al*., 2013; Suckling *et al*., 2014).

3.4.9 Concluding remarks and summary

Chapter 3 presents an overview of the presence and abundance of pteropods at P3, in order to elucidate their population dynamics and life history. An understanding of pteropod population dynamics in areas where they are keystone components of ecosystem (Lalli & Gilmar 1989; Hunt et al., 2008; Manno et al., 2017), is vital in order to discern any responses or vulnerabilities to predicted warming and acidification.

L. helicina dominated pteropod populations, with overall abundance being greatest in the summer and lowest in the winter. *L. retroversa* were the next most abundant, although numbers were much less than *L. helicina* and did not vary with season. Additionally, the thecosome pteropods *Clio piatkowskii*, *Peraclis* cf. *valdiviae* and *C. pyramidata* f. *excise* were recorded within the Scotia

Sea for the first time. A sudden drop in abundance occurred in the autumn which corresponded to the sedimentation peak phenomenon which was most likely due to an ontogenic migration event in response to a concurrent drop in food supply. The spawning of both *L. helicina* and *L. retroversa* was protracted and synchronised with the phytoplankton bloom between spring and early autumn, overwintering as juveniles and adults.

There were four distinct generations of *L. retroversa* over the year with no overlapping cohorts and a seasonal life cycle strategy which is completed in 1-7 months. Those which are spawned in the spring and summer rapidly grow to maturity, utilising the abundant food supply, however, they reach a smaller size than the autumn and winter cohorts, which grow at a slower rate. The cohorts of *L. helicina* were overlapping, with continuous recruitment into the population between the spring the autumn. No adult or large juvenile *L. helicina* were entrapped over the sampling period therefore, the full life history or specific cohorts could not be tracked. Consequently, it should be noted that there is uncertainty in outlining *L. helicina* cohorts. Based on highly extrapolated growth rates, it takes 2.1- 2.7 years to spawn.

This study provides new insight into the population dynamics and life history of pteropods in the northern Scotia Sea and assesses the relevance of sediment traps as effective tools for monitoring remote populations of pteropods which might otherwise be inaccessible for net sampling.

4   A historic baseline for the vertical and biogeographical distribution of pteropods across the Polar Front

4.1 Introduction
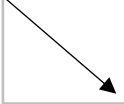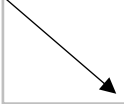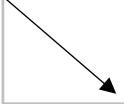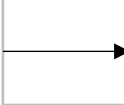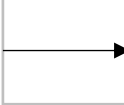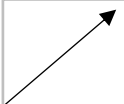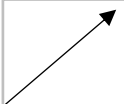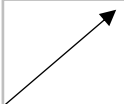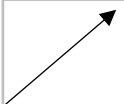
4.1.1 Euthecosome pteropods as indicators for future change in high-latitude ecosystems

Climate change is predicted to severely alter contemporary marine ecosystems (Doney *et al.,* 2012; Hoegh-Guldberg and Bruno, 2010). Specifically, changes in temperature, pH, oxygen concentration and the availability of food will modify ecosystem structure, function and adaptive capacity (IPCC, 2014). To establish a means of evaluating and managing the effects of these environmental drivers on ecosystems, a suite of environmental indicators have been proposed, which are often species that are particularly vulnerable to environmental change. These species act as an early warning signal, providing key information on the assessment of ecosystem health (Halpern *et al.,* 2012; Harwell *et al.,* 1999). Ecosystem health is a term used in environmental management where the goal is for an ecosystem to be productive, resilient and organised (Rapport, 1989).

Euthecosomatous (shelled and holoplanktonic) pteropods have been identified as potential candidates for indicating the onset of ocean acidification (Bednaršek *et al.,* 2017), since they have been shown to decrease calcification (Comeau *et al.,* 2009; 2010; Lischka *et al.,* 2011) and exhibit shell dissolution (Bednaršek *et al.,* 2012; Lischka and Riebesell, 2012) within waters undersaturated with respect to aragonite, $\Omega_{Ar} \leq 1$. Such alterations to pteropod shells could impact swimming, ability to evade predation, feeding and sinking rates (Adhikari *et al*., 2016; Lalli and Gilmer, 1989) (Section 1.6). Furthermore, when pteropods are exposed to multiple environmental drivers, changes in physiology, survival and vertical distribution have been observed (Section 1.1.3). These studies contribute to our growing understanding of the response of pteropods to environmental change, however, they focus on short term responses (<1 month) in experiments conducted at the physiological and individual level (Manno *et al.,* 2017). Long-term time series (16- 58 years) of pteropod abundance have assessed population level responses to environmental conditions (Table 4.1). Such long-term studies have indicated a variety of trends with no strong evidence linking abundances to ocean acidification or warming. However, this lack of association between

abundances and oceanic change is possibly due to the use of large regional averages to represent environmental conditions, and generalisation across multiple species and life stages, illustrating the need for more regional, species-specific studies. As well as variations in abundance distribution, pteropods can also respond on a population level to environmental change through the alteration of vertical distribution, phenology of life history events (e.g. spawning), latitudinal range and local extinctions, however, currently our knowledge of these aspects is lacking.

Table 4.1. An overview of long-term time series studies investigating the change in abundance of pteropods over time. A mixture of taxonomic resolutions were utilised between studies so the smallest resolution for each study is given (for example 'Thecosomes' include all shelled pteropods while 'Limacinidae' includes only *Limacina* species). The location abbreviations are: NEA: Northeast Atlantic, NWA: Northwest Atlantic, CC: California Current, NEP: Northeast Pacific, MED: Mediterranean Sea

Pteropods	Location	Abundance	Period	Study
Thecosomes, *C. limacina*	NEA	↘	1958- 2010	Beare *et al.,* 2013
Limacinidae, *C. limacina*	NEA	↘	1960- 2009	Beaugrand *et al.,* 2013
L. helicina helicina	NEP	↘	1979-2010	Mackas and Galbraith, 2012
Limacinidae	NWA	→	1958- 2006	Head and Pepin, 2010
Thecosomes	NEA	→	1977-2004	Kane, 2007
L. helicina	CC	→	1951- 2008	Ohman *et al.,* 2009
L. helicina antarctica, *S. australis*	SWA	→	1994- 2009	Loeb and Santora, 2013
Thecosomes	CC	→	1951- 2005	Lavaniegos and Ohman, 2007
Thecosomes	NWA	↗	1977-2009	Kane, 2011
C. pyramidata	NEP	↗	1979-2010	Mackas and Galbraith, 2011
C. pyramidata	CC	↗	1951- 2008	Ohman *et al.,* 2009
Limacinidae, Cavoliniidae, Creseidae	MED	↗	1967-2003	Howes *et al.,* 2015

Baseline datasets are vital starting points for monitoring population level changes associated with environmental climate change. These datasets outline the distribution and abundance of an organism before exposure to an event. The need to establish a baseline for pteropod population dynamics and distributions is especially pressing in rapidly changing regions such as in high-latitudes (Manno *et al.,* 2017; Doney *et al.,* 2009; Fabry *et al.,* 2009). These ecosystems are forecast to be affected by ocean acidification soonest, since low temperatures enhance the solubility of carbon dioxide and carbonate ion concentrations are already naturally low (Fabry *et al.,* 2009). *In-situ* dissolution of pteropod shells has already been observed where undersaturation is enhanced due to upwelling of deep-water (Bednaršek *et al*., 2012a) and beneath sea ice (Peck *et al*., 2016). Furthermore, polar regions are some of the fastest warming areas on earth, meaning organisms here are facing a multitude of synchronous changes to their environment (Bromwich *et al.,* 2013; Huang *et al.,* 2017).

The Southern Ocean is experiencing warming and acidification at one of the highest rates of any ocean. Within the Scotia Sea, there has been an increase in temperature of ~2.3°C (winter) and ~0.9°C (summer) between 1925- 2006 (<100 m) (Whitehouse *et al.,* 2006; 2008), while seasonal undersaturation of aragonite is expected by 2038 (McNeil and Matear, 2008). Euthecosome pteropods are key ecological species within the Southern Ocean (Lalli & Gilmar 1989; Hunt et al., 2008; Manno et al., 2017). Consequently, any changes to pteropod populations could potentially have large ramifications on ecosystem function. Due to logistical difficulties in sampling, there are fewer observations on the distribution of pteropods in the Southern Hemisphere (15%) in comparison to the Northern Hemisphere (85%) (Bednaršek *et al*., 2012b; Manno *et al.,* 2017) (Figure 1.1.). With so few data points in the Southern Ocean, our knowledge of pteropod populations is incomplete; particularly in terms of population dynamics and abundances. With little baseline data, we are unable to establish if population level responses of pteropods to environmental change are occurring. Therefore, in this chapter I aim to develop a baseline to define *in-situ,* species-specific, regional population dynamics and abundances from which we can assess subsequent change.

4.1.2 Establishing a baseline for pteropod population characteristics

The *Discovery Investigations,* a series of British funded scientific research cruises, gathered one of the earliest and most comprehensive collection of plankton samples in the Southern Ocean between 1925-1951. Thousands of depth-discrete samples targeting the entire plankton assemblage, alongside physical oceanographic measurements, primarily within the South Atlantic sector, were collected (Kemp *et al.,* 1929). The *Discovery Investigation* collection is still maintained by the Natural History Museum (London) and is readily available for further study. These samples have been fundamental in understanding Southern Ocean zooplankton composition and distribution as well as detailing the life history of key species (Ward *et al.,* 2013). Here I will use these data for establishing a baseline from which we can assess whether changes to pteropod populations are occurring.

An exact date for the beginning of the industrial era is debated (Lewis and Maslin, 2015), however, the Intergovernmental Panel on Climate Change (IPCC) defines this as when industrial growth began in Britain (1750 AD), which led to a sudden increase in fossil fuel use and greenhouse gas emissions. Climate models estimate that the pH in the South Atlantic fell below the natural range of inter-annual variability between 1900- 1930, while sea surface temperatures may breach this natural range by 2030- 2060 (Henson *et al.,* 2017). Furthermore, wintertime (McNeil and Matear, 2008) and summertime (Bjork *et al.,* 2014) aragonite undersaturation is suggested to occur by 2030 south of the Polar Front. The rate of atmospheric CO_2 rise and sea surface warming has been increasing since 1960 (Henson *et al.,* 2017; Joos and Spahni, 2008). The annual mean atmospheric temperatures over the Western Antarctic Peninsula have increased 3°C since 1951 (King, 1994; Turner *et al*., 2005) with an associated surface ocean warming of 1°C (Meredith and King, 2005). Around South Georgia surface temperatures have also increased between 1925 and 2006 by ~2.3°C in winter and by ~0.9°C in summer (Whitehouse *et al.,* 2006; 2008). As the *Discovery Investigations* plankton samples were collected between 1925- 1951,

the impact of anthropogenic climate change, particularly on earlier samples, is likely to be minimal. These samples represent the earliest, most comprehensive means of assessing the population dynamics and abundance of pteropods before the impact of anthropogenic change in the Scotia Sea.

4.1.3 The study region and rationale

Most of the open Southern Ocean is classed as High Nutrient Low Chlorophyll (HNLC) where lack of iron limits phytoplankton growth (Wadley *et al.,* 2014; Boyd *et al.,* 2000). However, parts of the Scotia Sea have significant productivity and endemic biodiversity (Whitehouse *et al.,* 2012; Atkinson *et al.,* 2012; Hogg *et al.,* 2011). Here, the Polar Front, which is a strong jet of the Antarctic Circumpolar Current (ACC), transports iron into the Scotia Sea from topographic features, fuelling one of the largest phytoplankton blooms in the Southern Ocean (Korb *et al.,* 2005; Korb and Whitehouse, 2004). The Scotia Sea supports high mesozooplankton biomass and biodiversity (Atkinson *et al.,* 2012) as well as commercially important fisheries and Antarctic krill (Gregory *et al.,* 2017). Further to the north, part of the ACC forms the Sub-Antarctic Front (SAF) which similarly sustains productive waters north of the Falkland Islands (Arkhipkin *et al.,* 2013). Between the Falklands and South Georgia, the Polar Front partitions the distribution of species through a division in water mass characteristics as well as through advection (Venables *et al.,* 2012; Ward *et al.,* 2003; Pakhomov *et al.,* 2000).

The Scotia Sea's unique hotspots of biodiversity are under threat, being one of the fastest warming areas in the world. Since seasonal temperature variation is from 6 °C (April) to <1 °C (September) at P3, this warming trend means certain species may be experiencing temperatures towards their upper thermal limits (Venables *et al.,* 2012; Tarling *et al.,* 2018). The Scotia Sea has been identified as a conservation priority, because of the unique characteristics of its fauna (Hogg *et al.,* 2011). Scotia Sea species are likely either to be at the limit of their tolerance of environmental conditions (range-edge species) or be specifically adapted to this region with narrow tolerance thresholds (endemic species) and

so likely to be susceptible to rapid environmental change (Hogg *et al.*, 2011). Previous studies of the northern Scotia Sea have found both *L. retroversa,* a boreal species, and *L. helicina,* a true polar species, which are at the most southern and northern limits of their biogeographical distributions, respectively (Ward *et al.,* 2003; Hunt *et al.,* 2008). Consequently, it would be expected that any changes in environmental conditions would be reflected in the abundance and population dynamics of these pteropod species. The combination of rapid environmental change with populations that reside at their range edge, makes this region an ideal focus for establishing a baseline of pteropod population dynamics and distributions. Furthermore, there is an overlap between sampling stations of the *Discovery Investigations* and that of more recent cruises (Tarling *et al.,* 2018) enabling the potential for future assessment.
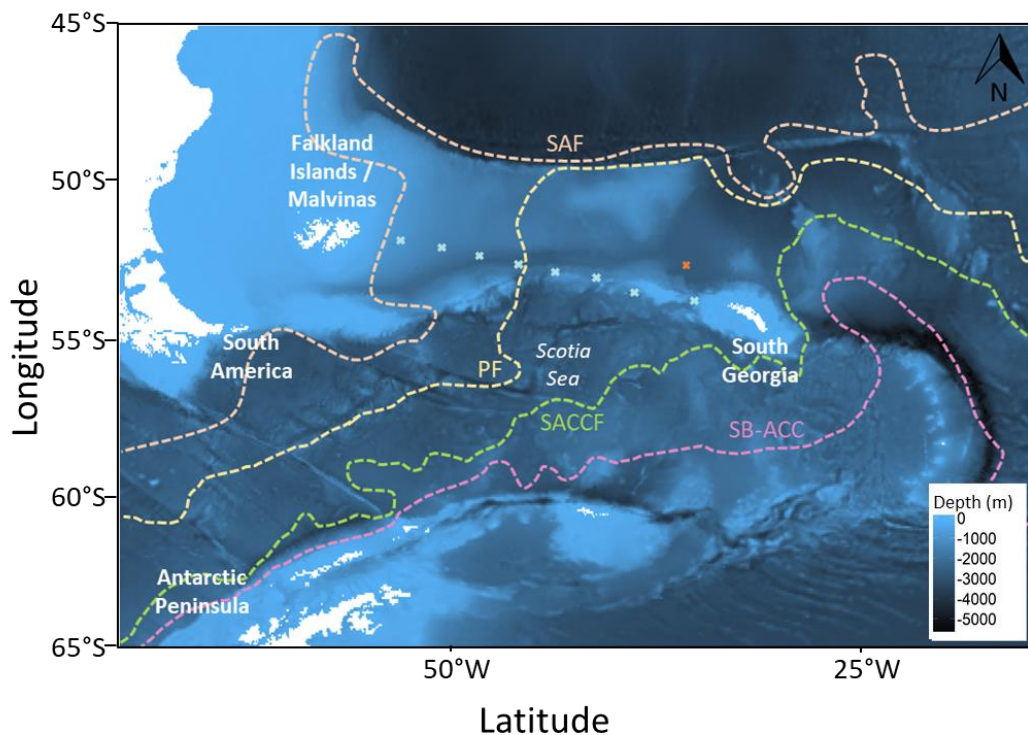
Figure 4-1. An overview of the study region and stations (✖) used to define a baseline for pteropod population abundances and dynamics. Dashed lines indicate the position of the Sub-Antarctic Front (SAF) (━ ━), Polar Front (PF) (━ ━), Southern Antarctic Circumpolar Current Front (SACCF) (━ ━) and the Southern Boundary of the Antarctic Circumpolar Current (SB-ACC) (━ ━). Positions of the SAF, PF and SB-ACC were taken from Orsi *et al.* (1995), while the position of the SACCF was from Thorpe *et al.* (2002). The orange cross (✖) gives the position of P3, which was discussed in Chapter 3.

4.1.4 Chapter Aims

Chapter 4 aims to develop a baseline to define *in-situ,* species-specific population dynamics and abundances of pteropods across the Polar Front between South Georgia and the Falkland Islands. This baseline will be determined using *Discovery investigation* samples that were collected prior to significant anthropogenic impact on their environment, allowing future studies to assess any subsequent changes to this population which may be attributable to global climate change. In order to define this baseline, three specific aspects will be evaluated:

1.   Pteropod species occurrence and range
2.   Vertical distribution and diurnal migration
3.   Size distribution with depth

4.2 Materials and Methods

4.2.1 Sampling stations

A transect of 8 stations was sampled between 26th February and 3rd March 1930 by the R.R.S. *William Scoresby* during the *Discovery Investigations* (Figure 4.2.). This transect stretched 1100 km between the Falkland Islands and South Georgia across the Polar Front. Locations of sampling stations were estimated by Anonymous (1929) using celestial navigation to the nearest nautical mile.

All stations along the transect were completed within 6 days, with the plankton and hydrographical samples on each station usually being completed in a 12-hour window. We assume that there was minimal change in hydrographical conditions over this 12-hour sampling window and thus hydrogeographic conditions represent those that the pteropods resided within. Station 525 (located between 524 and 526 on the transect) was not analysed as samples at this station were only collected to a depth of 150 m and plankton samples were not available. The station coordinates, dates and times are given in Table 4.2.
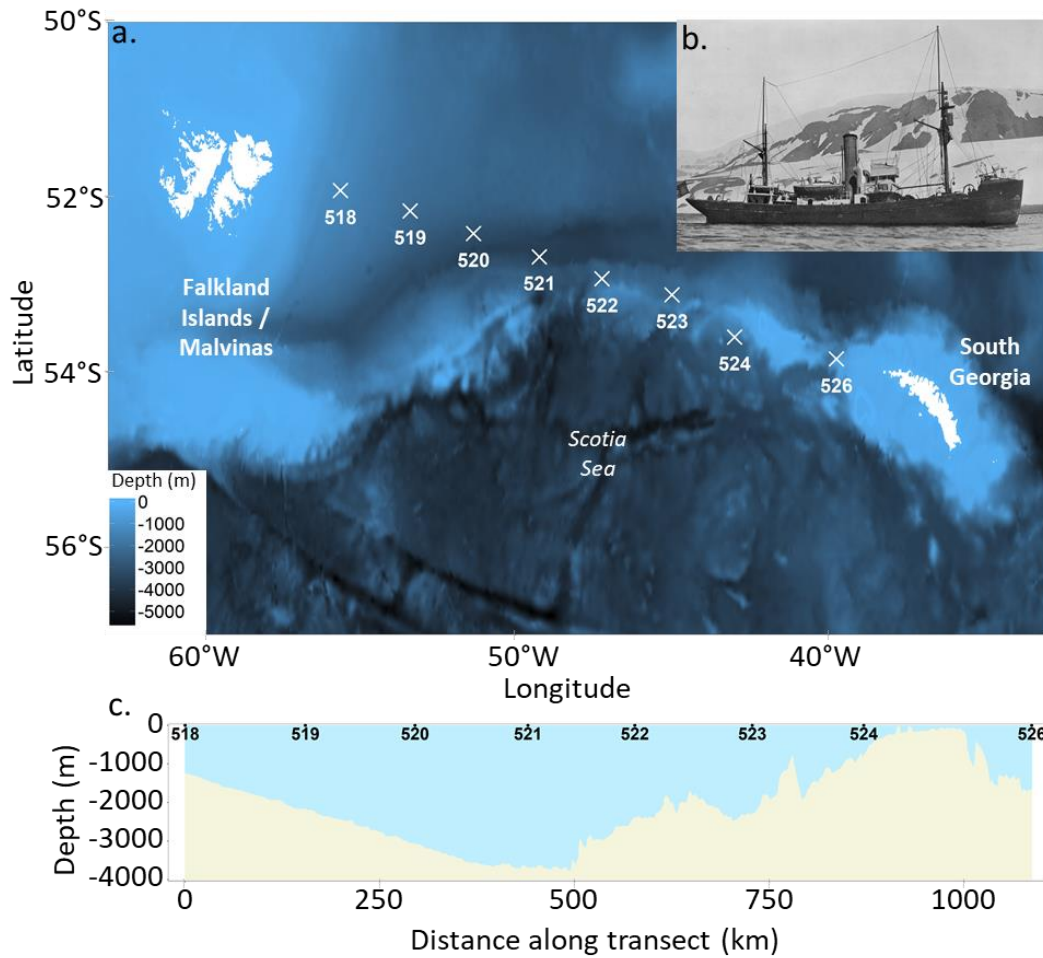
Figure 4-2. A transect of 8 stations (**a**) which was sampled between 26th February and 3rd March 1930 by the R.R.S. *William Scoresby* (image from Kemp *et al.,* 1929) (**b**) during the *Discovery Investigations*. These stations were distributed on a 1100 km transect between the Falkland Islands and South Georgia (**c**).

Table 4.2. Details of the stations along a transect between the Falkland Islands and South Georgia (Scotia Sea) sampled between 26th February and 3rd March 1930.

Station	Sea floor depth (m)	Date sampled	Latitude (°S)	Longitude (°W)	Time (GMT)	Day/ Night
518	1434	26/02/1930	51.93	55.58	00:05	Night
519	2135	26/02/1930	52.16	53.36	10:55	Day
520	3088	27/02/1930	52.42	51.33	21:50	Night
521	3674	28/02/1930	52.68	49.23	09:50	Day
522	2392	28/02/1930	52.93	47.23	22:35	Night
523	2263	02/03/1930	53.12	45.00	11:35	Day
524	1832	03/03/1930	53.60	43.00	07:50	Day
526	1626	03/03/1930	53.85	39.75	10:30	Day

4.2.2 Plankton sample collection

At each station, six depth-discrete plankton samples were obtained using an N70v net (Figure 4.3a) as follows: 50 m– surface, 100–50 m, 250–100 m, 500–250 m, 750–500 m and 1000–750 m. Extensive details of the net construction are given in Kemp *et al.* (1929). Briefly, the N70v was 70 cm in diameter with a collar of ~6 mm knotted mesh, a middle section of 41 threads per inch (equivalent to ~440 μm) and a rear section of 86 threads per inch (equivalent to ~195 μm) (Ward *et al.*, 2012). The net was deployed to the deepest of each of the 6 depths while open, hauled to the shallowest of the pair, and then closed via a messenger weight which triggered the closing mechanism; throttling the net. Nets were deployed with accumulator springs which reduce upwards movement and accidental catch as the ship rolls (Currie and Foxton, 1956). This approach makes contamination of each depth horizon with those above it possible (Grice and Hülsemann, 1968), although Kemp *et al.* (1929) considered this minimal. The *Discovery Investigations* did not use flow-meters when collecting plankton samples, but consistently hauled the nets up vertically at 1 m/sec. To allow comparison of the abundance of pteropods within *Discovery Investigation* samples with those collected during other expeditions, the filtration volume was calculated. This was achieved by using the net diameter and the height of the water column sampled with the assumption that the flow rate was constant at 1

m/sec. Pteropod counts (see Section 4.2.6.) were then standardised to the number of individuals per m^3 based on this estimated filtration volume (filtration volumes are reported in Table A4.1.).

Clogging of nets with dense phytoplankton can reduce net catches; causing increased net outflow and hindering sample sorting. However, there were no notes of this occurring within the station log (Anonymous, 1929) and no samples had an extremely high abundance of phytoplankton within them, so it was not considered an issue.

Once the net was retrieved, samples were placed into a bucket on deck, with added menthol crystals as an anaesthetic, until samples could be processed. Where there was an abundance of pteropods "a few drops" of 1% chloral hydrate were added as an alternative anaesthetic, although this was not recorded when adopted. Samples were then fixed using 10% formalin and "weak spirit" comprising of methylated spirits. Where there were "bulk collections of plankton" (Kemp *et al.,* 1929, pp. 218), samples were immediately neutralised by the addition of 5 grams of borax (sodium tetraborate) per litre although, it was not recorded when this occurred. Samples of each depth were stored in small glass tubes stoppered with cotton wool (Figure 4.3b) placed together within a larger screw top jar filled with the fixative (Figure 4.3c). Therefore, every depth within a station shared the same fixation solution. This means any artefact of fixation would be consistent for each depth within a station, but not between stations. Section 4.2.5. discusses the condition of the pteropods on the transect.

Figure 4-3. An overview of the plankton net, sample storage and inspection technique. (**a**) is the N70v plankton net (image from Kemp *et al.,* 1929) used by the R.R.S. *William Scoresby* during the *Discovery Investigations* between 26th February and 3rd March 1930. (**b**) Separate depth horizons were collected from a single station which were stored together in a larger jar (**c**). Samples were inspected using a Doncaster plankton sorting tray (**d**).

4.2.3 Environmental data collection

Temperature and salinity measurements were made from the surface at depths of 10, 20, 30, 40, 50, 60, 80, 100, 150, 200, 300, 400, 600, 800, 1000, 1500, 2000, 2500 and 3000 m or to just above to the sea floor. Since the R.R.S. *William Scoresby* had insufficient space, no oxygen, hydrogen-ion or phosphate measurements were made as were done on the R.R.S. *Discovery* (Kemp *et al.,* 1929).

The depth of the samples was estimated using recording sheaves which measure the length of wire paid out. However, this depends on the size and weight of the instrument being used as well as the swell. Therefore, recording sheaths were calibrated with a second reading obtained from reversing thermometers (Richter and Wiese, Berlin) attached to the Ekman reversing bottles (for measuring temperature). One of these reversing thermometers was protected against pressure, and the other unprotected allowing the depth at the moment a messenger arrives to be derived using a simple formula (for more details see

Kemp *et al.,* 1929). Both depth readings were occasionally recorded for other stations not on the transect and were generally within a few meters each other, meaning that we can reliably interpret the depths given (Ward *et al.,* 2014).

Temperatures were determined using Nansen-Pettersson (for depths <400 m) and Ekman reversing (for depths >400 m) water bottles (Richter and Wiese, Berlin). Nansen-Petterson bottles comprise of a thermometer in a water chamber insulated by a number of concentric jackets. A messenger system is used to trigger water sample collection at the required depth and then it is hauled to the surface for the temperature to be read. Temperatures are liable to rise on recovery of deep samples due to expansion of the water samples, therefore Ekman reversing bottles were used for all depths greater than 400 m. Ekman water bottles reverse on contact with the messenger system, cutting off the mercury column at that point before being hauled to the surface. Very small contractions and expansions may occur in the 'cut-off' mercury column therefore, a secondary thermometer is used in the same bottle and a simple formula is used on the difference (more details in Kemp *et al.,* 1929).

Salinity was analysed from water samples collected in Nansen-Pettersson (for depths <400 m) and Ekman reversing (for depths >400 m) water bottles. Salinity was calculated via determining the chloride concentration within a sample by a titration against silver nitrate of a known strength, using potassium chromate as an indicator.

4.2.4 Biogeochemical zones and frontal locations

Stations were grouped into two zones separated by the Polar Front. The position of the Polar Front was determined through examination of temperature and salinity profiles created using 'ggplot2{ggplot}' (Wickham, 2009) and potential temperature-salinity profiles. Seawater potential temperature was calculated using 'oce{swTheta}' (Kelly and Richards, 2017) from the *in-situ* temperatures recorded within the Discovery reports station list (Anonymous, 1929) using a reference pressure of 0 dbar. To visualise the thermohaline structure of each

station, potential temperature-salinity plots were created using 'oce{plot.TS}' (Kelly and Richards, 2017). Temperature and salinity were given to two decimal places which is sufficient to identify the position of the Polar Front. The conditions at each station were compared to the biogeochemical zones defined by Pollard *et al.* (2002) and the frontal positions approximated by Orsi *et al.* (1995) (see Section 4.3.1. for further details). Frontal positions, as defined by Orsi *et al.* (1995), were mapped using 'orsifronts{orsifronts}' onto bathymetric maps using 'marmap{plot}' (Pante and Simon-Bouhet, 2013).

4.2.5 Assessment of pteropod condition

Pteropod shells are extremely susceptible to breakage from net sampling, particularly where nets are not motion compensated (Howes *et al.,* 2014). Care was taken to retrieve the net smoothly and at a constant rate by accounting for the swell (Kemp *et al.,* 1929). Broken parts of pteropod shells were relatively rare within the samples, furthermore shells had few scratches or damaged apertures. Therefore, shell breakage is unlikely to have affected abundance estimates.

Some of the samples within the *Discovery Investigation* collection were not preserved using the best techniques. For example, some of the samples were not buffered initially, causing dissolution of calcium carbonate structures. Furthermore, crustaceans were sometimes brittle and missing some tissue. The original formalin was replaced within the last 20 years with fresh buffered formalin to stop carbonate dissolution (Ward. P., pers. comm.). The Falkland-South Georgia transect was selected since organisms seemed to be in excellent condition with no signs of calcium carbonate shell dissolution or damage under inspection with a light microscope (Olympus SZX16 fitted with a Cannon EOS 60D). To investigate if there were any signs of dissolution on pteropod shells, a small sub-sample (n= 4) of *L. retroversa* were examined under a variable pressure scanning electron microscope (SEM) (TM3000, Hitachi) (Figure 4-4). See Section 5.2.5. for a description of shell dissolution under a light and SEM microscope. There were no signs of shell dissolution on any areas of the shell therefore, I assume that this population did not encountered waters undersaturated with respect to aragonite.
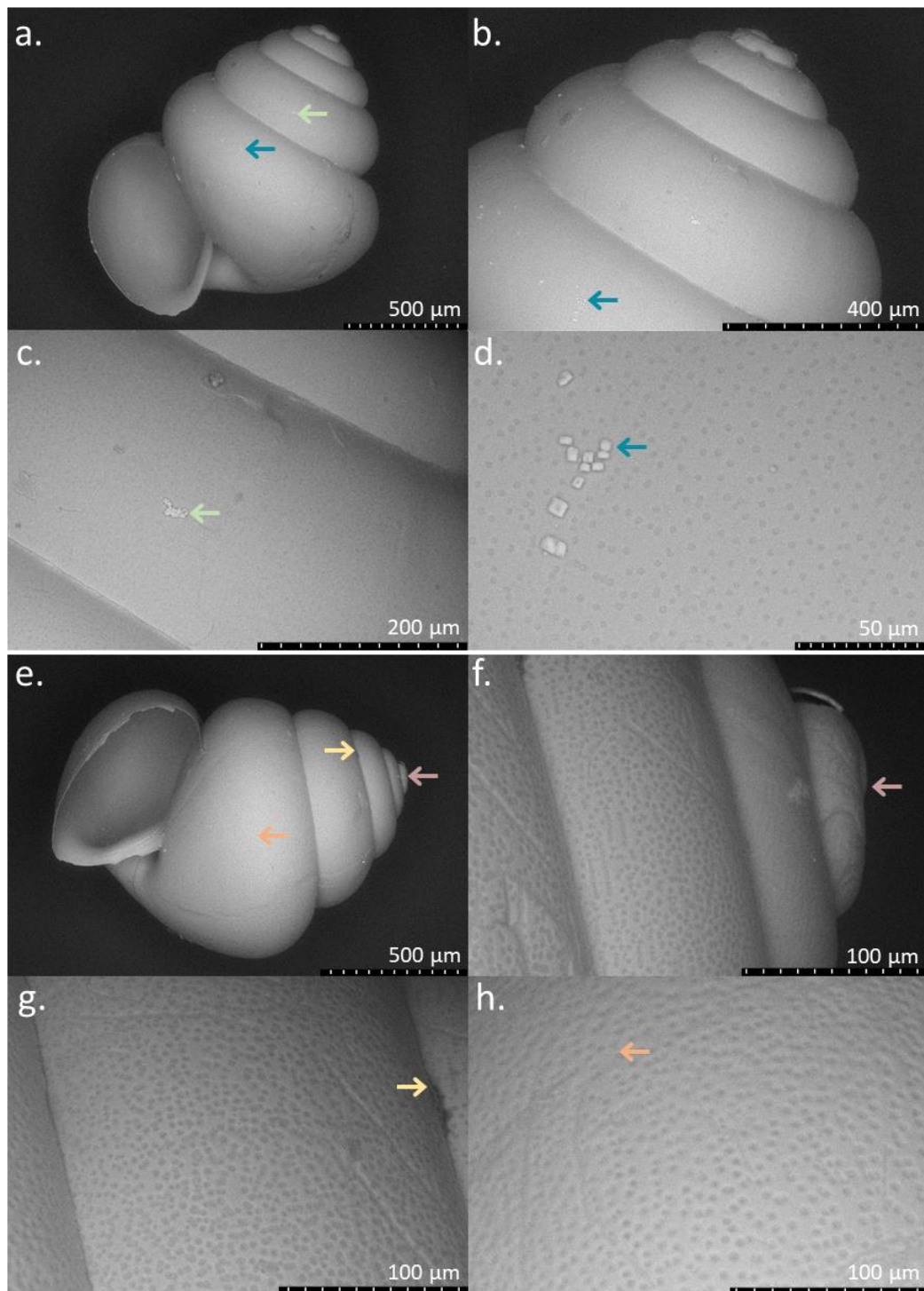
Figure 4-4. SEM microscope images of two specimens of *L. retroversa australis* (specimen 1= **a- d**, specimen 2= **e- h**) from station 521 which were collected 28/02/1930 by the R.R.S. *William Scoresby* during the *Discovery Investigations*. The outer shell surface remains smooth and intact with no changes in texture suggestive of shell dissolution. Coloured arrows point to the same point on the shell to show image location.

4.2.6 Pteropod abundance and shell size distribution

Since pteropods have a relatively high sinking rate, it is difficult to ensure homogenous sub-sampling when using plankton splitting techniques (See Section 3.2.3. for more detail), therefore, samples were analysed in their entirety to prevent any bias. Larger organisms were removed first by handpicking from a white sorting tray. Afterwards, samples were inspected under a dissection microscope (Olympus SZX16) using a Doncaster plankton sorting tray (Figure 4.3d). Extant Euthecosome pteropod species are well described and identification of unbroken specimens was carried out to species level using Lalli and Gilmer (1989), van der Spoel (1976) and MSIP (2017). As veligers (larvae) of *Limacina helicina antarctica* and *Limacina retroversa australis* are difficult to distinguish, having few shell whorls, individuals smaller than 0.3 mm were classed as *Limacina* spp. The diameter of each pteropod was measured using an eyepiece reticule across the aperture line. On *L. helicina* and *Limacina* spp the line of aperture was orientated from the growing edge to the shell edge over the protoconch. On *L. retroversa* the line of aperture passed from the protoconch and down the axis of coiling to the shell edge (also known as spire height) (see Section 3.2.4. for further details).

Gymnosome species contract to varying degrees during the preservation process having no calcareous shell, meaning body measurements are not reliable. Therefore, none were taken. Two species of gymnosomes were found along the transect, *Spongiobranchaea australis* and *Clione limacina antarctica* with both being specialist predators on thecosome pteropods. These species were pooled together as 'gymnosomes' since they both are specialist pteropods predators which occur at a low abundance.

A mixture analysis was applied to the shell size of each species to discern whether specific size classes were present across the entire population within each depth horizon using 'mixdist{mix}' (Macdonald and Du, 2012) (see Section 3.2.5. for further details).

4.3 Results

4.3.1 Hydrography of the transect

Surface water down to 80 m was well mixed at each station with little variation in temperature (max range 0.95°C). At station 519 and stations 522-526, from 80 m to ~150 m temperatures rapidly decreased (by 0.98-2.65°C), reaching a temperature minimum, before increasing again (by 1.07- 1.90°C) at 400 m depth (Figure 4-5). Stations 520 and 521 displayed a uni-directional decline in temperature from the surface to 400 m. There was little variation in salinity down to 150- 200 m (max range 0.11). Then, salinity steadily increased between 200 m to 1500 m reaching a maximum of 34.73. There was little variation in temperature (1.2°C difference) and salinity (max range 0.52) from 400 m to the sea floor at all stations. Potential temperature-salinity plots (Figure 4-6) indicated that station 519 may include a different water parcel to 518 and 520, with the haline structure being more like stations 522-526. Despite this, salinity did not significantly vary ($\chi^2_{2,155}$ = 31.1, P = 0.15) between stations 518-521 and 522-526. However, stations 518-521 were significantly warmer than stations 522-526 ($\chi^2_{2,159}$ = 31.1, P < 0.001). No interleaving was evident between 100- 400 m which is often observed close to fronts (Orsi et $al.,$ 1995).

Using the thermohaline structures described above, each station was then placed within a hydrographic zone using the definitions of Pollard et $al.$ (2002). There were no stations where salinity decreased with depth, therefore, this transect does not cross into the Sub-Antarctic Zone, which is situated between the Sub-Antarctic Front and the Sub-tropical Front. At stations 518, 520 and 521, salinity increases and temperature decreases with depth with no evidence of a subsurface salinity minimum nor a marked subsurface temperature minimum of 2°C. Therefore, these stations were within the Polar Frontal Zone, which is situated between the Sub-Antarctic Front and the Polar Front. There was a clear difference in subsurface temperature between stations 521 and 522 suggesting that the Polar Front is between these stations, which agrees with the average location estimated by Orsi et $al.,$ (1995) (Figure 4.1). Stations 522-526 all had a clear subsurface temperature minimum of <2°C with the underlying water being

warmer placing them within the Antarctic Zone. Interestingly, station 519 also had a subsurface temperature minimum of <2°C, however, its surface temperature and salinity profiles are more like stations within the Polar Frontal Zone. It is possible that station 519 contains an eddy of seawater from the Antarctic Zone. Individual temperature and salinity profiles are presented in Figure A4.1.
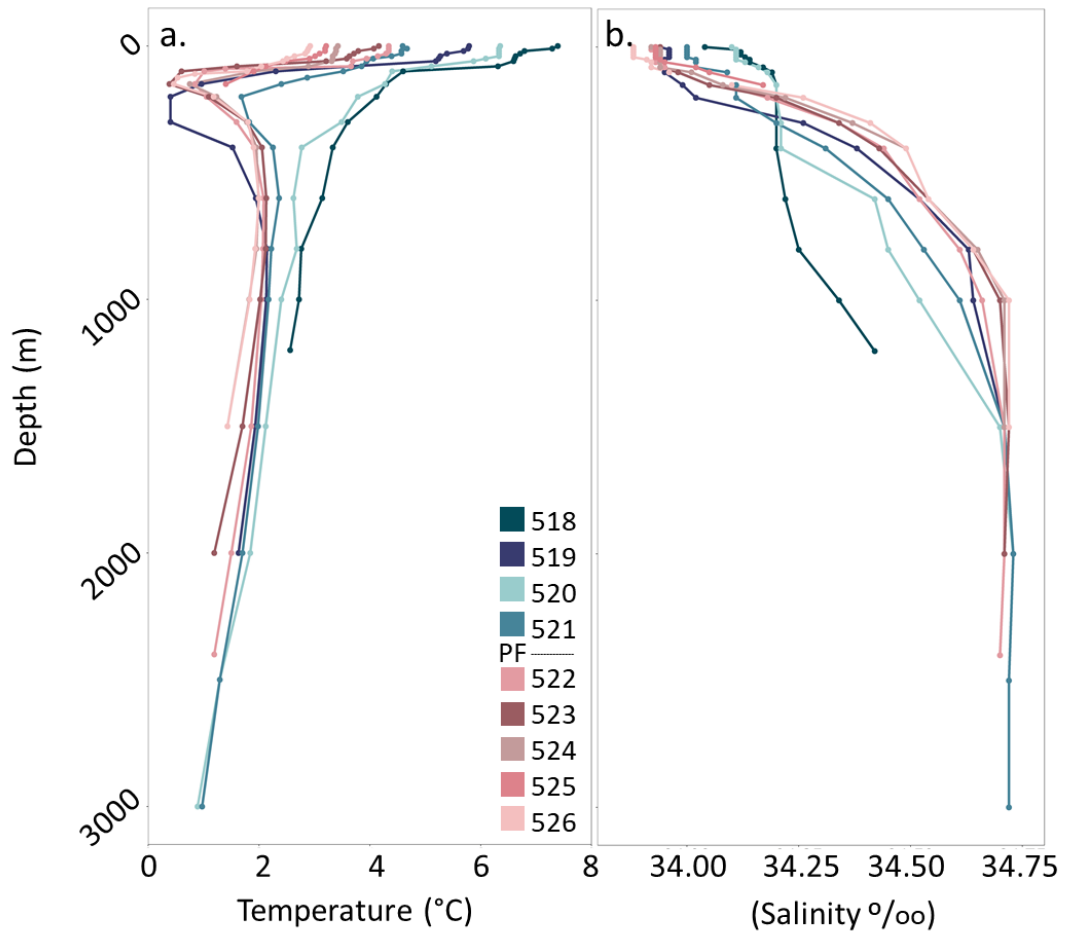
Figure 4-5. Temperature (°C) (**a.**) and Salinity (**b.**) profiles of each station (coloured) taken along a transect between the Falkland Islands and South Georgia by the R.R.S. *William Scoresby* during the *Discovery Investigations* between 26th February and 3rd March 1930. Insets detail the temperature and salinity profiles in the top 1000 m. PF is the estimated location of the Polar Front. Stations within the Polar Frontal Zone are coloured in blue while stations coloured in red are within the Antarctic Zone.
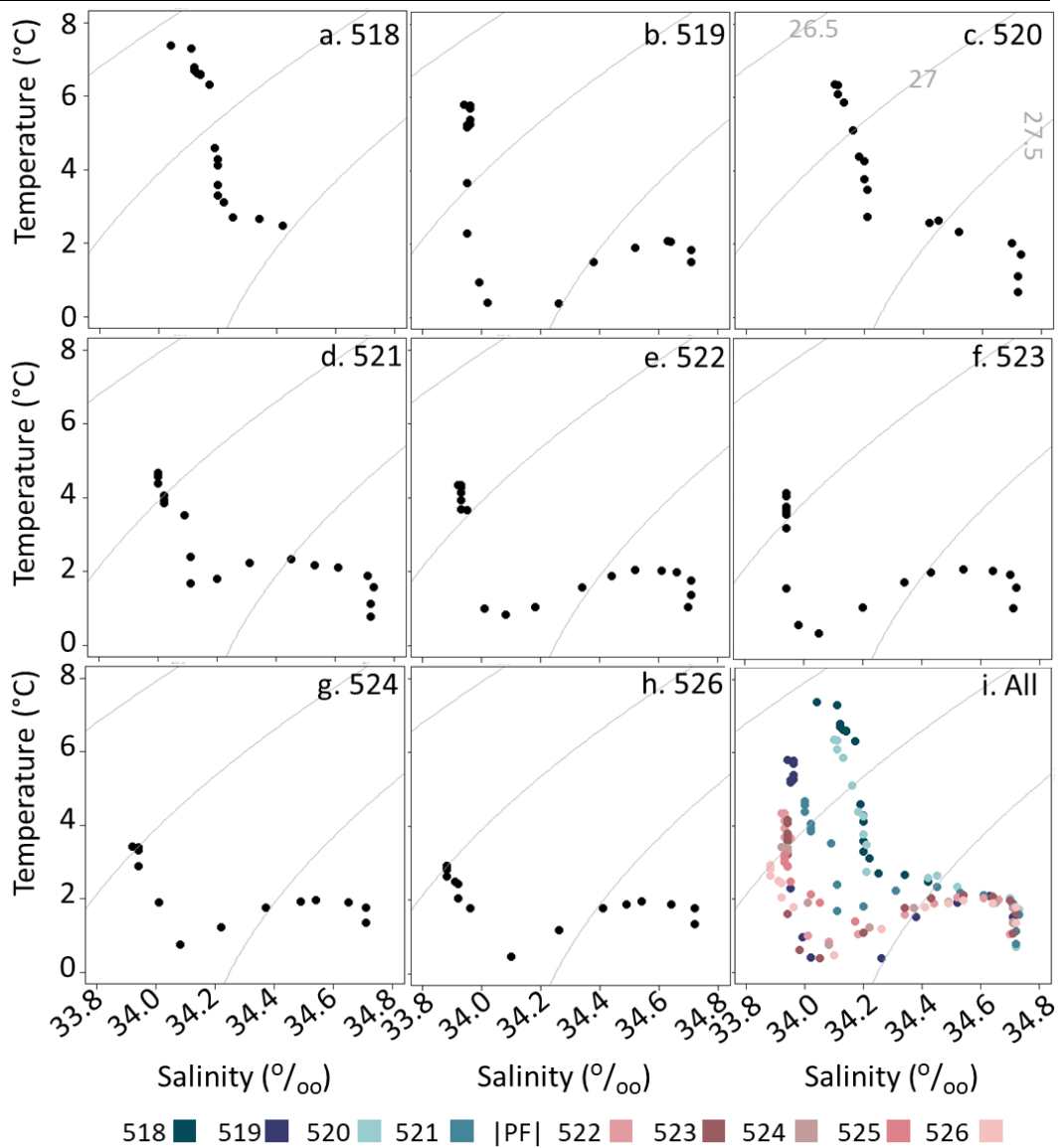
Figure 4-6. Potential temperature-salinity diagrams of each station (**a-h**) and combined (**i**) taken along a transect between the Falkland Islands and South Georgia by the R.R.S. *William Scoresby* during the *Discovery Investigations* between 26th February and 3rd March 1930. Neutral density (θ) contours are in grey. Stations within the Polar Frontal Zone are coloured in blue while stations coloured in red are within the Antarctic Zone.

4.3.2 Pteropod species occurrence and distribution

A total of 24,108 pteropods were identified from the *Discovery Investigation* Falkland Island to South Georgia transect completed in 1930, consisting of two species of thecosome and two species of gymnosome (Figure 4-7) pteropods. Stations within the Polar Frontal Zone (stations 518- 521) were dominated by *Limacina retroversa australis* (hereafter *L. retroversa* in Chapter 4), accounting

for 49.1- 83.2% of the total pteropod community sampled here. *Limacina helicina antarctica* (hereafter *L. helicina* in Chapter 4) were present on the edge of the Polar Frontal Zone (station 521) and at all stations within the Antarctic Zone (stations 522- 526) (Figure 4.8). The absolute abundance of *L. retroversa* in the Polar Frontal Zone was significantly higher in comparison to the Antarctic Zone ($\chi^2_{1,7}$ = 6.47, *P* = 0.011) and *vice-versa* for *L. helicina* ($\chi^2_{1,7}$ = 4.38, *P* = 0.036). *L. retroversa* absolute abundance within the Polar Frontal Zone increased from 108.46 ind. m^{-3} at station 518 to 230.83 ind. m^{-3} at station 521 (Figure 4-9). On entering the Antarctic Zone at station 522 the abundance of *L. retroversa* dropped to 1.15 ind. m^{-3}. *L. helicina* were present in much lower abundances compared to *L. retroversa.* At the boundary stations between the two zones (521-522), abundances of *L. helicina* were 0.28 ind. m^{-3} and 0.68 ind. m^{-3} respectively.

Veligers were present at all stations and accounted for around half of the pteropod population (42.9- 59.4%) except at the stations at the extreme ends of the transect where they were less abundant (station 518: 14.3% and station 526: 39.8%) (Figure 4-10 4.10). Veligers had a much greater relative abundance in the Polar Frontal Zone compared to the Antarctic Zone ($\chi^2_{1,7}$ = 4.05, *P* = 0.044). The abundance of *Limacina* veligers increased between station 518 and 521 from 19.75 ind. m^{-3} to 457.34 ind. m^{-3} before declining within the Antarctic Zone (station 522: 2.37 ind. m^{-3}) (Figure 4.9).

Gymnosomes contributed 0.7- 2.9 % of the population in the Antarctic Zone and 1.2- 11. 1% in the Polar Frontal Zone (Figure 4-10 4.10). While gymnosomes were present at all stations, their absolute abundance was significantly higher in the Polar Frontal Zone ($\chi^2_{1,7}$ = 18.59, *P* < 0.001) than in the Antarctic Zone. Gymnosome abundance increased from station 518 (3.63 ind. m^{-3}) to 520 (3.80 ind. m^{-3}). In the Antarctic Zone, gymnosome abundance was much lower at 0.1 ind. m^{-3} (Figure 4-10 4.9).
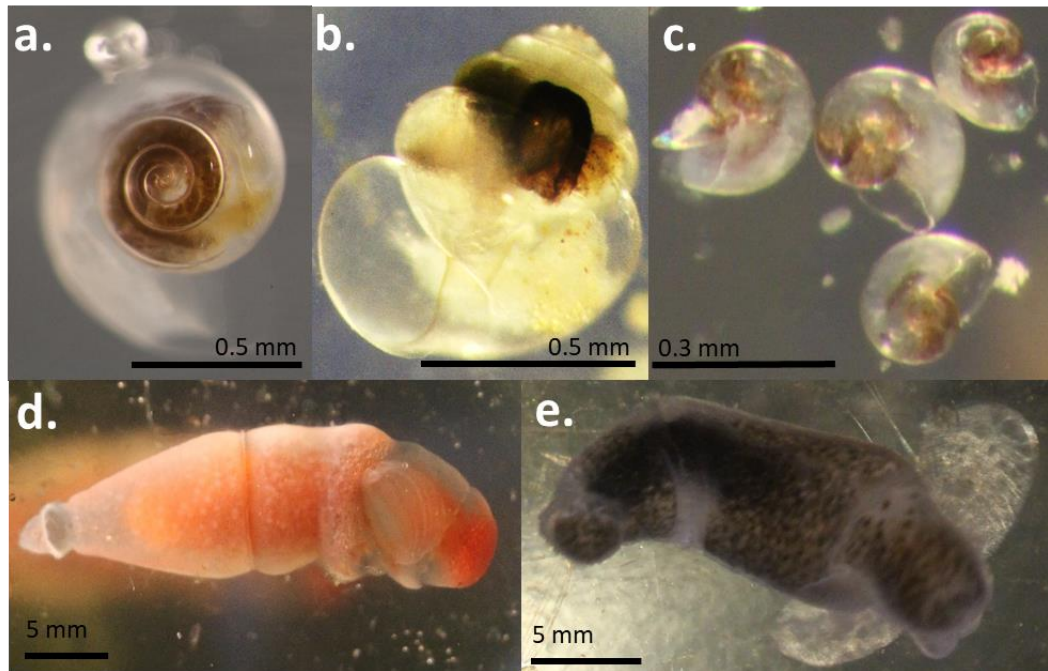
Figure 4-7. Pteropod species and groups identified across a transect between the Falkland Islands and South Georgia where **a**. *Limacina helicina antarctica,* **b**. *Limacina retroversa*, **c**. *Limacina* species veligers, **d**. *Clione limacina antarctica* and **e**. *Spongiobranchaea australis*. Images **a-c** are of individuals collected by the R.R.S. *William Scoresby* during the *Discovery Investigations* between 26th February and 3rd March 1930. Images **d-e** are of living individuals collected north of South Georgia (28/11/2015, 52.8052°S, 40.08624°W).
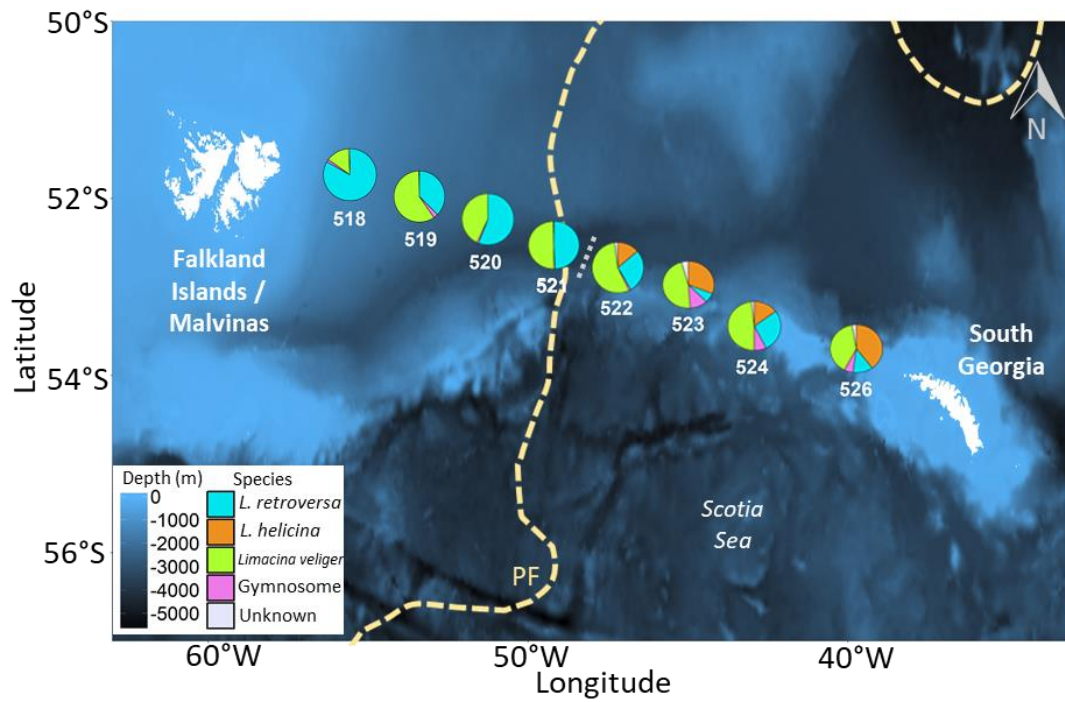
Figure 4-8. The population distribution and relative abundance of pteropods between the Falkland Islands and South Georgia. Samples were taken by the R.R.S. *William Scoresby* during the *Discovery Investigations* between 26th February and 3rd March 1930. The yellow dotted line (— —) indicates the climatological mean position of the Polar Front (PF) taken from Orsi *et al*., 1995 and the grey dotted line (▪ ▪ ▪) the PF position during the transect sampling.
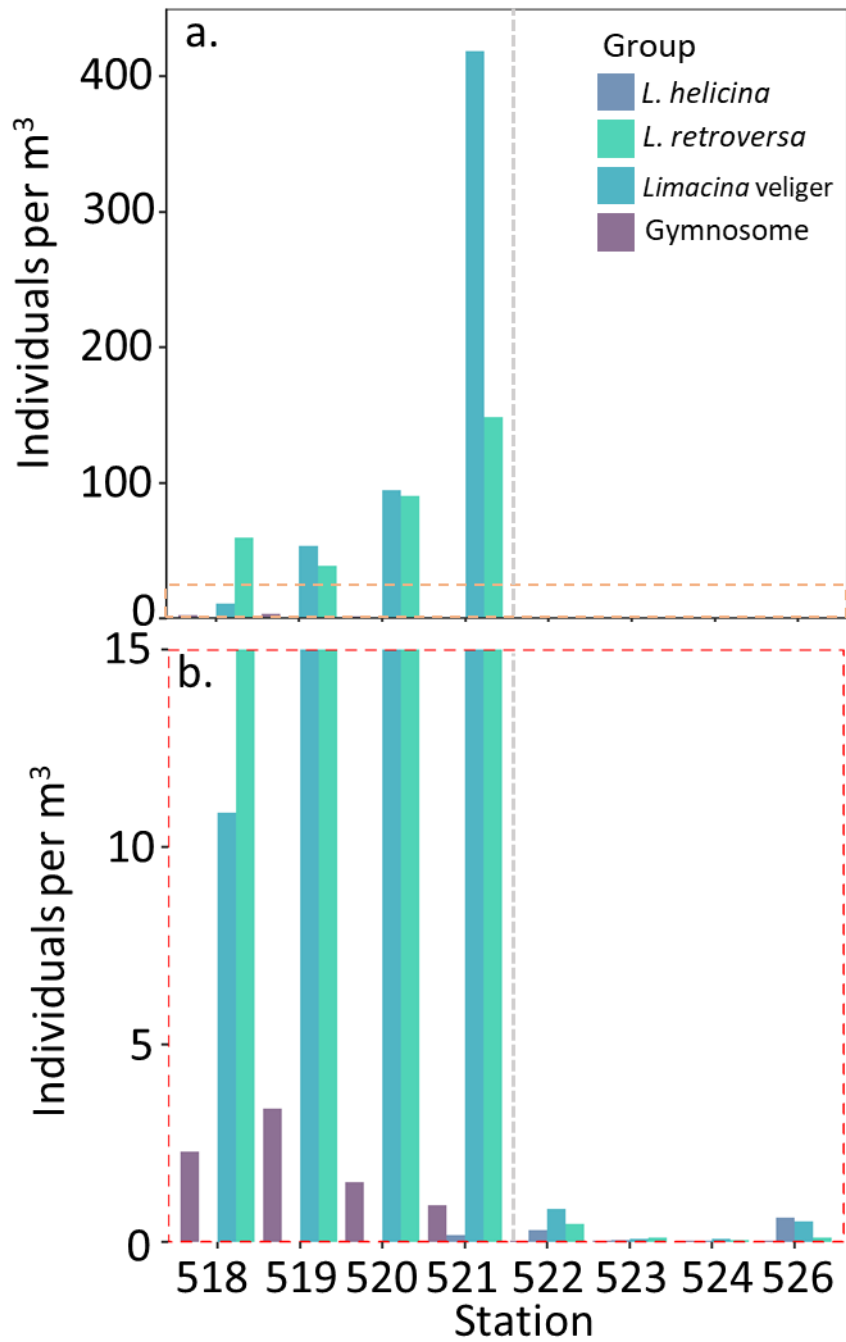
Figure 4-9. The average number of individuals per m³ for each station along the transect taken by the R.R.S. *William Scoresby* during the *Discovery Investigations* between 26th February and 3rd March 1930. Plot **b.** is an expanded view of plot **a.** The grey dashed line (---) is the position of the Polar Front during the transect where stations 518-521 are in the Polar Frontal Zone and 522-526 in the Antarctic Zone.
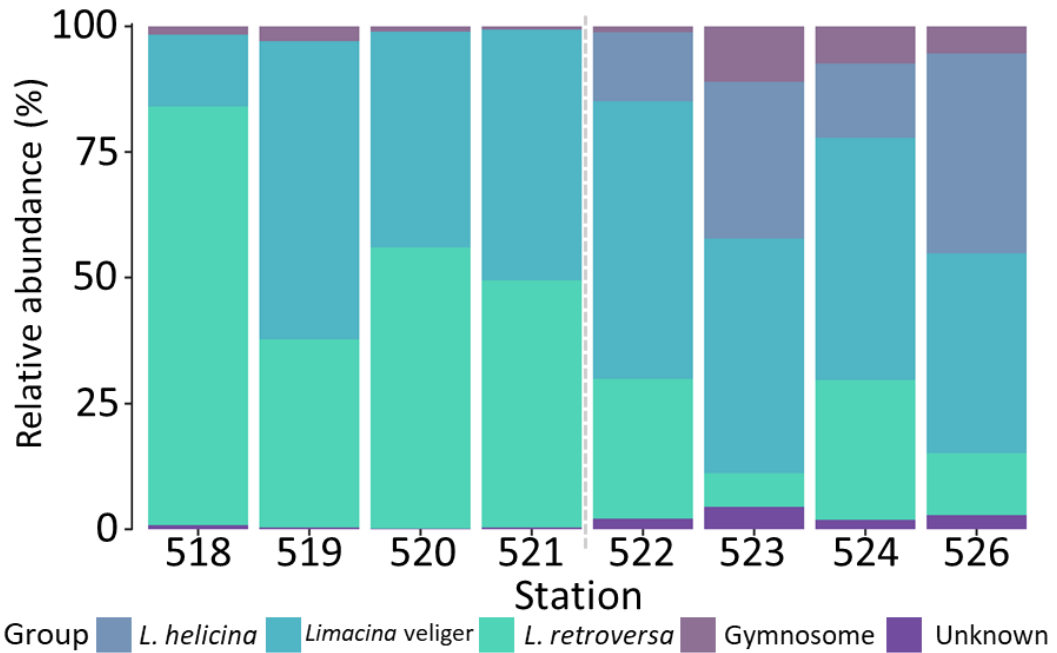
Figure 4-10. Percentage abundance of pteropods recorded at each station along a transect between the Falkland Islands and South Georgia. The grey dashed line (   ) is the position of the Polar Front during the transect where stations 518-521 are in the Polar Frontal Zone and 522-526 in the Antarctic Zone.

4.3.3 Vertical distribution of pteropods between day and night

All 4 pteropod groups identified along the Falkland Island- South Georgia transect were present throughout the water column down to 1000 m. Pteropods were most abundant at 50-100 m (mean 26.65 ind. m^{-3}) and 0-50 m (8.26 ind. m^{-3}) (Figure 4.12). The relative abundance of each pteropod group for each depth horizon is presented in Figure 4.11.
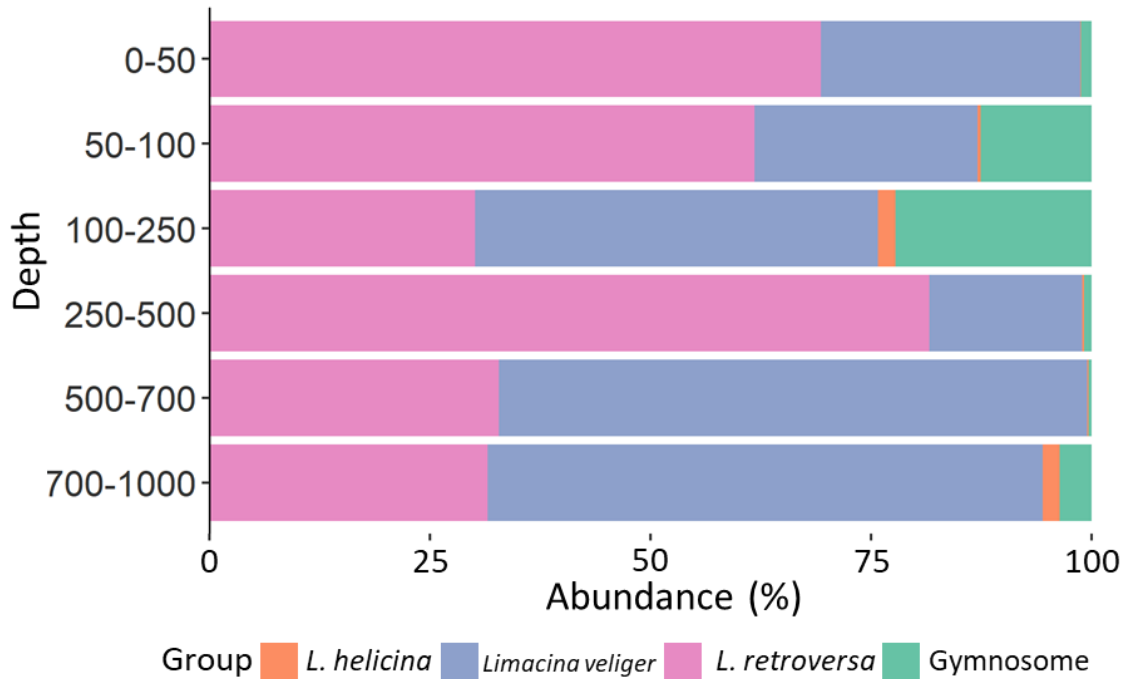
Figure 4-11. Percentage abundance of pteropods recorded at each depth along a transect from the Falkland Islands to South Georgia taken by the R.R.S. *William Scoresby* during the *Discovery Investigations* between 26th February and 3rd March 1930.

4.3.3.1   L. retroversa

The number of individuals per m^3 of *L. retroversa* significantly varied with depth (GLM: $\chi^2_{5,47}$ = 9.23, *P*= 0.002) (Figure 4.12b). The peak abundance of *L. retroversa* occurred at the surface (*TukeyHSD: P* <0.001) (0-50 m max: 118.95 ind. m^{-3} and 50-100 m, max 568.84 ind. m^{-3}). Additionally, a smaller peak in abundance of *L. retroversa* occurred at 500-700 m (*TukeyHSD: P* <0.001) (70.52 ind. m^{-3}). There were significantly less *L. retroversa* at 250-500 m (max 2.70 ind. m^{-3}) and at 700-1000 m (max 7.69 ind. m^{-3}) (*TukeyHSD: P* <0.001) in comparison to all other depths.

The depth distribution of *L. retroversa* significantly changed between day and night (GLM: $\chi^2_{12,47}$ = 6.835, *P* <0.001) (Figure 4.13). In the daytime peak abundance was over 0-50m and 50-100 m, while at night the number of *L. retroversa* significantly increased at 0-50 m (*TukeyHSD: P* <0.001), 100-250 m (*TukeyHSD: P* <0.002) and 500-700 m (*TukeyHSD: P* <0.001).

4.3.3.2 L. helicina

L. helicina were abundant throughout the water column, with a peak in the number of individuals at 50-100 m during the day and night (0.01- 0.1 ind. m^{-3}) (Figure 4.13) (GLM: $\chi^2_{5,47}$ = 0.38, *P*= 0.050). There was a secondary peak in abundance at 700-1000 m during the day and at 250-500 m during the night (*TukeyHSD: P*= 0.049).

4.3.3.3 Limacina veligers

The majority of veligers were found in the upper 100 m of the water column (GLM: $\chi^2_{12,47}$ = 6.26, *P* <0.001) (Figure 4.12). During the day, most veligers were found at 50-100 m (*TukeyHSD: P* <0.001) with a smaller number at 0-50 m depth (*TukeyHSD: P* <0.003) and a low number at all other depths (*TukeyHSD: P* >0.05) (Figure 4.12Figure 4-13). The number of veligers significantly reduced during night time at 50-100 m depth (*TukeyHSD: P* <0.001) and increased at 0-50 m (*TukeyHSD: P* <0.04) (Figure 4.13).

4.3.3.4 Gymnosome spp

There was significant variation in abundance of gymnosomes with depth during the day and night (GLM: $\chi^2_{5,47}$ = 16.466, *P* <0.001) (Figure 4.13). During the day, gymnosomes were most abundant at 100-250 m (*TukeyHSD: P*= 0.029) and to a lesser extent at 250-500 m (*TukeyHSD: P*= 0.031). While they were present throughout the entire water column, there were very few at the surface (0-50 m). The depth distribution of gymnosomes altered significantly between day and night (GLM: $\chi^2_{5,47}$ = 16.466, *P* <0.001). At night, gymnosomes were mostly found at 0-50 m depth. They were more abundant at 50-100 m at night and 100-250 m depth in the daytime (*TukeyHSD: P*= 0.023). Furthermore, there were significantly fewer gymnosomes at 250-500 m at night than in the day (*TukeyHSD: P*= 0.024).
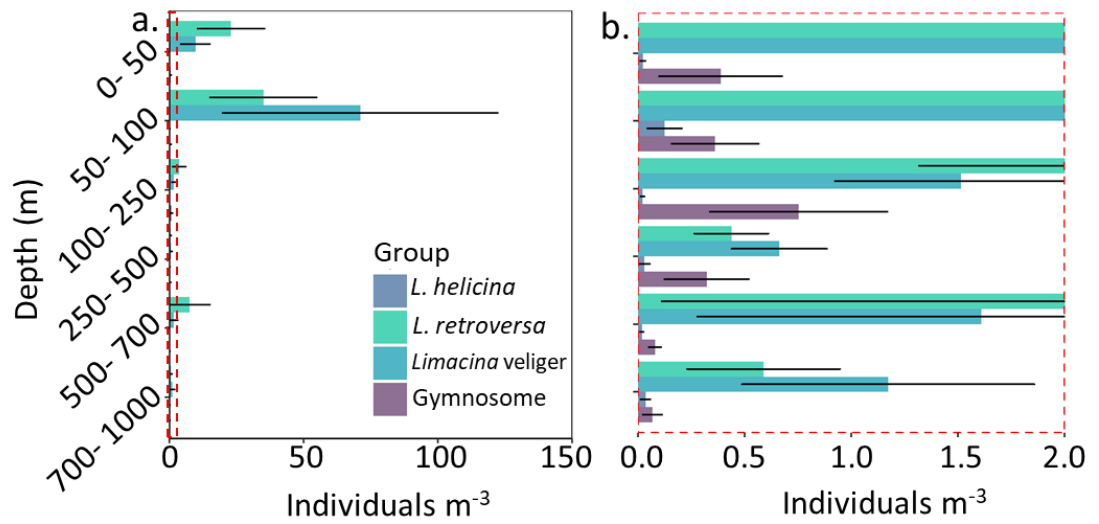
Figure 4-12. The mean number of individuals per m³ with depth across the transect stretching from the Falkland Islands to South Georgia. **a** is the complete distribution while **b** details the red dashed box. Bars denote standard deviation.
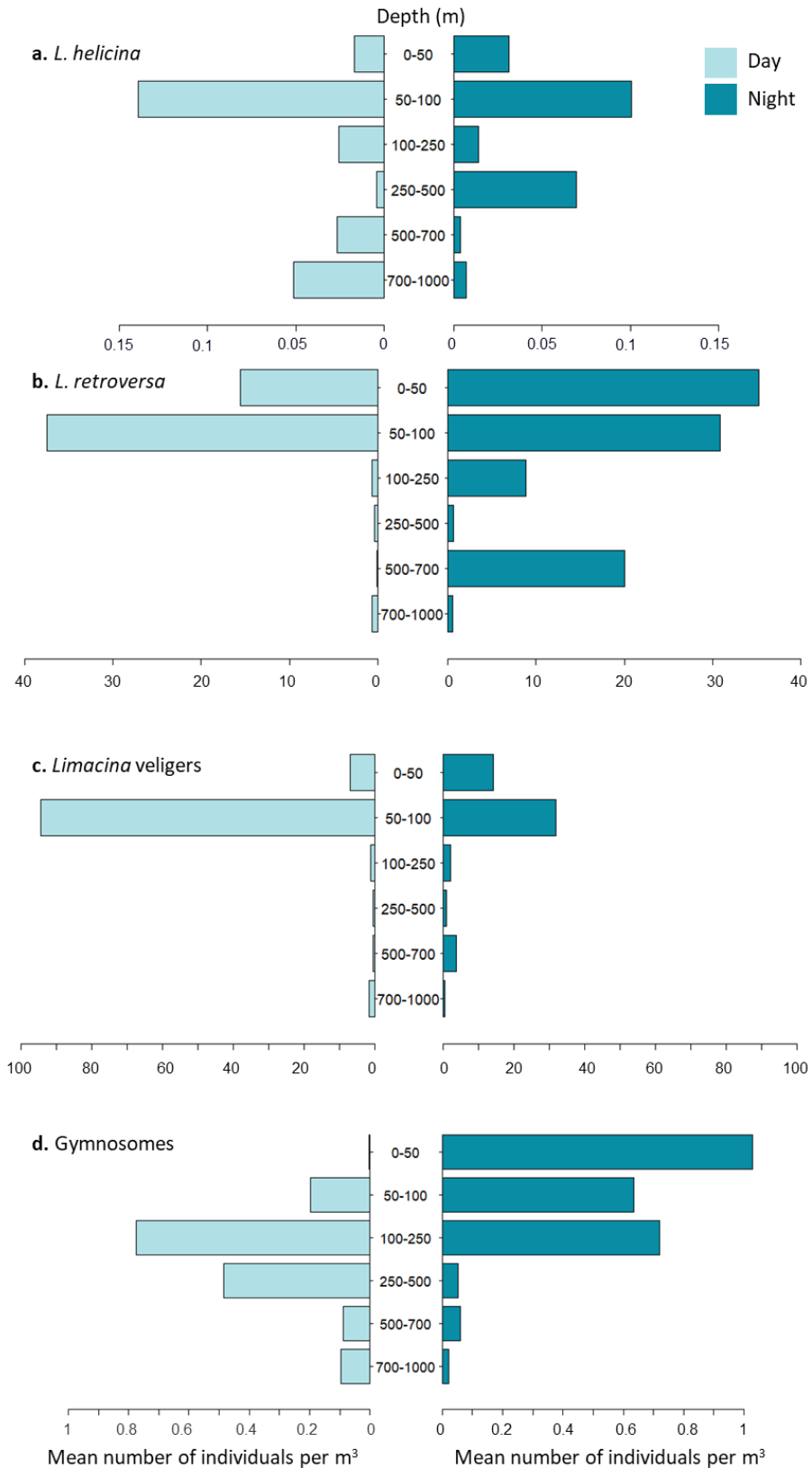
Figure 4-13. The mean number of individuals per m³ of pteropods sampled between **day** and **night** with depth. Individuals were counted across a transect stretching from the Falkland Islands to South Georgia between 26th February and 3rd March 1930.

4.3.4 Pteropod size distribution with depth

4.3.4.1 L. retroversa

The size-depth distribution of *L. retroversa* was significantly different between the day and night (GLM: $\chi^2_{13,12797}$ = 27.96, *P* <0.001) (Figure 4.14a). From day to night there was a shift to smaller *L. retroversa* at 0-50 m (mean day: 0.42 mm, night: 0.39 mm) and larger *L. retroversa* at 50-100 m (mean day: 0.37 mm, night: 0.41 mm) (*TukeyHSD: P* <0.001). However, there was no change in the size distribution of *L. retroversa* below 100 m between day and night (*TukeyHSD: P* >0.05). During the day, *L. retroversa* at 0-50 m were larger than those at 50-100 m, 100-250 m and 700-1000 m (*TukeyHSD: P* <0.001) (GLM: $\chi^2_{13,12797}$ = 27.96, *P* <0.001). At night, *L. retroversa* at 50-100 m were significantly larger than those at 0-50 m, 100-250 m and 500-750 m (*TukeyHSD: P* <0.001) but similar in size to specimens at all other depths (*TukeyHSD: P* >0.05). Additionally, at night, *L. retroversa* at 500-700 m (0.46 mm) were larger than those at 50-100 m, 100-250 m and 700-1000 m (*TukeyHSD: P* <0.001) (*TukeyHSD: P* >0.05).

4.3.4.2 L. helicina

There was no significant difference in the size distribution of *L. helicina* at any depth between day and night (GLM: $\chi^2_{13,112}$ = 33.682, *P* >0.05) (Figure 4.14b). Individuals during the day at 700-1000 m depth (0.41 mm) were significantly larger than those at 500-700 m depth (0.33 mm) (*TukeyHSD: P* =0.01) and 50-100 m depth (0.33 mm) (*TukeyHSD: P* =0.02), while there was no significant difference in *L. helicina* size between depths at night (*TukeyHSD: P* >0.05).

4.3.4.3 Limacina veligers

The size of *Limacina* veligers at each depth did not change between day and night (GLM: $\chi^2_{13,10908}$ = 11.39, *P* >0.05) (Figure 4.14c). However, there was a significant variation in size between each of the depths (GLM: $\chi^2_{13,10908}$ = 11.39, *P* <0.001). Veligers at 700-1000 m (0.23 mm) were smaller than those at all other depths (*TukeyHSD: P* <0.05) except at 500-700 m (0.24 mm) (*TukeyHSD: P* >0.05). Furthermore, those at 0-50 m (0.29 mm) were larger than those below 100 m (*TukeyHSD: P* <0.02).

4.3.4.4 Pteropod size cohorts

Following previous estimates of life stage sizes, no adult *L. helicina* or *L. retroversa* were collected across the transect; only juveniles and veligers (Lalli and Gilmer, 1989). Mixture analyses of *L. helicina* (Figure 4.15) and *L. retroversa* (Figure 4.16) juvenile shell sizes within each station and depth horizon revealed there were no distinct groupings of size classes.
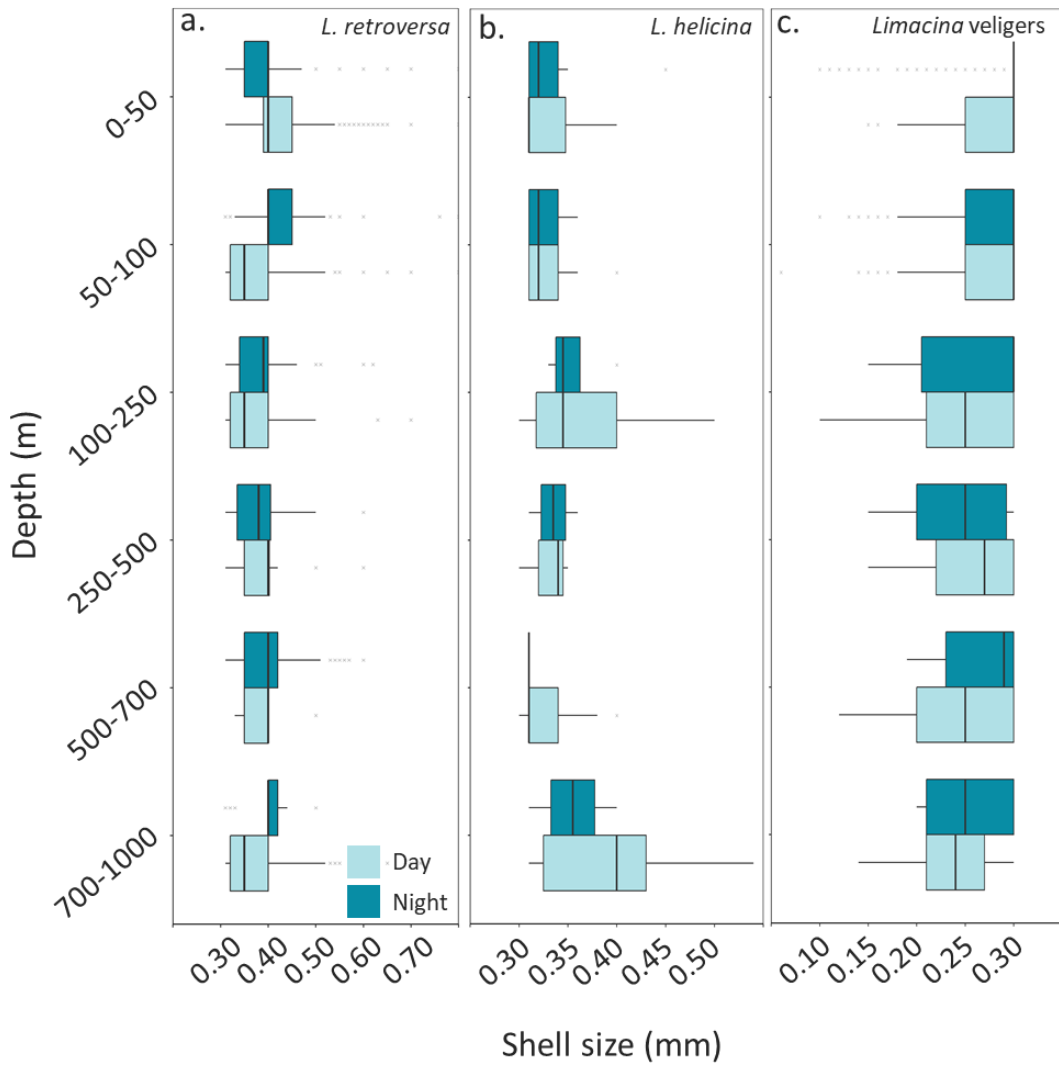
Figure 4-14. Shell size of *L. retroversa* (**a**), *L. helicina* (**b**) and Limacina veligers (**c**) for day and night. Pteropods were collected across a transect stretching from the Falkland Islands to South Georgia between 26th February and 3rd March 1930. One *L. helicina* (0.74 mm at 700-1000 m) and two *L. retroversa* being 3.23 mm (0-50 m) and 1.5 mm (500-700 m) were excluded as outliers.
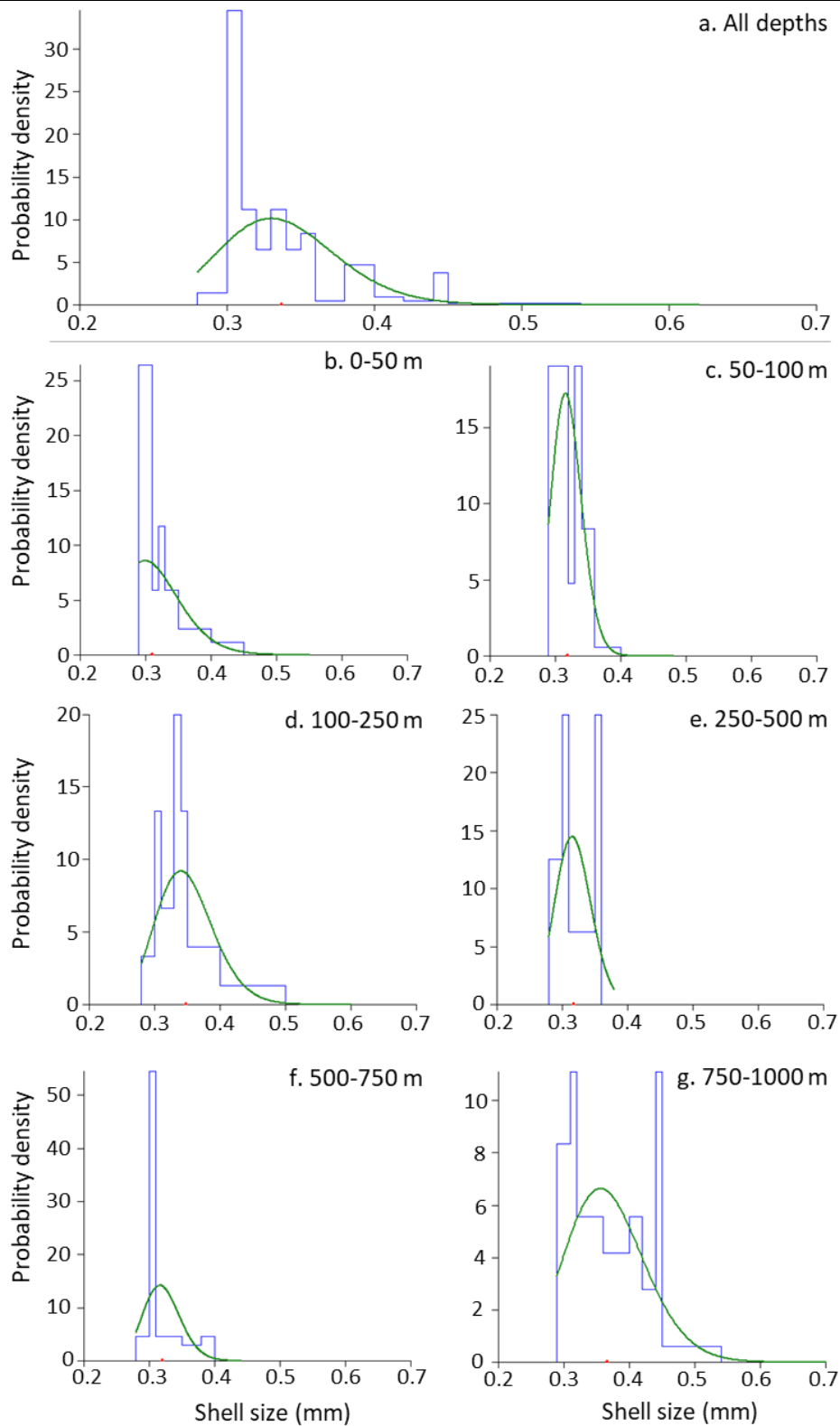
Figure 4-15. Mixture models fit to length-frequency data based on the shell width of living *L. helicina antarctica* for each depth across a transect stretching from the Falkland Islands to South Georgia between 26th February and 3rd March 1930. Mixture distributions were analysed using the *Mixdist* to identify whether distinct size cohorts were present at each depth. Blue lines represent the original length-frequency distribution and green lines are the sum of fitted distributions.
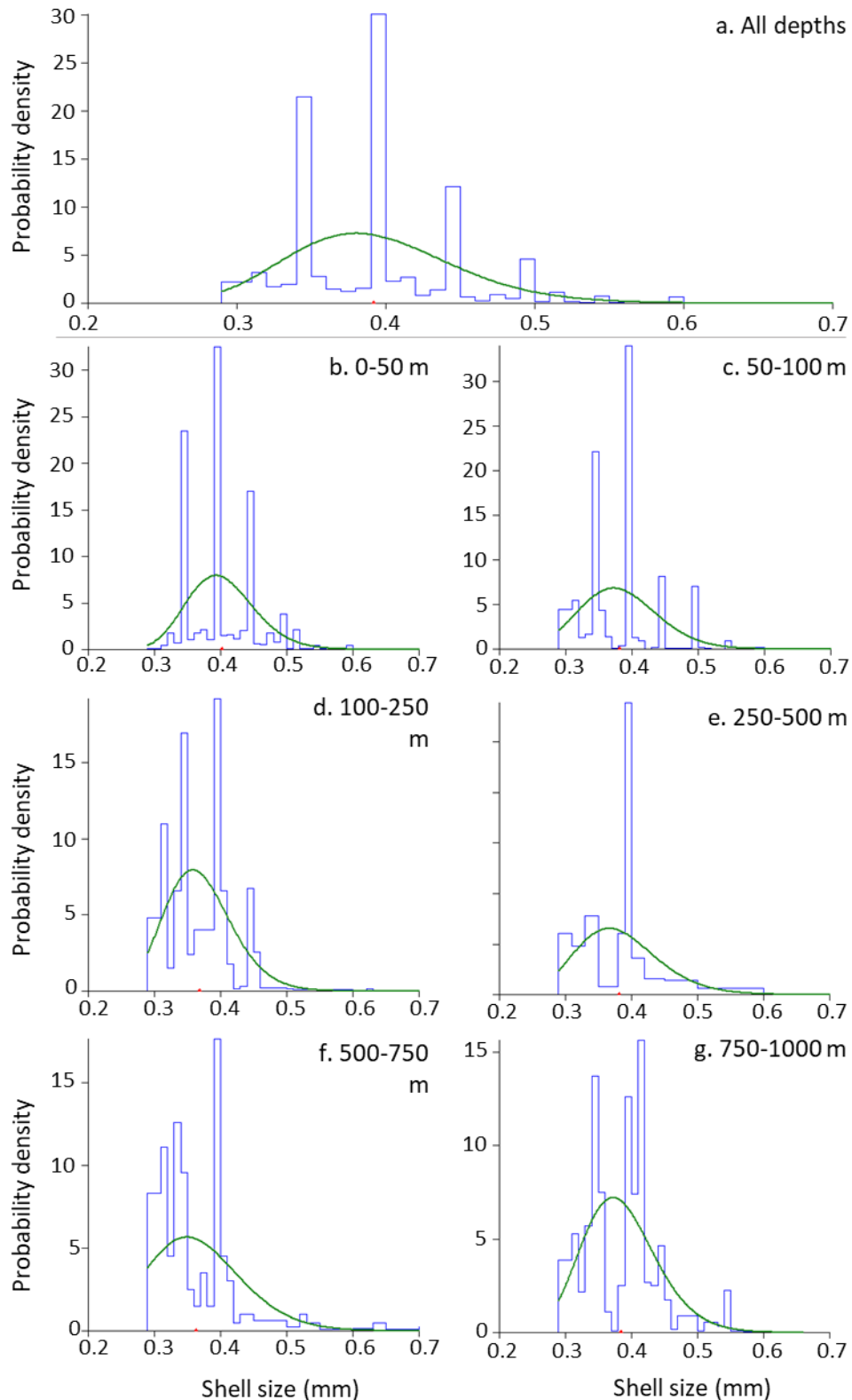
Figure 4-16. Mixture models fit to length-frequency data based on the shell width of living *L. retroversa australis* for each depth across a transect stretching from the Falkland Islands to South Georgia between 26th February and 3rd March 1930. Mixture distributions were analysed using the *Mixdist* to identify whether distinct size cohorts were present at each depth. Blue lines represent the original length-frequency distribution and green lines are the sum of fitted distributions.

4.4 Discussion

4.4.1 Considerations for the interpretation of the *Discovery Investigation* samples

No single net can reliably capture the full spectrum of plankton species and sizes (Voronina *et al.,* 1994). All nets have a degree of selectivity due to the mesh size (facilitating the escape of individuals of a certain shell size), avoidance behaviour and clogging (Riccardi, 2010; Voronina *et al.,* 1994). Nonetheless, net sampling remains the most common method of estimating plankton abundance.

The N70v net used by the R.R.S. *William Scoresby* had a middle section of mesh equivalent to ~440 µm and a rear section equivalent to ~195 µm. Therefore, it is likely that larval pteropods (individuals <300 µm) were under-sampled since they may have been able to escape through the mesh. Despite this, *Limacina* veligers were one of the most abundant pteropod groups sampled across the transect and individuals with shell diameters much smaller than this mesh size (60 µm) were captured. Net clogging from an abundance of phytoplankton can also cause loss of specific size classes or sample depths (particularly at the surface), however, there was no evidence of excessive phytoplankton quantities within the samples or log books so this was not considered an issue. The use of this mesh may lead to the underestimation of absolute veliger abundance, however, it will be standardised across all samples.

It is not ideal that the samples were collected at different times between day and night (within a four hour window). Despite this, the range of depths covered in each sample allows for some tolerance of the differences in times, especially considering the swimming speeds of the pteropods. Therefore, it is unlikely that the difference in collection time has impacted the depth distribution observed in this chapter.

Avoidance of the net may have resulted in under-sampling of pteropods over the transect. Juvenile and adult pteropods are faster and stronger swimmers than veligers and thus could outswim the net, skewing the data set towards smaller individuals. Pteropods of all sizes can sense turbulent motion and escape threats by rapid swimming or withdrawing their parapodia and rapidly sinking, with the

aid of their negatively buoyant shell, resulting in reduced levels of capture (Chang and Yen, 2012; Gilmer, 1974; Harbison and Gilmer, 1992). Despite adult *L. retroversa* being found, no larger (>0.74 mm) *L. helicina* were collected, which could be explained by their faster swimming speeds compared to *L. retroversa* (10-55 mm/s as opposed to 8 mm/s) (Adhikari *et al.,* 2016; Chang and Yen, 2012; Gilmer and Harbison, 1987). Alternatively, large *L. helicina* may undergo an ontogenetic migration as part of their life cycle in deeper water (see Chapter 3). Such behaviour has previously been observed in the Arctic for *L. helicina helicina,* but has not been reported for species in the Southern Ocean (Wang *et al.,* 2017; Kobayashi, 1974). It is postulated that this migration occurs at the end of summer, which is when this 1930 transect was completed. The *Discovery Investigations* sampled down to 1000 m, while seafloor depths ranged between 1434 and 3674 m. An Ontogenetic migration would therefore be missed if it extended below >1000 m.

Gymnosomes exhibit relatively slow swimming speeds, comparable to that of *L. retroversa* (1-7 mm/s) and so may have a similar evasion rate of nets. However, *Clione antarctica,* which is one of the two gymnosome species captured, lacks an escape swimming response (Borrell *et al.,* 2005; Gilmer and Lalli, 1990). Therefore, unlike thecosome species, it is less likely that gymnosomes reacted to turbulence produced by the net and escaped. We therefore assume that the abundance of gymnosomes was not impacted by sampling bias.

4.4.2 The diversity of pteropods across the Polar Front

Two species of thecosome pteropod were identified along the *Discovery Investigations* Falkland Island to South Georgia (FI-SG) transect sampled in 1930; *L. retroversa* and *L. helicina* (Figure 4.7) which are often the most common species found in the Polar Frontal and Antarctic Zones (Hunt *et al.,* 2008; Bernard and Froneman, 2009; Van der Spoel and Dadon, 1999; Roberts *et al.,* 2011; Howard *et al.,* 2011).

Modern-day investigations across the Southern Ocean have also identified *Clio pyramidata, Clio recurva, Clio piatkowskii* and *Limacina inflata* (van der Spoel *et*

al., 1997)*.* However, it is difficult to establish decisively whether these species were present during the transect and they were missed, or whether they were really absent. *Limacina inflata* are typically found in warmer waters (8 -28°C), therefore, it is not surprising these were not recorded within the northern Scotia Sea in 1930. *Clio piatkowskii* have mainly been recorded in the Weddell and Lazarev Seas with very few occurring towards the Polar Front (Chapter 3.; Hunt *et al.*, 2008; van der Spoel *et al.,* 1992; 1999), therefore, it is unlikely these would have been caught in 1930. *Clio recurva* have been recorded in the mesopelagic (200-1000 m) between Tasmania and Antarctica (Howard *et al.,* 2011; Van der Spoel and Dadon, 1999), but few records exist closer to South Georgia making it less likely that they would be captured. *Clio pyramidata* have often been recorded in the Polar Frontal and Antarctic Zone and might have been expected along the transect in 1930 (Akihaa *et al.,* 2017; Van der Spoel and Dadon, 1999; Hunt *et al.,* 2008; Roberts *et al.,* 2011; Howard *et al.,* 2011). The temperatures and salinities recorded along the transect in 1930 were well within the thermal tolerance of most Southern Ocean *C. pyramidata* formae today (Van der Spoel., 1992), therefore the environmental conditions were suitable. Furthermore, the gymnosome *Spongiobrachia australis* (Figure 4.7e) was present in the *Discovery Investigation* samples, a species which specialise on predating *C. pyramidata,* suggesting that *C. pyramidata* were present in 1930 (Mackas and Galbraith, 2012; Lalli and Gilmer, 1989). *C. pyramidata* are fast and strong swimmers compared to both *Limacina* species (see Section 4.4.1.), reaching speeds of ~40 mm/s (Davenport and Bebbington, 1990) and so larger individuals are more likely to be able to escape than the *Limacina* species. Despite this, we would expect to capture smaller individuals which have slower swimming speeds within the plankton nets. Further investigation of *Discovery samples* as well as alternative sampling techniques is needed to establish whether there is a true absence of *C. pyramidata* in the Scotia Sea during 1930.

4.4.3 The distribution of pteropods in the Polar Frontal and Antarctic Zones

The *Discovery Investigations* transect between the Falkland Islands and South Georgia crossed two major biogeographical zones; the Polar Frontal Zone and the Antarctic Zone separated by the Polar Front. The position of the Polar Front was similar to its modern-day location (Moore *et al.,* 1999; Belkin and Gordon, 1996; Orsi *et al.,* 1995; Gille, 1994). A clear shift in pteropod species assemblage occurred between the biogeographic zones, with *L. retroversa* mainly being affiliated with the Polar Frontal Zone, although ranging into the Antarctic Zone, and *L. helicina* only occurring within the Antarctic Zone. A similar distribution across the Polar Front has also been found in modern-day studies, with *L. retroversa* being recognised as a boreal, Polar Frontal species and *L. helicina* a true polar species (Akiha *et al.,* 2017; Hunt *et al.*, 2008; Chen and Be, 1964; Van der Spoel, 1967; 1976; Lalli and Gilmer, 1989). Therefore, the region between the Falkland Islands and South Georgia could be utilised as an important monitoring area for biogeographic changes in the distributions of pteropods since it encompasses both the southern range limit of *L. retroversa* and the northern range limit of *L. helicina.* It should be noted that the biogeographical ranges described in this chapter uses zones rather than geographical points due to the dynamic spatial nature of the Polar Front.

Temperature has been identified as the single most important physical variable in determining the latitudinal distributions of species (Parmesan and Yohe, 2003; Parmesan *et al.,* 2005). Recent biogeographical shifts of plankton have been associated with the warming of the sea surface near the Antarctic Peninsula (Montes-Hugo *et al.,* 2009) and in the North Atlantic (Beaugrand *et al.,* 2009; Hinder *et al.,* 2014). Previous studies have demonstrated that pteropods are sensitive to changes in temperature (Beaugrand *et al.,* 2013; Mackas and Galbraith, 2012; Siebel *et al.,* 2012; Mass *et al.,* 2011; Siebel *et al.,* 2007) (see Section 1.9). The most striking difference in environmental conditions between the Polar Frontal and Antarctic Zones was the sea surface temperature, with the Polar Frontal Zone being warmer than the Antarctic Zone.

Biogeographical shifts in association with temperature are mainly influenced by the strong relationship to physiological performance and an organism's optimal thermal niche (Pörtner, 2002). *L. retroversa* have been recorded to occupy waters between 5-9°C (<100 m) in the Argentine Sea (Dadon, 1990) and 2-12°C in the Northern hemisphere (Beckmann *et al.,* 1987; Bigelow, 1924; Chen and Be, 1964; Maas *et al.,* 2016). The optimal temperature for *L. retroversa australis* is estimated at 2-7°C (Van der Spoel and Heyman, 1983) with a thermal maximum of 18°C (Biglow, 1924). *L. retroversa* were found to occupy a temperature range of 0.7-6.9°C along the FI-SG transect in 1930, suggesting they can tolerate lower temperatures than this 2°C optimum. However, it is possible that *L. retroversa* individuals occupying temperatures below 2°C are functioning sub-optimally*.* From the *Discovery investigation* FI-SG transect, *L. retroversa* were found to be most abundant at 3.8°C which is within their proposed optimal range. Conversely, *L. helicina* are true polar pteropods, occupying a lower temperature range of -1.6-5.5°C in the Northern hemisphere, with a thermal maximum of 7°C (Van der Spoel and Hayman, 1983; Chen and Be, 1964). The *L. helicina* found along the FI-SG transect in 1930 occupied temperatures between 0.7- 4.2°C, being most abundant at 2.4°C.

In addition to warming in the Scotia Sea (Whitehouse *et al.,* 2008; 2006), it is expected that the Polar Front will migrate southwards over the coming decades (Sokolov and Rontoul, 2009). In order to persist in the face of such change, pelagic species may shift their geographical distribution to stay within their thermal limits (Bates *et al.,* 2014). Mackey *et al.,* (2012) constructed baseline distributions of a wide range of taxa within the Atlantic sector of the Southern Ocean and Bellingshausen Sea (<100 m) and predicted that all taxa, including pteropods, will shift polewards with 1°C of regional warming. Based on the temperature and zonal distributions found in Chapter 4, the biogeographic range of *L. helicina* is likely to contract closer to the Antarctic continent with future warming (although see Tarling *et al.,* 2018). In contrast, more suitable conditions for *L. retroversa* will become available, enabling their range to expand or shift southwards.

As well as the strong relationship between temperature and physiological performance, other ecological aspects also control biogeographical distributions including species interactions, trophodynamics and community composition (Richardson, 2008; Parmesan and Yoho, 2003). Gymnosomes were present at every station along the FI-SG transect in 1930, contributing 1.17- 11.11% of the pteropod population in the Polar Frontal Zone and 0.65- 2.90 % in the Antarctic Zone. The absolute abundance of gymnosomes was also lower in the Antarctic Zone in comparison to the Polar Frontal Zone. Physiologically, gymnosomes have a much higher thermal tolerance than their thecosome pteropod prey, with *Clione antarctica's* range being -1.7°C to 15.2°C and *Spongiobranchaea australis's* being 2.3- 13.2°C (Dymowska *et al.,* 2012; Dadon and Chauvon, 1998; van der Spoel, 1976). In the Discovery Investigations samples gymnosomes were found in waters between 0.68-6.90°C which is well within this tolerance range. It is unlikely therefore, that the distribution of gymnosomes was controlled by temperature along the FI-SG transect which was more correlated with *L. retroversa* and *L. helicina* distributions*.* Gymnosomatous pteropods are highly specialised predators which have evolved in concert with their thecosomatous relatives, which are their exclusive prey item (Seibel *et al.,* 2007; Gilmer and Lalli, 1990; Conover and Lalli, 1972). Therefore, the distribution of gymnosomes is most likely to match the population distribution of their prey items.

The FI-SG transect has no freshwater or sea ice influence, therefore, it is unlikely that salinity variability would be a major controlling factor for pteropod distributions. *L. retroversa* were collected within salinities ranging from 33.90- 34.72 and *L. helicina* at 33.80-34.70. *L. retroversa* are euryhaline, meaning they have a wide tolerance of salinities (30.1- 36.0). The tolerance window of *L. helicina* is narrower, being 33.55-36.14, which makes them more vulnerable to freshwater inflow which could be an influencing factor for more southern populations where there is more sea ice present, but not between the Falkland Islands and South Georgia (Dadon, 1990; Manno *et al.,* 2012; Gilmer, 1974; Kobayash, 1974).

4.4.4 The depth distribution of pteropods

Pteropods are mainly described as an epipelagic species (upper 200 m); co-occurring with phytoplankton which form a major part of their diet (Hunt *et al.*, 2008; Akiha *et al.,* 2017; Atkinson *et al.,* 1996; Wang *et al.,* 2017). However, a growing number of studies are finding pteropods within the mesopelagic (200-1000 m) with a much more varied diet (Hunt *et al.,* 2008; Wormuth, 1981; Bednaršek *et al.,* 2012a; Kobayashi, 1974). Bednaršek *et al.* (2012a) collated a large database of global pteropod abundance, with pteropods recorded at depths down to 2000 m. The highest biomass of pteropods along the Discovery Investigations FI-SG transect was found at 0-200 m with a rapid decrease to 1000 m, although, there were distinct regional differences. We found that all pteropod groups were present down to 1000 m, being most abundant at 50-100 m. This emphasises the need to sample down to >1000 m rather than concentrating on the epipelagic since this may result in underestimation of pteropod population abundances and distributions. The *Discovery Investigations* only sampled to 1000 m. It is possible that there were pteropods below this depth since the sea floor was between 1434 and 3674 m deep. This may impact abundance estimates as well as species distribution records (see Section 4.4.3).

Each species had its own distinct vertical distribution which altered between day and night, in agreement with Van der Spoel and Dadon, (1990). *L. retroversa* were most abundant in the upper 200 m during the day, while, at night they had a much wider depth distribution with many individuals migrating upwards to 0-50 m as well as descending to 500-700 m. Similarly, *L. helicina* were most abundant at the surface during the day with a second peak at 700-1000 m. At night, most individuals had migrated upwards to the surface (0-100 m) and 250-500 m. This differential depth distribution between day and night suggests that both *L. helicina* and *L. retroversa* undertake a weak vertical migration. In general, vertical migration to the surface at night is undertaken to reduce the risk of predation by visual predators and to feed in the area where food is most abundant (Hays, 2003; Gliwicz, 1986). Previous studies have also found an increase in the abundance of *L. retroversa* in the upper 50 m during the night (Chan and Bé, 1964; Beckmann *et al.* 1987; Wormuth, 1981). Surface densities of

L. helicina have also been observed to increase at night (Steinburg *et al.,* 2015; Atkinson *et al.,* 1996; Hunt *et al.,* 2008). While we show that both *L. helicina* and *L. retroversa* shift their vertical distribution at night, individuals were still most abundant at the surface during the day indicating that illumination is not the main control on vertical distribution.

All individuals of *L. helicina* and *L. retroversa* identified (maximum shell size <0.8 mm) were juveniles except for two adult *L. retroversa* (3.23 mm and 1.5 mm) (following Lalli and Gilmer, 1989). As discussed in Section 4.4.1. it is most likely that adult *L. helicina* and *L. retroversa* were either present at depths greater than 1000 m or were able to avoid the net by being faster and stronger swimmers than juveniles and veligers. Since adult pteropods are not represented in the baseline outlined in the current chapter, further work on the vertical and biogeographic range of the adult stages is needed.

There was no difference in the size distribution of juvenile *L. helicina* and *L. retroversa* with depth between day and night or between the Polar Frontal and Antarctic Zones. Similarly, Kobayashi (1974) found no differences in *L. helicina* shell sizes (0.4-0.7 mm) between depths during Arctic summer. The lack of size assortment with depth indicates that both small and large juveniles utilise the entire water column (<1000 m), with no skew of smaller individuals in the surface.

By comparing the depth distribution of gymnosomes and juvenile *Limacina*, it appears that *Limacina* are avoiding depths where gymnosomes are more abundant. Alternatively, this observation may be due to *Limacina* at this depth being predated on. Whether this observation is due to the cause or effect, it supports the idea that vertical migration by *Limacina,* like many other migrators, is most likely undertaken as a predator avoidance behaviour (Lampert, 1993). Gymnosomes displayed a clear vertical migration from the deeper layers in the day to the surface at night. During the day, gymnosomes were less abundant between 0-100 m while *L. helicina* and *L. retroversa* were most abundant. Furthermore, there were very few gymnosomes at 700-1000 m, which could explain the secondary peak abundance of *L. helicina* at these depths. At night,

the gymnosomes moved to the upper 0-250 m. While both *Limacina* species also moved upwards, both also congregated deeper in the water column (*L. retroversa:* 500-700 m; *L. helicina*: 250-500 m), reducing the vertical overlap with gymnosomes. It is likely that predation risk is a stronger factor in controlling juvenile pteropod distribution than food supply since adult pteropods are able to capture a variety of food sources within their large mucous nets (see Section 1.1).

The veligers of *Limacina* species (<0.3 mm), unlike juveniles, were predominantly present within the surface (<100 m) across the entire transect with no evidence of vertical movement between day or night. Veligers are probably constrained to the surface since they have limited swimming capabilities, relying on ciliated velums for locomotion rather than the characteristic wings which develop in the juvenile stage (Lalli & Gilmer 1989; Howes et al., 2014; Lebor, 1932). Since veligers have limited vertical movement, the benefit of residing in the food-rich surface layers, allowing increased growth rates (Dadon and deCidre, 1992), is greater than the threat of predation (as discussed in Section 4.4.4.). However, once individuals develop wings they utilise the entire water column sampled (<1000 m), avoiding the threat of predation by gymnosomes while maximising the time spent within food-rich surface layers. Therefore, the predator avoidance behaviour observed for juvenile *L. helicina* and *L. retroversa* is likely to be stage dependent.

Both gymnosomes and thecosome pteropods are themselves an important food-source to a host of other organisms including numerous carnivorous zooplankton, fish, mammals and birds (Pomerleau *et al.* 2012; Levasseur *et al.* 1994; Murphy *et al*, 2016; Litz *et al.,* 2016; Karnovsky *et al*. 2008). Since many of these are visual predators it would be beneficial to avoid surface layers during the day. However, both *Limacina* species remain in the upper 200 m during the daytime, while gymnosomes migrate deeper, suggesting other factors are also controlling their distribution. Interestingly, *Clione limacina* lacks an escape response from predators, while *Limacina* can detect turbulence from predators and rapidly sink to avoid them (Borrell *et al.,* 2005; Gilmer and Lalli, 1990). Therefore, *Clione limacina* may experience a greater threat from predation and

avoid the photic zone during the day. Gymnosomes and thecosome pteropods have coevolved highly specialised predation and evasion techniques in a predator-prey arms race (Seibel *et al.,* 2007). Because of this co-evolution, it is likely that the predator evasion techniques of *Limacina* are less effective against gymnosomes in comparison to visual predators. It would be more beneficial for *Limacina* to avoid gymnosomes and reside in the surface layers during the day despite the threat from visual predators.

4.4.5 Concluding remarks and summary

This Chapter contributes towards a fundamental baseline on the biogeographical range of pteropods before the impact of anthropogenic change in the Scotia Sea. This baseline is crucial for future comparisons and interpretation of pteropod ranges. Figure 4.17. gives a schematic summary of a historic baseline for the vertical and biogeographical distribution of pteropods across the Polar Front.

4.4.5.1 Biogeographical boundaries

This Chapter shows that the northern range of *L. helicina* is bounded by the Polar Front with the northern Antarctic Zone being the trailing edge of *L. helicina's* biogeographic range. Since the abundance of *L. retroversa* drops south of the Polar Front, the northern Antarctic Zone marks the southern, leading edge of its range. It is likely that the biogeographic ranges of both *Limacina* species are limited by their thermal tolerances. Contrastingly, gymnosomes were found across the entire transect, reflecting the abundance of the *Limacina* species rather than the temperature differences owing to their wide thermal niche and close predator-prey relationship with thecosome pteropods.

4.4.5.2 Vertical distribution

The differential depth distribution between day and night suggests that both *L. helicina* and *L. retroversa* undertake a weak vertical migration. This vertical migration was not only in response to illumination, but as a predator avoidance behaviour since vertical segregation between gymnosomes and their *Limacina* prey was identified. Vertical distribution was also dependent on life stage with veligers residing in the upper 100 m and juveniles being dispersed across all sampling depths (0-1000 m). The absence of adult *Limacina* also suggests that larger individuals may migrate to depths greater than 1000 m although, it is also possible that individuals were able to avoid the plankton nets.
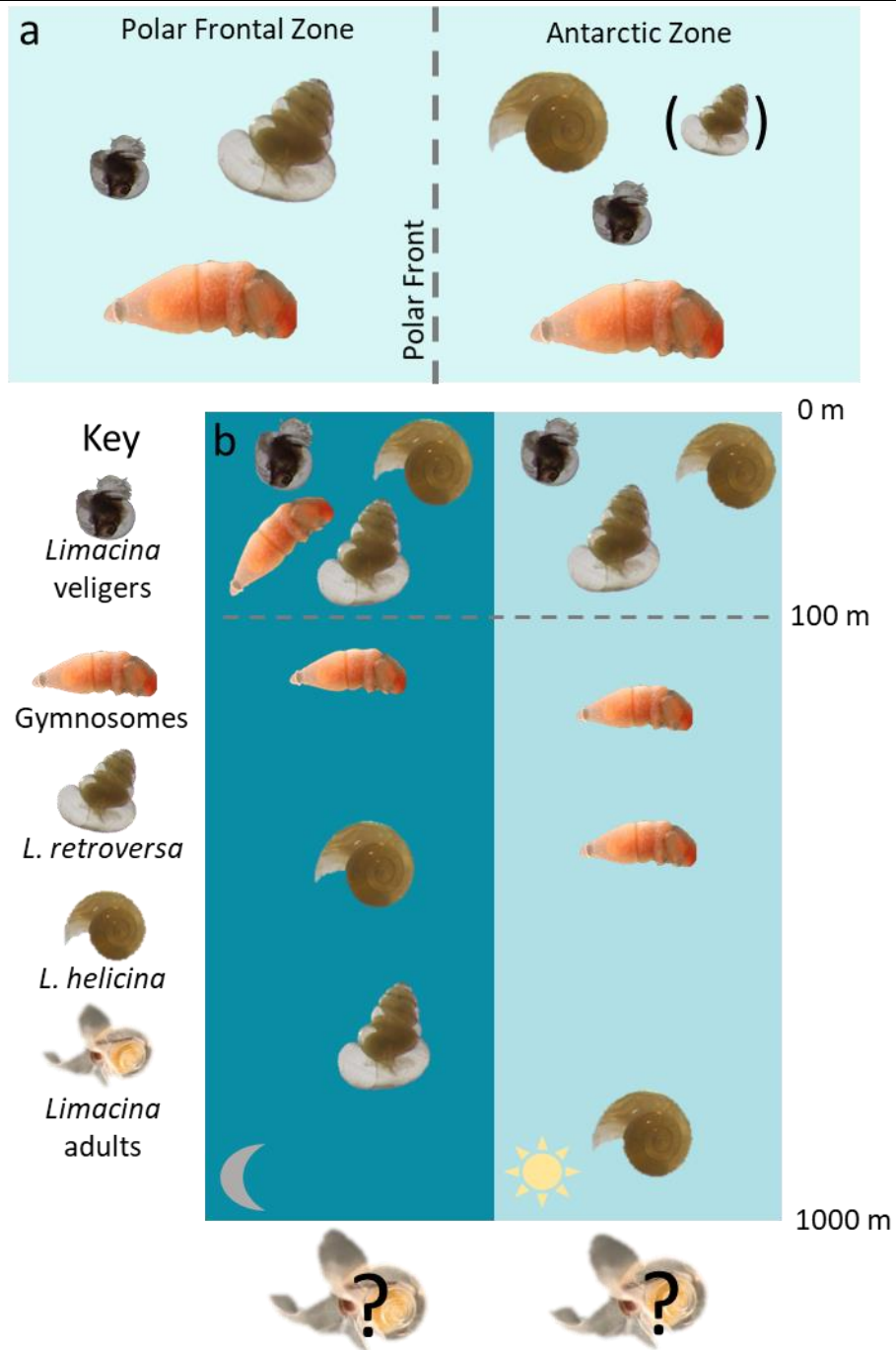
Figure 4-17. Schematic summary of a historic baseline for the vertical and biogeographical distribution of pteropods across the Polar Front. In (**a**) *L. helicina* are only found within the Antarctic Zone, while *L. retroversa* are less abundant here, mainly being present in the Polar Frontal Zone. Gymnosomes and veligers were present across the entire transect. In (**b**) Veligers were mainly present in the upper 100 m during the day and night. Both *L. helicina* and *L. retroversa* undertook a weak vertical migration to avoid gymnosomes between the day and night. No adult pteropods were captured so it is unknown where these individuals reside within the depth horizon.

5 Pteropod shell condition in relation to carbonate chemistry during the summer within the Scotia Sea

5.1 Introduction

The oceans have absorbed around 28% of emitted CO_2 since 1850 (Le Quéré *et al.,* 2016), leading to a globally averaged decrease in seawater pH of 0.1 (Raven *et al.,* 2005) and a reduction in the availability of carbonate ions (CO_3^{2-}), known collectively as ocean acidification. Bicarbonate ions are the building blocks for marine calcifying organisms to form biogenic calcium carbonate ($CaCO_3$) shells, skeletons or internal structures. A reduction in the availability of carbonate ions when Ω_{ar} is <1 will increase the energetic requirement for calcification as well as the dissolution of unprotected shells. Calcifiers within high-latitude ecosystems have been the focus of studies investigating the impact of ocean acidification, since they are expected to experience carbonate ion undersaturation first (McNeil and Sasse, 2016; Doney *et al.,* 2009).

Thecosome (shelled) pteropods have been identified as one of the most vulnerable calcifiers, since they are particularly abundant in polar oceans and they build their shells from aragonite, a polymorph of $CaCO_3$ that is ~50% more soluble in seawater than calcite (Mucci, 1983). Thecosome pteropods are one of the main planktonic producers of aragonite, attributing 20- 42% of the global pelagic carbonate budget (global sources and sinks of carbonate) (Bednaršek *et al.,* 2012; Manno *et al.,* 2007; 2009; Gangstø *et al.,* 2008). They contribute to the biological carbon pump through rapid sinking of faecal pellets, mucous webs, pseudo-faeces (mucous packages of inedible material) and mortality as well as the carbonate pump via the sinking of their shells (Pasternak *et al.,* 2017; Manno *et al.,* 2007; 2009). In the Ross Sea, up to 72% of organic carbon export during blooms can be attributed to *Limacina* species (Manno *et al.,* 2010) with their faecal pellets being responsible for up to 95.5% of biogenic flux (Accornero *et al*., 2003). Since pteropod abundance in the Ross Sea is similar to that in the Scotia Sea (Hunt *et al.,* 2008) it is likely that pteropods play a similar role in carbon flux.

5.1.1 Pteropods and shell dissolution

Numerous incubations of thecosome pteropods within conditions undersaturated with aragonite have demonstrated decreased calcification (Comeau *et al*., 2009; 2010; Lischka *et al*., 2011) and shell dissolution (Bednaršek

et al., 2012; Lischka and Riebesell, 2012) (Table 1.2). However, there is concern over the applicability of experimental incubations to natural populations since pteropods are notoriously difficult to culture owing to their fragile shells, handling sensitivity, poorly understood feeding mechanisms and undescribed buoyancy regulation (Howes *et al.,* 2014). Alternatively, areas which are naturally undersaturated with respect to aragonite can potentially be natural laboratories for considering the *in-situ* response of pteropods to anthropogenic ocean acidification, without some issues which accompany experimental studies. Wild caught pteropods from regions of upwelled deep water enriched with CO_2 along the U.S. west coast and in the northern Scotia Sea have all found evidence of *in-situ* shell dissolution (Bednaršek and Ohman 2015; Bednaršek *et al.,* 2014a; 2014b; 2012a; 2016). Furthermore, pteropods with shell dissolution have also been found along ice margins within the Greenland Sea after exposure to wintertime undersaturation (Peck *et al.,* 2016).

Aragonite saturation (Ω_{ar}) in high-latitude ecosystems is influenced by sea ice, freshwater inputs, temperature change, upwellings and biological activity (Hauri *et al.,* 2015; Fransson *et al.,* 2016) resulting in large spatiotemporal variation (Bakker *et al.,* 2016; Legge *et al.,* 2016). Consequently, to provide an adequate environmental context for pteropods, *in-situ* carbonate chemistry measurements should be coupled with pteropod sampling. Currently there is little overlap between *in-situ* sampling of pteropods and water column carbonate chemistry, therefore, we have limited understanding of the baseline conditions in which pteropods reside. A recent comprehensive overview by Manno *et al.* (2017) recommended further assessment of pteropod shell condition in relation to carbonate chemistry to improve our baseline knowledge of pteropod habitat, particularly in regions of rapid change, like the Scotia Sea (see Section 4.1.3.).

5.1.2 The role of the periostracum for pteropods

The shell microstructure of thecosome pteropods comprises of a lower cross-lamellar layer overlaid by a prismatic sheet, which is coated by a thin organic layer called the periostracum (Figure 5.1.). The main roles of the periostracum is to isolate the site of calcification from the surrounding seawater and provide a template for shell formation. Shell formation occurs in the extrapallial cavity by

increasing the carbonate ion concentration via active pumping and/or passive transport and encouraging the nucleation of aragonite crystals (Marin and Luquet, 2004). For crystallisation to occur, individuals elevate intracellular pH via the active removal of hydrogen ions, however, under acidified conditions, maintaining this pH gradient has a greater energetic cost (Jokiel, 2011). Many calcifying organisms have been shown to mitigate ocean acidification and continue shell formation by the regulation of intracellular pH. This regulation of intracellular pH during acidification has been measured directly using pH-sensitive probes and dyes in corals (Venn *et al.,* 2013) and calcifying echinoid larvae (Stumpp *et al.,* 2012), although intracellular pH reduced under acidified conditions. Reductions of intracellular pH of only 0.1–0.2 pH units have been associated with reduced cellular metabolism (Reipschlager and Portner, 1996). Experimental studies suggest that pteropods are able to maintain this gradient under short-term ocean acidification conditions since calcification continues, although, it is at a slower rate (Comeau *et al.,* 2010a; 2010b; Lischka *et al.,* 2011). Calcification may be able to continue at the normal rate or over longer time periods if there is sufficient food supply while experiencing aragonite undersaturation (Ramajo *et al.,* 2016). It is rare for pteropods to be supplied with food during experimental incubations since it is difficult to encourage feeding (Howes *et al.,* 2014), therefore, our current understanding of the ability for pteropods to maintain their intracellular pH in a food rich environment is limited.

As well as interfering with internal acid-base balance, ocean acidification can also cause the dissolution of unprotected shells. The periostracum acts as a protective layer, being an important component in determining the susceptibility of mollusc shells to dissolution (Ries *et al.,* 2009). Some *Mytilus* species are able to withstand conditions close to volcanic vents which are highly corrosive to $CaCO_3$ due to their thick periostracum, however, if it is breached, the underlying shell is rapidly dissolved (Tunnicliffe *et al.,* 2012; Rodolfo-Metalpa *et al.,* 2011).

Breaches to the periostracum may occur naturally from bacterial damage (Bausch *et al.,* 2018), failed predation attempts and epibionts, or un-naturally during sampling and culturing. Since the periostracum is secreted at the edge of

the mantle, once it has been damaged, an individual cannot repair it, therefore, the aragonite exposed after a breach will be susceptible to progressive dissolution if $\Omega_{ar} \leq 1$. If conditions are favourable, pteropods are able to thicken the inner shell wall to maintain shell integrity, although, this is likely to be at a metabolic cost (Peck *et al.,* 2018).

There is currently debate within the literature surrounding the effectiveness of the periostracum in protecting the shells of pteropods from aragonite undersaturation. Peck *et al.,* (2016a; 2016b) stipulate that shell dissolution only occurs when there has been a breach or perforation in the periostracum while Bednaršek *et al.,* (2016a; 2014a; 2012b) state that the periostracum is ineffective since it is extremely thin (>1 µm). If dissolution only occurs where there is a breach in the shell periostracum, it is possible that thecosome pteropods are not as vulnerable to ocean acidification as previously claimed. Further investigation into the effectiveness of the periostracum in protecting pteropod shells is needed to contribute to this debate.
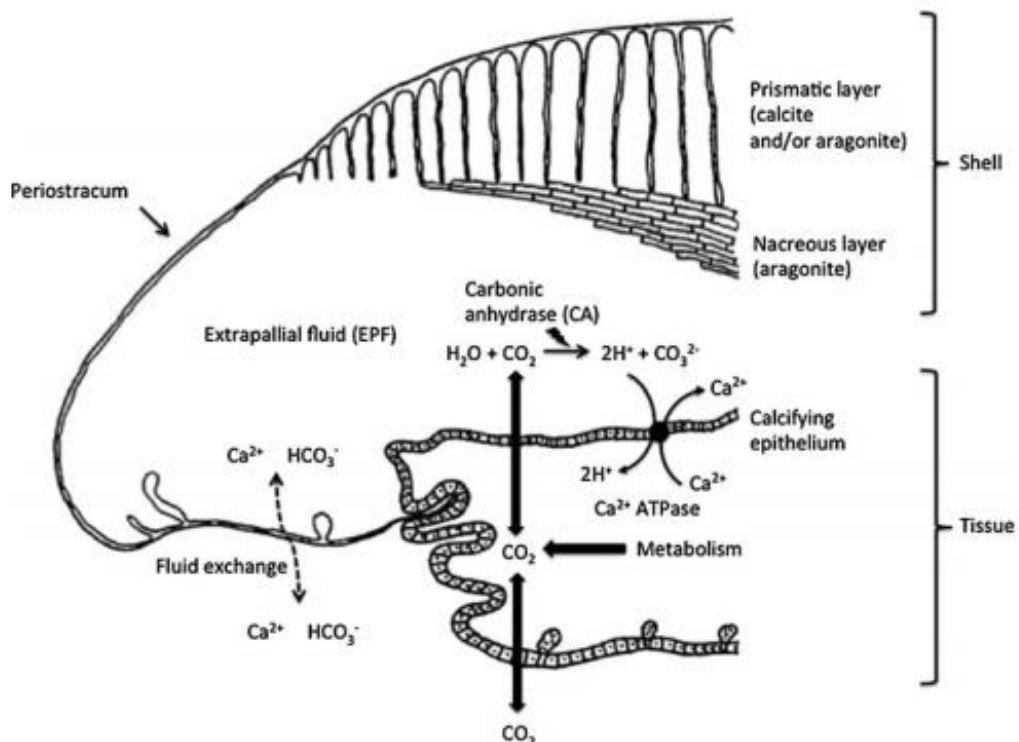
Figure 5-1. Calcification in a molluscan shell and the shell microstructure. Shell crystallisation occurs within the extrapallial space which is isolated by the periostracum. Image taken from Gazeau *et al.* (2013).

5.1.3 Chapter Aims

Chapter 5 aims to define the present day, *in-situ* state of *L. helicina antarctica* shells in relation to summer carbonate chemistry within the Scotia Sea. Water samples and pteropods were collected in parallel from areas of aragonite undersaturation ($\Omega_{ar} < 1$) and supersaturation ($\Omega_{ar} > 1$) during two research cruises in the austral summers of 2014 (JR304) and 2015 (JR15002). Three specific aspects will be investigated:

1. Station hydrography with focus on Ω_{ar} with depth
2. Vertical distribution of *L. helicina antarctica*
3. *In-situ* shell condition of *L. helicina antarctica*

5.2 Methods

5.2.1 Seawater sampling

Seawater sampling was carried out during two oceanographic cruises, JR304 and JR15002, on the R.R.S. *James Clark Ross* in 2014 and 2015, respectively (Table 5.1). A vertical profiler with a CTD (Conductivity-Temperature-Depth; SBE9Plus), was deployed at each station alongside pteropod sampling (see Section 5.2.4.) to characterise the water column structure. Seawater potential temperature was calculated using 'oce{swTheta}' (Kelly and Richards, 2017) using a reference pressure of 0 dbar and plotted using 'oce{plot.TS}' (Kelly and Richards, 2017). A Linear Discriminant Analysis was performed to disentangle which environmental factor explains the greatest dissimilarities between the stations. The model was created using 'lda{MASS}' (Venables and Ripley, 2002), while plots were created using 'plot.dudi{ade4}' (Dray and Dufour, 2007). The assumption of equal variances was checked using boxplots and equal covariance ellipses 'heplots{covEllipses}'. Homogeneity of variance-covariance matrices was tested using the Box's M-test 'heplots{boxM}' and levenes test 'base{leveneTest}. Both assumptions were met.

Water samples for Dissolved Inorganic Carbon (DIC) and Total Alkalinity (TA) were collected from 12 L Niskin bottles which were in a rosette (SBE32 carousel water sampler) around the CTD. All water samples were collected according to standard operating procedures (Dickson *et al.,* 2007). Samples were drawn from

the Niskin bottles into 250 mL borosilicate glass bottles through tygon tubing that had been soaked in seawater (Figure 5.2.). Bottles were rinsed twice and then overflowed for 25 seconds so that the bottle was flushed twice. Bottles were filled bottom up at a slow rate so that air bubbles were not introduced. A 2.5 mL headspace was created in the sample using a Pasteur pipette, to allow the sample to expand if warmed. Immediately after, 50 µL of saturated mercuric chloride ($HgCl_2$) solution was added to fix the sample and prevent any further biological activity from altering the organic and inorganic composition. The bottles were sealed using ground glass stoppers greased with Apiezon (silicone) grease, secured with elastic bands and then stored in darkness. Depending on the seafloor depth, 6-19 water samples were taken for each station. Furthermore, nine duplicate water samples were taken from four stations to quantify uncertainty that might arise from sampling and analysis. Depths of water sample collection was based on the needs of several other investigations and are therefore not uniform across sites, however a full profile was depth represented as much as logistically possible. The locations of the stations are shown in Figure 5.3 where frontal positions, as defined by Orsi *et al.* (1995), were mapped using 'orsifronts{orsifronts}' onto a bathymetric map using 'marmap{plot}' (Pante and Simon-Bouhet, 2013). The sample depths, dates, locations and the seafloor depths are given in Table 5.1.

Figure 5-2. (**a.**) Water samples were collected from Niskin bottles in a rosette around a CTD during two summer research cruises by the R.R.S. *James Clark Ross* (JR304; 2014 and JR15002; 2015) within the Scotia Sea (Southern Ocean). (**b.**) The total alkalinity and dissolved inorganic carbon of these water samples were measured using a VINDTA (Versatile INstrument for the Determination of Titration Alkalinity).
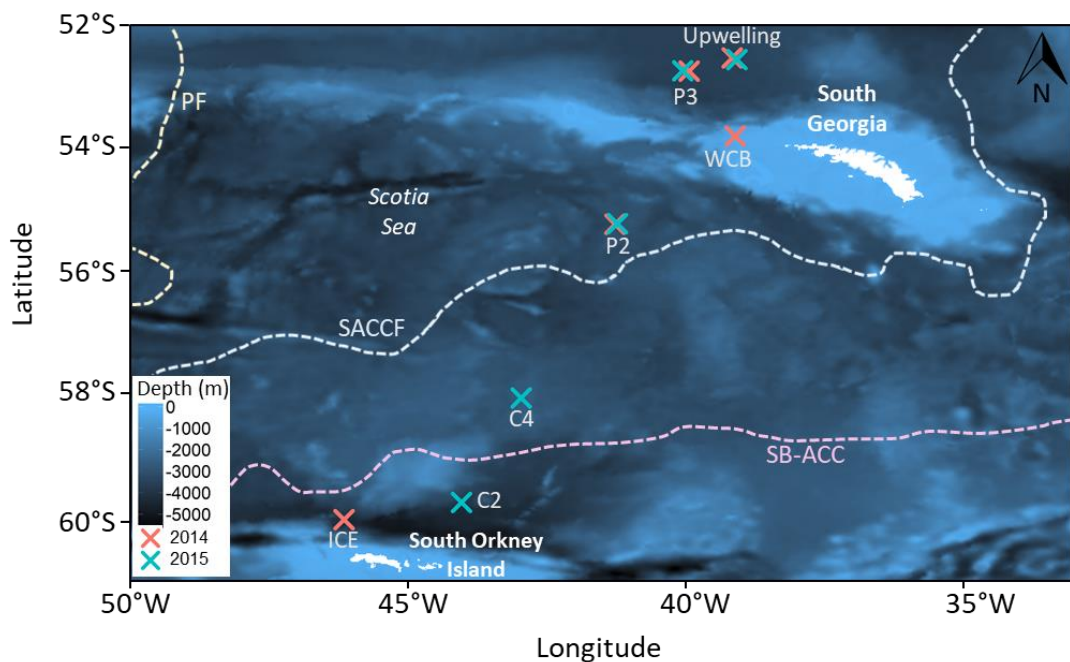
Figure 5-3. An overview of the study region and stations used to describe the carbonate chemistry of the Scotia Sea (Southern Ocean). Stations were sampled by the R.R.S. *James Clark Ross* during cruises JR304 in 2014 (✗) and JR15002 (✗) in 2015. Dashed lines indicate the position of the Polar Front (PF) (▬ ▬), Southern Antarctic Circumpolar Current Front (SACCF) (▬ ▬) and the Southern Boundary of the Antarctic Circumpolar Current (SB-ACC) (▬ ▬). Positions of the PF and SB-ACC were taken from Orsi *et al.* (1995), while the position of the SACCF was from Thorpe *et al.* (2002).

Table 5.1. Details of stations where water samples were collected for the analysis of carbonate chemistry within the Scotia Sea (Southern Ocean) during two research expeditions (JR304 in 2014 and JR15002 in 2015) by the *R.S.S. James Clark Ross*.

Station name	Sampling date	Latitude (°S)	Longitude (°W)	Seafloor depth (m)	Depths Sampled (m)
ICE	28/11/2014	59.9623	46.15975	4846	5, 11, 22, 41, 52, 62, 81, 102, 152, 404, 505, 607, 809, 1012, 1418, 1625, 1828, 2032.
C2	21/11/2015	59.6887	44.0543	4156	11, 101, 151, 201, 301, 501, 601, 801, 1001.
C4	21/11/2015	58.0229	42.9842	2847	11, 101, 201, 301, 401, 501, 603, 801.
P2	25/11/2014	55.2528	41.30237	3444	5, 41, 52, 62, 81, 102, 162, 203, 404, 505, 607, 809, 1418, 1625, 1828, 2032.
P2	22/11/2015	55.2426	41.2576	3357	57, 99, 101, 201, 801, 999, 1401, 1699, 1701, 1999, 2001, 2601.
P3	14/12/2014	52.8116	39.97267	3790	5, 19, 40, 51, 60, 100, 126, 176, 201, 303, 505, 607, 1011, 1418, 2029.
P3	28/11/2015	52.8052	40.0863	3361	9, 51, 101, 201, 301, 401, 601, 1001, 1401, 2001, 3001, 3735.
Upwelling	14/12/2014	52.6004	39.19965	3746	5, 11, 21, 40, 61, 81, 102, 126, 202, 304, 505, 606, 810, 1013.
Upwelling	09/12/2015	52.6272	39.1152	3740	5, 39, 71, 99, 203, 301, 401, 603, 1401, 1999, 2401, 2801, 3219, 3685.
WCB	09/12/2014	53.8477	39.14336	590	6, 22, 41, 62, 102, 151, 201.

5.2.2 Carbonate chemistry analysis

TA was measured by potentiometric titration (Mintrop *et al.,* 2000) and DIC by coulometry (UIC, coulometer model 5011, USA) (Johnson *et al.,* 1985) following the standard operating procedure by Dickson *et al.* (2007). Both TA and DIC were measured using a VINDTA (Versatile INstrument for the Determination of Titration Alkalinity, version 3C, Kiel, Germany) at the University of East Anglia (School of Environmental Sciences) (Figure 5.1.). The system was maintained at 25°C by continual movement of controlled temperature water around the glassware during analysis (mean for JR304 of 25.29°C, S.D. 0.41°C and for JR15002 of 25.53°C, S.D. 0.46°C). Samples from JR304 (2014) were analysed between 12/08/2015 and 19/08/2016 and samples from JR15002 (2015) were analysed between 10/11/2016 and 22/11/2016. For each day of analysis, the coulometric cell was cleaned with acetone and deionised water under slight pressure and dried overnight at 60°C. The drying agent (magnesium perchlorate) was also replaced daily to minimise the risk of contaminating the coulometric cell with water vapour. The VINDTA was calibrated against two 500 ml Certified Reference Material (CRM batch 133) each time a coulometer cell was replaced. The CRM batch was certified for total dissolved inorganic carbon using a Ruska electronic constant-volume manometer by the Scripps Institution of Oceanography.

The remaining variables of the carbonate system were calculated using the CO_2SYS programme (version 1.05; Lewis and Wallace, 1998; Pierrot *et al.,* 2006) using the constants of Mehrbach *et al.* (1973) refitted by Dickson and Millero (1987) and sulphate dissolution constants by Dickson (1990).

5.2.3 Precision of TA and DIC analysis

The overall instrument precision remained fairly constant while analysing both JR304 (10 individual CRM analyses) and JR15002 (20 individual CRM analyses), with the standard deviation being <2.4 μmol/kg for TA and <1.7 μmol/kg for DIC. Control plots (Dickson *et al.,* 2007) detail individual CRM values, overall means and standard deviations (Figure 5.4a-b). There were no points outside the control limits, so no corrections were needed. Short-term instrument precision

was determined by repeat sampling from the same CRM bottles. Standard deviations were calculated as the square root of the mean differences between duplicates (Legge *et al.,* 2017). The short-term deviation was lower than the long-term with TA <1.18 μmol/kg and DIC <0.76 μmol/kg. For JR15002, replicates were taken for each station at the same depth to indicate precision from sampling and analysis (Figure 5.4c-d). The variance between replicates was 3.9 μmol/kg for TA and 0.9 μmol/kg for DIC (from 9 duplicates). The replicate precision reflects differences in sampling, fixation, storage or analysis conditions as opposed to just the instrument precision as indicated by CRM's, which is why variance is greater (Figure 5.4e-f). Table A5.1. gives the standard deviations per cruise. Differences for both the in-bottle CRM and sample repeats were within the upper control limit, therefore, measurement precision was good throughout TA and DIC analysis.
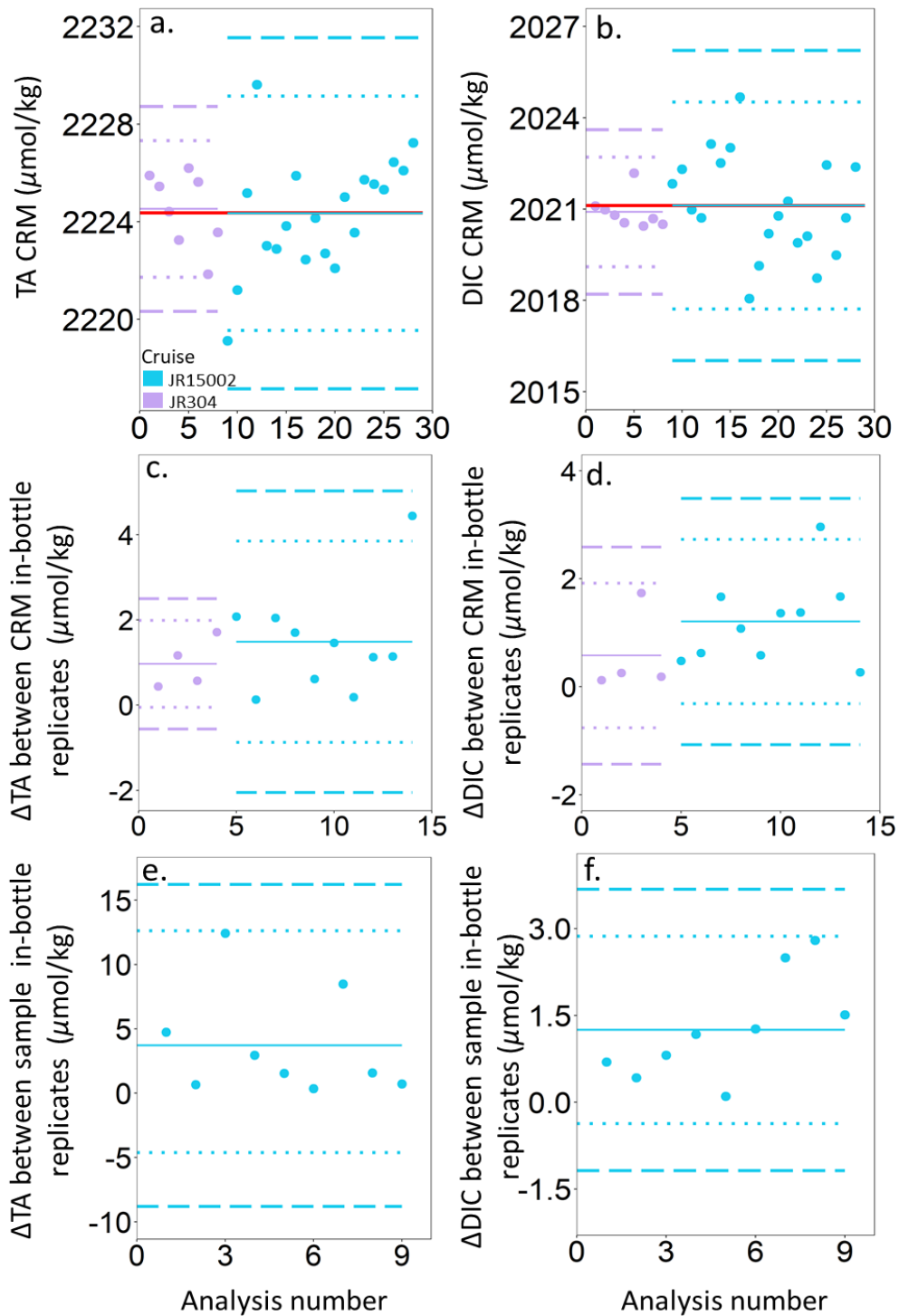
Figure 5-4. Control charts of Certified Reference Materials (CRM) (**a-b**), differences of in-bottle CRM replicates (**c-d**) and differences if in-bottle sample replicates (**e-f**) during TA (Total Alkalinity) and DIC (Dissolved Inorganic Carbon) analysis. The **solid lines** represent the means, **dotted lines** the upper and lower warning limits (±2 standard deviations from the mean) and **dashed lines** the upper and lower control limits (±3 standard deviations from the mean). The red solid line in a-b represents the CRM certified mean (batch 133; Scripps Institution of Oceanography). Colours represent the cruise (JR15002 and JR304) that was being analysed alongside these measures of precision.

5.2.4 Pteropod sampling and preservation

Limacina helicina antarctica specimens were collected alongside seawater samples and CTD measurements (see Section 5.2.1.). Individuals for shell condition analysis were gathered using a motion-compensated BONGO net (100 µm and 200 µm mesh sizes), vertically hauled from 200 m below the sea surface (Figure 2.1.). The motion compensation reduces stress on pteropods during collection as well as mechanical damage to shells. Samples were gently transferred from the cod-end into a bucket of ambient surface seawater and allowed to settle. Due to their high shell density, pteropods sink to the bottom of the bucket, allowing collection via a wide mouthed Pasteur pipette into a glass dish filled with ambient seawater. Individuals were examined under a light microscope (Olympus SZX16 mounted with a Cannon 60D camera) and their activity levels (i.e. whether they were actively swimming) were recorded. A small sub-sample of specimens were then individually rinsed in ultra-pure, pH-buffered (borax) fresh water three times before being placed in a specimen slide and air-dried.

The vertical distribution of *L. helicina antarctica* was estimated using depth discrete net samples (Table 5.2.) taken as close to the water sampling and CTD measurements as possible. It was assumed that there was little change in the seawater chemistry between sampling of seawater and the pteropods. Unfortunately, no depth discrete nets were deployed at stations C4 and C2. Pteropods were mainly sampled with a MOCNESS (Multiple Opening and Closing Net, with an Environmental Sensing System) which has a mouth opening of 1 m^2 and 9 x 330 µm mesh nets which are trawled over specified depth horizons. A mammoth multi-net was deployed at P3 in 2015 which has the same mouth opening, net number and mesh size as the MOCNESS. Since there was no motion compensation of the nets, pteropod shells were often badly damaged or scratched meaning individuals were not suitable for shell condition analysis. However, the presence or absence of pteropods was noted in each net sampled to determine the vertical range of pteropods. Due to time constraints and the samples needed for another application, I did not determine the abundance of pteropods in the net samples.

Table 5.2. Depth discrete net sampling used to estimate the vertical distribution of *L. helicina antarctica* within the Scotia Sea (Southern Ocean). Nets were deployed during two research expeditions (JR304 and JR15002).

Station name	Sampling date (Time(GMT))	Latitude (°S)	Longitude (°W)	Net type	Depths Sampled (m)
ICE	26/11/2014 (21:11)	59.97028	46.09907	MOCNESS	5-125, 125-250, 250-375, 500-375, 500-625, 625-750, 750-875, 875-1000
P2	29/11/2014 (07:23)	55.1655	41.31074	MOCNESS	5-125, 125-250, 250-375, 500-375, 500-625, 625-750, 750-875, 875-1000
P2	28/11/2014 (17:48)	55.2419	41.13365	MOCNESS	5-125, 125-250, 250-375, 500-375, 500-625, 625-750, 750-875, 875-1000
P2	30/11/2015 (20:45)	55.2544	41.2402	MOCNESS	5-125, 125-250, 250-375, 500-375, 500-625, 625-750, 750-875, 875-1000
P2	01/12/2015 (09:36)	55.2571	41.2369	MOCNESS	5-125, 125-250, 250-375, 500-375, 500-625, 625-750, 750-875, 875-1000
P3	09/12/2015 (02:45)	52.81184	40.08687	Mammoth	5-50, 50-100, 100-150, 150-200, 200-250, 250-300, 300-400, 400-700, 700-1000
P3	13/12/2014 (19:05)	52.75598	40.25841	MOCNESS	20-125, 125-250, 250-375, 500-375, 500-625, 625-750, 750-875, 875-1000
P3	14/12/2014 (02:39)	52.74735	40.26299	MOCNESS	20-125, 125-250, 250-375, 500-375, 500-625, 625-750, 750-875, 875-1000
Upwelling	14/12/2014 (13:07)	52.61696	39.28492	MOCNESS	5-125, 125-250, 250-375, 500-375, 500-625, 625-1000

5.2.5 Pteropod imaging

Pteropods taken from the motion compensated Bongo net from the stations P3, Upwelling and C4 collected were imaged for shell condition analysis. These stations were selected since they represent a range of undersaturation conditions with $\Omega_{ar} \leq 1$ occurring closest to the surface at the upwelling station and deepest at C4, with P3 being an intermediary. Six pteropods were selected from each station and year to assess shell condition given that numbers were limited since only individuals that were actively swimming after collection were used for shell condition analysis. Pteropods were imaged under a light microscope using both transmissive and reflected light (Olympus SZX16 mounted with a Cannon 60D camera) at the British Antarctic Survey (Cambridge) (Figure 5.5a-b). Specimens were then mounted onto stubs using carbon tape and imaged using a Hitachi 3400N variable pressure scanning electron microscope (SEM) at the Cavendish Laboratory's electron microscope suite (University of Cambridge) (Figure 5.5c-d). The variable pressure mode allows examination of non-conductive samples in their natural state without the need for splutter coating.
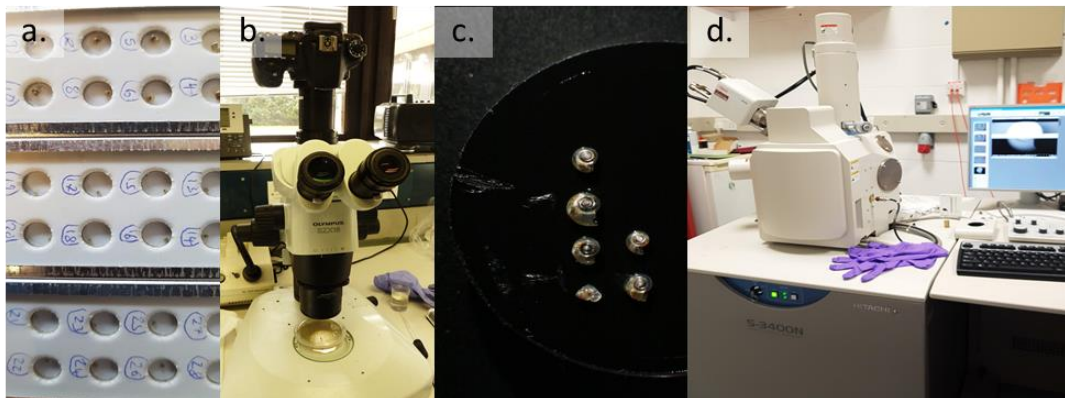
Figure 5-5. Sample preparation and imaging equipment used to assess the shell condition of *Limacina helicina antarctica* specimens collected from the Scotia Sea (Southern Ocean). (**a.**) Individuals were air dried and stored on a specimen slide (**b.**) before being imaged under a light microscope. (**c.**) Specimens were then mounted onto a stub coated in carbon tape and (**d.**) imaged using a Hitachi 3400N variable pressure scanning electron microscope.

5.2.6 Shell condition analysis

A transect of images was taken along the shell width (otherwise known as the line of aperture), crossing the protoconch. For each shell whorl an overview image was taken, then a feature would be selected (e.g. a scratch) to centre images taken at x1.2k, x2.5k and x4k magnification (Figure 5.6a). Shells were divided into four regions; protoconch, first whorl, inner whorls and outer whorls (Figure 5.6b). The shell condition was then assessed across SEM, reflected light and transmissive light images (Figure 5.7).

Any notable deviation in the texture of the shell surface (from smooth) were imaged and recorded (Figure 5.8.). Shell dissolution are regions where the shell has been eroded to expose either the prismatic or cross-lamellar layer, altering the shell texture. Changes in texture were classed using the dissolution categorisation scheme by Bednaršek *et al.* (2012a) which is:

- Type 0= no dissolution
- Type I= dissolution where there is some exposure of the upper prismatic layer and aragonite crystals appear as 'cauliflower heads'
- Type II= dissolution is where large areas of the prismatic layer have been removed to expose the cross-lamellar layer beneath
- Type III= dissolution where the cross-lamellar layer has been eroded to expose rods of aragonite.

In addition to changes in the shell texture, shell features were also observed, which were classified based on Gardner *et al.* (2018) as: 1. Scratches: narrow, linear depressions where the upper shell layers have been removed. 2. Pits: deep, defined holes within the shell surface. 3. Fractures; break through the shell, usually running across a whorl, which may or may not have been closed by regrowth. It was noted whether shell dissolution was associated with a shell feature. If shell dissolution was not associated with a specific feature, this was termed as 'generalised'.
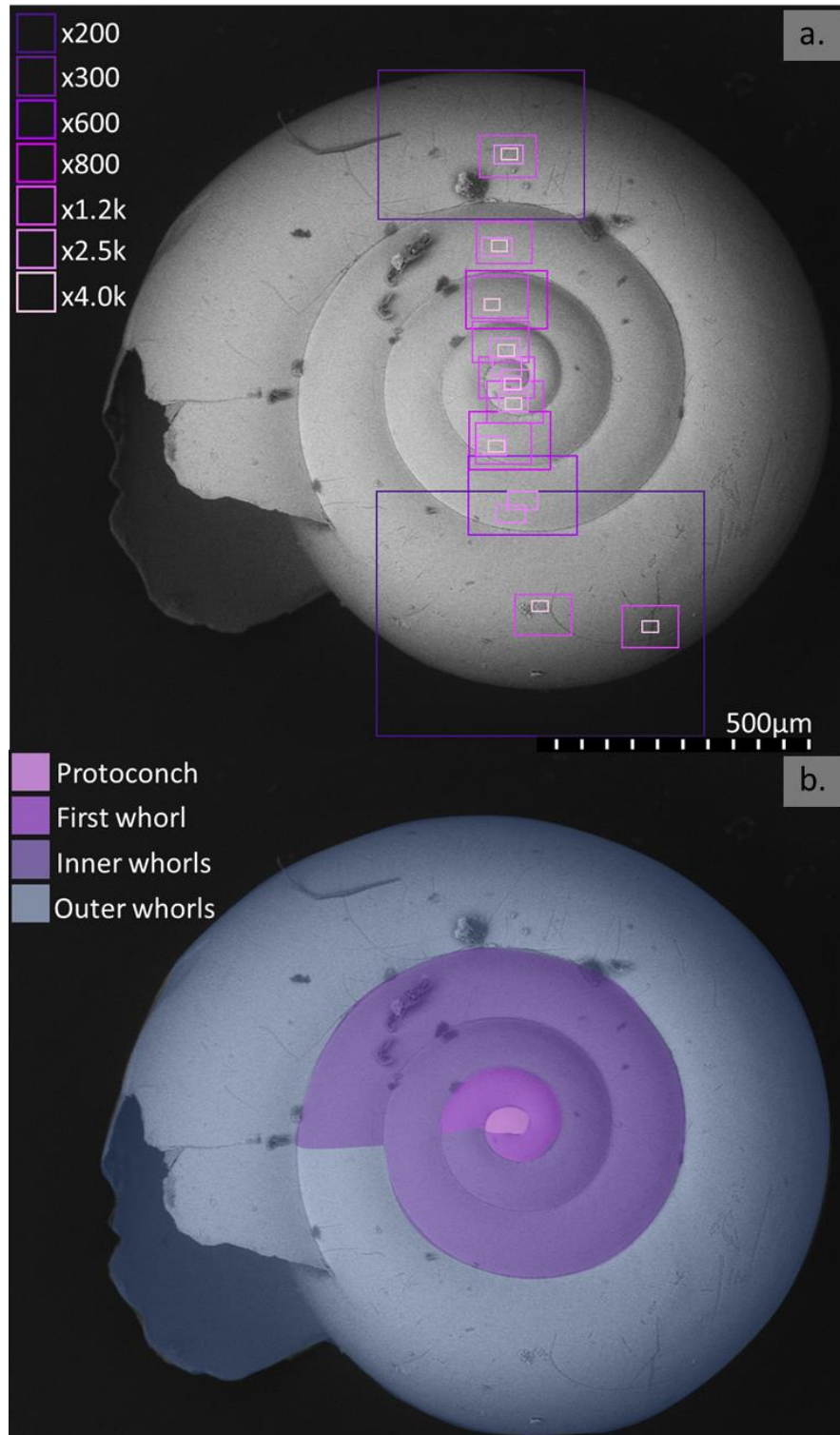
Figure 5-6. An overview of pteropod shell image positions taken with a variable pressure scanning electron microscope to assess *Limacina helicina antarctica* shell condition in relation to carbonate chemistry. (**a.**) is an image transect down the line of aperture where images were taken over a range of magnifications. (**b.**) gives the regions that the shell was divided into. Specimens were collected from the Scotia Sea in the summer of 2014 and 2015.

Figure 5-7. The shell condition of *L. helicina antarctica* was assessed across (**a.**) SEM, (**b.**) reflected light (**c.**) and transmissive light images to assess the *in-situ* shell condition of individuals.
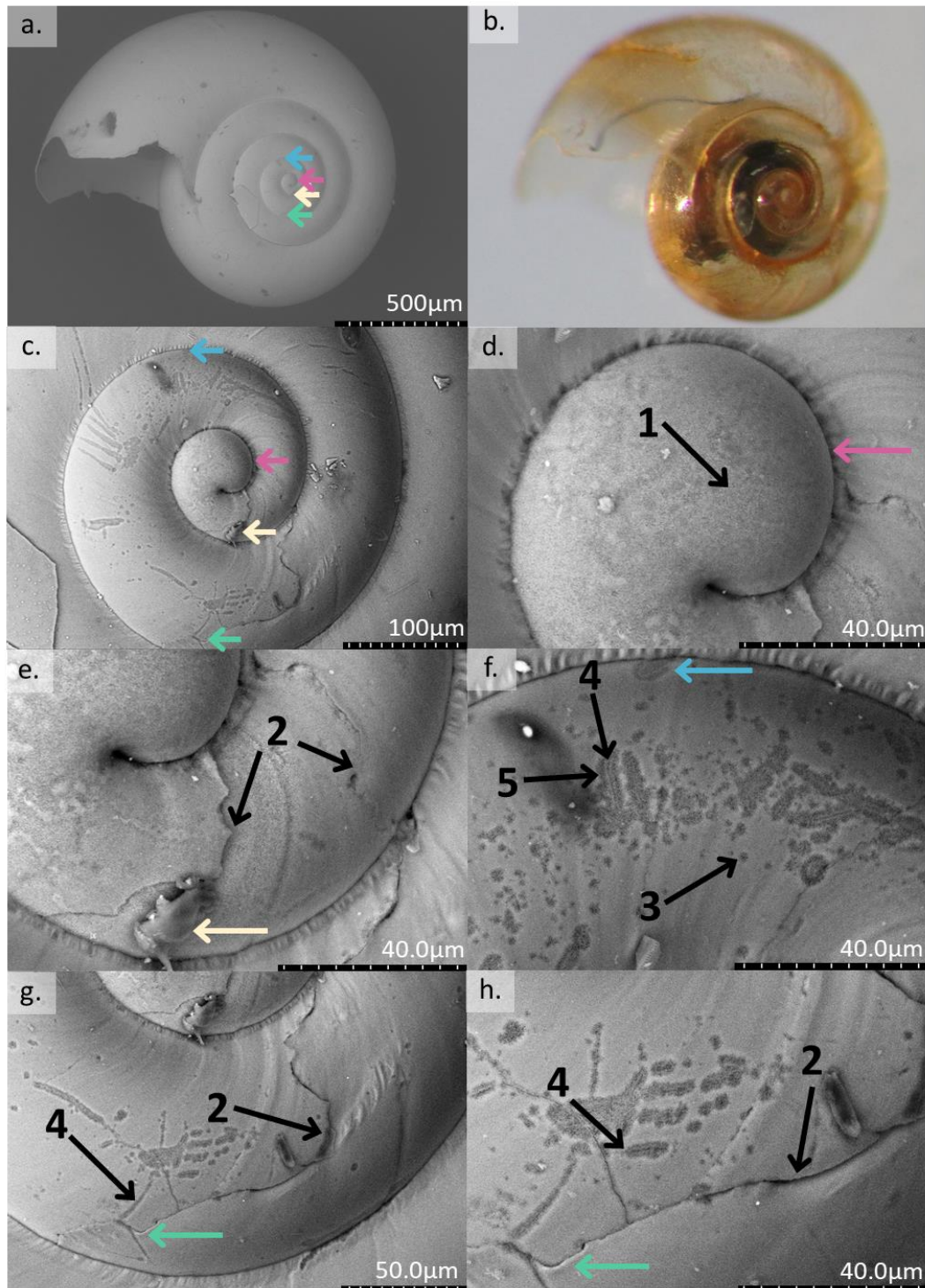
Figure 5-8. Examples of shell features present on *Limacina helicina antarctica* shells collected from the Scotia Sea in the austral summer of 2014 and 2015. Coloured arrows point to the same point on the shell to show image location. **1.** is a patch of 'generalised' dissolution which is not localised to a scratch, pit or break. **2.** are historical breaks. **3.** a pit. **4.** gives an example of a scratch and **5.** dissolution associated with a scratch. Images (**a, c-h**) were taken using a variable pressure scanning electron microscope and image **b.** a light microscope. The specimen was from the upwelling station in 2014 and uncoated.

5.3 Results

5.3.1 Station characteristics

5.3.1.1 *Temperature and Salinity*

Potential temperature-salinity plots indicate that stations P3, Upwelling and WCB have differing thermohaline structure to stations P2, C2, C4 and ICE (Figure 5.9). Stations P3, Upwelling and WCB all had a clear subsurface temperature minimum of <2°C (from Upper Circumpolar Deep Water), with the underlying water being warmer, which is characteristic of the Antarctic Zone (AAZ) (Pollard *et al.,* 2002) (Figure 5.10a). The Upper Circumpolar Deep Water is less prominent at stations P2, C2, C4 and ICE, with a sub-surface temperature maximum being present instead, placing them south of the Antarctic Circumpolar Current (SACCZ) (as defined by Pollard *et al.,* 2002). P2 is on average to the north of the SACCZ (Figure 5.3) however, its characteristics are an intermediate between the most northern and southern stations (Thorpe *et al.,* 2002). Stations in the SACCZ were cooler than those in the AAZ and slightly more saline in the upper 800 m in comparison to those in the AAZ however, all stations had salinities of around 34.6 below 800 m (Figure 5.10b). Individual temperature and salinity profiles are presented in A.5.2.
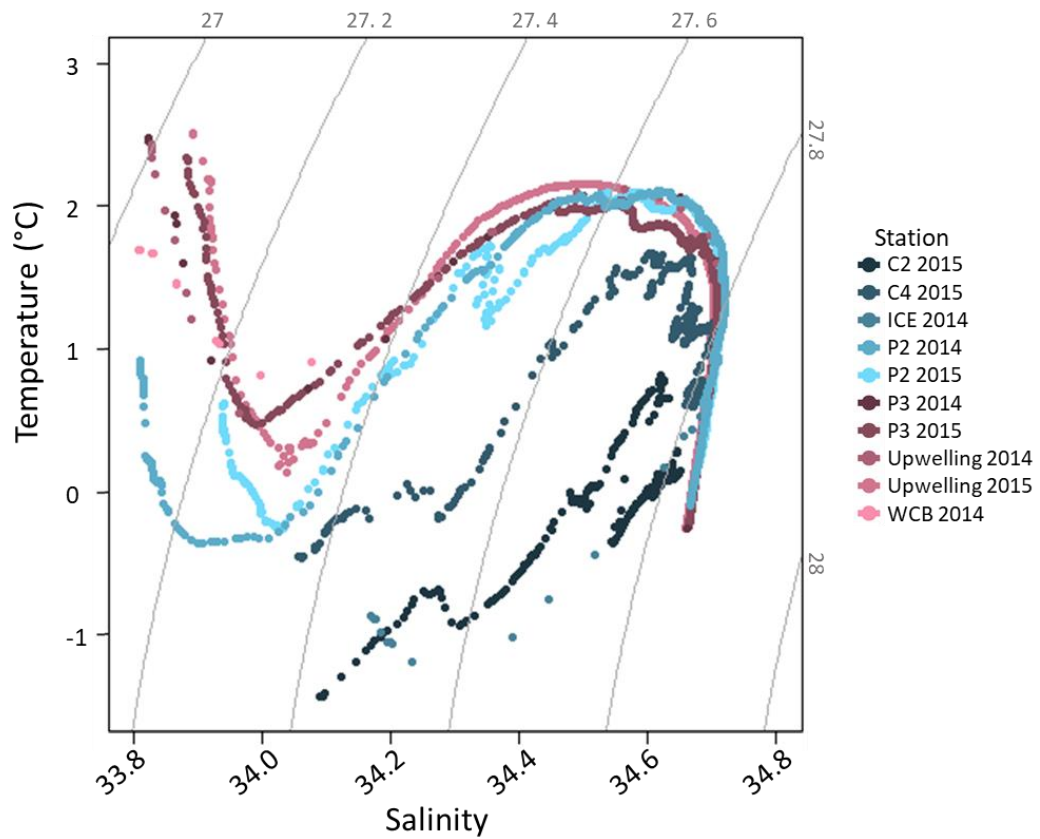
Figure 5-9. Potential temperature-salinity diagrams of each station and year from stations across the Scotia Sea during research expeditions JR304 in 2014 and JR15002 in 2015. Neutral density (θ) contours are in grey. Full depth data is used.
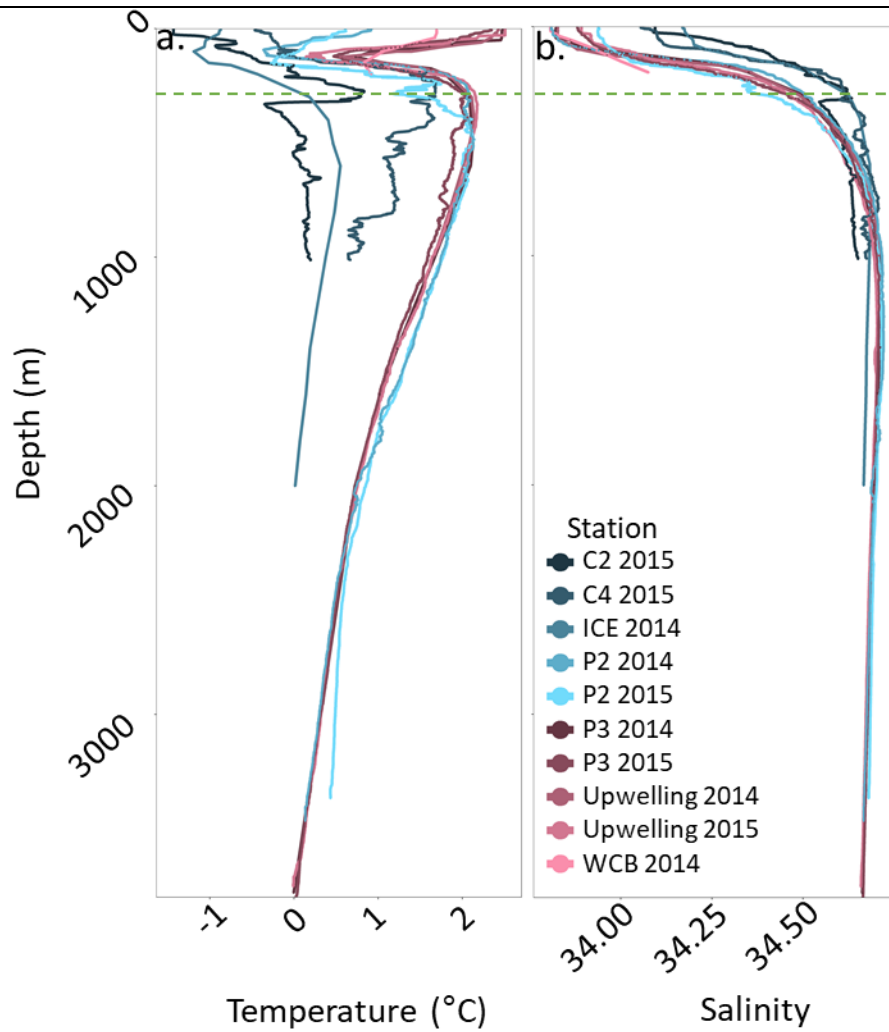
Figure 5-10. (**a.**) Temperature (°C) and (**b.**) Salinity profiles of each station
(coloured) situated within the Scotia Sea during two research expeditions, JR304
and JR15002.

5.3.1.2 Carbonate Chemistry

The depth of aragonite undersaturation ($\Omega_{ar} \leq 1$) varied between the stations sampled with ($\Omega_{ar} \leq 1$) occurring closest to the surface (300 m in 2014 and 200m in 2015) at the Upwelling station (Figure 5.11). The aragonite saturation horizon at P3 occurred at 600 m in 2014 and 400 m in 2015. The WCB approached $\Omega_{ar} \leq 1$ at 200 m however, deeper samples were not collected. P2 had an aragonite saturation horizon of 1400 m in 2014 and 800 m in 2015. The Ice station had a shallow region of water (~10 m) which was undersaturated with respect to aragonite, but below this it was supersaturated until 800 m where $\Omega_{ar} \leq 1$. No water with $\Omega_{ar} \leq 1$ was found at station C4. Individual TA, DIC and Ω_{ar} profiles for each station and year are given in Appendix A5.3. The stations P3, upwelling and C4 were selected as sites to investigate pteropod shell condition since they represent a range of aragonite saturation conditions, which are shown in more detail (<1000 m) in Figure 5.12.
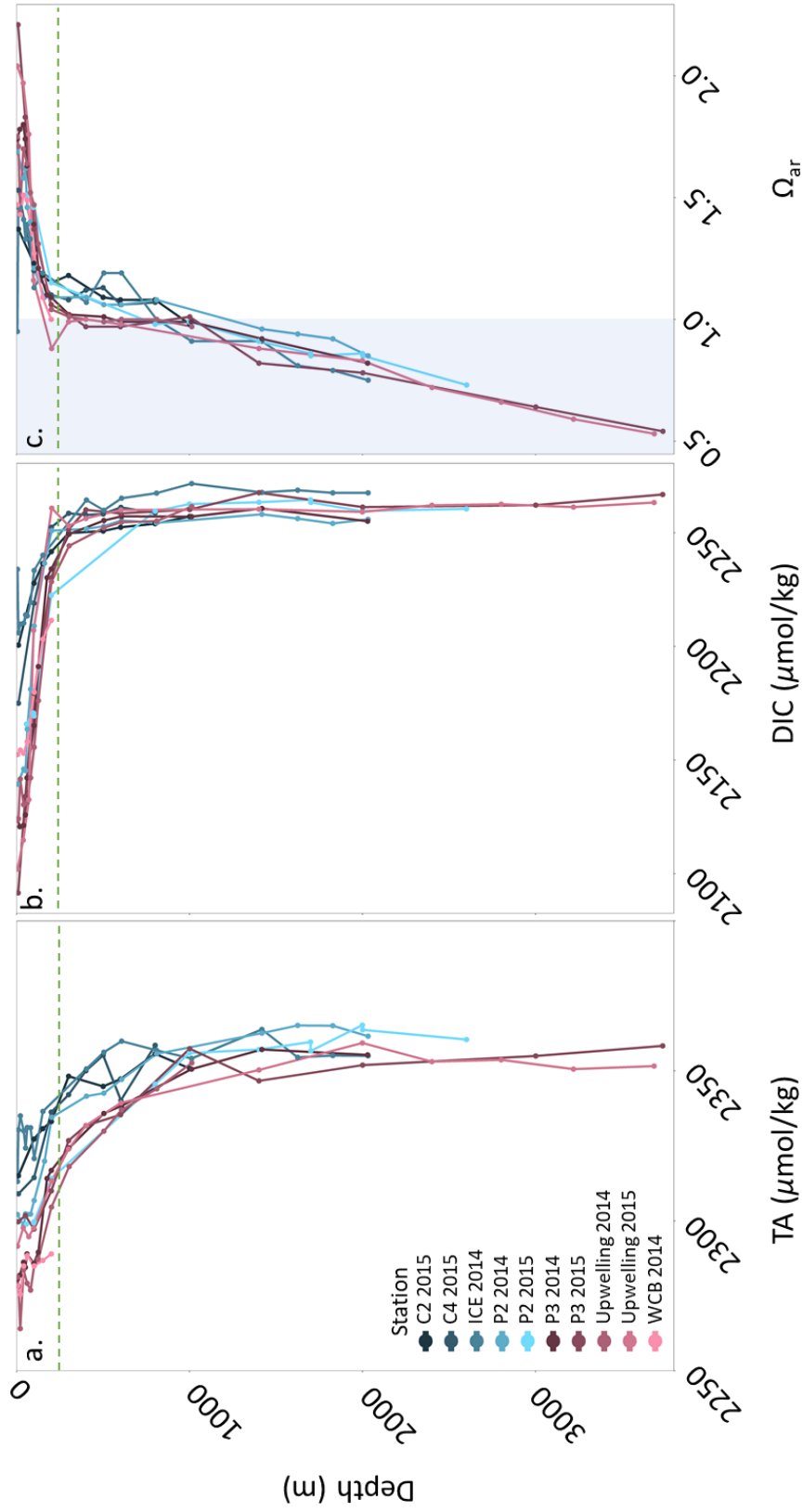
Figure 5-11 (**a.**) Total Alkalinity (TA), (**b.**) Dissolved Inorganic Carbon (DIC) and (**c.**) aragonite saturation (Ω_{ar}) profiles of each station (coloured) situated within the Scotia Sea sampled during research expeditions JR304 and JR15002. The grey shading is where the seawater is undersaturated with respect to aragonite ($\Omega_{ar} \leq 1$). The green dashed line is the maximum sampling depth of pteropod specimens.
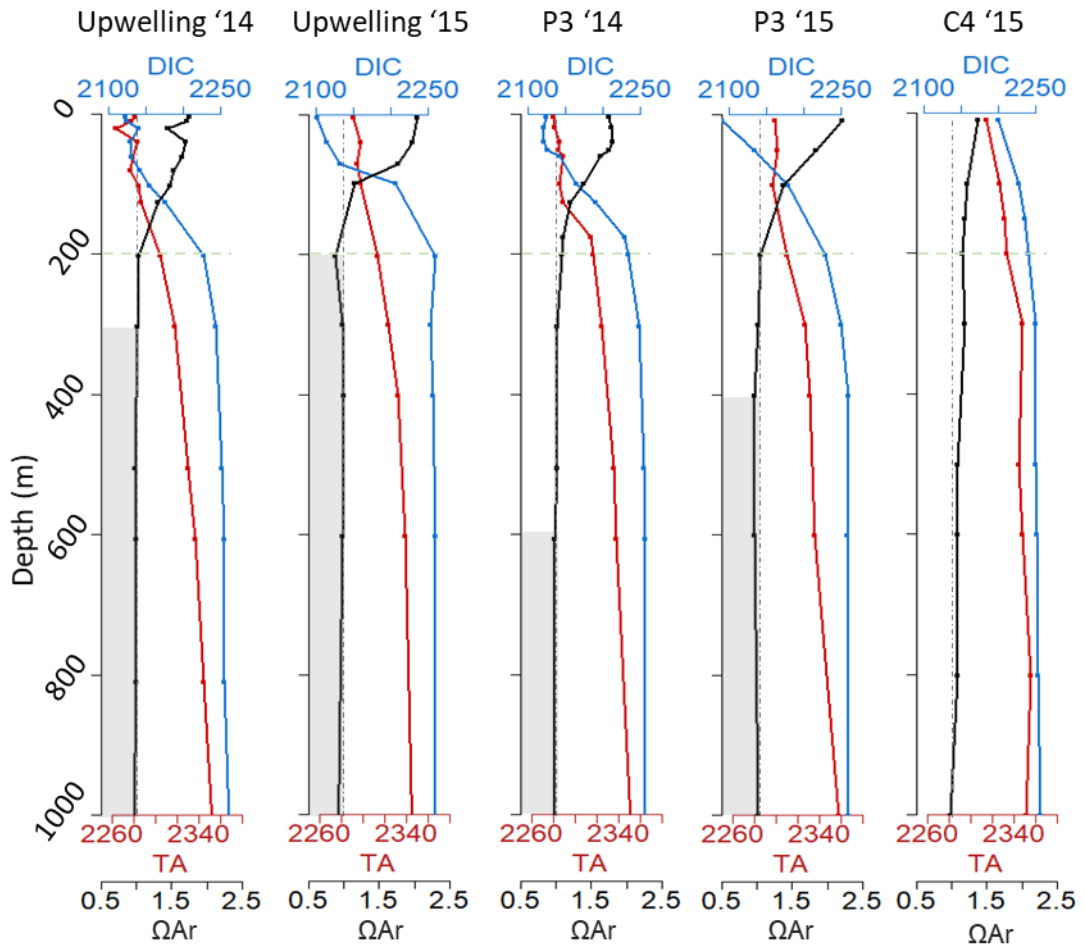
Figure 5-12. A focus on the Total Alkalinity (**TA**), Dissolved Inorganic Carbon (**DIC**) and aragonite saturation (Ω_{ar}) profiles of the stations P3, Upwelling and C4 where pteropods were collected for shell condition analysis. Stations are situated within the Scotia Sea (Southern Ocean) and were sampled during research expeditions JR304 and JR15002. The black dashed line is where $\Omega_{ar} = 1$, with the grey shading being where the seawater is undersaturated with respect to aragonite ($\Omega_{ar} \leq 1$). The green dashed line is the maximum sampling depth of pteropod specimens.

5.3.1.3   Interstation comparison

A Linear Discriminant Analysis (LDA) on the full depth profiles of TA, DIC, Ω_{ar}, temperature and salinity classified the stations into two distinct groups, being; Group 1. P3, Upwelling and WCB and Group 2. C2, C4, ICE and P2 (Figure 5.13a). The first linear discriminant explained 83% of dissimilarity between stations with aragonite saturation being the strongest loading after salinity and temperature (Table 5.3.). Therefore, aragonite saturation is the most important environmental variable out of those measured in explaining the difference between the stations sampled (Figure 5.13b). The second linear discriminant explained 11% of dissimilarities between stations with salinity being the strongest loading.

Table 5.3. Coefficients of linear discriminants computed by a linear discriminant analysis investigating which environmental variable explained the greatest dissimilarities between stations sampled within the Scotia Sea (Southern Ocean) during two research expeditions (JR304 in 2014 and JR15002 in 2015) by the R.S.S. *James Clark Ross*.

	LD1 (83 %)	LD2 (11 %)	LD3	LD4	LD5
TA	-0.037	0.050	-0.011	-0.119	-0.017
DIC	-0.054	0.063	-0.046	0.038	0.007
Ω_{ar}	-7.980	1.004	-5.602	4.213	-3.090
Temperature	1.278	0.244	-0.727	-0.385	0.018
Salinity	2.286	-13.644	1.262	7.040	-0.098
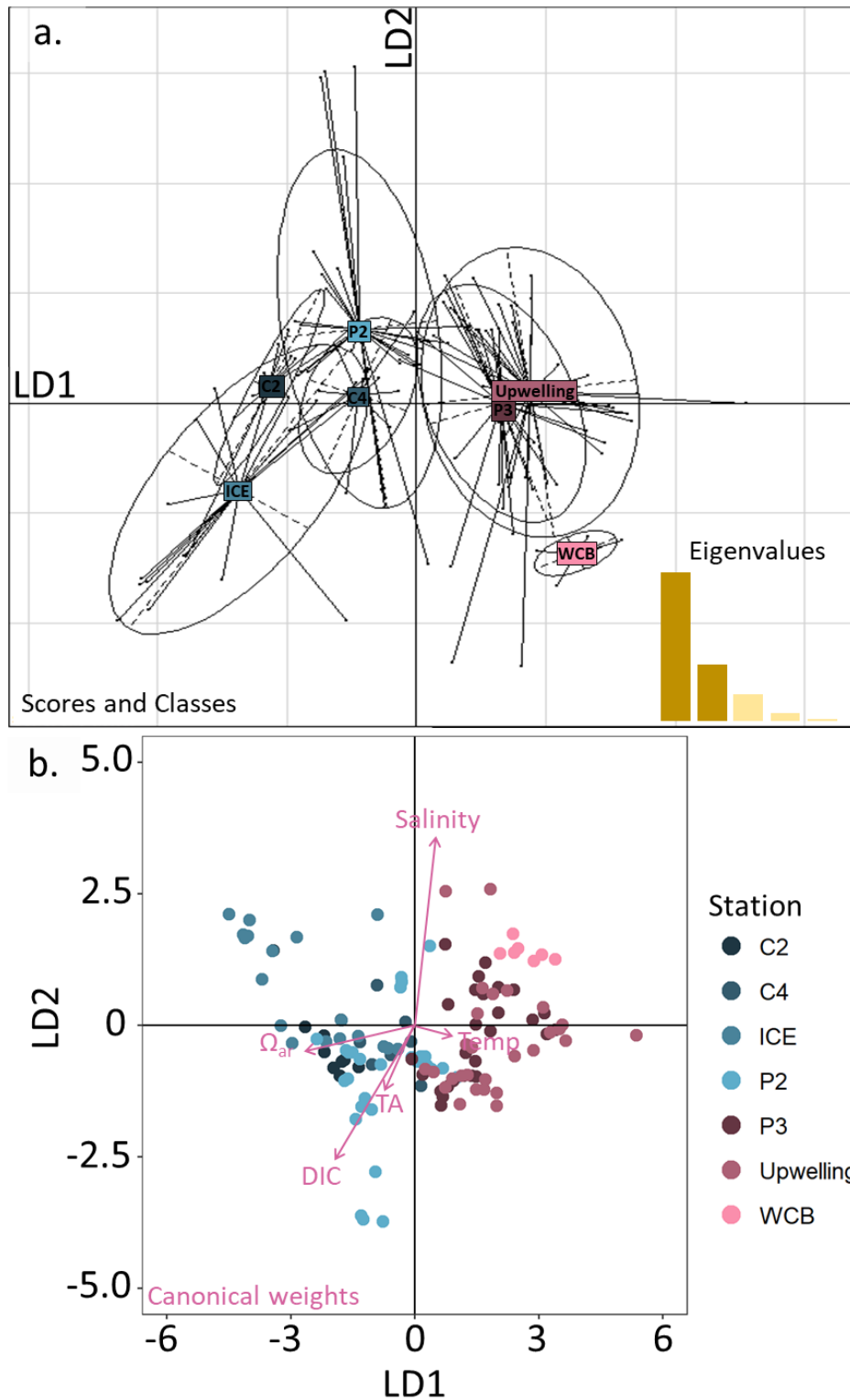
Figure 5-13. Linear Discriminant (LD) analysis plots investigating which environmental factor out of TA, DIC, Ω_{ar}, temperature and salinity explained the most dissimilarity between stations sampled within the Scotia Sea during the research expeditions JR304 and JR15002. (**a.**) gives the linear discriminant scores and classes while (**b.**) gives the Canonical weights of the environmental factors in relation to the stations.

5.3.2 Vertical distribution of pteropods

L. helicina antarctica were present within 90.1% of nets deployed between the surface and 1000 m (Figure 5.14) at the P3, Upwelling and P2 stations. Individuals were in every net sample between 0 and 300 m at all sites and were in most of the net samples down to 1000 m. The greatest number of pteropod absences within the nets occurred between 625-750 m. Abundances of *L. helicina antarctica* were occasionally extremely high (Figure 5.15).
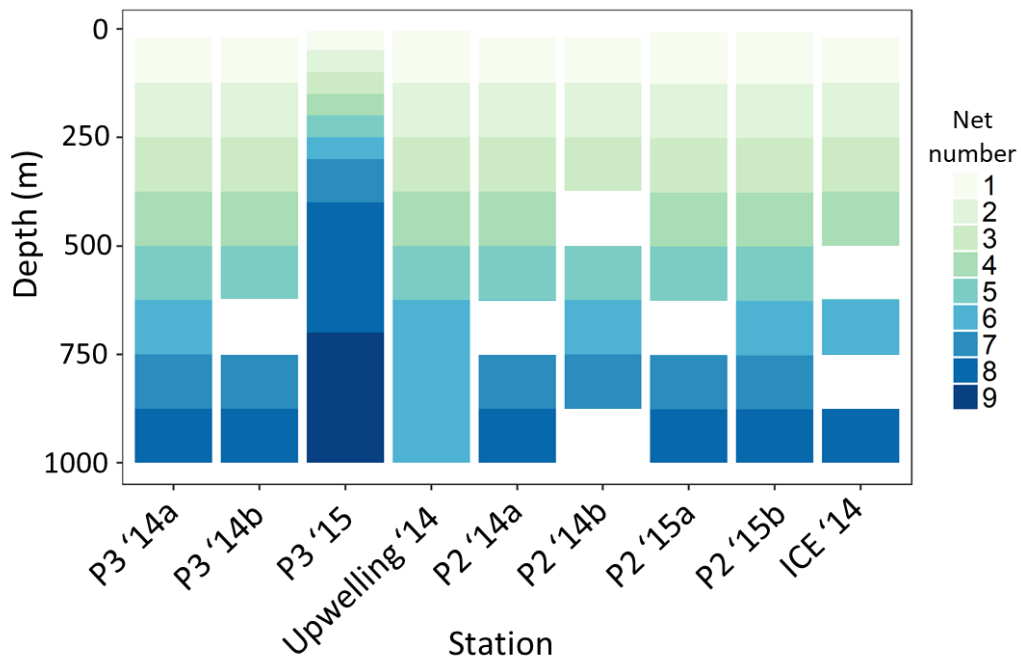
Figure 5-14. *L. helicina antarctica* presence and absence across stations with depth. Pteropods were sampled with depth discrete nets within the Scotia Sea during the research expeditions JR304 and JR15002. Colours indicate each net and the depth horizon which was sampled by that net. The white boxes indicate the absence of *L. helicina antarctica* within that net sample.

s
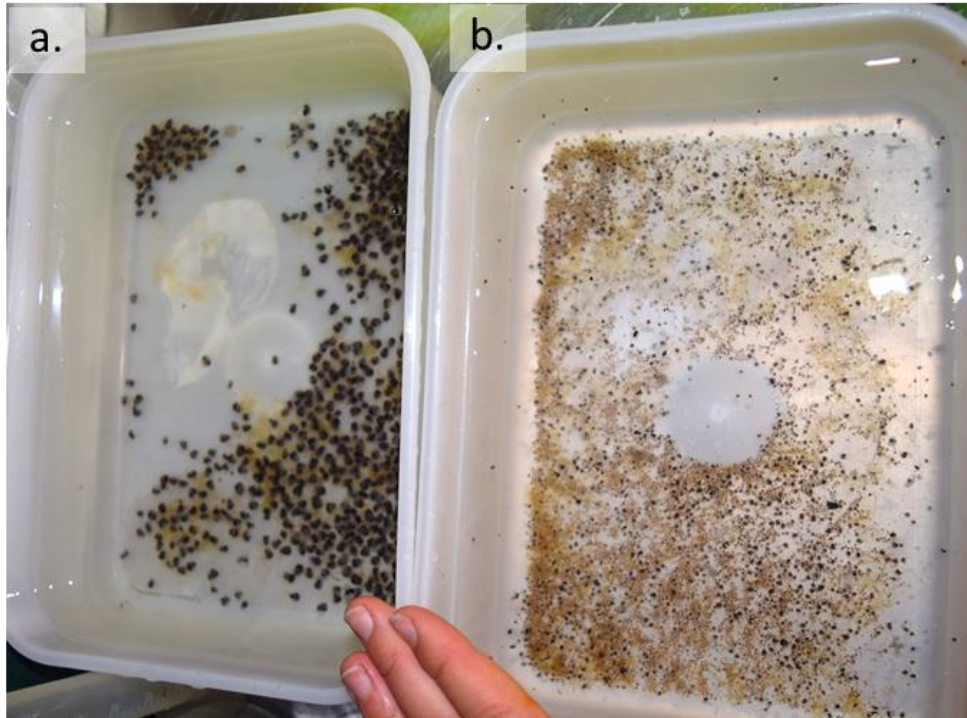
Figure 5-15. Pteropods were occasionally extremely abundant within the depth discrete MOCNESS samples. These *L. helicina antarctica* individuals were at 125-250 m (station P2; 2015) within the Scotia Sea (Southern Ocean). Within tray (**a.**) are *L. helicina antarctica* adults while in tray (**b.**) are juvenile *L. helicina antarctica.*

5.3.3 Shell condition analysis

Six specimens of *L. helicina antarctica* were selected for shell condition analysis from each of the Bongo net sample taken at the stations P3 (2014 and 2015), Upwelling (2014 and 2015) and C4 (2014). The average shell width across these samples was 1.36 mm (0.27 S.D.) (Figure 5.16) making them juveniles, based on measurements by Lalli and Gilmer (1989). As is typical of the sampling protocol used in these studies, I acknowledge that the sample size is small (n= 35) but it does exceed that of previous studies in on *in-situ* shell condition by Bednarsek et al. 2012b (n = 3 to 20) and Bednarsek et al. 2014 (n=10).
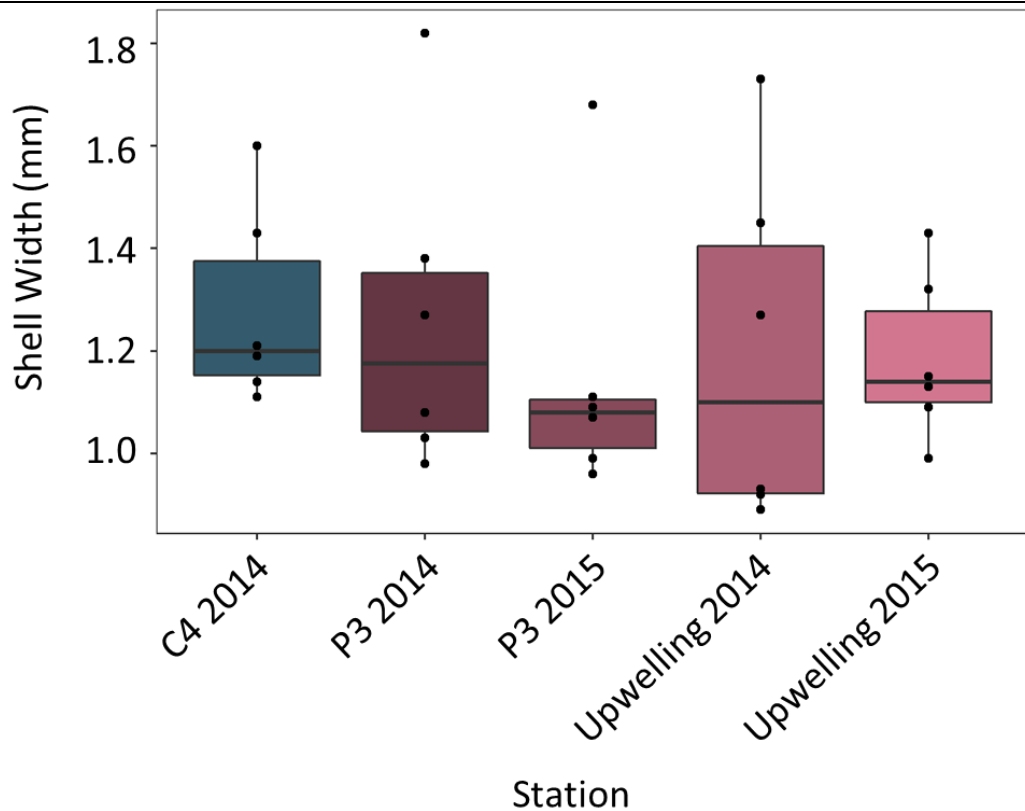
Figure 5-16. Shell width of *L. helicina antarctica* specimens recovered from the Scotia Sea using a BONGO net sampling from 0- 200 m depth and used for shell condition analysis. Each data point represents an individual.

5.3.3.1   Station C4

All six of the shells of *L. helicina antarctica* which were collected at station C4 appeared fully translucent when examined under a light microscope. Inspection under the SEM revealed some scratches, pits and historic fractures on all areas of the shell. The shell surrounding these features was fully transparent under a light microscope and the surface texture of the shell was uniformly smooth under the SEM, being type 0 on the Bednaršek *et al.* (2012a), corresponding to no dissolution on the dissolution scale (Figure 5.17).
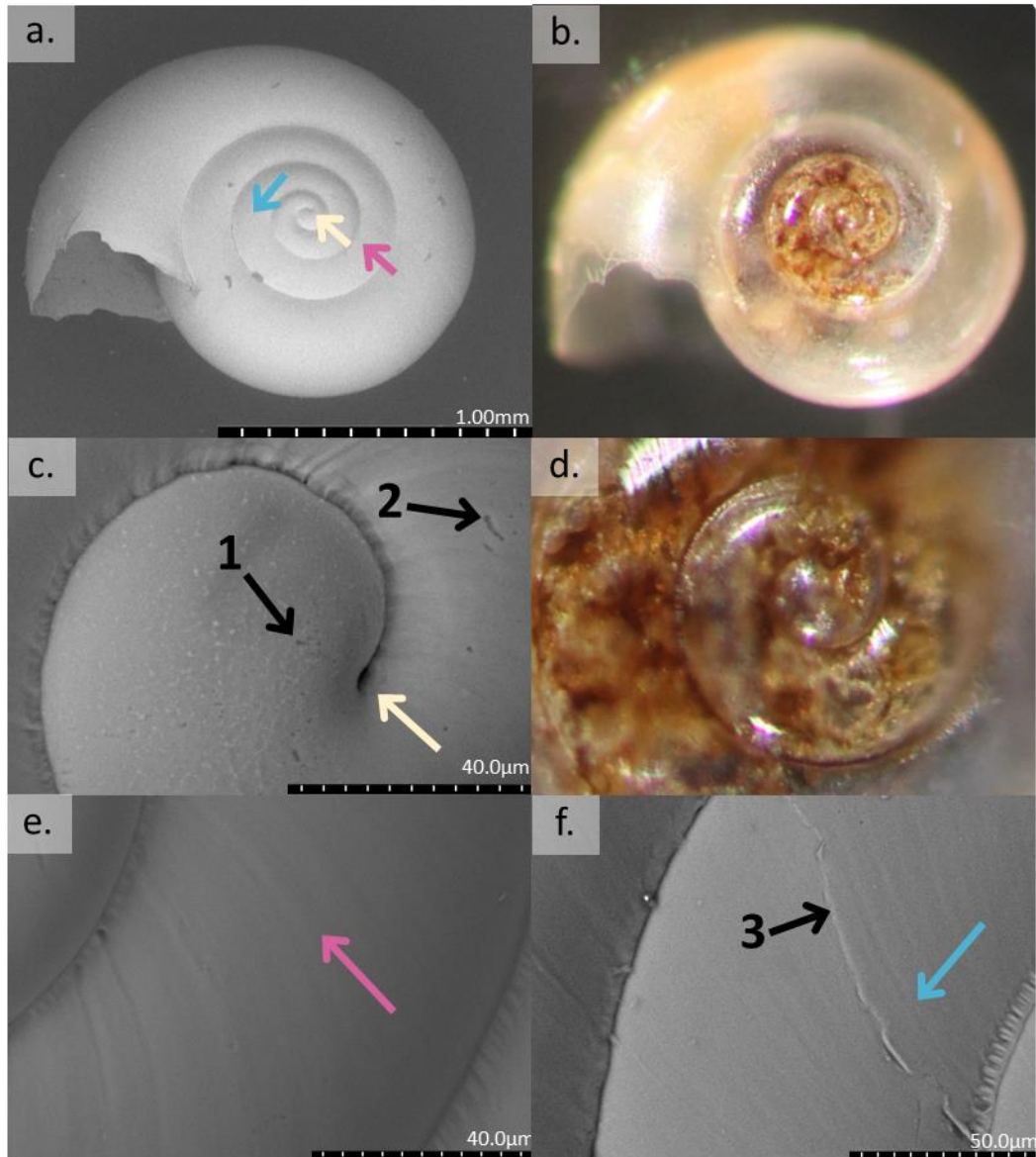
Figure 5-17. **(a, c, e** and **f.)** SEM and light (**b and d.**) microscope images of a *L. helicina antarctica* shell specimen from site C4 (2015) which was oversaturated with respected to aragonite. Images indicate no evidence of shell dissolution or opacity on any region of the shell or associated with pits (**1.**), scratches (**2.**) or fractures (**3.**). Coloured arrows point to the same point on the shell to show image location.

5.3.3.2   Stations P3 and Upwelling

All *L. helicina antarctica* shells which were collected from stations P3 (n= 6 in 2014 and n= 6 in 2015) (Figure 5.18) and Upwelling (n= 6 in 2014 and n= 6 in 2015) (Figure 5.19) had areas of the shell which appeared opaque under a light microscope. When examined with the SEM these opaque areas were found to exhibit a surface texture consistent with Type I dissolution on the Bednaršek *et*

al. (2012a) scale. All of the individuals (n= 12) from the Upwelling station and 91.67% (11 out of 12) of individuals from P3 had extensive regions of generalised dissolution (Figure 5.20). These regions of generalised dissolution, not associated with scratches, pits or fracture, were only present on the shell protoconch. The crossed-lamellar layer was not visible within any of the patches of generalised dissolution, which was therefore classed as type I (shallow dissolution) by Bednaršek *et al.* (2012a). Every shell from P3 and Upwelling stations had scratches and pits across all the shell regions, however, fractures were less frequent and never occurred on the protoconch. Dissolution which was associated with a scratch or pit was most common on the shell protoconch and inner whorls. In each case where there was dissolution associated with a shell feature, the surrounding shell had no evidence of dissolution under the SEM and was translucent under a light microscope. Where the scratch or fracture occurred at a whorl margin, the growth of the subsequent whorls continued around these features and moulded around them.
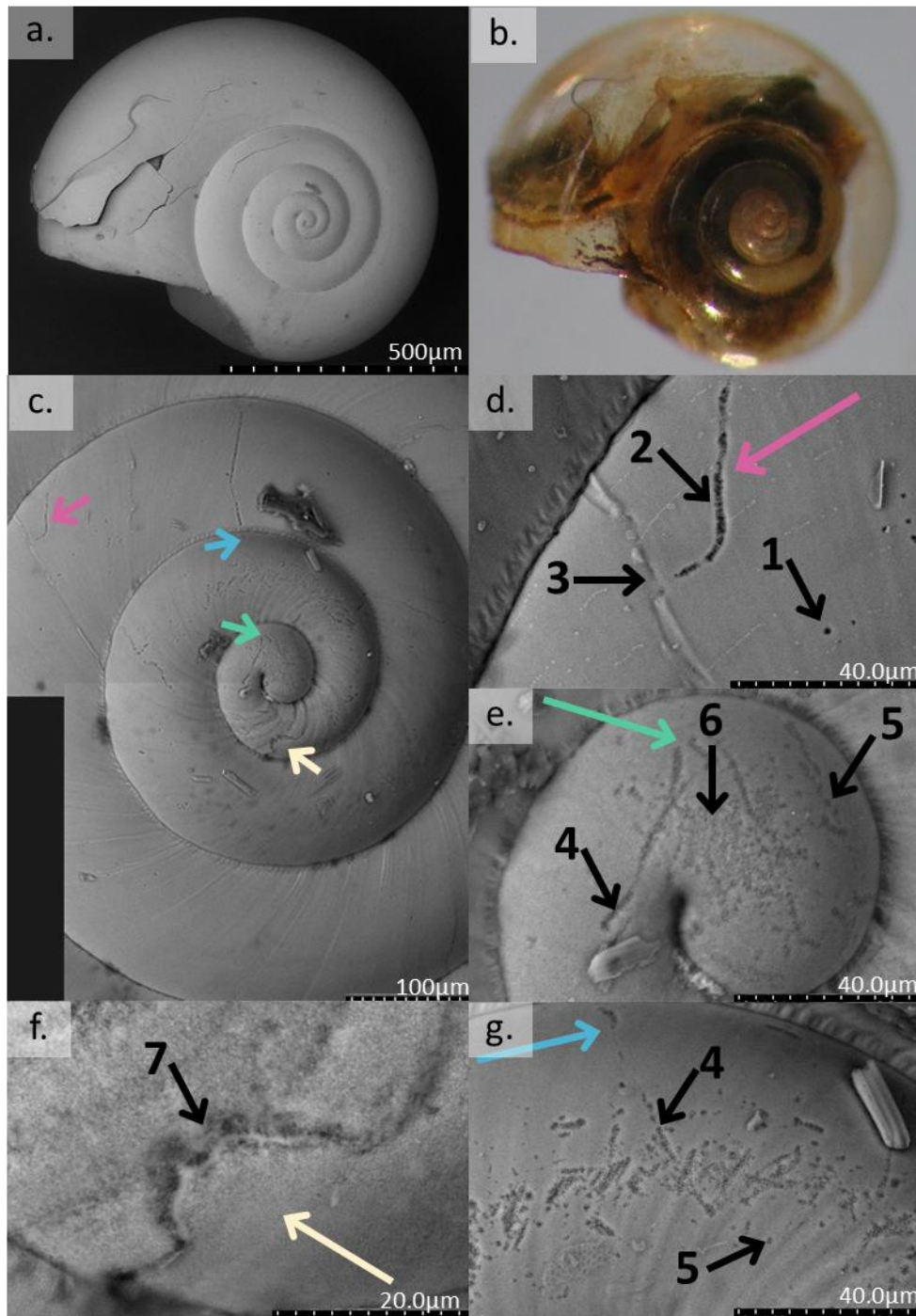
Figure 5-18. SEM (**a, c, d, e, f** and **g.**) and light (**b.**) microscope images of a *L. helicina antarctica* shell specimen from site P3 (2015) located in the Scotia Sea from 0- 200 m depth. Coloured arrows indicate the same point on the shell to show image location. Arrow **1.** is a pit, **2.** is a scratch and **3.** is a fracture on a central whorl with no associated dissolution. **4.** shows a scratch and **5.** a pit with associated dissolution around its edges. **6.** illustrates a region of generalised type I dissolution while **7.** shows a fracture with associated dissolution.
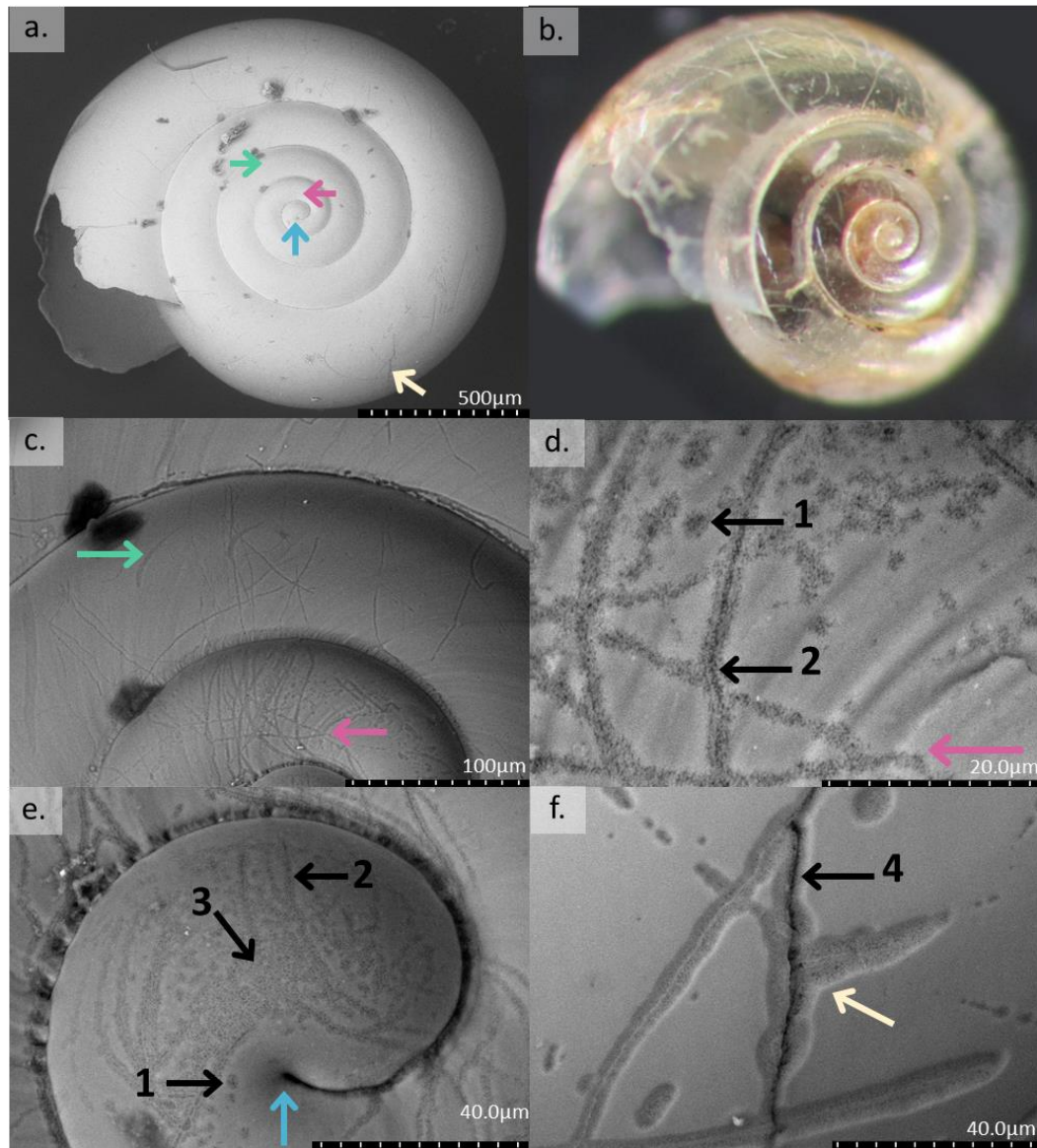
Figure 5-19. SEM (**a.**) and light microscope (**b.**) images of a *L. helicina antarctica* shell specimen from the Upwelling site (2015) located in the Scotia Sea from the upper 200 m. Coloured arrows point to the same point on the shell to show image location. The light microscope image clearly shows regions of opacity associated with dissolution. Arrow **1.** is a pit and **2.** is a scratch which have associated shell dissolution. Arrow **3.** illustrates a region of type 1 generalised dissolution on the shell protoconch. Arrow **4.** shows a region of dissolution that is accompanying a shell fracture.
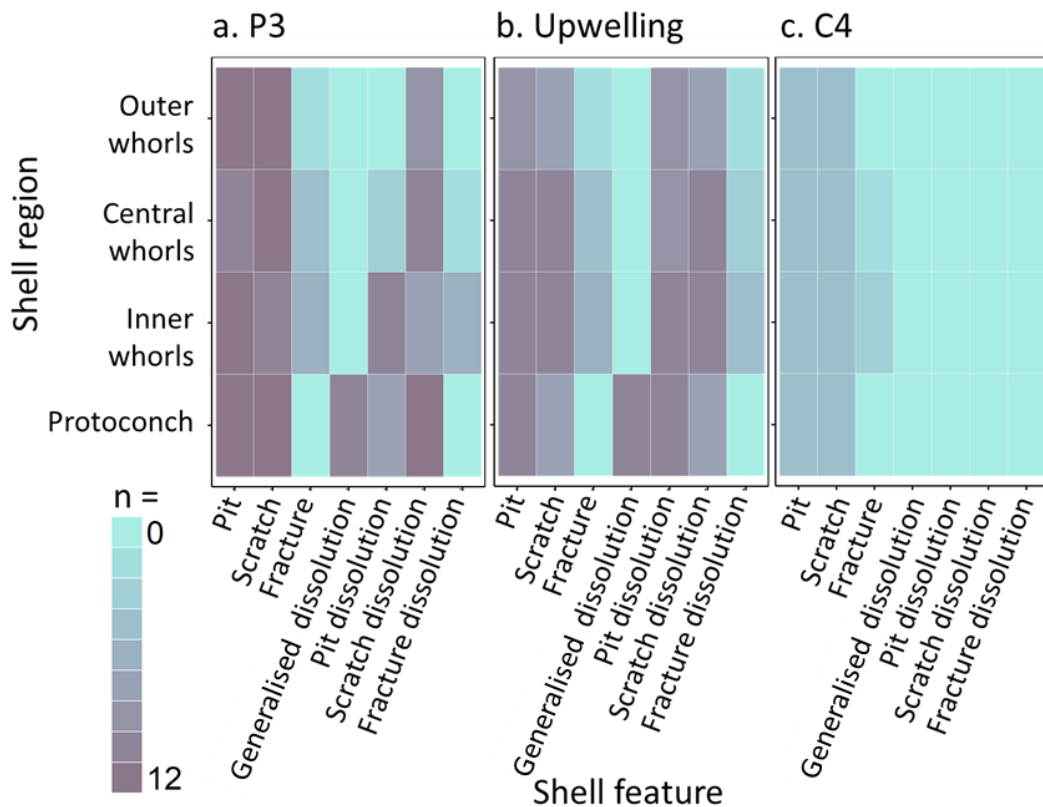
Figure 5-20. The presence of shell features within each shell region of *L. helicina antarctica* collected from sites P3 (**a.**) (n= 12), Upwelling (**b.**) (n= 12) and C4 (**c.**) (n= 6) located within the Scotia Sea during the summers of 2014-2015. Colours (**n**) are the number of specimens which had each shell feature present for each shell region.

5.4 Discussion

5.4.1 Aragonite saturation in the Scotia Sea

The depth of aragonite undersaturation ($\Omega_{ar} \leq 1$) occurred closest to the surface at the Upwelling station (300 m in 2014 and 200 m in 2015) and at P3 (600 m in 2014 and 400 m in 2015). Aragonite undersaturation in the upper water column at the Upwelling station was also documented by Bednaršek *et al.* (2012a) who found undersaturation of Ω_{ar} at 200 m in 2010. In 2010 the range of Ω_{ar} between 0-1000 m was 1.42- 0.94 (Bednaršek *et al.,* 2012a), reaching a low of 0.76 at 2000 m (Bednaršek *et al.,* 2010). The range of Ω_{ar} between 0-1000 m was similar in 2014 (1.75-0.99) and 2015 (Ω_{ar}= 2.04-0.88) to those found by Bednaršek *et al.,* 2012a), however, at 2000 m the water column had a higher aragonite saturation state of 0.97 (2014) and 0.83 (2015) than observed in 2010 by Bednaršek *et al.* (2012a) (0.76). As water undersaturated with respect to Ω_{ar} in the upper 600 m was observed at P3 and the Upwelling in 2014 and 2015, this suggests "near

surface" undersaturation covers a much larger area than previously reported by Bednaršek et al., (2012a). The aragonite saturation horizon was deeper at stations P2, C2 and ICE in comparison to P3 and the Upwelling, being at 800 m and 1000 m (2014 and 2015) and was not sampled at C4 between 0 and 800 m. Stations P3, Upwelling and WCB all had a clear subsurface temperature minimum of <2°C (from Upper Circumpolar Deep Water) therefore, undersaturation of aragonite at these stations could partially be explained by the upwelling of DIC enriched deep water. The phytoplankton bloom present at both P3 and the Upwelling station at the time of sampling (see Section 3.3.6.2.), may have resulted in the remineralisation of organic matter back to DIC at depth and may have contributed to the water to become undersaturated with respect to aragonite, as observed by Bates et al. (2013) and Anderson et al. (2010) in the Arctic Ocean. It is difficult to discern which process contributes the most to the shoaling of the lysocline without longer term measurements of the carbonate chemistry at stations P3 and the Upwelling. However, since the presence of Upper Circumpolar Deep Water is characteristic of the Antarctic zone and undersaturation with respect to aragonite is not widespread, I suggest it is the unique combination of upwelling water and the intense phytoplankton activity which results in aragonite undersaturation at stations P3 and Upwelling.

Regions of upwelling and intense phytoplankton blooms bring the saturation horizon of aragonite closer to the surface, where mixing with surface water usually increases Ω_{ar} to ≥ 1 since air-sea gas exchange will drive the system towards equilibrium with the atmosphere. However, increasing concentrations of atmospheric CO_2 are gradually reducing upper ocean Ω_{ar}. Currently, wintertime aragonite undersaturation at the surface is predicted to occur by 2030 south of the Polar Front and the lysocline is predicted to shoal (Orr et al., 2005; McNeil and Matear, 2008; Friedrich et al., 2012). Therefore, pteropods at stations P3 and Upwelling are likely to experience both summertime and wintertime undersaturation events in the near future.

5.4.2 Vertical distribution of *L. helicina antarctica*

L. helicina antarctica were present between 0- 1000 m depth at all stations in 2014 and 2015, irrespective of the saturation state of aragonite. Therefore, individuals at the P3 and Upwelling stations will have experienced water naturally undersaturated with aragonite (Ω_{ar} <1) while those at C4 will only have experienced water that was saturated with respect to aragonite. Within the Californian upwelling system, where the lysocline shoals to 200-400 m, the vertical distribution of *L. helicina helicina* was reported to have been restricted to the upper 400 m during the day and night, leading the authors to conclude that the pteropods were actively avoiding waters undersaturated with aragonite (Bednaršek *et al.,* 2014). In the Scotia Sea there was no obvious avoidance of undersaturated waters, with individuals being present down to 1000 m despite the saturation state of aragonite. The aragonite saturation state at the P3 and Upwelling stations between 0- 2000 m reaches a minimum of Ω_{ar}= 0.79, therefore, pteropods were not exposed to undersaturation as low as what is observed in the Californian Current system (Ω_{ar}= 0.56), which may explain why they were not limited vertically. Numerous local factors may influence the vertical distribution of pteropods including predation pressures, environmental conditions, species interactions and feeding regimes (See Section 4.4.4) and it is clear the undersaturation is not the main driver of pteropod vertical distribution within the Scotia Sea.

5.4.3 Natural shell condition of *L. helicina antarctica*

Naturally occurring dissolution of *L. helicina antarctica* shells was observed at both P3 and the Upwelling station within the Antarctic Zone of the Scotia Sea (Southern Ocean), where waters undersaturated with respect to aragonite were found at depths of 200-600 m. Previously *L. helicina antarctica* shell dissolution in the Scotia Sea has been reported in the summer of 2010 at the Upwelling station by Bednaršek *et al.* (2012a). The more widespread occurrence of shells exhibiting dissolution in this study is consistent with the larger area experiencing undersaturation in 2014 and 2015 than previously reported in 2010 by Bednaršek *et al.* (2012a). Furthermore, summertime shell dissolution is a

persistent phenomenon, having been observed during the summers of 2010 (Bednaršek *et al.,* 2012a), 2014 and 2015 (S*ee Section 5.4.1* for a comparison of findings).

Individuals from station C4, which was saturated with respect to aragonite, displayed scratches, pits and fractures to their shells, however, there was no associated dissolution, indicating that shell dissolution is likely to arise from contact with undersaturated aragonite conditions. Shell dissolution observed on shells from P3 and the Upwelling station was exclusively associated with scratches, pits and fractures, except on the protoconch, where generalised dissolution had occurred. The shell surrounding areas of dissolution remained fully transparent and undamaged, demonstrating that dissolution was restricted to discrete areas of existing shell damage. Breaches in the periostracum are likely due to from failed predation attempts, epibiont and bacterial activity, abrasion or mechanical damage (Bausch *et al.,* 2018; Peck *et al.,* 2016a). Therefore, individuals that experience undersaturated conditions are susceptible to shell dissolution where these breaches in the periostracum occur.

The fact that shell dissolution only occurred at specific sites on the juvenile shell (inner and outer shell whorls) in association with shell features, confirms the periostracum of *L. helicina antarctica* protects the aragonite shell beneath it, which was also demonstrated by Peck *et al.,* (2016a; 2016b) on Arctic *L. helicina helicina.* Generalised dissolution was observed on the protoconch of *L. helicina antarctica* shells from the P3 and Upwelling stations in 2014 and 2015, suggesting that the periostracum is only ineffective on the initial, larval shell (also observed with *L. helicina helicina* by Peck *et al*., 2016a). In contrast, Bednaršek *et al.* (2014a; 2016a; 2012a) concluded that the periostracum of *L. helicina antarctica* and *L. helicina helicina* was ineffective in protecting the entire shell from dissolution on exposure to Ω_{ar} <1. However, Bednaršek *et al.* (2014a; 2016a; 2012a) adopted a different methodology for preparing the pteropods before SEM imaging which involves the removal of the periostracum with plasma etching or H_2O_2. Pteropod shells have both an outer organic layer (periostracum), as well as numerous crystalline layers which contain intra-crystalline organic

components (Marin *et al.,* 1996). By exposing the shell to plasma etching or H_2O_2, there is a possibility that the intra-crystalline organic matrix is removed alongside the periostracum, creating a corroded appearance that may be misinterpreted as natural dissolution (Peck *et al.,* 2016b). H_2O_2 would leach through existing breaches in the periostracum with more ease than the intact periostracum, meaning removal of the intra-crystalline organic matrix would not be uniform across the shell, the definition of shell features (e.g. scratches) may be obscured and the resulting matrix-free areas may present a similar appearance to areas of generalised dissolution on untreated shells. Bednaršek *et al.* (2016a; 2014a; 2012a) also used plasma etching and sputter coating in preparation for SEM imaging. Non-uniform cohesion of the coating over a curved surface and granular or cracking to the metal film can produce artefacts which may be mistaken for dissolution at high magnification (Kirk *et al.,* 2009). Therefore, unless shells are examined under a variable pressure SEM without any chemical or laser preparation, it is difficult to interpret artificial from natural shell features (Sawyer *et al.,* 2008) making the comparison between the studies by Bednaršek *et al.* (2016a; 2014a; 2012a) with the current results difficult.

In the Scotia Sea, Type II and III dissolution to juvenile *L. helicina antarctica* was not observed on individuals collected in 2014 and 2015, with all *in-situ* dissolution being describes as Type 0 or Type I. In the Scotia Sea, the lowest Ω_{ar} observed in the upper 1000 m was $\Omega_{ar}=0.88$ (Upwelling station, 200 m depth, 2015), which is less undersaturated than the conditions adopted by incubation studies where deeper damage has been observed (See Table 1.2). However, in 2010 at the Upwelling station, Bednaršek *et al.* (2012a) observed juveniles with Type II and III damage across all whorls, despite the lowest level of aragonite saturation being $\Omega_{ar} = 0.94$. The presence of deeper shell dissolution may either be due to the individuals sampled experiencing much lower levels of aragonite saturation prior to sampling or due to the sample preparation (discussed above). The severity and extent of shell dissolution increases with the duration of exposure to $\Omega_{ar} <1$. Incubation studies have found a linear relationship between the severity of dissolution and the number of days exposed to $\Omega_{ar} <1$ (See Table 1.2), however, the seasonal variation in carbonate chemistry at P3 and the

Upwelling station, and so the time period that pteropods encounter undersaturated conditions, remains unknown.

Generalised dissolution, not associated with a shell feature, such as a fracture, scratch or pit, was only found on the protoconch of shells from the P3 and Upwelling stations. While no damage was visible on the protoconch using the protocol adopted, it is possible that microperforations were present on the periostracum, allowing water corrosive to aragonite to enter (Peck *et al.,* 2016b). However, since there were no regions of generalised dissolution present on the inner and outer shell whorls, this seems unlikely to be the case. The protoconch is the oldest part of the shell, being the larval shell, and so has been exposed to shell damage and undersaturation for the longest time. Therefore, this region is likely to accumulate progressive dissolution. In previous work I showed that larvae of *L. helicina antarctica* that were cultured in undersaturated conditions had generalised dissolution across the entire larval shell, leading the conclusion that the larval periostracum is ineffective (See Section 2.4.). This means that the protoconch is more susceptible to dissolution on exposure to undersaturation.

5.4.4 Concluding remarks and summary

Chapter 5 provides an overview of the present day, *in-situ* state of *L. helicina antarctica* shells in relation to carbonate chemistry within the Scotia Sea. I show that the region of aragonite undersaturation to the north of South Georgia is larger than previously recorded and is a long term feature, being present since at least 2010, which was identified by Bednaršek *et al.* (2012a). Pteropods were found at all stations down to 1000 m, regardless of the saturation state of aragonite. The shells of *L. helicina antarctica* gathered from C4 had scratches, pits and fractures however, there was no evidence of shell dissolution, suggesting no contact had been made with waters where Ω_{ar} ≤1. Individuals collected from stations P3 and Upwelling in both 2014 and 2015 also had scratches, pitting and fractures on their shells with shell dissolution being present. Regions of generalised dissolution, which were not associated with a shell feature, were present on the shell protoconch. All other shell dissolution,

which was found on inner and outer whorls, was associated with a shell feature such as a scratch, pit or fracture. Therefore, the periostracum on the inner and outer shell whorls is effective in protecting the aragonite shell beneath from waters where $\Omega_{ar} \leq 1$, except where there has been a breach. Conversely, the periostracum on the protoconch is less effective at protecting the underlying shell layers, allowing undersaturated water to penetrate and result in regions of generalised shell dissolution, even if a breach is not present.

6 Overall thesis key findings and synthesis

6.1 Thesis overview

The purpose of this thesis is to elucidate the impact of rising anthropogenic CO_2 and warming on the physiology and life history of pteropods in the Scotia Sea. The Scotia Sea is an ideal natural laboratory, since pteropods are highly abundant and widespread over a range of rapidly changing oceanographic and ecological regimes. I particularly focussed on the region to the north of South Georgia; a hotspot of productivity and diversity that is affected by a multitude of environmental drivers. I cultured early stage pteropods under ocean acidification and warming conditions predicted to occur in 2100 (Chapter 2), constrained the life cycle and population dynamics of pteropods (Chapter 3), established a historical baseline describing the vertical and biogeographical distribution of pteropods (Chapter 4) and investigate the *in-situ* pteropod shell condition in relation to the prevailing carbonate chemistry of the sea water (Chapter 5). To achieve my thesis aims, I participated on two oceanographic cruises where I collected a variety of net, sediment trap and oceanographic samples and incubated and cultured pteropods under predicted modern and future ocean acidification and warming conditions. Additionally, I examined a historical transect of samples collected in 1930 before the occurrence of considerable influence of anthropogenic ocean acidification and warming on the Scotia Sea.

In this synthesis I first present key findings from each Chapter (Section 6.2.) and then draw overall conclusions from the Chapters (Section 6.3.) to highlight areas for future research (Section 6.4.).

6.2 Chapter overviews and key findings

6.2.1 Chapter 2

In Chapter 2, veligers of *L. helicina antarctica* were cultured for the first time in conditions that simulate the predicted increases in temperature (warming) and more extensive undersaturation of aragonite (acidification) in the Scotia Sea. I calculate that:

- Veligers of *L. helicina antarctica* are vulnerable to warm, acidified and acidified-warm oceanic conditions predicted for 2100 in the Scotia Sea, given the increase in occurrences of shell malformation and mortality. Increased mortality was mainly driven by exposure to acidified conditions. No change in survival has been found in all the previous studies on juvenile and adult life stages of *L. helicina helicina* (Busch *et al.,* 2014; Comeau *et al.,* 2012a; Lischka *et al.,* 2011; Lischka and Riebesell, 2012). My results show that early life stages of *L. helicina* have a high vulnerability to acidification and warming.
- Warming resulted in shell malformation, acidification in shell etching and acidification and warming in both shell malformation and etching. Therefore, the impacts of warming and acidification on veliger shell morphology are distinct. However, veliger shell diameter increased during exposure to all treatments, indicating resilience of veliger calcification to oceanic change
- Generalised dissolution across the shell surface suggests that the periostracum, which protects the subsequent shell, is ineffective in protecting veliger shells (protoconch) from acidification.

6.2.2 Chapter 3

In Chapter 3, I analysed samples collected over a one-year period from a sediment trap deployed on a moored platform located in the northern Scotia Sea to assess the population dynamics and life history of current pteropod populations. I calculate that:

- *L. retroversa* start spawning at 1-7 months while *L. helicina* spawn at 2.1-2.7 years. Therefore, *L. helicina* and *L. retroversa* have distinct life cycles which are likely to be differentially impacted by warming and acidification depending on season and longevity. Previously, the life cycle and longevity of *L. retroversa australis* and *L. helicina antarctica* was poorly parametrised and it was assumed that *L. retroversa australis* and *L.*

helicina antarctica started spawning respectively at 1 and 1- 3 years (Bednaršek *et al.,* 2012a; Hunt *et al.*, 2008).

- Spawning of both *L. helicina* and *L. retroversa* in the Scotia Sea only occurs from spring to autumn, with individuals overwintering as juveniles and adult, with the early life stages of both species only being present in the summer. Previously there was disagreement as to whether early life stages overwinter (Bednaršek et al., 2012a; Hunt et al., 2008). My results highlight that only the less vulnerable life stage (such as juveniles and adults) will be exposed to seasonal aragonite undersaturation predicted to occur during the winter from 2030 south of the Polar Front (McNeil and Matear, 2008).

- In the autumn the majority of *L. helicina* juveniles and adults migrate from 400 m water depth, most likely to deeper water in response to a concurrent drop in food supply. Some juveniles overwinter around 400 m water depth and continue to grow to large juveniles. I believe it is likely that these overwintering juveniles do not reach maturity by the spring although it is possible that upon reaching a large enough size before spring they were able to escape or avoid the sediment trap. Therefore, a variety of overwintering strategies are undertaken by *L. helicina,* which can potentially result in differential exposure of sub-populations to the wintertime surface aragonite undersaturation predicted to occur in the near future.

- Numerous species that have never been reported in the northern Scotia Sea were collected, such as; *Clio piatkowskii*, *Peraclis* cf. *valdiviae* and *C. pyramidata* f. *excise*. My results emphasise that sediment traps are an effective technique for long-term, remote sampling of pteropods in regions which might be periodically inaccessible for net sampling.

6.2.3 Chapter 4

In Chapter 4, I utilised historical net samples collected during the *Discovery Investigations* to provide a baseline of pteropod distribution and abundance across the Polar Front between South Georgia and the Falkland Islands. This transect covered an area which previously had few investigations into pteropod populations (Figure 1.1). The samples were collected in 1930, prior to significant anthropogenic impact of ocean acidification and warming on the Scotia Sea. I demonstrated that:

- The Antarctic Zone is the trailing and leading edge of *L. helicina's* and *L. retroversa's* biogeographic range, respectively. Both *L. helicina* and *L. retroversa* are bounded by the Polar Front, being likely limited by their

thermal tolerances. My results suggest that a future change in the position of the Polar Front or continued warming could consequently shift the pteropod population in this region from being dominated by *L. helicina* to *L. retroversa*, possibly resulting in a range retraction of *L. helicina.*

- Both *L. helicina* and *L. retroversa* juveniles and adults undertake a weak diurnal vertical migration in response to light intensity; feeding in relatively shallow waters during the night and retreating to deeper depths during the day to avoid predators. In contrast, *Limacina* veligers mainly reside in the upper 100 m of the water column. In the future, it is projected that surface waters will become undersaturated with respect to aragonite alongside shoaling of the aragonite lysocline (McNeil and Matear, 2008). Veligers may have little refuge from surface waters undersaturated with respect to aragonite while juveniles and adults may experience a narrowing of suitable habitat. Increased exposure to conditions where $\Omega_{ar} \leq 1$ may reduce veliger survivorship and increase shell dissolution, potentially impacting the population stability in these areas.

- Gymnosomes, the specialist predator of thecosome pteropods, were not bound by the Polar Front. Instead, Gymnosome abundance mirrors that of *Limacina* prey species rather than temperature differences, owing to their wide thermal niche and close predator-prey relationship with thecosome pteropods. This result suggests that gymnosomes are likely to follow the distribution of their prey if a range-shift occurs rather than be bounded by tolerances to surrounding environmental conditions.

6.2.4 Chapter 5

Chapter 5 assessed the current condition of *L. helicina antarctica* shells in the Scotia Sea, in relation to the prevailing aragonite saturation state during the austral summer. I demonstrated that:

- The geographic area of aragonite undersaturation to the north of South Georgia is a persistent feature and larger than previously recorded by Bednaršek *et al.* (2012a). This natural gradient in aragonite saturation state provides an ideal natural laboratory for testing the impact of aragonite undersaturation for understanding pteropod physiology and population dynamics.

- In sites where $\Omega_{ar} \leq 1$ occurred below 200- 600 m, shell dissolution on outer whorls of *L. helicina* collected at 200 m was exclusively associated with a pre-existing shell feature such as a scratch, pit or fracture. Generalised dissolution, not associated with a shell feature, was only present on the protoconch in agreement with what I observed on

incubation of veligers in conditions where $\Omega_{ar} \leq 1$ (Chapter 2). My results help to resolve the current debate in the literature over the effectiveness (Peck *et al.,* 2016a; 2016b) versus the ineffectiveness (Bednaršek *et al.* (2014a; 2016a) of the periostracum in protecting pteropod shells from conditions undersaturated with respect to aragonite. In particular, I show that the periostracum is effective on the outer whorls of the juvenile shell in isolating the underlying aragonite layers from waters where $\Omega_{ar} \leq 1$, but is less effective on the protoconch (inner) shell regions which developed during the veliger stage.

6.3 Chapter synthesis

In this thesis I establish that pteropods in the Scotia Sea have some resistance to a range of oceanographic and ecological regimes, including waters which are undersaturated with respect to aragonite. Furthermore, I found that there are large spatiotemporal variations in the population dynamics and life history of *L. helicina antarctica* and *L. retroversa australis*. Future predictions and investigations into the impact of oceanic change on Southern Ocean pteropods need to focus on single species over local scales since wider generalisations are unlikely to be representative of their true responses.

In Chapter 5 I highlight that the northern Scotia Sea provides an ideal natural laboratory for considering the *in-situ* response of pteropods to conditions where $\Omega_{ar} \leq 1$. Currently, sites where the aragonite saturation of sea water is $\Omega_{ar} \leq 1$ are mainly found in higher latitude ecosystems (McNeil and Sasse, 2016; Sabine *et al.,* 2004; Doney *et al.,* 2009; Fabry *et al.,* 2008), however, surface water aragonite undersaturation is expected to be a wider spread phenomenon by 2100 (IPCC, 2013; Friedrich *et al.,* 2012) (Figure 6.1.). Within the Scotia Sea, the area of summertime undersaturation of aragonite within the upper 600 m is larger than recorded in 2010, occurring at both the Upwelling station and P3. Conditions where $\Omega_{ar} \leq 1$ were present at both these stations were associated respectively with the upwelling of CO_2-laden deep water and intense phytoplankton productivity (Section 3.3.6.2.). These sites of natural aragonite undersaturation can be utilised to inform predictions in other areas which have yet to experience aragonite undersaturation.
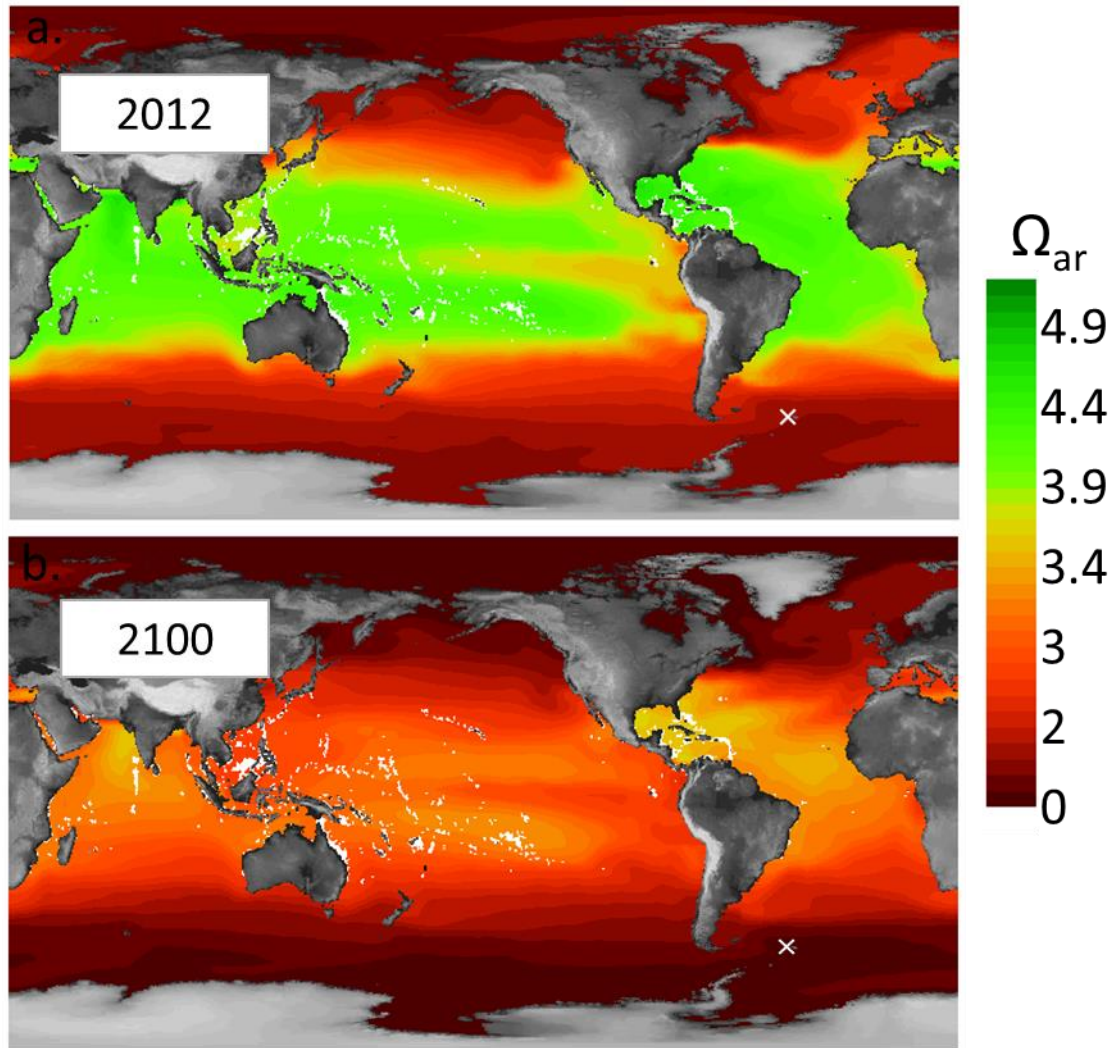
Figure 6-1. Surface saturation state of aragonite (Ω_{ar}) in (**a.**) 2012 and (**b.**) 2100 simulated by the using the Max Planck Institute for Meteorology Earth System Model (MPI-ESM) using historical data and the A1B greenhouse gas emission scenario during the 21st century. The cross (✕) indicates the position of station P3. Modified from Friedrich *et al.* (2012).

During the spring and summer of 2015, aragonite undersaturation shoaled to 400 m at P3 (Section 5.4.1.) where both *L. helicina* and *L. retroversa* veligers and juveniles were abundant (Section 3.4.2. and 5.4.1.). Furthermore, very few dead veligers were observed in the sediment trap (Section 3.3.2.) and there was still sufficient recruitment into the juvenile stages for the population to continue over several generations (Section 3.4.4.). Converse to the *in-situ* observations at P3, I found that that the survival rate of cultured *L. helicina antarctica* veligers is ~61% on exposure to waters where $\Omega_{ar} \leq 1$, in comparison to ~97% survival rate within waters where $\Omega_{ar} \geq 1$ (Section 2.4.1.). It should be noted that the cultured

veligers were unfed, and so survival rates are likely to be lower than if food was provided. However, the mortality rates of cultured veligers did not increase with prolonged exposure to acidified conditions (Section 2.4.1.) suggesting those which died may have had particularly sensitive genotypes to acidification. The continued removal of genotypes that are vulnerable to acidification may ultimately lead to a population which is more resistant to acidification (Timpane-Padgham *et al.*, 2017).

L. retroversa have a seasonal life cycle strategy with non-overlapping generations while *L. helicina antarctica'*s longer life cycle spans numerous seasons with several overlapping cohorts at any one time (Section 3.4.4.). The number of contemporary size groups within the *L. helicina* population suggests a life cycle of over a year. This strategy, of overlapping cohorts, is more robust against unfavourable environmental conditions such as reduced food supply or an aragonite undersaturation event. For *L. helicina*, since all life stages co-exist, vulnerability of one cohort is not detrimental to the stability of the overall population. Conversely, there is no overlap of life stages in the life cycle of *L. retroversa* meaning, if one cohort is removed, the entire population is vulnerable. If intolerable conditions occurred prior to the cohort of *L. retroversa* reaching sexual maturity, a population bottleneck or local extinction may result. Therefore, based on the assumption of a static population which is not advected from the sampling area, on exposure to a short-term acidification and warming *L. helicina* is most likely to be a winner, while *L. retroversa* will be a loser. Despite this, repeated or prolonged exposure to unfavourable conditions is likely to impact all cohorts and if there is reduced recruitment over an extended period, the population of *L. helicina* would also be under threat. Such a progressive population decline was observed in the Ross Sea, where long-term food shortages due to reduced primary productivity eventually led to the short-term localised extinction of *L. helicina* (Maas *et al.,* 2011; Seibel and Dierssen, 2003).

Veligers sampled in 1930 (Section 4.3.3.) were mainly found within the first 100 m of the water column. Conversely, the high abundance of veligers collected in the sediment trap deployed at 400m in P3 suggests that veligers may have a

vertical distribution deeper than 100m (Section 3.3.4.). Veligers are limited by their reduced swimming capacity (Lalli & Gilmer 1989; Howes et al., 2014) and only reside where there is a plentiful food supply (Section 4.3.3.3). The *Discovery samples* were collected across the open ocean where phytoplankton is likely to be confined to the surface. Conversely, the sediment trap was situated in a region of upwelling, meaning phytoplankton are likely to be at deeper depths due to the enhanced supply of macronutrients. Therefore, veligers found in the polar frontal zone reside closer to the surface in comparison to those at the upwelling region, mirroring the distribution of food supply. The presence of juvenile *L. helicina* and *L. retroversa* collected within the sediment trap in Chapter 3 (Section 3.3.4.) agrees with the baseline vertical distribution established in Chapter 4 (Section 4.3.3.). This is likely because adults and juveniles undertake a vertical migration in response to light intensity and predator presence, rather than food supply, which are similar across the polar frontal zone and the upwelling region.

I found that *L. helicina* and *L. retroversa* undertake protracted spawning from spring to autumn, in parallel to the prolonged phytoplankton bloom at P3 (Section 3.4.3.). There is disagreement in the literature as to when pteropods spawn in the Southern Ocean (See Table 3.1.) and whether they overwinter as veligers in a diapause state, as *L. helicina* have been observed to do in the Arctic (Hunt, 2008; Lischka and Riebesell, 2016). However, in Section 3.4.4. I start to elucidate that individuals of both *L. helicina* and *L. retroversa* overwinter as juveniles and adults, with no veligers being present during the winter. Since aragonite undersaturation occurred at P3 and the Upwelling station in the summer (Section 5.4.1.), all life stages (veligers, juveniles and adults) were exposed to conditions where $\Omega_{ar} \leq 1$ in this part of the year (Section 3.4.4.). Furthermore, all the life stages continue growth despite experiencing $\Omega_{ar} \leq 1$ (Section 2.3.2), which was confirmed in veligers within cultured conditions (Section 2.4.1.). Continued shell growth indicates that individuals were still capable of maintaining the necessary concentration of carbonate ions within their interpallial space to calcify new shell, despite the greater energetic demand needed under conditions where $\Omega_{ar} \leq 1$ in the summer (Hoshijima *et al.,* 2017).

Previous studies in the Arctic fjords show that *L. helicina* and *L. retroversa* cease growth when sea water is undersaturated with respect to aragonite during the winter months (Hunt, 2008; Lischka and Riebesell, 2016). Considering both observations of continued shell growth during summer (this study) and reduced shell growth during the winter (Hunt, 2008; Lischka and Riebesell, 2016) suggests that the availability of food may potentially play a relevant role in the ability of pteropod to counteract ocean acidification. Little data exists on the wintertime carbonate chemistry at P3, however, it is predicted that $\Omega_{ar} \leq 1$ will occur by 2030 in surface water during the winter south of the Polar Front (McNeil and Matear, 2008) with widespread undersaturation of aragonite by 2100 (Friedrich *et al.,* 2012; Orr *et al.,* 2005). Since wintertime $\Omega_{ar} \leq 1$ events in the Scotia Sea will coincide with lower quality and quantity of food supply than the summer months (Section 3.4.3.), individuals may not be able to maintain a steady rate of shell growth (Deppeler and Davidson, 2017 *and references therein*). However, pteropods are omnivores therefore, it is possible that overwintering individuals may still be able to acquire a sufficient food supply despite a change in composition.

In Chapter 5 I show that shell dissolution was found on every *L. helicina antarctica* juvenile collected at 200 m depth to the north of South Georgia where waters were naturally undersaturated with respect to aragonite below 200- 600 m (Section 5.4.3.). Two types of shell dissolution were identified, either being in association with a pre-existing shell feature such as a pit, fracture or scratch, or being generalised across the shell surface (Section 5.4.3.). According to Peck *et al* (2016a), dissolution, which was associated with a shell feature within waters where $\Omega_{ar} \leq 1$, occurs because the periostracum has been breached. Bednaršek *et al.* (2016a) suggested that generalised dissolution occurs due to the periostracum being ineffective while Peck *et al.* (2016b) suggested that generalised dissolution occurs because of microperforations within the periostracum and/or a different nature of the periostracum covering the protoconch (the remnant veliger shell).

Here, generalised dissolution was observed on the protoconch of juveniles collected from the northern Scotia Sea region (Section 5.4.3.). Furthermore, shell dissolution was observed on every *L. helicina antarctica* veliger which was cultured in conditions where $\Omega_{ar} \leq 1$ (Section 2.4.3.). While it is possible that microperforations to the periostracum could have been present on individuals collected from the northern Scotia Sea (P3 and Upwelling stations), there was no feasible mechanism for microperforations or any other mechanism of periostracum breaching to occur on the cultured veliger (Section 2.2.1.). Therefore, it is most likely that the periostracum of veliger shells is ineffective at protecting the underlying aragonite from dissolution as previously suggested by Peck *et al.,* (2016a). This lack of protection to the veliger shell means that the early life history stages of *L. helicina antarctica* are especially vulnerable to shell dissolution. Furthermore, since the periostracum cannot be repaired or replaced, the protoconch remains vulnerable to dissolution throughout an individual's life cycle. Nevertheless, generalised dissolution did not occur on juvenile shell whorls of *L. helicina antarctica* collected within the Scotia Sea (Section 5.3.3.) indicating that the periostracum formed after metamorphosis into this life stage is effective at protecting the aragonitic part of the shell in waters which are undersaturated with respect to aragonite.
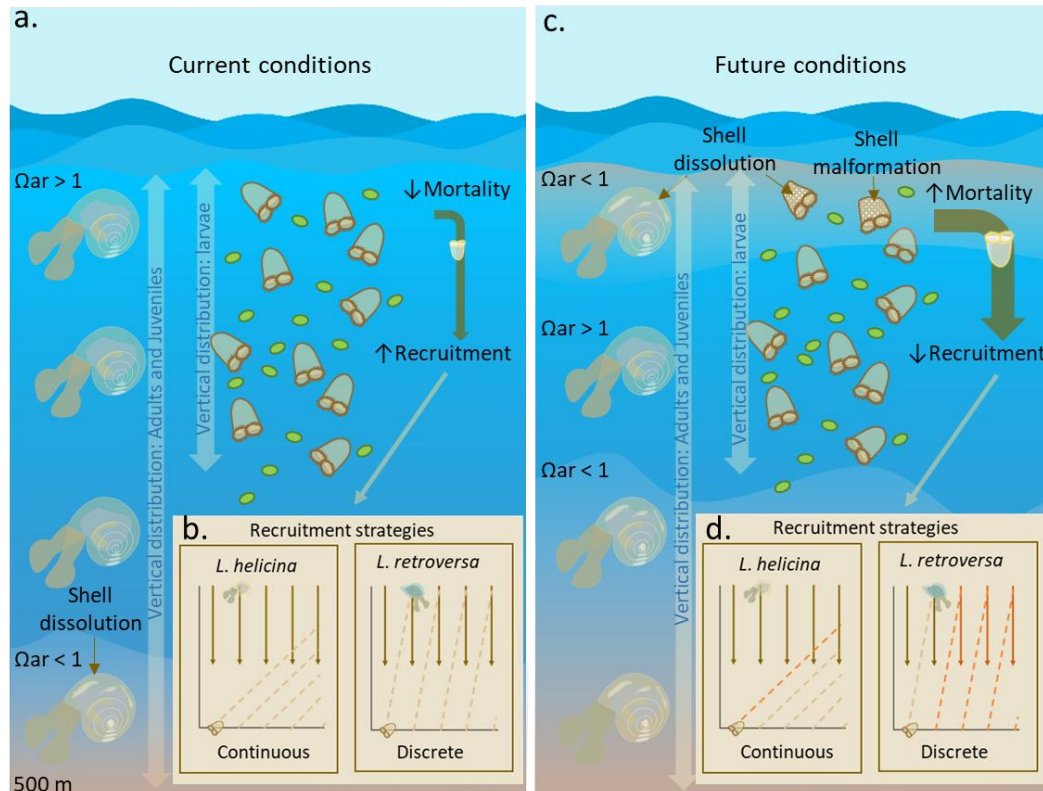
Figure 6-2. Overall synthesis of the main findings of this thesis. Under (**a.**) current conditions, adult and juvenile pteropods undertake a vertical migration over 1000 m from the surface. In an upwelling region, these individuals experience conditions that are undersaturated with respect to aragonite (Ωar < 1) within the lysocline, causing shell dissolution where there are breaches in the periostracum and on the shell protoconch (larval shell). (**b.**) *L. helicina* continuously spawn over the summer and there is continuous recruitment while *L. retroversa* have a discrete spawning and recruitment strategy. Larvae are confined in vertical distribution to food rich layers, meaning there is no contact with the lysocline. Under (**c.**) future conditions the lysocline is predicted to shoal closer to the surface and surface waters are predicted to be undersaturated with respect to aragonite alongside warming. Therefore, larvae will be exposed to water which is warmer and where Ωar < 1, causing reduced shell size, shell dissolution and shell malformation. Mortality rate of larvae will increase (brown arrow) and recruitment will decrease. **(d.)** Since *L. helicina* continuously spawn, if one cohort of larvae is removed (orange line) it can be replaced (subsequent brown lines). However, if one cohort of *L. retroversa* larvae is removed, they can only be replaced through migration from other regions.

6.4 Future work

The data presented in this thesis have added to our understanding of the impact of a changing ocean on pteropod life history and physiology, however, several aspects warrant further investigation.

In Chapter 5, I gave an overview of the summertime carbonate chemistry across the Scotia Sea which compliments a number of existing datasets (GLODAP; SOCAT). However, wintertime measurements of carbonate chemistry are rare, so our knowledge of the current conditions which pteropods experience is incomplete. It is vital to understand the baseline environmental conditions that pteropods reside in for further exploration into the adaptive capacity, and potential resilience, which exists in pteropods populations. Furthermore, a better knowledge of the conditions which pteropods already experience will give a more accurate environmental context to manipulation experiments and help inform relevant exposure conditions.

As demonstrated in Chapter 3, sediment traps moored at a variety of depths can elucidate pteropod population dynamics and the environment that they reside in. Furthermore, sediment traps can sample the pteropod population during the winter in areas which are otherwise inaccessible with nets. The continued analysis of pteropods collected within the sediment trap at P3 will utilise this ideal natural laboratory which is experiencing rapid environmental change to inform us of long term population trends and dynamics in the two key thecosome species. Furthermore, continued sampling may elucidate the population dynamics of the adult stages of *L. helicina antarctica.* Ultimately, sediment trap data can be combined with particle tracking models and carbonate chemistry datasets to model the exposure history (e.g. number of 'undersaturation days') of pteropods to waters where $\Omega_{ar} \leq 1$, as applied by Bednaršek *et al.,* (2017). The challenge would be to account for complex frontal and eddy components of the notably dynamic northern Scotia Sea.

In Chapter 2 *L. helicina antarctica* were cultured under acidified and warm conditions predicted in 2100 for 5 days under starvation conditions. Longer term (months to years) incubations could be conducted to observe the success rate of

veliger metamorphosis to the juvenile and adult stages in waters where $\Omega_{ar} \leq 1$. Furthermore, it is possible that exposure to environmental perturbations during early life stages may cause latent effects on later life stages such as a lower tolerance to environmental drivers and a greater susceptibility to predation and parasitism. Multi-generational studies on pteropods could inform whether latent effects occur and help elucidate population scale effects of environmental drivers, however, this would require improved culturing and incubation techniques. The long-term culturing of pteropods is currently problematic, with difficulties in allowing natural behaviours and encouraging pteropods to feed (Howes *et al.,* 2014). It is therefore important to develop culturing techniques which may encourage more natural behaviours. I believe this can be achieved through adopting the innovative developments made in aquaculture for rearing gelatinous planktonic organisms, such as using variants of kreisel tanks for rearing jellyfish (Purcell *et al.,* 2013). Kreisel systems have a flow which keeps the organism in suspension, encouraging natural swimming and feeding behaviours while enabling manipulation of water conditions. Furthermore, the constant flux of water through the kreisel system will enable a more stable carbonate chemistry system despite the addition of food, which poses a problem for closed systems.

It is critical to understand how pteropods balance energetic requirements when exposed to undersaturated conditions and the impact that food supply has on this balance. Nevertheless, the effects of ocean acidification and warming on the physiological functioning of pteropods remains poorly understood. Techniques such as metabolomics could be utilised to examine the how the metabolic profile of pteropods responds to changes in the external environment. Individuals can be flash frozen after an incubation design, similar to that utilised in Chapter 2, to reveal which proteins and lipids are up and down regulated on exposure to acidification and warming. Metabolomics have already been applied to some polar organisms to reveal the impact of exposure to warming and acidification in experimental incubations (Clark *et al.,* 2017; Mayor *et al.,* 2015), but have yet been applied to pteropod research. These studies indicated species-specific

responses to stress, such as the accumulation of anerobic end products and the production of heat shock proteins.

It has been shown that pteropods are able to continue calcification in undersaturated conditions when food availability is high, despite the extra energetic burden (Seibel *et al.,* 2012; Maas *et al.,* 2011). However, the majority of studies do not provide a food source (Howes *et al.,* 2014; Maas *et al.,* 2011). Further investigation into energetic budgets under a range of aragonite saturations and food regimes would enable prediction as to which combination of environmental conditions would be most damaging to pteropods populations. For this to be achieved, the local diet of the pteropods being investigated would need to be established. Duplicating a pteropods natural diet is vital during manipulative experimental investigations as the nutritional content and quality may act as an additional confounding factor during experimental manipulations. Furthermore, the quality and availability of food is likely to alter with season, therefore, the ability of an individual to maintain the intracellular environment and perform certain functions (such as shell growth and spawning) may vary seasonally depending on the nutritional value and availability of food. Information on pteropod diet can be gathered through gut content analysis. Replicating food sources realistically for incubations could involve harvesting and/or culturing what is naturally consumed or substituting it with an energetically similar food source. Previously, Gilmer and Harbison (1991) have examined the diet of *L. helicina helicina* collected during the Arctic summer, finding copepods, pteropods, tintinnids, diatoms and dinoflagellates within their gizzard and esophagus. While it is likely that Southern Ocean pteropods feed on similar groups, there is little data to confirm this. Future work should focus on characterising the suite of food sources that Southern Ocean pteoropods feed on in order to realistically mimic natural conditions during perturbation experiments.

Chapter 2 considered the impact of simultaneous warming and acidification on veliger pteropods, however, numerous other anthropogenic drivers are predicted to occur simultaneously including de-oxygenation, freshening, increased stratification and pollutants (Pörtner *et al.,* 2014). In combination with

ocean acidification, these drivers could cause interactive effects that may be additive, synergistic or antagonistic therefore additional multi-driver investigations are vital. The responses to multiple drivers are likely to be specific with region, habitat, species, and life history stage (Hobday and Lough, 2011). The possible impacts of these additional drivers on pteropods within the Southern Ocean is poorly understood, with most current research investigating response to single drivers (Table 1.2). Natural analogues for multiple driver combinations are rare or likely differ from future scenarios within the Scotia Sea, therefore, investigating pteropods within modern proxies is limited. Consequently, manipulative experiments are the most logical avenue to investigate the impact of multiple drivers on pteropods. There are many logistical constraints while investigating Southern Ocean pteropods which limits the number of possible drivers which can be investigated at any one time. Future studies may consider adopting a 'reduced' or 'collapsed' experimental design as suggested by Boyd *et al.* (2018) where several variables are combined into one or lower-order interactions are excluded. For example, to reduce the number of samples needed for investigating the impact of warming, acidification and food supply with several levels, we can identify the primary driver of interest (e.g. warming), and then only test the effects of this driver as one factor with all other drivers together. Alternatively, the single effects of each driver can be tested independently as well as the interactive effects, but not the two-way interactions.

In Chapter 5, I show that specimens of *L. helicina* which were exposed to aragonite undersaturation displayed shell dissolution (Section 5.4.3.). It is speculated that shell dissolution is a sub-lethal stressor, generating shell fragility which in turn can influence vulnerability to infection and predation, buoyancy regulation, swimming ability and acid-base homeostasis (Bergan *et al.,* 2017; Adhikari *et al.,* 2016; Norton, 1988). There is little research into the direct implications of shell dissolution for pteropods since current experimental techniques limit species interactions and natural behaviours, however, mesocosms provide an ideal opportunity to explore possible sub-lethal impacts. In an ideal world with unlimited funding and no logistical constraints, I believe

the next step for investigating the impact of environmental change on pteropods would be to incubate individuals on long time scales within large-scale manipulative mesocosm experiments alongside natural assemblages, such as those deployed in the KOSMOS project (Gran Canaria) which measure 13x 2m. Mesocosms have strong ecological relevance and species interactions can capture direct (e.g. shell dissolution) and indirect (e.g. susceptibility to predation) effects of oceanic change. Natural food supply can be utilised alongside diurnal and seasonal fluctuations in environmental conditions. Furthermore, there is a large enough space within mesocosms from pteropods to behave naturally, including the ability to deploy mucous webs and react to the presence of predators.

Overall, the continued monitoring of thecosome pteropod populations in the Scotia Sea, combined with bioassays and mesocosm work. This research approach will be crucial in identifying the continued threat to this taxa from rapid warming and ocean acidification.

7 Appendices

Table A2.1. Model selection parameters (residual deviance, residual degrees of freedom, delta AIC and AIC weight) for the top models (delta<4) predicting the effect of acidification and warming over time (days) on *Limacina helicina antarctica* mortality, shell morphology and shell size.

Variable	Predictor	R. Df	R. Dev	dAIC	Weight
Mortality	Acidified *Warm	296	258.96	0.0	0.41
	Acidified*Warm + Day	295	257.77	0.8	0.28
	Acidified*Warm + Day + Acidified:Day	294	257.05	2.1	0.15
	Acidified*Warm + Warm:Day + Acidified	294	257.73	2.8	0.10
	Acidified	298	266.73	3.8	0.06
Pitting	Acidified*Warm + Day	218	196.63	0.0	0.27
	Acidified*Warm + Day + Warm:Day	217	194.84	0.2	0.25
	Acidified*Warm + Day + Acidified:Day	217	195.97	1.3	0.14
	Acidified*Warm	219	200.93	2.3	0.09
	Acidified*Day + Warm + Warm:Day	217	194.83	0.2	0.25
Malformation	Acidified * Day + Warm	218	128.36	0.3	0.3
	Acidified + Warm + Day	219	130.07	0.0	0.0
	Acidified*Warm + Day	218	130.08	2.0	2.0
	Warm* Day + Acidified	218	129.97	1.9	1.9
	Acidified*Warm + Day + Acidified:Day	217	127.85	1.8	1.8
	Acidified * Day + Warm + Warm:Day	217	128.62	2.6	2.6
Etching	Acidified + Warm	220	25.04	0.0	0.43
	Acidified	221	28.68	1.6	0.19
	Warm + Acidified + Day	219	25.02	2.0	0.16
	Acidified*Warm	219	25.05	2.0	0.16

Table A2.2. Binomial (logit) generalised linear model comparing mortalities of larval *Limacina helicina antarctica* within control, ambient, acidified and acidified-warm conditions over time (days) using 300 observations with 297.45 null deviance.

Predictor	Estimate (S.E.)	Wald	*p*
Intercept	-3.99 (0.80)	-4.97	<0.001
Warm	1.61 (0.80)	2.01	0.04
Acidified	3.17 (0.76)	4.18	<0.001
Acidified-Warm	2.54 (0.77)	3.31	<0.001
Day 2	0.14 (0.53)	0.26	0.79
Day 3	0.51 (0.51)	1.00	0.32
Day 4	0.82 (0.50)	1.66	0.10
Day 5	0.27 (0.52)	0.52	0.61

Table A2.3. Binomial (logit) generalised linear model using a two-way factorial design estimating mortality of larval *Limacina helicina antarctica* within control, ambient, acidified and acidified-warm conditions over time (days) using 300 observations with 297.45 null deviance.

Predictor	Estimate (S.E.)	Wald	*p*
Intercept	-3.68 (0.89)	-4.12	<0.001
Warm	0.92 (0.86)	1.06	0.28
Acidified	3.01 (0.89)	3.38	<0.001
Day	0.15 (0.23)	0.69	0.49
Acidified:Warm	-1.67 (0.70)	-2.38	0.02
Acidified:Day	-0.10 (0.22)	-0.46	0.64
Warming:Day	0.062 (0.21)	0.30	0.76

Table A2.4. Summary of larval *Limacina helicina antarctica* mortalities/breakages within each treatment and across exposure times. These individuals were not considered for further analysis. Overall 223 larvae were analysed for changes in shell morphology.

		Number of deaths			
		Ambient	**Warm**	**Acidified**	**Acidified-Warm**
Exposure time (days)	**1**	0/0	0/6	6/1	3/1
	2	0/3	2/1	5/0	4/0
	3	1/1	2/0	6/1	4/0
	4	1/4	2/1	6/1	4/2
	5	0/1	2/0	5/0	3/0

Table A2.5. Gamma (identity) maximum likelihood generalised linear comparing shell size of larval *Limacina helicina antarctica* within control, ambient, acidified and acidified-warm conditions over time (days) using 223 observations with 3.38 null deviance.

Predictor	Estimate (S.E.)	t	p
Intercept	81.80 (0.73)	111.31	<0.001
Warm	0.98 (1.21)	0.81	0.42
Acidified	-2.92 (1.21)	-2.4	0.01
Acidified-Warm	-5.8 (1.08)	-5.34	<0.001
Day 2	8.2 (1.17)	7.04	<0.001
Day 3	14.77 (1.16)	12.72	<0.001
Day 4	29.02 (1.38)	22.1	<0.001
Day 5	31.2 (1.28)	24.33	<0.001
Acidified-Warm: Day 2	-4.29 (1.64)	-2.61	0.009
Acidified: Day 2	-0.37 (1.79)	-0.21	0.834
Warm: Day 2	-1.39 (1.76)	-0.79	0.428
Acidified-Warm: Day 3	0.86 (1.70)	0.51	0.612
Acidified: Day 3	-0.52 (1.89)	-0.28	0.783
Warm: Day 3	-1.31 (1.76)	-0.74	0.458
Acidified-Warm: Day 4	0.09 (2.03)	0.05	0.963
Acidified: Day 4	-3.02 (2.12)	-1.42	0.16
Warm: Day 4	-7.21 (1.97)	-3.64	<0.001
Acidified-Warm: Day 5	-2.03 (1.84)	-1.10	0.271
Acidified: Day 5	-4.07 (1.98)	-2.05	0.041
Warm: Day 5	-9.43 (1.89)	-4.98	<0.001

Table A2.6. Gamma (identity) generalised linear model fit by using a two-way factorial design estimating the impact on shell size of exposing larval *Limacina helicina antarctica* to control, ambient, acidified and acidified warm conditions to fit 223 observations with 3.38 null deviance.

Predictor	Estimate (S.E.)	t	P
Intercept	75.33 (0.97)	77.54	<0.001
Warm	0.07 (1.29)	0.05	0.95
Acidified	-6.03 (1.29)	-4.67	<0.001
Day	7.55 (0.32)	23.96	<0.001
Acidified:Warm	-0.76 (1.08)	-0.70	0.48
Acid:Day	0.72 (0.38)	1.88	0.061
Warm:Day	-0.79 (0.38)	-2.06	0.039

Table A2.7. Binomial (logit) generalised linear model estimating the presence of malformation, pitting and etching on larval *Limacina helicina antarctica* shells incubated within control, ambient, acidified and acidified-warm conditions over time (days) using 223 observations with 277.5, 251.35, 307.16 null deviance respectively

Variable	Predictor	Estimate (S.E.)	Wald	*p*
Malformation	Intercept	-6.75 (0.94)	-7.15	<0.001
	Warm	3.72 (0.69)	5.35	<0.001
	Acidified	0.72 (0.76)	0.96	0.34
	Acidified-Warm	5.16 (0.79)	6.56	<0.001
	Day 2	1.08 (0.77)	1.41	0.16
	Day 3	2.94 (0.77)	3.82	<0.001
	Day 4	4.71 (0.87)	5.41	<0.001
	Day 5	4.42 (0.84)	5.29	<0.001
Pitting	Intercept	-3.86 (0.89)	-4.32	<0.001
	Warm	3.96 (0.88)	4.48	<0.001
	Acidified	2.84 (0.90)	3.13	<0.001
	Acidified-Warm	3.49 (0.89)	3.93	<0.001
	Day 2	0.04 (0.48)	0.09	0.93
	Day 3	-0.22 (0.49)	0.09	0.67
	Day 4	-0.18 (0.51)	-0.36	0.72
	Day 5	-1.03 (0.53)	-1.92	0.05
Etching	Intercept	-5.84 (1.59)	-3.67	<0.001
	Warm	1.66 (1.20)	1.38	0.17
	Acidified	11.55 (2.78)	4.16	<0.001
	Acidified-Warm	11.74 (2.79)	4.21	<0.001
	Day 2	-0.32 (1.59)	-0.19	0.84
	Day 3	2.56 (1.37)	1.87	0.06
	Day 4	-0.35 (1.62)	-0.22	0.83
	Day 5	-0.34 (1.57)	-0.22	0.83

Table A2.8. Binomial (logit) generalised linear model using a two-way factorial design estimating the presence of malformation, pitting and etching on larval *Limacina helicina antarctica* shells incubated within control, ambient, acidified and acidified-warm conditions over time (days) using 223 observations with 277.5, 251.35, 307.16 null deviance respectively.

Variable	Predictor	Estimate (S.E.)	Wald	p
Malformation	Intercept	-13.53 (3.19)	-4.24	<0.001
	Warm	6.82 (1.75)	3.91	<0.001
	Acidified	1.47 (1.26)	1.16	0.24
	Acidified-Warm	0.92 (1.38)	0.67	0.50
	Day	2.17 (0.59)	3.67	<0.001
Pitting	Intercept	-2.09 (0.79)	-2.64	<0.01
	Warm	2.21 (0.80)	2.76	<0.01
	Acidified	2.23 (0.79)	2.82	<0.01
	Day	-0.28 (0.22)	-1.29	0.19
	Acidified:Warm	-2.36 (0.79)	-2.98	<0.01
	Acid:Day	-0.04 (0.16)	-0.27	0.78
	Warm:Day	0.20 (0.19)	1.06	0.28
Etching	Intercept	-4.49 (1.70)	-2.63	<0.01
	Warm	1.32 (1.72)	0.77	0.44
	Acidified	10.11 (3.02)	3.35	<0.001
	Day	-0.24 (0.52)	-0.45	0.65
	Acidified:Warm	0.11 (2.27)	0.04	0.96
	Acid:Day	0.24 (0.62)	0.38	0.70
	Warm:Day	0.29 (0.57)	0.49	0.62

Table A2.9. Factorial analysis comparing shell size of larval *Limacina helicina antarctica* within control, ambient, acidified and acidified-warm conditions over time (days) using 223 observations.

Test	Predictor	Estimate	*z*	*p*
Shell size	Intercept	75.33	77.549	<0.001
	Warm	0.07	0.051	0.96
	Acidified	-6.03	-4.677	<0.001
	Day	7.55	23.963	<0.001
	Acidified: Warm	-0.76	-0.703	0.48
	Acidified: Day	0.72	1.882	0.06
	Warm: Day	-0.79	-2.068	0.04

Treatment conditions
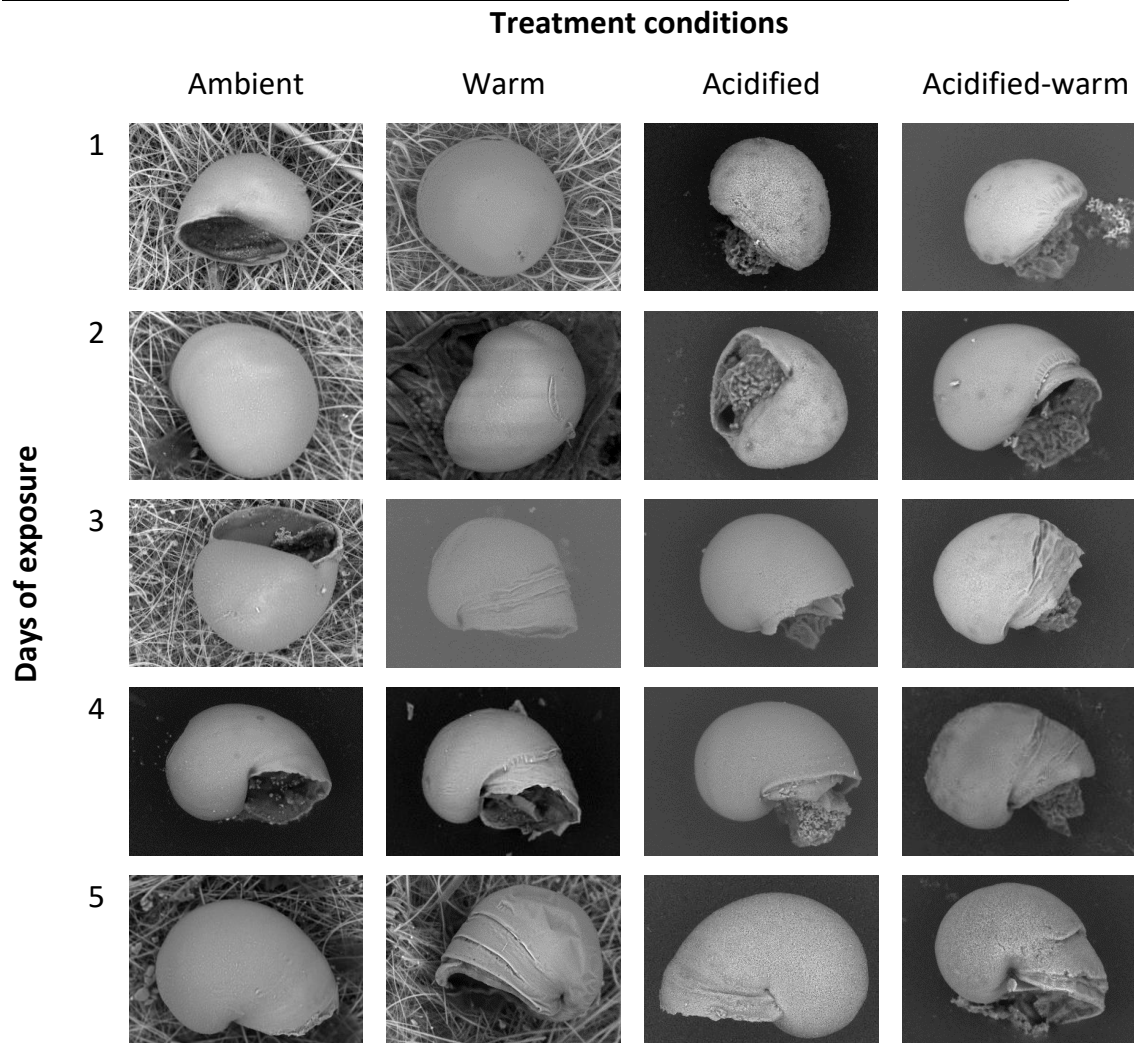
Figure A2.1. Scanning Electron microscope images of larval *Limacina helicina antarctica* after exposure to ambient, warm, acidified and acidified-warm conditions for 1-5 days. All larvae were alive upon harvesting.
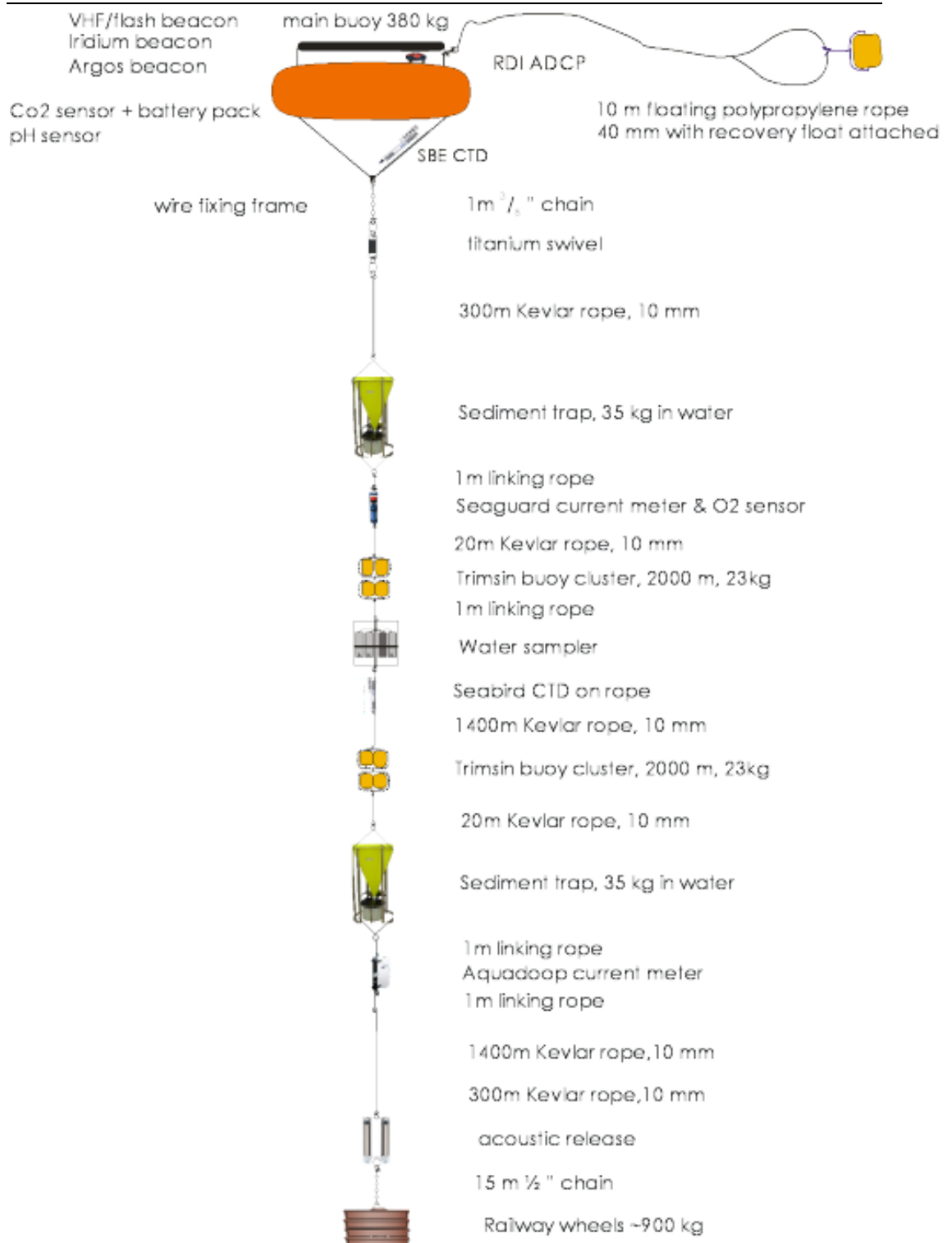
Figure A3.1. Arrangement of the instruments deployed on the mooring at station P3 (Scotia Sea) between December 2014 and March 2015. Image taken directly from the JR304 cruise report.
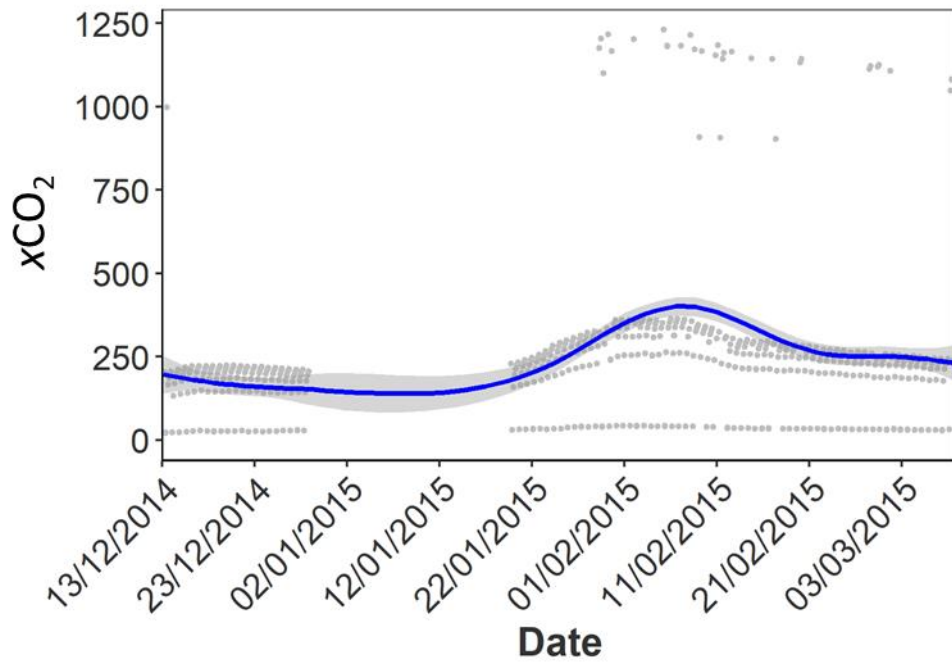
Figure A3.2. Seawater xCO_2 (parts per million, Pro-OCEANUS) measurements taken at 200 m depth at station P3 (Scotia Sea) between December 2014 and March 2015. All measurements collected are presented. An *in-situ* calibration was not carried out. A locally weighted scatterplot smoothing (LOESS) curve is fitted to the data points.

Table A3.3. Mixture analysis chi-squared, means and standard errors of *L. retroversa* (L.R.) and *L. helicina* (L.H.) cohorts based on the shell width of *L. helicina* and spire height of *L. retroversa* individuals. Individuals were entrapped within a sediment trap at 200 m at station P3 (Southern Ocean) between December 2014 and March 2015.

Month	Model	L.R. χ^2	L.R. d.f.	L.R. P	L.H. χ^2	L.H. d.f.	P
Dec	Lognormal	2.72	8	0.95	15.51	23	0.88
	Normal	2.56	8	0.95	21.78	26	0.70
	Gamma	2.65	8	0.95	15.40	23	0.88
	Weibull	2.59	8	0.96	14.99	23	0.9
Jan	Lognormal	14.98	24	0.41	105.54	47	>0.01
	Normal	13.30	24	0.96	385.54	47	0
	Gamma	25.43	24	0.38	105.24	47	>0.01
	Weibull	24.39	27	0.61	7181.64	48	0
Feb	Lognormal	53.56	41	0.09	128.61	55	>0.01
	Normal	45.93	38	0.18	1114.39	54	0
	Gamma	45.73	38	0.18	154.49	55	>0.01
	Weibull	47.63	38	0.14	2798.61	54	0
Mar	Lognormal	21.98	13	0.05	86.08	50	>0.01
	Normal	24.31	13	0.03	167.12	50	>0.01
	Gamma	22.71	13	0.04	82.68	50	>0.01
	Weibull	67.47	14	>0.01	3920.19	50	0
Apr	Lognormal	21.09	12	0.5	36.47	60	0.991
	Normal	21.01	12	0.5	32.20	57	0.997
	Gamma	21.06	12	0.5	32.16	57	0.997
	Weibull	22.64	15	0.09	32.52	56	0.99
May	Lognormal	59.66	71	0.82	27.33	25	0.34
	Normal	67.80	74	0.68	23.01	25	0.58
	Gamma	59.57	71	0.83	25.47	25	0.44
	Weibull	70.45	74	0.59	24.52	25	0.49
June	Lognormal	55.35	60	0.65	24.32	23	0.39
	Normal	55.28	60	0.65	25.09	23	0.35
	Gamma	55.07	60	0.66	24.56	23	0.37
	Weibull	57.73	60	0.55	27.01	23	0.26
July	Lognormal	42.08	43	0.51	19.22	10	0.03
	Normal	35.51	43	0.78	19.55	10	0.03
	Gamma	39.89	43	0.63	19.32	10	0.03
	Weibull	32.89	43	0.86	22.19	10	0.01
Aug	Lognormal	41.46	48	0.73	56.59	10	>0.01
	Normal	37.80	48	0.85	16.70	11	0.12
	Gamma	39.71	48	0.79	58.19	10	>0.01
	Weibull	39.21	48	0.81	61.56	11	>0.01
Sep	Lognormal	34.15	26	0.13	18.59	16	0.29
	Normal	29.91	26	0.27	21.36	15	0.13
	Gamma	32.36	26	0.18	21.34	16	0.16
	Weibull	28.76	26	0.32	23.49	15	0.07
Oct	Lognormal	2.51	4	0.64	81.89	20	>0.01
	Normal	2.97	4	0.56	81.17	20	>0.01
	Gamma	2.49	4	0.65	81.49	20	>0.01
	Weibull	2.83	4	0.58	80.62	20	>0.01
Nov	Lognormal	14.82	18	0.67	107.06	62	>0.01
	Normal	15.22	18	0.64	128.28	62	>0.01
	Gamma	14.94	18	0.67	107.99	62	>0.01
	Weibull	14.19	18	0.71	80.62	20	>0.01
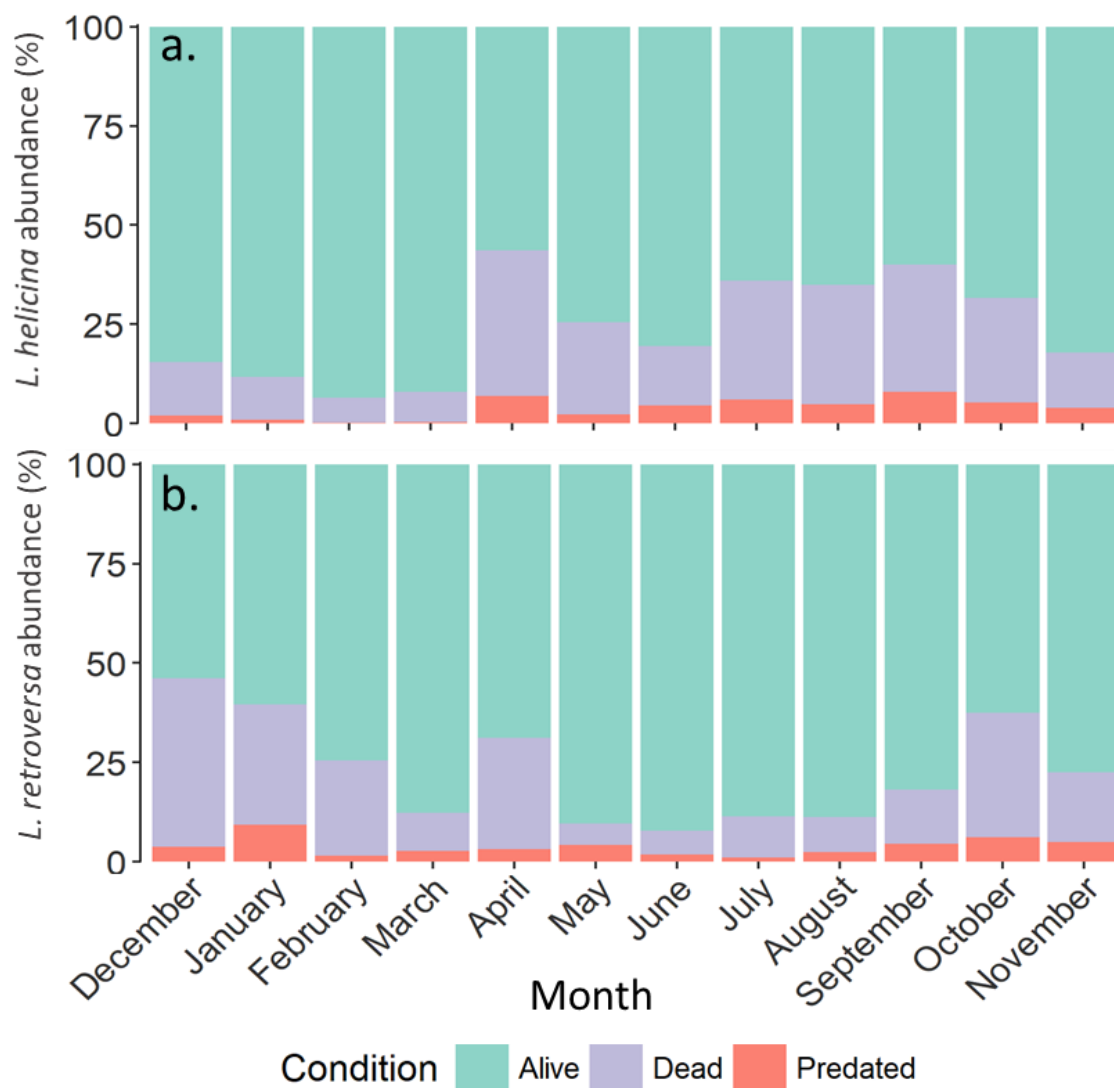
Figure A3.448-1. Monthly abundance (%) of *L. helicina* (**a.**), *L. retroversa* (**b.**) that were alive (green), dead (purple) or predated (orange). Pteropods were entrapped within a sediment trap at 200 m at station P3 (Southern Ocean) between December 2014 and March 2015.

Table A4.1. Details of the filtration volumes of nets used by the R.R.S. *William Scoresby* during the *Discovery Investigations*.

Depth sampled (m)	Volume filtered (m^3)
0-50	19.24
50-100	19.24
100-250	57.73
250-500	96.21
500-750	96.21
750-1000	96.21
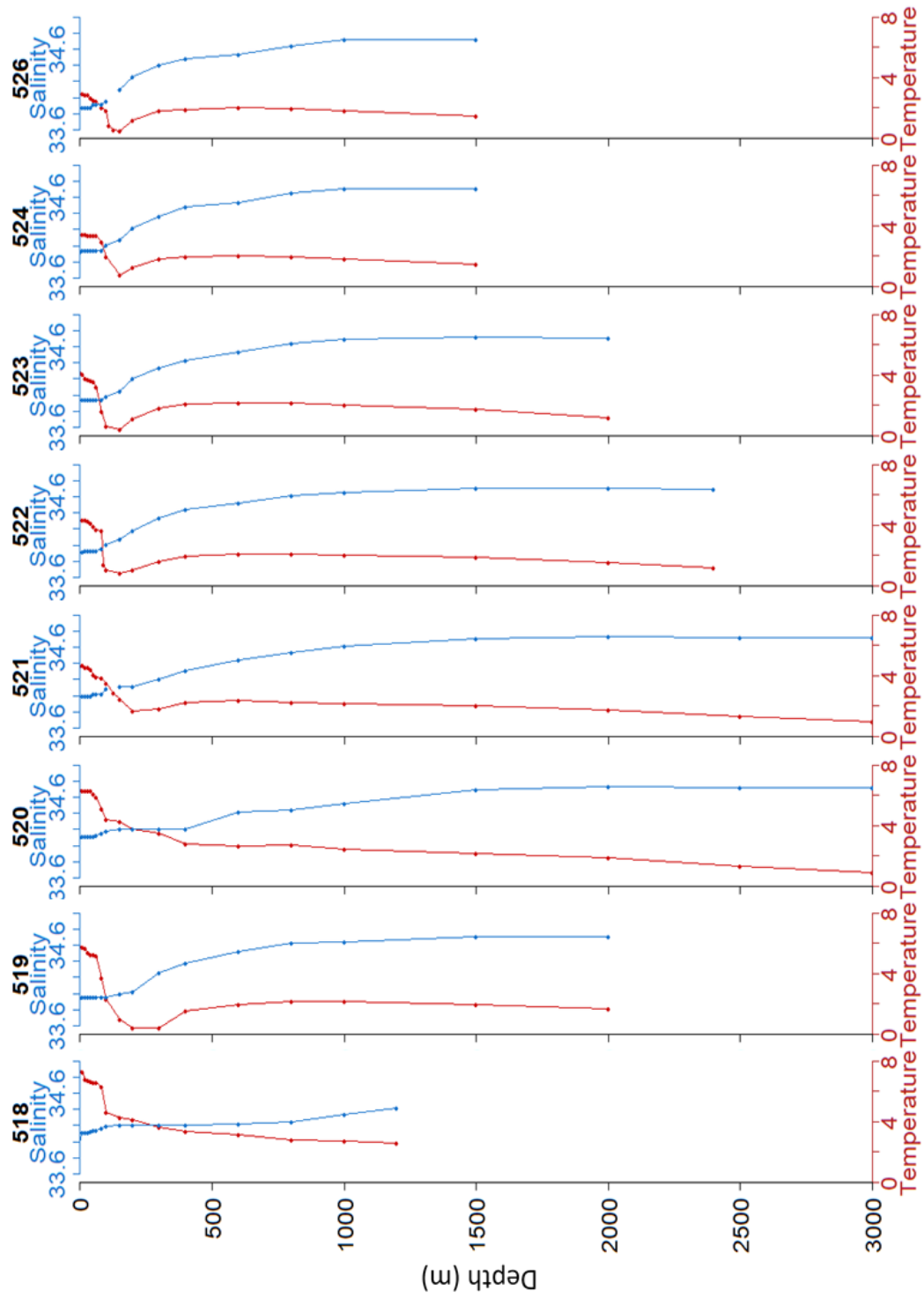
Figure A4.1. Temperature (°C) and Salinity profiles taken by the R.R.S. *William Scoresby* during the *Discovery Investigations* between 26th February and 3rd March 1930. Each profile corresponds to a station on a transect where 518 is closest to the Falkland Islands and 526 to South Georgia.

Table A5.1. Measures of precision (standard deviations) during the analysis of Total Alkalinity (TA) and Dissolved Inorganic Carbon (DIC) for two cruises, JR304 (2014) and JR15002 (2015), by *the R.S.S. James Clark Ross* within the Scotia Sea (Southern Ocean).

Cruise name	Overall precision (μmol/kg)		Short-term precision (μmol/kg)		Replicate precision (μmol/kg)	
	TA	DIC	TA	DIC	TA	DIC
JR304	1.4	0.9	0.51	0.67	-	-
JR15002	2.4	1.7	1.18	0.76	3.9	0.9
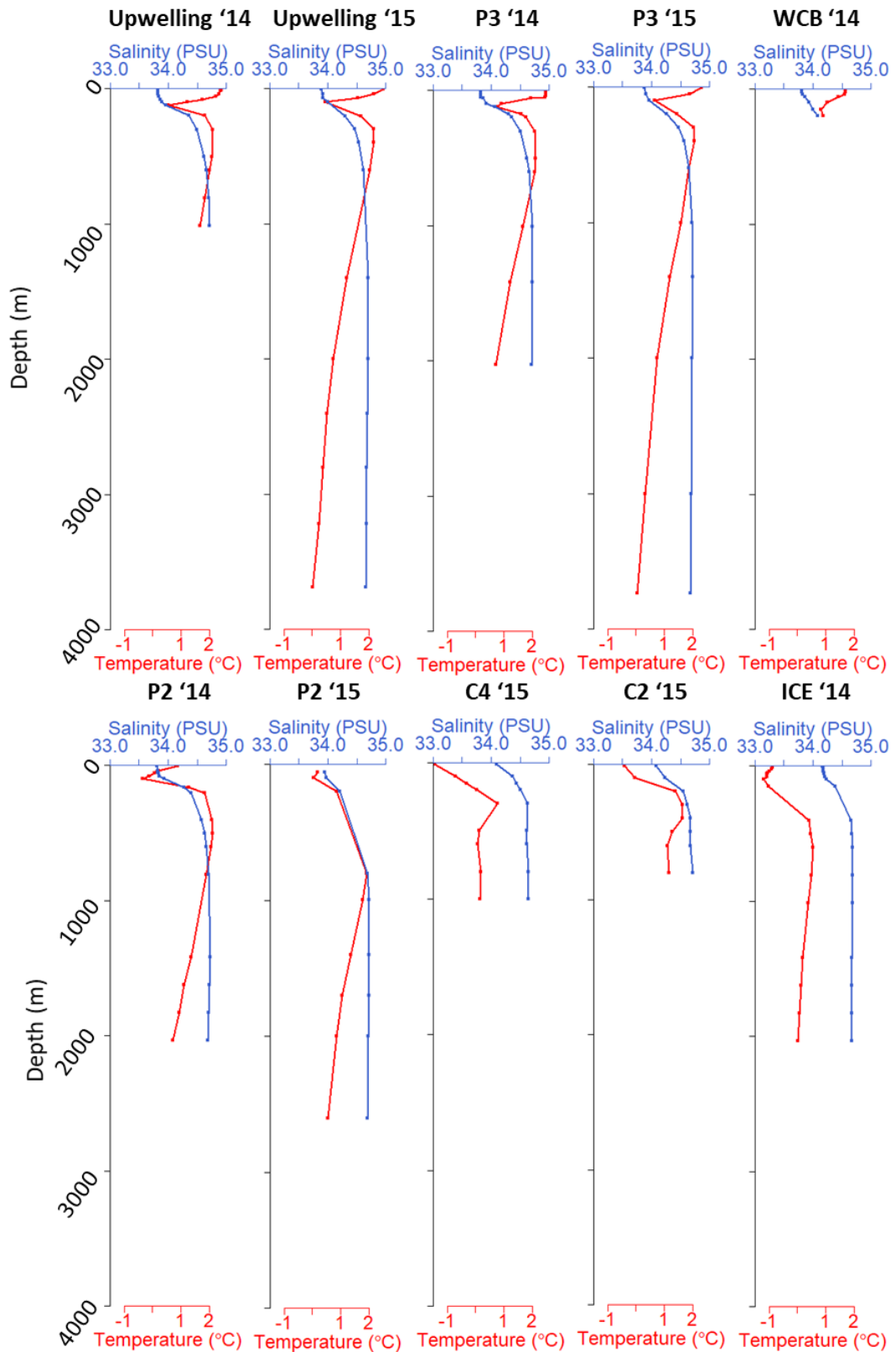
Figure A5.2. Individual temperature and salinity profiles of each station and year measured during two summer research cruises JR304; 2014 and JR15002; 2015) by the R.R.S. *James Clark Ross* (within the Scotia Sea (Southern Ocean)
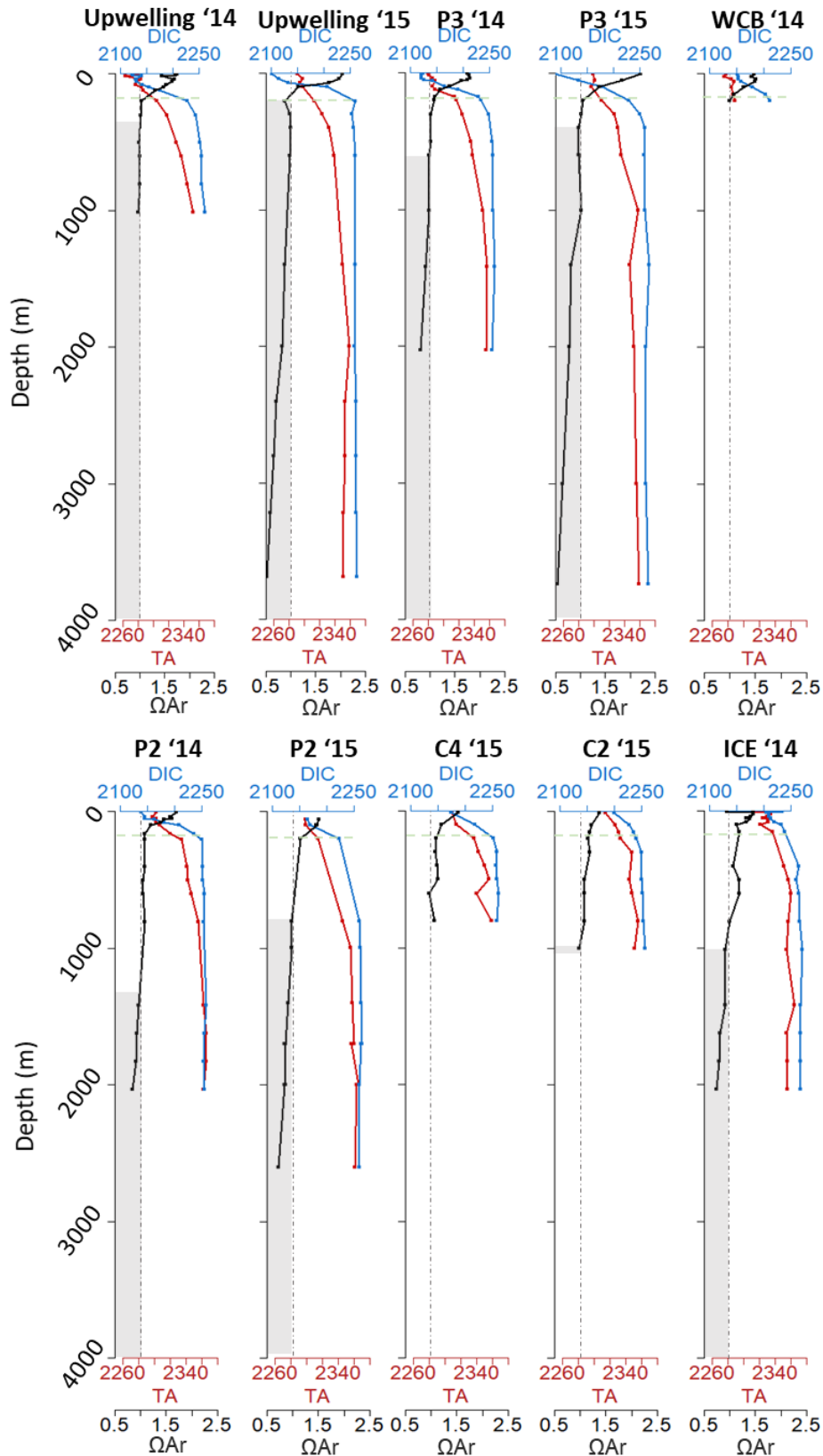
Figure A5.3. Total Alkalinity (TA), Dissolved Inorganic Carbon (DIC) and aragonite saturation state (Ω_{ar}) measured during two summer research cruises JR304; 2014 and JR15002; 2015) by the R.R.S. *James Clark Ross* (within the Scotia Sea (Southern Ocean). The dashed line is where $\Omega_{ar} = 1$ while the grey is the depth of the lysocline.

8 References

Accornero, A., Manno, C., Esposito, F.G.M.C. and Gambi, M.C., 2003. The vertical flux of particulate matter in the polynya of Terra Nova Bay. Part II. Biological components. Antarctic Science, 15(2), pp.175-188.

Adhikari, D., Webster, D.R. and Yen, J., 2016. Portable tomographic PIV measurements of swimming shelled Antarctic pteropods. Experiments in Fluids, 57(12), pp.180-189.

Agresti, A. and Coull, B.A., 1998. Approximate is better than 'exact' for interval estimation of binomial proportions. The American Statistician, 52(2), pp.119-126.

Akiha, F., Hashida, G., Makabe, R., Hattorid, H. and Sasaki, H., 2017. Distribution in the abundance and biomass of shelled pteropods in surface waters of the Indian sector of the Antarctic Ocean in mid-summer. Polar Science. 12, pp. 12-18.

Almogi-Labin, A., Hemleben, C. and Deuser, W.G., 1988. Seasonal variation in the flux of euthecosomatous pteropods collected in a deep sediment trap in the Sargasso Sea. Deep Sea Research Part A. Oceanographic Research Papers, 35(3), pp.441-464.

Anderson, L.G., Tanhua, T., Björk, G., Hjalmarsson, S., Jones, E.P., Jutterström, S., Rudels, B., Swift, J.H. and Wåhlstöm, I., 2010. Arctic ocean shelf–basin interaction: An active continental shelf CO_2 pump and its impact on the degree of calcium carbonate solubility. Deep Sea Research Part I: Oceanographic Research Papers, 57(7), pp.869-879.

Anonymous., 1929. Station list 1929-1931, The Discovery reports, vol. 4. Cambridge university press. London.

Anthony, K.R., Kline, D.I., Diaz-Pulido, G., Dove, S. and Hoegh-Guldberg, O., 2008. Ocean acidification causes bleaching and productivity loss in coral reef builders. Proceedings of the National Academy of Sciences. 105(45), pp.17442-17446

Arkhipkin, A., Brickle, P. and Laptikhovsky, V., 2013. Links between marine fauna and oceanic fronts on the Patagonian Shelf and Slope. Arquipélago. Life and Marine Science, 30, pp.19-37.

Atkinson, A., Shreeve, R.S., Pakhomov, E.A., Priddle, J., Blight, S.P. and Ward, P., 1996. Zooplankton response to a phytoplankton bloom near South Georgia, Antarctica. Marine Ecology Progress Series, 144, pp.195-210.

Atkinson, A., Ward, P., Hunt, B.P.V., Pakhomov, E.A. and Hosie, G.W., 2012. An overview of Southern Ocean zooplankton data: abundance, biomass, feeding and functional relationships. CCAMLR Science, 19, pp.171-218.

Auzoux-Bordenave, S., Badou, A., Gaume, B., Berland, S., Helléouet, M., Milet, C. and Huchette, S., 2010. Ultrastructure, chemistry and mineralogy of the growing

shell of the European abalone Haliotis tuberculata. Journal of Structural Biology, 171, pp.277–290.

Auzoux-Bordenave, S., Brahmi, C., Badou, A., De Rafélis, M. and Huchette, S., 2015. Shell growth, microstructure and composition over the development cycle of the European abalone Haliotis tuberculata. Marine biology, 162(3), pp.687-697.

Almogi-Labin, A., Schmiedel, G., Hemleben, C., Siman-Tov, R., Segl, M. and Meischner, D. 2000. The influence of the NE winter monsoon on productivity changes in the Gulf of Aden, NW Arabian Sea, during the last 530 kyr as recorded by foraminifera, *Marine Micropaleontology*, 40, 295–319.

Bakker, D.C.E., Pfeil, B., Landa, C., Metzl, N., O'Brien, K., Olsen, A., Smith, K., Cosca, C., Harasawa, S., Jones, S., Nakaoka, S., Nojiri, Y., Schuster, U., Steinhoff, T., Sweeney, C., Takahashi, T., Tilbrook, B., Wada, C., Wanninkhof, R., Alin, S., Balestrini, C., Barbero, L., Bates, N., Bianchi, A., Bonou, F., Boutin, J., Bozec, Y., Burger, E., Cai, W., Castle, R., Chen, L., Chierici, M., Currie, K., Evans, W., Featherstone, C., Feely, R., Fransson, A., Goyet, C., Greenwood, N., Gregor, L., Hankin, S., Hardman-Mountford, N., Harlay, J., Hauck, J., Hoppema, M., Humphreys, M., Hunt, C., Huss, B., Ibánhez, J., Johannessen, T., Keeling, R., Kitidis, V., Körtzinger, A., Kozyr, A., Krasakopoulou, E., Kuwata, A., Landschützer, P., Lauvset, S., Lefèvre, N., Lo Monaco, C., Manke, A., Mathis, J., Merlivat, L., Millero, F., Monteiro, P., Munro, D., Murata, A., Newberger, T., Omar, A., Ono, T., Paterson, K., Pearce, D., Pierrot, D., Robbins, L., Saito, S., Salisbury, J., Schlitzer, R., Schneider, B., Schweitzer, R., Sieger, R., Skjelvan, I., Sullivan, K., Sutherland, S., Sutton, A., Tadokoro, K., Telszewski, M., Tuma, M., van Heuven, S., Vandemark, D., Ward, B., Watson, A. and Xu, S., 2016. A multi-decade record of high-quality fCO_2 data in version 3 of the Surface Ocean CO_2 Atlas (SOCAT). Earth System Science Data, 8(2), pp.383-413.

Bandel, K. and Hemleben, C., 1995. Observations on the ontogeny of thecosomatous pteropods (holoplanktic Gastropoda) in the southern Red Sea and from Bermuda. Marine Biology, 124(2), pp.225-243.

Baragi, L.V. and Anil, A.C., 2015. Interactive effect of elevated pCO_2 and temperature on the larval development of an inter-tidal organism, *Balanus amphitrite* Darwin (Cirripedia: Thoracica). Journal of experimental marine biology and ecology, 471, pp.48-57.

Barton, K. 2016. MuMIn: Multi-Model Inference. R package version 1.15.6. https://CRAN.R-project.org/package=MuMIn [last accessed 03/05/16].

Bates, N.R., Orchowska, M.I., Garley, R. and Mathis, J.T., 2013. Summertime calcium carbonate undersaturation in shelf waters of the western Arctic Ocean how biological processes exacerbate the impact of ocean acidification. Biogeosciences, 10(8), pp.5281-5309.

Bathmann, U.V., Noji, T.T. and von Bodungen, B., 1991. Sedimentation of pteropods in the Norwegian Sea in autumn. Deep Sea Research Part A. Oceanographic Research Papers, 38(10), pp.1341-1360.

Bausch, A.R., Gallego, M.A., Harianto, J., Thibodeau, P., Bednaršek, N., Havenhand, J.N. and Klinger, T., 2018. Influence of bacteria on shell dissolution in dead gastropod larvae and adult *Limacina helicina* pteropods under ocean acidification conditions. Marine Biology, 165(2), pp.40-52.

Beare, D., McQuatters-Gollop, A., van der Hammen, T., Machiels, M., Teoh, S.J. and Hall-Spencer, J.M., 2013. Long-term trends in calcifying plankton and pH in the North Sea. PLoS One, 8(5), e61175.

Beaugrand, G., McQuatters-Gollop, A., Edwards, M. and Goberville, E., 2013. Long-term responses of North Atlantic calcifying plankton to climate change. Nature Climate Change, 3(3), pp.263-267.

Beaugrand, G., Reid, P. C., Ibanez, F., Lindley, J. A. and Edwards, M., 2002. Reorganization of North Atlantic marine copepod biodiversity and climate. Science, 296, pp.1692-1694.

Beckmann, W., Auras, A. and Hemleben, C., 1987. Cyclonic cold-core eddy in the eastern North Atlantic. III. Zooplankton. Marine Ecology Progress Series, 39, pp.165-173.

Bednaršek, N. and Ohman, M.D., 2015. Changes in pteropod distributions and shell dissolution across a frontal system in the California Current System. Marine Ecology Progress Series, 523, pp.93-103.

Bednaršek, N., Feely, R.A., Reum, J.C.P., Peterson, B., Menkel, J., Alin, S.R. and Hales, B., 2014. *Limacina helicina* shell dissolution as an indicator of declining habitat suitability owing to ocean acidification in the California Current Ecosystem. Proceedings of the Royal Society, 281(1785), e20140123.

Bednaršek, N., Harvey, C.J., Kaplan, I.C., Feely, R.A. and Moz, J., 2016. Pteropods on the edge: Cumulative effects of ocean acidification, warming and deoxygenation. Progress in Oceanography, 145, pp.1-24.

Bednaršek, N., Johnson, J. and Feely, R.A., 2016. Comment on Peck *et al*: Vulnerability of pteropod (Limacina helicina) to ocean acidification: shell dissolution occurs despite an intact organic layer. Deep Sea Research Part II: Topical Studies in Oceanography, 127, pp.53–56.

Bednaršek, N., Klinger, T., Harvey, C.J., Weisberg, S., McCabe, R.M., Feely, R.A., Newton, J. and Tolimieri, N., 2017. New ocean, new needs: Application of pteropod shell dissolution as a biological indicator for marine resource management. Ecological Indicators, 76, pp.240-244.

Bednaršek, N., Mozina, J., Vuckovic, M., Vogt, M., O'Brien, C. and Tarling, G.A., 2012c. Global distribution of pteropods representing carbonate functional type biomass. Earth System Science Data Discussions, 5, pp.317-350.

Bednaršek, N., Tarling, G.A., Bakker, D.C.E., Fielding, S. and Feely, R. A., 2014a. Dissolution dominating calcification process in polar pteropods close to the point of aragonite undersaturation. PloS One, 9(10), e109183.

Bednaršek, N., Tarling, G.A., Bakker, D.C.E., Fielding, S., Cohen, A., Kuzirian, A., McCorkle, D., Lézé, B. and Montagna, R., 2012a. Description and quantification of pteropod shell dissolution: A sensitive bioindicator of ocean acidification. Global Change Biology, 18(7), pp.2378-2388.

Bednaršek, N., Tarling, G.A., Bakker, D.C.E., Fielding, S., Jones, E.M., Venables, H.J., Ward, P., Kuzirian, A., Lézé, B., Feely, R.A. and Murphy, E.J., 2012b. Extensive dissolution of live pteropods in the Southern Ocean. Nature Geoscience, 5(12), pp.881-885.

Bednaršek, N., Tarling, G.A., Fielding, S. and Bakker, D.C.E., 2012b. Population dynamics and biogeochemical significance of *Limacina helicina antarctica* in the Scotia Sea (Southern Ocean). Deep Sea Research Part II: Topical Studies in Oceanography, 59, pp.105-116.

Begon, M., Townsend, C.R. and Harper, J.L., 2006. Ecology: from individuals to ecosystems, 4th Edition, Wiley-Blackwell.

Belkin, I.M. and Gordon, A.L., 1996. Southern Ocean fronts from the Greenwich meridian to Tasmania. Journal of Geophysical Research: Oceans, 101(C2), pp.3675-3696.

Bergan, A.J., Lawson, G.L., Maas, A.E. and Wang, Z.A., 2017. The effect of elevated carbon dioxide on the sinking and swimming of the shelled pteropod *Limacina retroversa*. ICES Journal of Marine Science, 74(7), pp.1893-1905.

Bernard K. S. and Froneman. P.W., 2005. Trophodynamics of selected mesozooplankton in the west-Indian sector of the Polar Frontal Zone, Southern Ocean, Polar Biology. 28, pp.594-606.

Bernard, K.S. and Froneman, P.W., 2005. Trophodynamics of selected mesozooplankton in the west-Indian sector of the Polar Frontal Zone, Southern Ocean. Polar Biology, 28(8), pp.594-606.

Bernard, K.S. and Froneman, P.W., 2009. The sub-Antarctic euthecosome pteropod, *Limacina retroversa*: Distribution patterns and trophic role. Deep Sea Research Part I: Oceanographic Research Papers, 56(4), pp.582-598.

Bigelow, H.B., 1926. Plankton of the offshore waters of the Gulf of Maine. US Government Printing Office. pp.40-2.

Bijma, J., Pörtner, H.O., Yesson, C. and Rogers, A.D., 2013. Climate change and the oceans- What does the future hold? Marine pollution bulletin, 74(2), pp.495-505.

Björk, M.M., Fransson, A., Chierici, M. and Torstensson, A., 2014. Ocean acidification state in western Antarctic surface waters: controls and interannual variability. Biogeosciences, 11, pp.57-73.

Björk, M.M., Fransson, A., Torstensson, A. and Chierici, M., 2014. Ocean acidification state in western Antarctic surface waters: controls and interannual variability. Biogeosciences, 11(1), pp.57-73.

Blain, S., Tréguer, P., Belviso, S., Bucciarelli, E., Denis, M., Desabre, S., Fiala, M., Jézéquel, V.M., Le Fèvre, J., Mayzaud, P. and Marty, J.C., 2001. A biogeochemical study of the island mass effect in the context of the iron hypothesis: Kerguelen Islands, Southern Ocean. Deep Sea Research Part I: Oceanographic Research Papers, 48(1), pp.163-187.

Böer, M., Gannefors, C., Kattner, G., Graeve, M., Hop, H. and Falk-Petersen, S., 2005. The Arctic pteropod *Clione limacina*: seasonal lipid dynamics and life-strategy. Marine Biology, 147(3), pp.707-717.

Borrell, B.J., Goldbogen, J.A. and Dudley, R., 2005. Aquatic wing flapping at low Reynolds numbers: swimming kinematics of the Antarctic pteropod*, Clione antarctica*. Journal of Experimental Biology, 208(15), pp.2939-2949.

Borrione, I. and Schlitzer, R., 2013. Distribution and recurrence of phytoplankton blooms around South Georgia, Southern Ocean. Biogeosciences, 10(1), pp.217-231.

Boyd, P.W., Collins, S., Dupont, S., Fabricius, K., Gattuso, J.P., Havenhand, J., Hutchins, D.A., Riebesell, U., Rintoul, M.S., Vichi, M. and Biswas, H., 2018. Experimental strategies to assess the biological ramifications of multiple drivers of global ocean change. Global change biology, 24(6), pp.2239-2261.

Boyd, P.W., Dillingham, P.W., McGraw, C.M., Armstrong, E.A., Cornwall, C.E., Feng, Y. Y., Hurd, C.L., Gault-Ringold, M., Roleda, M.Y., Timmins-Schiffman, E. and Nunn, B.L. 2015. Physiological responses of a Southern Ocean diatom to complex future ocean conditions. Nature Climate Change, 6, pp.207-213.

Boyd, P.W., Watson, A.J., Law, C.S., Abraham, E.R., Trull, T., Murdoch, R., Bakker, D.C., Bowie, A.R., Buesseler, K.O., Chang, H. and Charette, M., 2000. A mesoscale phytoplankton bloom in the polar Southern Ocean stimulated by iron fertilization. Nature, 407(6805), pp.695-702.

Brennand, H.S., Soars, N., Dworjanyn, S.A., Davis, A.R. and Byrne, M., 2010. Impact of ocean warming and ocean acidification on larval development and calcification in the sea urchin *Tripneustes gratilla*. PloS one, 5(6), e11372.

Brennand, H.S., Soars, N., Dworjanyn, S.A., Davis, A.R. and Byrne, M., 2010. Impact of ocean warming and ocean acidification on larval development and calcification in the sea urchin Tripneustes gratilla. PloS one, 5(6), e11372.

Bromwich, D.H., Nicolas, J.P., Monaghan, A.J., Lazzara, M.A., Keller, L.M., Weidner, G.A. and Wilson, A.B., 2013. Central West Antarctica among the most rapidly warming regions on Earth. Nature Geoscience, 6(2), pp.139.

Buesseler, K.O., Antia, A.N., Chen, M., Fowler, S.W., Gardner, W.D., Gustafsson, O., Harada, K., Michaels, A.F., Rutgers van der Loeff, M., Sarin, M. and Steinberg, D.K., 2007. An assessment of the use of sediment traps for estimating upper ocean particle fluxes. Journal of Marine Research, 65(3), pp.345-416.

Burridge, A.K., Hörnlein, C., Janssen, A.W., Hughes, M., Bush, S.L., Marlétaz, F., Gasca, R., Pierrot-Bults, A.C., Michel, E., Todd, J.A. and Young, J.R., 2017. Time-calibrated molecular phylogeny of pteropods. PLoS One, 12(6), e0177325.

Busch, D.S., Maher, M., Thibodeau, P. and McElhany, P., 2014. Shell condition and survival of Puget Sound pteropods are impaired by ocean acidification conditions. PloS one, 9(8), e105884.

Byrne, M. and Przeslawski, R., 2013. Multistressor impacts of warming and acidification of the ocean on marine invertebrates' life histories. Integrative and comparative biology, 53(4), pp.582-596.

Byrne., M. 2011. Impact of ocean warming and ocean acidification on marine invertebrate life history stages: vulnerabilities and potential for persistence in a changing ocean. In: Gibson, R., Atkinson, R., Gordon, J., Smith, I. and Hughes, D., 2011. Oceanography and marine biology. Oceanography and Marine Biology Annual Reviews. 49, pp.1-42.

Cermeño, P., Teixeira, I.G., Branco, M., Figueiras, F.G. and Marañón, E., 2014. Sampling the limits of species richness in marine phytoplankton communities. Journal of Plankton Research, 36(4), pp.1135-1139.

Chang, Y. and Yen, J., 2012. Swimming in the intermediate Reynolds range: kinematics of the pteropod Limacina helicina. Integrative and Comparative Biology, 52(5), pp.597-615

Chen, C. 1968. Pleistocene pteropods in pelagic sediments. Nature, 219, 1145-1149.

Chen, C. and Bé, A.W., 1964. Seasonal distributions of euthecosomatous pteropods in the surface waters of five stations in the Western North Atlantic. Bulletin of Marine Science, 14(2), pp.185-220.

Chiarini, F., Capotondi, L., Dunbar, R.B., Giglio, F., Mammì, I., Mucciarone, D.A., Ravaioli, M., Tesi, T. and Langone, L., 2013. A revised sediment trap splitting procedure for samples collected in the Antarctic sea. Methods in Oceanography, 8, pp.13-22.

Chiu, Y., Chen, H., Lee., S. and Chen, C., 2002. Morphometric analysis of shell and operculum variations in the viviparid snail, *Cipangopaludina chinensis* (Mollusca: Gastropoda) in Taiwan. Zoological Studies, 41(3), pp.321-331.

Clark, D., Lamare, M. and Barker, M., 2009. Response of sea urchin *pluteus* larvae (Echinodermata: Echinoidea) to reduced seawater pH: a comparison among a tropical, temperate, and a polar species. Marine biology, 156(6), pp.1125-1137.

Clark, M.S., Sommer, U., Sihra, J.K., Thorne, M.A., Morley, S.A., King, M., Viant, M.R. and Peck, L.S., 2017. Biodiversity in marine invertebrate responses to acute warming revealed by a comparative multi-omics approach. Global change biology, 23(1), pp.318-330.

Collier, R., Dymond, J., Honjo, S., Manganini, S., Francois, R. and Dunbar, R., 2000. The vertical flux of biogenic and lithogenic material in the Ross Sea: moored sediment trap observations 1996–1998. Deep Sea Research Part II: Topical Studies in Oceanography, 47(15), pp.3491-3520.

Collins M, Knutti R, Arblaster J, Dufresne JL, Fichefet T, Friedlingstein P, Gao X, Gutowski WJ, Johns T, Krinner G, Shongwe M, Tebaldi C, Weaver AJ, Wehner M, 2013. The Physical Science Basis. Contribution of Working Group I to the Fifth Assessment Report of the Intergovernmental Panel on Climate Change Stocker TF, Qin D, Plattner GK, Tignor M, Allen SK, Boschung J, Nauels A, Xia Y, Bex V, Midgley PM (eds.). Cambridge University Press, Cambridge, United Kingdom and New York, USA.

Comeau, S., Alliouane, S., Gattuso, J., June, P., Pen, O., Alliouane, S. and Gattuso, J., 2012. of ocean acidification on overwintering juvenile Arctic pteropods *Limacina helicina*. Marine Ecology Progress Series, 456, pp.279-284.

Comeau, S., Gorsky, G., Alliouane, S. and Gattuso, J.P., 2010b. Larvae of the pteropod *Cavolinia inflexa* exposed to aragonite undersaturation are viable but shell-less. Marine Biology, 157(10), pp.2341-2345.

Comeau, S., Gorsky, G., Jeffree, R., Teyssie, J.L. and Gattuso, J.P., 2009. Impact of ocean acidification on a key Arctic pelagic mollusc (*Limacina helicina*). Biogeosciences, 6(9), pp.1877-1882.

Comeau, S., Jeffree, R., Teyssié, J.L. and Gattuso, J.P., 2010a. Response of the Arctic pteropod *Limacina helicina* to projected future environmental conditions. PloS One, 5(6): e11362.

Conover, R.J. and Lalli, C.M., 1974. Feeding and growth in Clione limacina (Phipps), a pteropod mollusc. II. Assimilation, metabolism, and growth efficiency. Journal of Experimental Marine Biology and Ecology, 16(2), pp.131-154.

Constable, A.J., Melbourne-Thomas, J., Corney, S.P., Arrigo, K.R., Barbraud, C., Barnes, D.K., Bindoff, N.L., Boyd, P.W., Brandt, A., Costa, D.P. and Davidson, A.T., 2014. Climate change and Southern Ocean ecosystems I: how changes in physical

habitats directly affect marine biota. Global Change Biology, 20(10), pp.3004-3025.

Crelier, A.M., Dadon, J.R., Isbert-Perlender, H.G., Nahabedian, D.E. and Daponte, M.C., 2010. Distribution patterns of chaetognata, polychaeta, pteropoda and salpidae off south georgia and south orkney islands. Brazilian Journal of Oceanography, 58(4), pp.287-298.

Cripps, G., Lindeque, P. and Flynn, K.J., 2014. Have we been underestimating the effects of ocean acidification in zooplankton? Global Change Biology, 20(11), pp.3377-3385.

Currie, R.I. and Foxton, P., 1956. The Nansen closing method with vertical plankton nets. Journal of the Marine Biological Association of the United Kingdom, 35(3), pp.483-492.

Dadon, J.R. and de Cidre, L.L., 1992. The reproductive cycle of the Thecosomatous pteropod Limacina retroversa in the western South Atlantic. Marine Biology, 114(3), pp.439-442.

Dadon, J.R., 1990. Annual cycle of *Limacina retroversa* in Patagonian waters. American Malacological Bulletin, 8(1), pp.77-84.

Davenport, J. and Bebbington, A., 1990. Observations on the swimming and buoyancy of some thecosomatous pteropod gastropods. Journal of Molluscan Studies, 56(4), pp.487-497.

Deacon, G.E.R., 1982. Physical and biological zonation in the Southern Ocean. Deep Sea Research Part A. Oceanographic Research Papers, 29(1), pp.1-15.

Deppeler, S.L. and Davidson, A.T., 2017. Southern Ocean phytoplankton in a changing climate. Frontiers in Marine Science, 4, pp.40-47.

Dickson A.G., 1990. Standard potential of the reaction: AgCl(s) + 1/2 H2(g) = Ag(s) + HCl(aq), and the standard acidity constant of the ion HSO4- in synthetic sea water from 273.15 to 318.15 K. K. Journal of Chemical Thermodynamics, 22, pp.113-127.

Dickson, A.G. and Millero, F.J., 1987. Comparison of the equilibrium constants for the dissociation of carbonic acid in seawater media. Deep Sea Research Part I: Oceanographic Research Papers, 34 (111), pp.1733-1743.

Dillon, R.T. 2000. The ecology of freshwater molluscs. Cambridge University Press, Cambridge.

Doney, S., Ruckelshaus, M., Emmett Duffy, J., Barry, J., Chan, F., English, C., Galindo, H., Grebmeier, J., Hollowed, A., Knowlton, N., Polovina, J., Rabalais, N., Sydeman, W. and Talley, L., 2012. Climate Change Impacts on Marine Ecosystems. Annual Review of Marine Science, 4(1), pp.11-37.

Doney, S.C., Fabry, V.J., Feely, R.A. and Kleypas, J.A., 2009. Ocean Acidification: The Other CO2 problem. Annual Review of Marine Science, 1(1), pp.169-192.

Dray, S. and Dufour, A.B. 2007. The ade4 package: implementing the duality diagram for ecologists. Journal of Statistical Software. 22(4), pp.1-20.

Drits A. V., E. G. Arashkevich, A. B. Nikishina, V. M. Sergeeva, K. A. Solovyev, and M. V. Flint., 2015. Mesozooplankton grazing impact on phytoplankton in the northern regions of the Kara Sea in autumn, Oceanology, 55, pp.595–605.

Dupont, S. and Thorndyke, M.C., 2009. Impact of CO_2 driven ocean acidification on invertebrate's early life-history; what we know, what we need to know and what we can do. Biogeosciences, 6, pp.3109–3131.

Duquette, A., McClintock, J.B., Amsler, C.D., Pérez-Huerta, A., Milazzo, M. and Hall-Spencer, J.M., 2017. Effects of ocean acidification on the shells of four Mediterranean gastropod species near a CO_2 seep. Marine Pollution Bulletin. 124(2), 917-928.

Dymowska, A.K., Manfredi, T., Rosenthal, J.J. and Seibel, B.A., 2012. Temperature compensation of aerobic capacity and performance in the Antarctic pteropod, *Clione antarctica*, compared with its northern congener, *C. limacina*. Journal of Experimental Biology, 215(19), pp.3370-3378.

Fabry, V.J. and Deuser, W.G., 1992. Seasonal changes in the isotopic compositions and sinking fluxes of euthecosomatous pteropod shells in the Sargasso Sea. Paleoceanography, 7(2), pp.195-213.

Fabry, V.J., McClintock, J.B., Mathis, J.T. and Grebmeier, J.M., 2009. Ocean acidification at high-latitudes: the bellwether. Oceanography, 22(4), pp.160-171.

Fabry, V.J., Seibel, B.A., Feely, R.A. and Orr, J.C., 2008. Impacts of ocean acidification on marine fauna and ecosystem processes. ICES Journal of Marine Science, 65(3), pp.414-432.

Falk-Petersen, S., Sargent, J.R., Kwasniewski, S., Gulliksen, B. and Millar, R.M., 2001. Lipids and fatty acids in Clione limacina and Limacina helicina in Svalbard waters and the Arctic Ocean: trophic implications. Polar Biology, 24(3), pp.163-170.

Feely, R.A., Doney, S.C. and Cooley, S.R., 2009. Ocean acidification: Present conditions and future changes in a high-CO_2 world. Oceanography, 22(4), pp.36-47.

Flores, H., Hunt, B.P., Kruse, S., Pakhomov, E.A., Siegel, V., van Franeker, J.A., Strass, V., Van de Putte, A.P., Meesters, E.H. and Bathmann, U., 2014. Seasonal changes in the vertical distribution and community structure of Antarctic macrozooplankton and micronekton. Deep Sea Research Part I: Oceanographic Research Papers, 84, pp.127-141.

Flores, H., van Franeker, J.A., Cisewski, B., Leach, H., Van de Putte, A.P., Meesters, E.H., Bathmann, U. and Wolff, W.J., 2011. Macrofauna under sea ice and in the open surface layer of the Lazarev Sea, Southern Ocean. Deep Sea Research Part II: Topical Studies in Oceanography, 58(19-20), pp.1948-1961.

Foo, A.F. and Byrne, M., 2017. Marine gametes in a changing ocean: Impacts of climate change stressors on fecundity and the egg. Marine environmental research. 128, pp.12-24.

Forbes, A.E. and Chase, J.M., 2002. The role of habitat connectivity and landscape geometry in experimental zooplankton metacommunities. Oikos, 96(3), pp.433-440.

Francis-Pan, T.C.F., Applebaum, S.L. and Manahan, D.T., 2015. Experimental ocean acidification alters the allocation of metabolic energy. Proceedings of the National Academy of Sciences, pp.201416967.

Fransson, A., Chierici, M., Hop, H., Findlay, H.S., Kristiansen, S. and Wold, A., 2016. Late winter-to-summer change in ocean acidification state in Kongsfjorden, with implications for calcifying organisms. Polar Biology, 39(10), pp.1841-1857.

Friedrich, T., Timmermann, A., Abe-Ouchi, A., Bates, N.R., Chikamoto, M.O., Church, M.J., Dore, J.E., Gledhill, D.K., Gonzalez-Davila, M., Heinemann, M. and Ilyina, T., 2012. Detecting regional anthropogenic trends in ocean acidification against natural variability. Nature Climate Change, 2(3), pp.167-171.

Fyfe, J.C., 2006. Southern Ocean warming due to human influence. Geophysical Research Letters, 33(19), e19701.

Gangstø, R., Gehlen, M., Schneider, B., Bopp, L., Aumont, O. and Joos, F., 2008. Modeling the marine aragonite cycle: changes under rising carbon dioxide and its role in shallow water $CaCO_3$ dissolution. Biogeosciences, 5(4), pp.1057-1072.

Gannefors, C., Böer, M., Kattner, G., Graeve, M., Eiane, K., Gulliksen, B., Hop, H. and Falk-Petersen, S., 2005. The Arctic sea butterfly *Limacina helicina*: lipids and life strategy. Marine Biology, 147(1), pp.169-177.

Gardner, J., Manno, C., Bakker, D.C., Peck, V.L. and Tarling, G.A., 2018. Southern Ocean pteropods at risk from ocean warming and acidification. Marine biology, 165(1), pp.8-18.

Gardner, L.D., Mills, D., Wiegand, A., Leavesley, D. and Elizur, A., 2011. Spatial analysis of biomineralization associated gene expression from the mantle organ of the pearl oyster *Pinctada maxima*. BMC genomics, 12(1), pp.455.

Gardner, W.D., 2000. Sediment trap sampling in surface waters. Cambridge University Press, Cambridge. pp. 240-284.

Gardner, W.D., Biscaye, P.E. and Richardson, M.J., 1997. A sediment trap experiment in the Vema Channel to evaluate the effect of horizontal particle

fluxes on measured vertical fluxes. Journal of Marine Research, 55(5), pp.995-1028.

Gattuso, J.P. and Lavigne, H., 2009. Approaches and software tools to investigate the impact of ocean acidification. Biogeosciences, 6(10), pp.2121-2133.

Gattuso, J.P., Gao, K., Lee, K., Rost, B. and Schulz, K.G., Approaches and tools to manipulate the carbonate chemistry., 2011. In: Riebesell, U., Fabry, V.J. and Hansson, L. (2011) Guide to best practices for ocean acidification research and data reporting. Publications Office of the European Union, Luxembourg, pp.243–258.

Gattuso, J.P., Magnan, A., Billé, R., Cheung, W.W., Howes, E.L., Joos, F., Allemand, D., Bopp, L., Cooley, S.R., Eakin, C.M. and Hoegh-Guldberg, O., 2015. Contrasting futures for ocean and society from different anthropogenic CO_2 emissions scenarios. Science, 349(6243), pp.4722.

Gaylord, B., Kroeker, K.J., Sunday, J.M., Anderson, K.M., Barry, J.P., Brown, N.E., Connell, S.D., Dupont, S., Fabricius, K.E., Hall-Spencer, J.M. and Klinger, T., 2015. Ocean acidification through the lens of ecological theory. Ecology, 96(1), pp.3-15.

Gazeau, F., Parker, L.M., Comeau, S., Gattuso, J.P., O'Connor, W.A., Martin, S., Pörtner, H.O. and Ross, P.M., 2013. Impacts of ocean acidification on marine shelled molluscs. Marine Biology, 160(8), pp.2207-2245.

Gelman, A. and Su, Y., 2016. Arm: Data analysis using regression and multilevel/hierarchical models; R package version 1.8-6. Cambridge University Press.

Gelman, A., Jakulin, A., Pittau, M.G. and Su, Y.S. 2008. A weakly informative default prior distribution for logistic and other regression models. The Annals of Applied Statistics, 2(4), pp.1360-1383.

Gerhardt, S., Groth, H., Rühlemann, C. and Henrich, R., 2000. Aragonite preservation in late Quaternary sediment cores on the Brazilian Continental Slope: implications for intermediate water circulation. International Journal of Earth Sciences, 88(4), pp.607-618.

Ghiselin, M.T. 1969. The evolution of hermaphroditism among animals. Quarterly Review of Biology, 44, pp.189–208.

Gille, S.T. 2002. Warming of the Southern Ocean since the 1950s. Science, 295 (5558), pp.1275–1277.

Gille, S.T., 1994. Mean sea surface height of the Antarctic Circumpolar Current from Geosat data: Method and application. Journal of Geophysical Research: Oceans, 99(C9), pp.18255-18273.

Gilmer R.W. and Harbison G.R. 1986. Morphology and field behaviour of pteropod molluscs: feeding methods in the families Cavoliniidae, Limacinidae and Peraclididae (Gastropoda: Thecosomata). Marine Biology, 91(1), pp.47–57.

Gilmer, R.W. and Harbison, G.R., 1991. Diet of *Limacina helicina* (Gastropoda: Thecosomata) in Arctic waters in midsummer. Marine Ecology Progress Series, 77(2-3), pp.125-134.

Gilmer, R.W. and Lalli, C.M., 1990. Bipolar variation in Clione, a gymnosomatous pteropod. American Malacological Bulletin, 8(1), pp.67-75.

Gilmer, R.W., 1974. Some aspects of feeding in thecosomatous pteropod molluscs. Journal of Experimental Marine Biology and Ecology, 15(2), pp.127-144.

Gliwicz, Z., 1986. A lunar cycle in zooplankton. Ecology. 67(4), pp.883-897.

GLODAP (Global Ocean Data Analysis Project). National Centre for Atmospheric Research Staff. Last modified 31 Jan 2014. "The Climate Data Guide: GLODAP: GLobal Ocean Data Analysis Project for Carbon." Retrieved from https://climatedataguide.ucar.edu/climate-data/glodap-global-ocean-data-analysis-project-carbon [last accessed 18/08/2018].

GOFS., 1989, U.S. GOFS Working Group on Sediment Trap Technology and Sampling Report 10. Sediment Trap Technology and Sampling, pp.18.

Gordon, A. L., Georgi, D. T., and Taylor, H. W., 1977. Antarctic Polar Frontal Zone in the western Scotia Sea- summer 1975. Journal Physical Oceanography, 7, pp.309-328.

Gosselin, L.A. and Qian, P.Y., 1997. Juvenile mortality in benthic marine invertebrates. Marine Ecology Progress Series, 146, pp.265-282.

Green, M.A., Waldbusser, G.G., Reilly, S.L., Emerson, K. and O'Donnell, S., 2009. Death by dissolution: sediment saturation state as a mortality factor for juvenile bivalves. Limnology and Oceanography, 54(4), pp.1037-1047.

Gregory, S., Collins, M.A. and Belchier, M., 2017. Demersal fish communities of the shelf and slope of South Georgia and Shag Rocks (Southern Ocean). Polar Biology, 40(1), pp.107-121.

Grice, G.D. and Hülsemann, K., 1968. Contamination in Nansen-type vertical plankton nets and a method to prevent it. Deep Sea Research and Oceanographic Abstracts. 15(2), pp.229-233.

Guo, X., Huang, M., Pu, F., You, W. and Ke, C., 2015. Effects of ocean acidification caused by rising CO_2 on the early development of three mollusks. Aquatic Biology, 23(2), pp.147-157.

Gutt, J., Bertler, N., Bracegirdle, T.J., Buschmann, A., Comiso, J., Hosie, G., Isla, E., Schloss, I.R., Smith, C.R., Tournadre, J. and Xavier, J.C. 2015. The Southern Ocean ecosystem under multiple climate change stresses-an integrated circumpolar assessment. Global change biology, 21(4), pp.1434-1453.

Halpern, B.S., Longo, C., Hardy, D., McLeod, K.L., Samhouri, J.F., Katona, S.K., Kleisner, K., Lester, S.E., O'Leary, J., Ranelletti, M. and Rosenberg, A.A., 2012. An

index to assess the health and benefits of the global ocean. Nature, 488(7413), pp.615.

Harbison, G.R. and Gilmer, R.W., 1986. Effects of animal behavior on sediment trap collections: implications for the calculation of aragonite fluxes. Deep Sea Research Part A. Oceanographic Research Papers, 33(8), pp.1017-1024.

Harper, E.M., 1997. The molluscan periostracum: an important constraint in bivalve evolution. Palaeontology, 40(1), pp.71-98.

Harwell, M.A., Myers, V., Young, T., Bartuska, A., Gassman, N., Gentile, J.H., Harwell, C.C., Appelbaum, S., Barko, J., Causey, B. and Johnson, C., 1999. A framework for an ecosystem integrity report card: examples from south Florida show how an ecosystem report card links societal values and scientific information. BioScience, 49(7), pp.543-556.

Hauri, C., Doney, S.C., Takahashi, T., Erickson, M., Jiang, G. and Ducklow, H.W., 2015. Two decades of inorganic carbon dynamics along the Western Antarctic Peninsula. Biogeosciences Discuss, 12, pp.6929-6969.

Hauri, C., Friedrich, T. and Timmermann, A., 2016. Abrupt onset and prolongation of aragonite undersaturation events in the Southern Ocean. Nature Climate Change. 6, pp.172-176.

Hays G. C. 2003. A review of the adaptive significance and ecosystem consequences of zooplankton diel vertical migration. Hydrobiologia. 503(1-3), pp.163-170.

Head, E.J. and Pepin, P., 2010. Spatial and inter-decadal variability in plankton abundance and composition in the Northwest Atlantic (1958–2006). Journal of Plankton Research, 32(12), pp.1633-1648.

Heinze, C., Meyer, S., Goris, N., Anderson, L., Steinfeldt, R., Chang, N., Le Quéré, C. and Bakker, D.C.E. 2015. The ocean carbon sink: Impacts, vulnerabilities and challenges. Earth System Dynamics, 6(1), pp.327-358.

Henson, S.A., Beaulieu, C., Ilyina, T., John, J.G., Long, M., Séférian, R., Tjiputra, J. and Sarmiento, J.L., 2017. Rapid emergence of climate change in environmental drivers of marine ecosystems. Nature communications, 8, pp.14682.

Highfield, J.M., Eloire, D., Conway, D.V., Lindeque, P.K., Attrill, M.J. and Somerfield, P.J., 2010. Seasonal dynamics of meroplankton assemblages at station L4. Journal of plankton research, 32(5), pp.681-691.

Hinder, S., Gravenor, M., Edwards, M., Ostle, C., Bodger, O., Lee, P., Walne, A. and Hays, G., 2013. Multi-decadal range changes vs. thermal adaptation for north east Atlantic oceanic copepods in the face of climate change. Global Change Biology, 20(1), pp.140-146.

Hodgson, E.E., Essington, T.E. and Kaplan, I.C., 2016. Extending vulnerability assessment to include life stages considerations. PloS one, 11(7), pp.e0158917.

Hoegh-Guldberg, O. and Bruno, J.F., 2010. The impact of climate change on the world's marine ecosystems. Science, 328(5985), pp.1523-1528.

Hogg, O.T., Barnes, D.K. and Griffiths, H.J., 2011. Highly diverse, poorly studied and uniquely threatened by climate change: an assessment of marine biodiversity on South Georgia's continental shelf. PLoS One, 6(5), e19795.

Hop, H., Pearson, T., Hegseth, E.N., Kovacs, K.M., Wiencke4, C., Kwasniewski, S., Eiane, K., Mehlum, F., Gulliksen, B., Wlodarska-Kowalczuk, M. and Lydersen, C., 2002. The marine ecosystem of Kongsfjorden, Svalbard. Polar Research, 21(1), pp.167-208.

Hopes, A. and Mock, T., 2001. Evolution of Microalgae and Their Adaptations in Different Marine Ecosystems. eLS, pp.1-9.

Hoshijima, U., Wong, J.M. and Hofmann, G.E., 2017. Additive effects of pCO_2 and temperature on respiration rates of the Antarctic pteropod *Limacina helicina antarctica*. Conservation physiology, 5(1), pp.cox064.

Hoshijima, U., Wong, J.M. and Hofmann, G.E., 2017. Additive effects of pCO_2 and temperature on respiration rates of the Antarctic pteropod *Limacina helicina antarctica*. Conservation physiology, 5(1), pp.64-72.

Howard, W.R., Roberts, D., Moy, A.D., Lindsay, M.C.M., Hopcroft, R.R., Trull, T.W. and Bray, S.G., 2011. Distribution, abundance and seasonal flux of pteropods in the Sub-Antarctic Zone. Deep Sea Research Part II: Topical Studies in Oceanography, 58(21-22), pp.2293-2300.

Howes, E.L., Bednaršek, N., Büdenbender, J., Comeau, S., Doubleday, A., Gallager, S.M., Hopcroft, R.R., Lischka, S., Maas, A.E., Bijma, J. and Gattuso, J.P., 2014. Sink and swim: a status review of thecosome pteropod culture techniques. Journal of Plankton Research, 36(2), pp.299-315.

Howes, E.L., Stemmann, L., Assailly, C., Irisson, J.O., Dima, M., Bijma, J. and Gattuso, J.P., 2015. Pteropod time series from the North Western Mediterranean (1967-2003): impacts of pH and climate variability. Marine Ecology Progress Series, 531, pp.193-206.

Hsiao, S.C., 1939. The reproductive system and spermatogenesis of *Limacina* (Spiratella) *retroversa* (Flem.). The Biological Bulletin, 76(1), pp.7-25.

Huang, J., Zhang, X., Zhang, Q., Lin, Y., Hao, M., Luo, Y., Zhao, Z., Yao, Y., Chen, X., Wang, L. and Nie, S., 2017. Recently amplified arctic warming has contributed to a continual global warming trend. Nature Climate Change, 7(12), pp.875.

Hunt, B., Strugnell, J., Bednaršek, N., Linse, K., Nelson, R.J., Pakhomov, E., Seibel, B., Steinke, D. and Würzberg, L., 2010. Poles apart: the "bipolar" pteropod species *Limacina helicina* is genetically distinct between the Arctic and Antarctic oceans. PLoS One, 5 (3), e9835.

Hunt, B.P. and Pakhomov, E.A., 2003. Mesozooplankton interactions with the shelf around the sub-Antarctic Prince Edward Islands archipelago. Journal of Plankton Research, 25(8), pp.885-904.

Hunt, B.P.V., Pakhomov, E.A., Hosie, G.W., Siegel, V., Ward, P. and Bernard, K., 2008. Pteropods in Southern Ocean ecosystems. Progress in Oceanography, 78(3), pp.193-221.

Iersel, T.P.V. and van der Spoel, S., 1986. Schizogamy in the planktonic opisthobranch Clio a previously undescribed mode of reproduction in the Mollusca. International journal of invertebrate reproduction and development, 10(1), pp.43-50.

IPCC, 2014. Climate Change 2014. Impacts, Adaptation and Vulnerability: Regional Aspects. Contribution of Working Group II to the Fifth Assessment Report of the Intergovernmental Panel on Climate Change [Field, C.B., V.R. Barros, D.J. Dokken, K.J. Mach, M.D. Mastrandrea, T.E. Bilir, M. Chatterjee, K.L. Ebi, Y.O. Estrada, R.C. Genova, B. Girma, E.S. Kissel, A.N. Levy, S. MacCracken, P.R. Mastrandrea, and L.L. White (eds.)]. Cambridge University Press, Cambridge, United Kingdom and New York, NY, USA, pp.1132

IPCC. Climate Change 2013: The Physical Science Basis. Contribution of Working Group I to the Fifth Assessment Report of the Intergovernmental Panel on Climate Change., 2013. Chapter 13, [Stocker, T.F., Qin, D. Plattner, G.K. Tignor, M. Allen, S.K. Boschung, J. Nauels, A. Xia, Y. Bex V. and Midgley P.M. (eds.)]. Cambridge University Press, pp.1535.

James, A., Pitchford, J.W. and Brindley, J., 2003. The relationship between plankton blooms, the hatching of fish larvae, and recruitment. Ecological Modelling, 160(1-2), pp.77-90.

Jennings, R.M., Bucklin, A., Ossenbrügger, H. and Hopcroft, R.R., 2010. Species diversity of planktonic gastropods (Pteropoda and Heteropoda) from six ocean regions based on DNA barcode analysis. Deep Sea Research Part II: Topical Studies in Oceanography, 57(24), pp.2199-2210.

Johnson, K.M., King, A.E. and Sieburth, J.M., 1985. Coulometric TCO_2 analyses for marine studies; an introduction. Marine Chemistry, 16(1), pp.61-82.

Jokiel, P. L. 2011. Ocean acidification and control of reef coral calcification by boundary layer limitation of proton flux. Bulletin of Marine Science. 87, pp.639-657.

Jones, E.M., Bakker, D.C.E., Venables, H.J. and Hardman-Mountford, N.J. 2015. Seasonal cycle of CO_2 from the sea ice edge to island blooms in the Scotia Sea, Southern Ocean. Marine Chemistry, 177, pp.490-500.

Jones, E.M., Bakker, D.C.E., Venables, H.J., Watson, A.J. and Georgia, S. 2012. Dynamic seasonal cycling of inorganic carbon downstream of South Georgia, Southern Ocean. Deep-Sea Research Part II, 59-60, pp.25-35.

Joos, F. and Spahni, R., 2008. Rates of change in natural and anthropogenic radiative forcing over the past 20,000 years. Proceedings of the National Academy of Sciences, 105(5), pp.1425-1430.

Joyce, T.M., Zenk, W. and Toole, J.M., 1978. The anatomy of the Antarctic Polar Front in the Drake Passage. Journal of Geophysical Research: Oceans, 83(C12), pp.6093-6113.

Kane, J. 2011. Inter-decadal variability of zooplankton abundance in the Middle Atlantic Bight. Journal of Northwest Atlantic Fishery Science., 43. pp.81-92.

Kane, J., 2007. Zooplankton abundance trends on Georges Bank, 1977–2004. ICES journal of marine science, 64(5), pp.909-919.

Kapsenberg, L., Kelley, A.L., Shaw, E.C., Martz, T.R. and Hofmann, G.E., 2015. Near-shore Antarctic pH variability has implications for the design of ocean acidification experiments. Scientific Reports, 5, pp.9638-9645.

Karnovsky, N.J., Hobson, K.A., Iverson, S. and Hunt, G.L., 2008. Seasonal changes in diets of seabirds in the North Water Polynya: a multiple-indicator approach. Marine Ecology Progress Series, 357, pp.291-299.

Kelley, D. and Richards, C., 2017. oce: Analysis of Oceanographic Data. R package version 0.9-22. https://CRAN.R-project.org/package=oce [last accessed 12/03/18].

Kemp, S., Hardy, A.C. and Mackintosh, N.A., 1929, The Discovery investigations, objects, equipment and methods. Discovery Reports, Cambridge university press. 1, pp.141-232.

King, J.C., 1994. Recent climate variability in the vicinity of the Antarctic Peninsula. International Journal of Climatology, 14(4), pp.357-369.

Kirk, S.E., Skepper, J.N. and Donald, A.M., 2009. Application of environmental scanning electron microscopy to determine biological surface structure. Journal of microscopy, 233(2), pp.205-224.

Kobayashi, H.A., 1974. Growth cycle and related vertical distribution of the thecosomatous pteropod Spiratella ("Limacina") helicina in the central Arctic Ocean. Marine Biology, 26(4), pp.295-301.

Kopczyńska, E.E., Fiala, M. and Jeandel, C., 1998. Annual and interannual variability in phytoplankton at a permanent station off Kerguelen Islands, Southern Ocean. Polar Biology, 20(5), pp.342-351.

Korb, R.E. and Whitehouse, M., 2004. Contrasting primary production regimes around South Georgia, Southern Ocean: large blooms versus high nutrient, low chlorophyll waters. Deep Sea Research Part I: Oceanographic Research Papers, 51(5), pp.721-738.

Korb, R.E., Whitehouse, M.J., Thorpe, S.E. and Gordon, M., 2005. Primary production across the Scotia Sea in relation to the physico-chemical environment. Journal of Marine Systems, 57(3), pp.231-249.

Kroeker, K.J., Kordas, R.L., Crim, R., Hendriks, I.E., Ramajo, L., Singh, G.S., Duarte, C.M. and Gattuso, J.P., 2013. Impacts of ocean acidification on marine organisms: Quantifying sensitivities and interaction with warming. Global Change Biology, 19 (6), pp.1884–1896.

Lalli CM, Conover RJ., 1976. Microstructure of the veliger shells of gymnosomatous pteropods (Gastropoda: Opisthobranchia). Veliger, 18, pp.237–240.

Lalli, C.M. and Gilmer, R.W., 1989. Pelagic snails: the biology of holoplanktonic gastropod mollusks. Stanford University Press.

Lalli, C.M. and Wells, F.E., 1978. Reproduction in the genus *Limacina* (Opisthobranchia: Thecosomata). Journal of Zoology, 186, pp.95–108.

Lampert, W. 1993. Ultimate causes of diel vertical migration of zooplankton: new evidence for the predator avoidance hypothesis. *Diel vertical migration of zooplankton,* 1, 79-88.

Landschützer, P., Gruber, N., Bakker, D.C., Stemmler, I. and Six, K.D., 2018. Strengthening seasonal marine CO_2 variations due to increasing atmospheric CO_2. Nature Climate Change, 8, pp.146-150.

Lavaniegos, B.E. and Ohman, M.D., 2007. Coherence of long-term variations of zooplankton in two sectors of the California Current System. Progress in Oceanography, 75(1), pp.42-69.

Lavergne, S., Mouquet, N., Thuiller, W. and Ronce, O., 2010. Biodiversity and climate change: integrating evolutionary and ecological responses of species and communities. Annual review of ecology, evolution, and systematics, 41, pp.321-350.

Lavigne, H. and Gattuso, J.P., 2010. Seacarb: Seawater carbonates chemistry with R package version 3.1.3. http://CRAN.R-project.org/package=seacarb [last accessed 03/05/16].

Le Quéré, C., Moriarty, R., Andrew, R., Peters, G., Ciais, P., Friedlingstein, P., Jones, S., Sitch, S., Tans, P., Arneth, A., Boden, T., Bopp, L., Bozec, Y., Canadell, J., Chini, L., Chevallier, F., Cosca, C., Harris, I., Hoppema, M., Houghton, R., House, J., Jain, A., Johannessen, T., Kato, E., Keeling, R., Kitidis, V., Klein Goldewijk, K., Koven, C., Landa, C., Landschützer, P., Lenton, A., Lima, I., Marland, G., Mathis, J., Metzl, N., Nojiri, Y., Olsen, A., Ono, T., Peng, S., Peters, W., Pfeil, B., Poulter, B., Raupach, M., Regnier, P., Rödenbeck, C., Saito, S., Salisbury, J., Schuster, U., Schwinger, J., Séférian, R., Segschneider, J., Steinhoff, T., Stocker, B., Sutton, A., Takahashi, T., Tilbrook, B., van der Werf,

G., Viovy, N., Wang, Y., Wanninkhof, R., Wiltshire, A. and Zeng, N., 2015. Global carbon budget 2014. Earth System Science Data, 7(1), pp.47-85.

Lebour, M.V., 1932. *Limacina retroversa* in Plymouth waters. Journal of the Marine Biological Association of the United Kingdom, 18(1), pp.123-126.

Lee, R.F., Hagen, W. and Kattner, G., 2006. Lipid storage in marine zooplankton. Marine Ecology Progress Series, 307(1863), pp.273-306.

Legge, O.J., Bakker, D.C., Meredith, M.P., Venables, H.J., Brown, P.J., Jones, E.M. and Johnson, M.T., 2017. The seasonal cycle of carbonate system processes in Ryder Bay, West Antarctic Peninsula. Deep Sea Research Part II: Topical Studies in Oceanography, 139, pp.167-180.

Lenth, R., 2002. lsmeans: Least-Squares Means. R package version 2.20-23. http://CRAN.R-project.org/package=lsmeans [last accessed 03/05/16].

Levasseur, M., Keller, M.D., Bonneau, E., D'amours, D. and Bellows, W.K., 1994. Oceanographic basis of a DMS-related Atlantic cod (*Gadus morhua*) fishery problem: blackberry feed. Canadian Journal of Fisheries and Aquatic Sciences, 51(4), pp.881-889.

Levitus, S., Antonov, J.I., Boyer, T.P. and Stephens, C., 2000. Warming of the world ocean. Science, 287(5461), pp.2225-2229.

Lewis, E. and Wallace, D.W.R. 1998. Program developed for CO_2 system calculations. Technical Report ORNL/CDIAC-105. Carbon Dioxide Information Analysis Center, Oak Ridge National Laboratory, US Department of Energy, Oak Ridge, TN, USA.

Lewis, S.L. and Maslin, M.A., 2015. Defining the anthropocene. Nature, 519(7542), pp.171-180.

Linsley R.M. and Javidpour M., 1980. Episodic growth in Gastropoda. Malacologia. 20(1), pp.153–160.

Lischka, S. and Riebesell, U., 2012. Synergistic effects of ocean acidification and warming on overwintering pteropods in the Arctic. Global Change Biology, 18 (12), pp.3517–3528.

Lischka, S. and Riebesell, U., 2016. Metabolic response of Arctic pteropods to ocean acidification and warming during the polar night/twilight phase in Kongsfjord (Spitsbergen). Polar Biology, 40(6), pp.1211-1227.

Lischka, S., Büdenbender, J., Boxhammer, T. and Riebesell, U., 2011. Impact of ocean acidification and elevated temperatures on early juveniles of the polar shelled pteropod *Limacina helicina*: Mortality, shell degradation, and shell growth. Biogeosciences, 8, pp.919–932.

Litz, M.N., Miller, J.A., Copeman, L.A., Teel, D.J., Weitkamp, L.A., Daly, E.A. and Claiborne, A.M., 2017. Ontogenetic shifts in the diets of juvenile Chinook Salmon:

new insight from stable isotopes and fatty acids. Environmental biology of fishes, 100(4), pp.337-360.

Loeb, V.J. and Santora, J.A., 2013. Pteropods and climate off the Antarctic Peninsula. Progress in oceanography, 116, pp.31-48.

Lutz, V.A., Segura, V., Dogliotti, A.I., Gagliardini, D.A., Bianchi, A.A. and Balestrini, C.F., 2009. Primary production in the Argentine Sea during spring estimated by field and satellite models. Journal of Plankton Research, 32(2), pp.181-195.

Maas, A.E., Elder, L.E., Dierssen, H.M. and Seibel, B.A., 2011. Metabolic response of Antarctic pteropods (Mollusca: Gastropoda) to food deprivation and regional productivity. Marine Ecology Progress Series, 441, pp.129-139.

Maas, A.E., Lawson, G.L. and Wang, Z.A., 2016. The metabolic response of thecosome pteropods from the North Atlantic and North Pacific Oceans to high CO_2 and low O_2. Biogeosciences, 13(22), pp.6191.

Maas, A.E., Wishner, K.F. and Seibel, B.A., 2012a. Metabolic suppression in thecosomatous pteropods as an effect of low temperature and hypoxia in the eastern tropical North Pacific. Marine Biology, 159(9), pp.1955-1967.

Maas, A.E., Wishner, K.F. and Seibel, B.A., 2012b. The metabolic response of pteropods to acidification reflects natural CO_2-exposure in oxygen minimum Zones. Biogeosciences. 9, pp.747-757.

Macdonald, P. and Juan, D., 2012. Mixdist: Finite Mixture Distribution Models. R package version 0.5-4. https://CRAN.R-project.org/package=mixdist [last accessed 03/05/16].

Mackas, D.L. and Galbraith, M.D., 2011. Pteropod time-series from the NE Pacific. ICES Journal of Marine Science, 69(3), pp.448-459.

Mackenzie, C.L., Ormondroyd, G.A., Curling, S.F., Ball, R.J., Whiteley, N.M. and Malham, S.K., 2014. Ocean warming, more than acidification, reduces shell strength in a commercial shellfish species during food limitation. PloS one, 9(1), e86764.

Makabe, R., Hattori, H., Sampei, M., Darnis, G., Fortier, L. and Sasaki, H., 2016. Can sediment trap-collected zooplankton be used for ecological studies? Polar Biology, 39(12), pp.2335-2346.

Manno, C., Accornero, A. and Umani, S.F., 2009. Importance of the contribution of *Limacina helicina* faecal pellets to the carbon pump in Terra Nova Bay (Antarctica), Journal of plankton research. 32(2), pp.145-152.

Manno, C., Bednaršek, N., Tarling, G., Peck, V., Comeau, S., Adhikari, D., Bakker, D., Bauerfeind, E., Bergan, A., Berning, M., Buitenhuis, E., Burridge, A., Chierici, M., Flöter, S., Fransson, A., Gardner, J., Howes, E., Keul, N., Kimoto, K., Kohnert, P., Lawson, G., Lischka, S., Maas, A., Mekkes, L., Oakes, R., Pebody, C., Peijnenburg, K., Seifert, M., Skinner, J., Thibodeau, P., Wall-Palmer, D. and Ziveri,

P., 2017. Shelled pteropods in peril: Assessing vulnerability in a high CO_2 ocean. Earth-Science Reviews, 169, pp.132-145.

Manno, C., Morata, N. and Primicerio, R., 2012. *Limacina retroversa's* response to combined effects of ocean acidification and sea water freshening. Estuarine, Coastal and Shelf Science, 113, pp.163–171.

Manno, C., Peck, V.L. and Tarling, G.A., 2016. Pteropod eggs released at high pCO2 lack resilience to ocean acidification. Scientific reports, 6, e25752.

Manno, C., Sandrini, S., Tositti, L. and Accornero, A., 2007. First stages of degradation of *Limacina helicina* shells observed above the aragonite chemical lysocline in Terra Nova Bay(Antarctica). Journal of Marine Systems, 68(1–2), pp.91-102.

Manno, C., Tirelli, V., Accornero, A. and Umani, S.F., 2009. Importance of the contribution of *Limacina helicina* faecal pellets to the carbon pump in Terra Nova Bay (Antarctica). Journal of Plankton Research, 32(2). pp.145-152.

Marin, F. and Luquet, G., 2004. Molluscan shell proteins. Comptes Rendus Palevol, 3(6-7), pp.469-492.

Martin, J.H., Gordon, R.M. and Fitzwater, S.E., 1990. Iron in Antarctic waters. Nature, 345(6271), pp.156-158.

Matson, P.G., Martz, T.R. and Hofmann, G.E., 2011. High-frequency observations of pH under Antarctic sea ice in the southern Ross Sea. Antarctic Science, 23(6), pp.607-613.

Mayor, D.J., Sommer, U., Cook, K.B. and Viant, M.R., 2015. The metabolic response of marine copepods to environmental warming and ocean acidification in the absence of food. Scientific reports, 5, pp.13690.

McCulloch, M., Falter, J., Trotter, J. and Montagna, P., 2012. Coral resilience to ocean acidification and global warming through pH up-regulation. Nature Climate Change, 2(4), 1-5.

McGowan John A. and Fraundorf Vernie J. 1966. The relationship between size of net used and estimates of zooplankton diversity. Limnology and Oceanography, 11(4), pp.456-469.

McNeil, B.I. and Matear, R.J., 2008. Southern Ocean acidification: a tipping point at 450 ppm atmospheric CO_2. Proceedings of the National Academy of Sciences of the United States of America, 105(48), pp.18860-4.

McNeil, B.I. and Sasse, T.P., 2016. Future ocean hypercapnia driven by anthropogenic amplification of the natural CO_2 cycle. Nature, 529(7586), p.383-391.

Mehrbach, C., Culberson, C.H., Hawley, J.E. and Pytkowicx, R.M., 1973. Measurement of the apparent dissociation constants of carbonic acid in

seawater at atmospheric pressure. Limnology and Oceanography, 18, pp.897–907.

Melzner, F., Stange, P., Trübenbach, K., Thomsen, J., Casties, I., Panknin, U., Gorb, S.N. and Gutowska, M.A., 2011. Food supply and seawater pCO_2 impact calcification and internal shell dissolution in the blue mussel *Mytilus edulis*. PloS one, 6(9), e24223.

Meredith, M.P. and King, J.C., 2005. Rapid climate change in the ocean west of the Antarctic Peninsula during the second half of the 20th century. Geophysical Research Letters, 32(19). pp.1-8.

Meredith, M.P., Watkins, J.L., Murphy, E.J., Cunningham, N.J., Wood, A.G., Korb, R., Whitehouse, M.J., Thorpe, S.E. and Vivier, F., 2003. An anticyclonic circulation above the northwest Georgia rise, Southern Ocean. Geophysical research letters, 30(20). pp.1-6.

Mintrop, L., Pérez, F.F., González Dávila, M., Santana Casiano, J.M. and Körtzinger, A., 2000. Alkalinity determination by potentiometry: Intercalibration using three different methods. *Ciencias Marinas*, 26(1). pp.23-27,

Mock, T. and Thomas, D.N., 2008. Microalgae in polar regions: linking functional genomics and physiology with environmental conditions. In Psychrophiles: From Biodiversity to Biotechnology (pp. 285-312). Springer, Berlin, Heidelberg.

Montes-Hugo, M., Doney, S.C., Ducklow, H.W., Fraser, W., Martinson, D., Stammerjohn, S.E. and Schofield, O., 2009. Recent changes in phytoplankton communities associated with rapid regional climate change along the western Antarctic Peninsula. Science, 323(5920), pp.1470-1473.

Moore, J.K., Abbott, M.R. and Richman, J.G., 1999. Location and dynamics of the Antarctic Polar Front from satellite sea surface temperature data. Journal of Geophysical Research: Oceans, 104(C2), pp.3059-3073.

Morton, J.E., 1954. The biology of Limacina retroversa. *Journal of the Marine Biological Association of the United Kingdom*, *33*(2), pp.297-312.

Mostofa, K.M.G., Liu, C., Zhai, W., Minella, M., Vione, D., Gao, K., Minakata, D., Arakaki, T., Yoshioka, T., Hayakawa, K. and Konohira, E., 2016. Reviews and syntheses: Ocean acidification and its potential impacts on marine ecosystems. Biogeosciences, 13, pp.1767–1786.

MSIP., 2017. Marine species identification portal. http://species-identification.org/index.php [last accessed 08/07/2017].

Mucci, A., 1983. The solubility of calcite and aragonite in seawater at various salinities, temperatures, and one atmosphere total pressure. American Journal of Science, 283, pp.780–799.

NASA; Ocean Biology. 2018. MODIS-Aqua/Mapped. https://oceandata.sci.gsfc.nasa.gov/MODIS-Aqua/Mapped/ [last accessed 10/01/2018].

Noji, T.T., Bathmann, U.V., Bodungen, B.V., Voss, M., Antia, A., Krumbholz, M., Klein, B., Peeken, I., Noji, C.I.M. and Rey, F., 1997. Clearance of picoplankton-sized particles and formation of rapidly sinking aggregates by the pteropod, *Limacina retroversa*. Journal of Plankton Research, 19(7), pp.863-875.

Norton, S.F., 1988. Role of the gastropod shell and operculum in inhibiting predation by fishes. Science, 241(4861), pp.92-94.

Oakes, R.L., Peck, V.L., Manno, C. and Bralower, T.J., 2019. Impact of preservation techniques on pteropod shell condition. Polar Biology, 42(2), pp.257-269.

Ohman, M.D., Lavaniegos, B.E. and Townsend A.W., 2009. Multi-decadal variations in calcareous holozooplankton in the California Current System: Thecosome pteropods, Heteropods, and foraminifera, Geophysical Research Letters., 36(18), pp.28-34.

Orr, J., Fabry, V., Aumont, O., Bopp, L., Doney, S., Feely, R., Gnanadesikan, A., Gruber, N., Ishida, A., Joos, F., Key, R., Lindsay, K., Maier-Reimer, E., Matear, R., Monfray, P., Mouchet, A., Najjar, R., Plattner, G., Rodgers, K., Sabine, C., Sarmiento, J., Schlitzer, R., Slater, R., Totterdell, I., Weirig, M., Yamanaka, Y. and Yool, A., 2005. Anthropogenic ocean acidification over the twenty-first century and its impact on calcifying organisms. Nature, 437(7059), pp.681-686.

Orsi, A.H., Whitworth III, T. and Nowlin Jr, W.D., 1995. On the meridional extent and fronts of the Antarctic Circumpolar Current. Deep Sea Research Part I: Oceanographic Research Papers, 42(5), pp.641-673.

OSPAR/ICES, 2014, Final Report to OSPAR of the Joint OSPAR/ICES Ocean Acidification Study Group (SGOA). ICES advisory committee, ACOM:67.

Pakhomov, E.A. and Froneman, P.W., 2004. Zooplankton dynamics in the eastern Atlantic sector of the Southern Ocean during the austral summer 1997/1998—Part 2: Grazing impact. Deep Sea Research Part II: Topical Studies in Oceanography, 51(22), pp.2617-2631.

Pakhomov, E.A., Froneman, P.W., Wassmann, P., Ratkova, T. and Arashkevich, E., 2002. Contribution of algal sinking and zooplankton grazing to downward flux in the Lazarev Sea (Southern Ocean) during the onset of phytoplankton bloom: a lagrangian study. Marine Ecology Progress Series, 233, pp.73-88.

Pakhomov, E.A., Perissinotto, R., McQuaid, C.D. and Froneman, P.W., 2000. Zooplankton structure and grazing in the Atlantic sector of the Southern Ocean in late austral summer 1993: Part 1. Ecological zonation. Deep Sea Research Part I: Oceanographic Research Papers, 47(9), pp.1663-1686.

Pansch, C., Nasrolahi, A., Appelhans, Y.S. and Wahl, M., 2013. Tolerance of juvenile barnacles (*Amphibalanus improvisus*) to warming and elevated pCO2. Marine Biology, 160(8), pp.2023-2035.

Pante, E. and Simon-Bouhet, B., 2013. marmap: A Package for Importing, Plotting and Analysing Bathymetric and Topographic Data in R. PLoS ONE, 8(9), e73051.

Paranjape, M., 1968. The egg mass and veligers of Limacina helicina Phipps. Veliger, 10, pp.322–326.

Parker, L.M., Ross, P.M., O'Connor, W.A., Pörtner, H.O., Scanes, E. and Wright, J.M., 2013. Predicting the response of molluscs to the impact of ocean acidification. Biology, 2(2), pp.651-692.

Parmesan, C., and Yohe, G., 2003. A globally coherent fingerprint of climate change impacts across natural systems. Nature, 421, pp.37-42.

Parmesan, C., Gaines, S., Gonzalez, L., Kaufman, D.M., Kingsolver, J., Townsend Peterson, A. and Sagarin, R., 2005. Empirical perspectives on species borders: from traditional biogeography to global change. Oikos, 108(1), pp.58-75.

Pasternak, A.F., Drits, A.V. and Flint, M.V., 2017. Feeding, egg production, and respiration rate of pteropods *Limacina* in Arctic seas. Oceanology, 57(1), pp.122-129.

Pechenik, J.A., 1987. Environmental influences on larval survival and development. Reproduction of marine invertebrates, 9, pp.551-608.

Peck, V.L., Oakes, R.L., Harper, E.M., Manno, C. and Tarling, G.A., 2018. Pteropods counter mechanical damage and dissolution through extensive shell repair. Nature communications, 9(1), pp.264.

Peck, V.L., Tarling, G.A., Manno, C. and Harper, E.M. 2016a. Reply to comment by Bednaršek *et al*. Deep-Sea Research Part II: Topical Studies in Oceanography, 127, pp.57–59.

Peck, V.L., Tarling, G.A., Manno, C. and Harper, E.M., 2016b. Response to comment "Vulnerability of pteropod (Limacina helicina) to ocean acidification: Shell dissolution occurs despite an intact organic layer" by Bednaršek *et al*. Deep-Sea Research Part II: Topical Studies in Oceanography, 127, pp.57-59.

Peck, V.L., Tarling, G.A., Manno, C., Harper, E.M. and Tynan, E. 2016c. Outer organic layer and internal repair mechanism protects pteropod Limacina helicina from ocean acidification. Deep Sea Research Part II: Topical Studies in Oceanography, 127, pp.41–52.

Peterson, W. and Dam, H.G., 1990. The influence of copepod "swimmers" on pigment fluxes in brine-filled vs. ambient seawater-filled sediment traps. Limnology and Oceanography, 35(2), pp.448-455.

Pierrot, D.E.L. and Wallace, D.W.R. 2006. MS Excel program developed for CO_2 System Calculations. ORNL/CDIAC-105, Oak Ridge, Tennessee, Carbon Dioxide Information Analysis Centre Oak Ridge Natl. Lab., US Department of Energy.

Pollard, R.T., Lucas, M.I. and Read, J.F., 2002. Physical controls on biogeochemical zonation in the Southern Ocean. Deep Sea Research Part II: Topical Studies in Oceanography, 49(16), pp.3289-3305.

Poloczanska, E.S., Brown, C.J., Sydeman, W.J., Kiessling, W., Schoeman, D.S., Moore, P.J., Brander, K., Bruno, J.F., Buckley, L.B., Burrows, M.T. and Duarte, C.M., 2013. Global imprint of climate change on marine life. Nature Climate Change, 3(10), pp.919.

Pomerleau, C., Lesage, V., Ferguson, S.H., Winkler, G., Petersen, S.D. and Higdon, J.W., 2012. Prey assemblage isotopic variability as a tool for assessing diet and the spatial distribution of bowhead whale Balaena mysticetus foraging in the Canadian eastern Arctic. Marine Ecology Progress Series, 469, pp.161-174.

Pörtner, H., 2001. Climate change and temperature-dependent biogeography: oxygen limitation of thermal tolerance in animals. Naturwissenschaften, 88(4), pp.137-146.

Pörtner, H.O., 2002. Physiological basis of temperature-dependent biogeography: trade-offs in muscle design and performance in polar ectotherms. Journal of Experimental Biology, 205(15), pp.2217-2230.

Pörtner, H.O., 2008. Ecosystem effects of ocean acidification in times of ocean warming: A physiologist's view. Marine Ecology Progress Series, 373, pp.203-217.

Przeslawski, R., Ahyong, S., Byrne, M., Worheides, G. and Hutchings, P., 2008. Beyond corals and fish: the effects of climate change on noncoral benthic invertebrates of tropical reefs. Global Change Biology, 14, pp.2773-2795.

Purcell, J.E., Baxter, E.J. and Fuentes, V.L., 2013. Jellyfish as products and problems of aquaculture. Advances in aquaculture hatchery technology, 13(1), pp.404-430.

R Development Core Team., 2015. R: A language and environment for statistical computing. R Foundation for Statistical Computing, version 3.1.3. https://cran.r-project.org [last accessed 03/05/16].

Ramajo, L., Pérez-León, E., Hendriks, I.E., Marba, N., Krause-Jensen, D., Sejr, M.K., Blicher, M.E., Lagos, N.A., Olsen, Y.S. and Duarte, C.M., 2016. Food supply confers calcifiers resistance to ocean acidification. Scientific reports, 6(19374), pp.1-6.

Rapport, D.J., 1989. What constitutes ecosystem health?. Perspectives in biology and medicine, 33(1), pp.120-132.

Raven, J., Caldeira, K., Elderfield, H., Hoegh-Guldberg, O., Liss, P., Riebesell, U., Shepherd, J., Turley, C. and Watson, A., 2005. Ocean acidification due to

increasing atmospheric carbon dioxide. The Royal Society. Policy document 12/05. pp.1-31.

Redfield, A.C., 1939. The history of a population of *Limacina retroversa* during its drift across the Gulf of Maine. The Biological Bulletin, 76(1), pp.26-47.

Reipschläger, A. and Pörtner, H.O., 1996. Metabolic depression during environmental stress: the role of extracellular versus intracellular pH in Sipunculus nudus. Journal of experimental biology, 199(8), pp.1801-1807.

Reisdorph, S.C. and Mathis, J.T., 2014. The dynamic controls on carbonate mineral saturation states and ocean acidification in a glacially dominated estuary. Estuarine, Coastal and Shelf Science, 144, pp.8-18.

Riccardi, N., 2010. Selectivity of plankton nets over mesozooplankton taxa: implications for abundance, biomass and diversity estimation. Journal of Limnology, 69(2), pp.287-296.

Richardson, A. J., 2008. In hot water: Zooplankton and climate change. ICES Journal of Marine Science, 65, pp.279-295.

Riebesell, U. and Gattuso, J.P., 2014. Lessons learned from ocean acidification research. Nature Climate Change, 5(1), pp.12.

Ries, J.B., 2011a. Skeletal mineralogy in a high CO_2 world. Journal of Experimental Marine Biology and Ecology, 403(1–2), pp.54-64.

Ries, J.B., 2011b. A physicochemical framework for interpreting the biological calcification response to CO_2 induced ocean acidification. Geochimica et Cosmochimica Acta, 75(14), pp.4053-4064.

Ries, J.B., Cohen, A.L. and McCorkle, D.C., 2009. Marine calcifiers exhibit mixed responses to CO2-induced ocean acidification. Geology, 37(12), pp.1131-1134.

Robbins, L.L., Wynn, J.G., Lisle, J.T., Yates, K.K., Knorr, P.O., Byrne, R.H., Liu, X., Patsavas, M.C., Azetsu-Scott, K. and Takahashi, T., 2013. Baseline monitoring of the western Arctic Ocean estimates 20% of Canadian Basin surface waters are undersaturated with respect to aragonite. PloS one, 8(9), e73796.

Roberts, D., Howard, W.R., Moy, A.D., Roberts, J.L., Trull, T.W., Bray, S.G. and Hopcroft, R.R., 2011. Inter-annual pteropod variability in sediment traps deployed above and below the aragonite saturation horizon in the Sub-Antarctic Southern Ocean. Polar Biology, 34(11), pp.1739-1750.

Robinson, J.O.S.I.E., Popova, E.E., Srokosz, M.A. and Yool, A., 2016. A tale of three islands: Downstream natural iron fertilization in the Southern Ocean. Journal of Geophysical Research: Oceans, 121(5), pp.3350-3371.

Rodolfo-Metalpa, R., Houlbrèque, F., Tambutté, É., Boisson, F., Baggini, C., Patti, F.P., Jeffree, R., Fine, M., Foggo, A., Gattuso, J.P. and Hall-Spencer, J.M., 2011.

Coral and mollusc resistance to ocean acidification adversely affected by warming. Nature Climate Change, 1(6), pp.308.

Rudd, M.A., 2014. Scientists perspectives on global ocean research priorities. Frontiers in Marine Science, 1, pp.36-42.

Sabine, C.L., Feely, R.A., Gruber, N., Key, R.M., Lee, K., Bullister, J.L., Wanninkhof, R., Wong, C.S.L., Wallace, D.W., Tilbrook, B. and Millero, F.J., 2004. The oceanic sink for anthropogenic CO2. Science, 305(5682), pp.367-371.

Sallée, J.-B. 2018. Southern Ocean warming. *Oceanography* 31(2):52–62, https://doi.org/10.5670/oceanog.2018.215.

Sawyer, L., Grubb, D. and Meyers, G. 2011. Polymer microscopy. 3rd ed. New York: Springer, pp.130- 246.

Schneider, C.A., Rasband, W.S. and Eliceiri, K.W., 2012. NIH Image to ImageJ: 25 years of image analysis. Nature methods, 9(7), pp.671.

Schram, J.B., Schoenrock, K.M., McClintock, J.B., Amsler, C.D. and Angus, R.A., 2015. Multi-frequency observations of seawater carbonate chemistry on the central coast of the western Antarctic Peninsula. Polar Research, 34(1), pp.25582.

Schulz, K.G., Barcelose Ramos, J., Zeebe, R.E. and Riebesell, U., 2009. CO_2 perturbation experiments: similarities and differences between dissolved inorganic carbon and total alkalinity manipulations. Biogeosciences, 6(10), 2145-2153.

Seibel, B.A. and Dierssen, H.M., 2003. Cascading trophic impacts of reduced biomass in the Ross Sea, Antarctica: Just the tip of the iceberg? The Biological Bulletin, 205(2), pp.93-97.

Seibel, B.A., Dymowska, A. and Rosenthal, J., 2007. Metabolic temperature compensation and coevolution of locomotory performance in pteropod molluscs. Integrative and Comparative Biology, 47(6), pp.880-891.

Seibel, B.A., Maas, A.E. and Dierssen, H.M., 2012. Energetic plasticity underlies a variable response to ocean acidification in the pteropod, *Limacina helicina* antarctica. PLoS One, 7(4), e30464.

Small, D.P., Calosi, P., Boothroyd, D., Widdicombe, S. and Spicer, J.I., 2016. The sensitivity of the early benthic juvenile stage of the European *lobster Homarus gammarus* (L.) to elevated pCO_2 and temperature. Marine biology, 163(3), p.53.

SOCAT, (Surface Ocean CO_2 Atlas), Bakker *et al.* (2016) A multi-decade record of high quality fCO_2 data in version 3 of the Surface Ocean CO_2 Atlas (SOCAT). Earth System Science Data, (8), pp.383-413.

Sokolov, S. and Rintoul, S.R., 2009. Circumpolar structure and distribution of the Antarctic circumpolar current fronts: 2. Variability and relationship to sea surface height. Journal of Geophysical Research: Oceans, 114(C4), pp.1-14.

Somero, G.N. 2010. The physiology of climate change: how potentials for acclimatization and genetic adaptation will determine 'winners' and 'losers'. Journal of Experimental Biology, 213(6), pp.912-920.

Starr, M., Himmelman, J.H. and Therriault, J.C., 1990. Direct coupling of marine invertebrate spawning with phytoplankton blooms. Science, 247(4946), pp.1071-1074.

Stumpp, M., Hu, M., Melzner, F., Gutowska, M., Dorey, N., Himmerkus, N., Holtmann, W., Dupont, S., Thorndyke, M. and Bleich, M., 2012. Acidified seawater impacts sea urchin larvae pH regulatory systems relevant for calcification. Proceedings of the National Academy of Sciences, 109(44), pp.18192-18197.

Sturdevant, M.V., Orsi, J.A. and Fergusson, E.A., 2012. Diets and trophic linkages of epipelagic fish predators in coastal Southeast Alaska during a period of warm and cold climate years, 1997–2011. Marine and Coastal Fisheries, 4(1), pp.526-545.

Suckling, C.C., Clark, M.S., Beveridge, C., Brunner, L., Hughes, A.D., Harper, E.M., Cook, E.J., Davies, A.J. and Peck, L.S., 2014. Experimental influence of pH on the early life-stages of sea urchins II: increasing parental exposure times gives rise to different responses. Invertebrate reproduction and development, 58(3), pp.161-175.

Tarling, G.A., Ward, P. and Thorpe, S.E., 2018. Spatial distributions of Southern Ocean mesozooplankton communities have been resilient to long-term surface warming. Global change biology, 24(1), pp.132-142.

Thabet, A.A., Maas, A.E., Lawson, G.L. and Tarrant, A.M. 2015. Life cycle and early development of the thecosomatous pteropod *Limacina retroversa* in the Gulf of Maine, including the effect of elevated CO_2 levels. Marine Biology, 162(11), pp.2235-2249.

Thomas, J.A., Welch, J.J., Lanfear, R. and Bromham, L., 2010. A generation time effect on the rate of molecular evolution in invertebrates. Molecular biology and evolution, 27(5), pp.1173-1180.

Thorp, J.H. and Covich, A.P., 2009. Ecology and classification of North American freshwater invertebrates. Academic press. New York.

Thorpe, S.E., Heywood, K.J., Brandon, M.A. and Stevens, D.P., 2002. Variability of the southern Antarctic Circumpolar Current front north of South Georgia. Journal of Marine Systems, 37(1-3), pp.87-105.

Timpane-Padgham, B.L., Beechie, T. and Klinger, T., 2017. A systematic review of ecological attributes that confer resilience to climate change in environmental restoration. PLoS One, 12(3), e0173812.

Tunnicliffe, V., Davies, K.T., Butterfield, D.A., Embley, R.W., Rose, J.M. and Chadwick Jr, W.W., 2009. Survival of mussels in extremely acidic waters on a submarine volcano. Nature Geoscience, 2(5), pp.344.

Turner, J., Colwell, S.R., Marshall, G.J., Lachlan-Cope, T.A., Carleton, A.M., Jones, P.D., Lagun, V., Reid, P.A. and Iagovkina, S., 2005. Antarctic climate change during the last 50 years. International journal of Climatology, 25(3), pp.279-294.

Van der Spoel and Dadon, S. 1999. Pteropoda. In: Boltovskoy, D. South Atlantic Zooplankton. Leiden: Backhuys Publishers, Leiden. pp.649-706.

Van der Spoel, S. and Heyman, R.P., 2013. A comparative atlas of zooplankton: biological patterns in the oceans. Springer Science & Business Media. Berlin.

Van der Spoel, S., 1970. Morphometric data on Cavoliniidae, with notes on a new form of *Cuvierina columnella* (Rang, 1827) (Gastropoda, Pteropoda). Basteria, 34(5/6), pp.103-151.

Van der Spoel, S., 1973. Growth, reproduction and vertical migration *in Clio pyramidata* Linne, 1767 forma lanceolata (Lesueur, 1813), with notes on some other Cavoliniidae (Mollusca, Pteropoda). Beaufortia, 21(281), pp.117-134.

Van der Spoel, S., Schalk, P.H. and Bleeker, J., 1992. *Clio piatkowskii*, a mesopelagic pteropod new to science (Gastropoda, Opisthobranchia). Beaufortia, 43(1), pp.1-6.

Vaughan, D.G., Marshall, G.J., Connolley, W.M., Parkinson, C., Mulvaney, R., Hodgson, D.A., King, J.C., Pudsey, C.J. and Turner, J., 2003. Recent rapid regional climate warming on the Antarctic Peninsula. Climatic change, 60(3), pp.243-274.

Venables, W. N. & Ripley, B. D. 2002. Modern Applied Statistics with S. Fourth Edition. Springer, New York.

Venn, A.A., Tambutté, E., Holcomb, M., Laurent, J., Allemand, D. and Tambutté, S., 2013. Impact of seawater acidification on pH at the tissue-skeleton interface and calcification in reef corals. Proceedings of the National Academy of Sciences, 110(5), pp.1634-1639.

Voronina, N.M., Kosobokova, K.N. And Pakiiomov, E.A., 1994. size structure of antarctic metazoan plankton according to united net, trawl, and water bottle data. Russian Journal of aquatic Ecology, 3(2), pp.137-142.

Wadley, M.R., Jickells, T.D. and Heywood, K.J., 2014. The role of iron sources and transport for Southern Ocean productivity. Deep Sea Research Part I: Oceanographic Research Papers, 87, pp.82-94.

Waldbusser, G.G., 2011, August. The causes of acidification in Chesapeake Bay and consequences to oyster shell growth and dissolution. Journal of Shellfish Research 30(2), pp.559-560.

Waldbusser, G.G., Brunner, E.L., Haley, B.A., Hales, B., Langdon, C.J., Prahl, F.G. 2013. A developmental and energetic basis linking larval oyster shell formation to acidification sensitivity. Geophysical Research Letters, 40, pp.2171-2176.

Waldbusser, G.G., Hales, B., Langdon, C.J., Haley, B.A., Schrader, P., Brunner, E.L., Gray, M.W., Miller, C.A., Gimenez, I. 2015a. Saturation-state sensitivity of marine bivalve larvae to ocean acidification. Nature Climate Change, 5, pp.273-280.

Waldbusser, G.G., Hales, B., Langdon, C.J., Haley, B.A., Schrader, P., Brunner, E.L., Gray, M.W., Miller, C.A., Gimenez, I., Hutchinson, G. 2015b. Ocean acidification has multiple modes of action on bivalve larvae. PloS one, 10, e0128376.

Waldbusser, G.G., Hales, B., Langdon, C.J., Haley, B.A., Schrader, P., Brunner, E.L., Gray, M.W., Miller, C.A., Gimenez, I. 2015a. Saturation-state sensitivity of marine bivalve larvae to ocean acidification. Nature Climate Change, 5, pp.273-280.

Waldbusser, G.G., Hales, B., Langdon, C.J., Haley, B.A., Schrader, P., Brunner, E.L., Gray, M.W., Miller, C.A., Gimenez, I., Hutchinson, G. 2015b. Ocean acidification has multiple modes of action on bivalve larvae. PloS one, 10, e0128376.

Wall-Palmer, D., Smart, C.W. and Hart, M.B., 2013. In-life pteropod shell dissolution as an indicator of past ocean carbonate saturation. Quaternary Science Reviews, 81, pp.29-34.

Wang, K., 2014. The life cycle of the pteropod *Limacina helicina* in Rivers Inlet, Doctoral dissertation, University of British Columbia. British Columbia, Canada.

Wang, K., Hunt, B.P., Liang, C., Pauly, D. and Pakhomov, E.A., 2017. Reassessment of the life cycle of the pteropod Limacina helicina from a high resolution interannual time series in the temperate North Pacific. ICES Journal of Marine Science, 74(7), pp.1906-1902.

Wang, L., Jian, Z., Chen, J., 1997. Late Quaternary pteropods in the South China Sea: carbonate preservation and paleoenvironmental variation. Marine Micropaleontology, 32, 115-126.

Ward, P., Atkinson, A., Murray, A.W.A., Wood, A.G., Williams, R. and Poulet, S.A., 1995. The summer zooplankton community at South Georgia: biomass, vertical migration and grazing. Polar Biology, 15(3), pp.195-208.

Ward, P., Grant, S., Brandon, M., Siegel, V., Sushin, V., Loeb, V. and Griffiths, H., 2004. Mesozooplankton community structure in the Scotia Sea during the CCAMLR 2000 Survey: January–February 2000. Deep Sea Research Part II: Topical Studies in Oceanography, 51(12-13), pp.1351-1367.

Ward, P., Whitehouse, M., Brandon, M., Shreeve, R. and Woodd-Walker, R., 2003. Mesozooplankton community structure across the Antarctic Circumpolar

Current to the north of South Georgia: Southern Ocean. Marine Biology, 143(1), pp.121-130.

Watanabe, Y., Yamaguchi, A., Ishida, H., Harimoto, T., Suzuki, S., Sekido, Y., Ikeda, T., Shirayama, Y., Mac Takahashi, M., Ohsumi, T. and Ishizaka, J., 2006. Lethality of increasing CO_2 levels on deep-sea copepods in the western North Pacific. Journal of Oceanography, 62(2), pp.185-196.

Watson, S.A., Southgate, P.C., Tyler, P.A. and Peck, L.S. 2009. Early Larval Development of the Sydney Rock Oyster Saccostrea glomerata under near-future predictions of CO_2 driven ocean acidification. Journal of shellfish research, 28(3), pp.431-437.

Weiss, I.M., Tuross, N., and Addadi, L.I.A. 2002. Mollusc larval shell formation: amorphous calcium carbonate is a precursor phase for aragonite, Journal of Experimental Zoology, 491, pp.478-491.

Wernberg, T., Smale, D. A. and Thomsen, M.S. 2012. A decade of climate change experiments on marine organisms: Procedures, patterns and problems. Global Change Biology, 18(5), pp.1491–1498.

Węsławski, J.M., Stempniewicz, L., Mehlum, F. and Kwaśniewski, S., 1999. Summer feeding strategy of the little auk (Alle alle) from Bjørnøya, Barents Sea. Polar Biology, 21(3), pp.129-134.

Whitehouse, M.J., Atkinson, A., Korb, R.E., Venables, H.J., Pond, D.W. and Gordon, M., 2012. Substantial primary production in the land-remote region of the central and northern Scotia Sea. Deep Sea Research Part II: Topical Studies in Oceanography, 59, pp.47-56.

Whitehouse, M.J., Meredith, M.P., Rothery, P., Atkinson, A., Ward, P. and Korb, R.E. 2008. Rapid warming of the ocean around South Georgia, Southern Ocean, during the 20th century: Forcings, characteristics and implications for lower trophic levels. Deep Sea Research Part I: Oceanographic Research Papers, 55(10), pp.1218–1228.

Wickham. H. (2009) ggplot2: Elegant Graphics for Data Analysis. Springer-Verlag New York.

Wiens, J. A. (1989). Spatial scaling in ecology. Functional ecology, 3(4), pp.385-397.

Wilbur, K.M. and Owen, G. 1964. Growth. In: Physiology of Mollusca, K.M. Wilbur and C.M. Yonge, Physiology of Mollusca, Academic Press, New York. pp.211–242.

Wilbur, K.M. and Yonge, C.M., 2013. Physiology of mollusca. Volume 1, Academic Press. pp.4-51.

Willis, K.J., Cottier, F.R. and Kwaśniewski, S., 2008. Impact of warm water advection on the winter zooplankton community in an Arctic fjord. Polar Biology, 31(4), pp.475-481.

Winter, D.F., Banse, K. and Anderson, G.C., 1975. The dynamics of phytoplankton blooms in Puget sound a fjord in the North-Western United States. Marine Biology, 29(2), pp.139-176.

WoRMS (2017). World register of Marine Spices. http://www.marinespecies.org/index.php [last accessed 14/07/17]

Wormuth, J.H., 1981. Vertical distributions and diel migrations of Euthecosomata in the northwest Sargasso Sea. Deep Sea Research Part A. Oceanographic Research Papers, 28(12), pp.1493-1515.

Yamamoto-Kawai, M., McLaughlin, F.A. and Carmack, E.C., 2011. Effects of ocean acidification, warming and melting of sea ice on aragonite saturation of the Canada Basin surface water. Geophysical Research Letters, 38(3). e3601.

Yamamoto-Kawai, M., McLaughlin, F.A., Carmack, E.C., Nishino, S. and Shimada, K., 2009. Aragonite undersaturation in the Arctic Ocean: effects of ocean acidification and sea ice melt. Science, 326(5956), pp.1098-1100.

Zeileis, A. and Hothorn, T. 2002. Diagnostic checking in regression relationships. R News, 2(3), pp.7-10.